Characterization of TMEFF2; its role in tumour progression and development of targeting strategies for anti-cancer therapy.

by

Katarzyna Gaweł-Bęben

Extracellular Matrix (ECM) in Repair & Remodelling

Cardiff University School of Dentistry

Cardiff, UK

A thesis submitted to the Cardiff University for the degree of Doctor of Philosophy

PhD Project Supervisors:

Dr Vera Knäuper

Dr Ann Ager

August 2013

DECLARATION

This work has not been submitted in substance for any other degree or award at this or any other university or place of learning, nor is being submitted concurrently in candidature for any degree or other award.

Signed ……..... (candidate) Date ……

STATEMENT 1

This thesis is being submitted in partial fulfilment of the requirements for the degree of Doctor of Philosophy.

Signed ……..... (candidate) Date ……

STATEMENT 2

This thesis is the result of my own independent work/investigation, except where otherwise stated. Other sources are acknowledged by explicit references. The views expressed are my own.

Signed ……..... (candidate) Date ……

STATEMENT 3

I hereby give consent for my thesis, if accepted, to be available for photocopying and for inter-library loan, and for the title and summary to be made available to outside organisations.

Signed ……..... (candidate) Date ……

STATEMENT 4: PREVIOUSLY APPROVED BAR ON ACCESS

I hereby give consent for my thesis, if accepted, to be available for photocopying and for inter-library loans **after expiry of a bar on access previously approved by the Academic Standards & Quality Committee.**

Signed ……..... (candidate) Date ……

Acknowledgments

I would like to thank my supervisors, Vera Knäuper and Ann Ager for motivating and inspiring me from the very first day of my PhD.

This work could not be completed without the help and support of my great colleagues: Magdalena Adamczyk, Lea Bauer, Andreas Heil and Tim Wanger – thank you very much.

I would also like to thank Łukasz for encouraging me to accept every challenge and supporting me during difficult times.

Abstract

TMEFF2 (transmembrane protein with EGF-like and two follistatin motifs 2) is a transmembrane protein expressed in brain and prostate and over-expressed in prostate cancer (Uchida et al. 1999; Horie et al. 2000). The role of TMEFF2 in prostate cancer is controversial. Several data indicate that TMEFF2 has cancer-promoting activity (Glynne-Jones et al. 2001; Ali and Knäuper 2007), while others suggest that TMEFF2 inhibits progression of cancer (Gery et al. 2002; Gery and Koeffler 2003). TMEFF2 is cleaved by membrane-anchored proteases, including disintegrin and metalloproteases (ADAMs) and γ-secretase (Ali and Knäuper 2007), but the biological meaning of TMEFF2 shedding is not known. It was hypothesized that the opposing findings describing the role of TMEFF2 in prostate cancer result from proteolytic processing of TMEFF2 by different proteases which are co-expressed with TMEFF2 in prostate cancer cells, such as the type II transmembrane serine proteases (TTSPs), prostasin and ADAMs. To support this hypothesis co-expression of TMEFF2 and serine proteases was analyzed in prostate cancer cell lines and clinical samples. The shedding of TMEFF2 by ADAMs and serine proteases was investigated using HEK293 cells expressing AP/V5 TMEFF2 or shedding resistant AP/V5 $\Delta_{303\text{-}320}$TMEFF2 mutant (Ali and Knäuper 2007). The data obtained from AP activity assay and Western blot analysis of cell lysates showed that TMEFF2 is cleaved by serine proteases (matriptase and hepsin) and ADAMs (ADAM9, ADAM12). Moreover, serine proteases and ADAMs cleave TMEFF2 in different positions, generating several soluble TMEFF2 fragments. To establish the biological role of TMEFF2 processing, N-terminal TMEFF2 fragments predicted to be generated by TTSPs and ADAMs were expressed in *E. coli* and mammalian cells. Preliminary experiments using HEK293 and PNT2-C2 cells indicated that soluble TMEFF2 does not signal through ErbB receptors and suggested several signaling pathways that might be regulated by TMEFF2. The fate of TMEFF2 C-terminus following ectodomain shedding was examined by confocal microscopy and Western blotting, indicating that TMEFF2 cytoplasmic domain is likely degraded following the release of TMEFF2-ECD.

Table of content

List of Figures

Chapter 1: Introduction

Chapter 2: Materials and methods

Chapter 3: Expression of TMEFF2 and serine proteases in prostate cancer

Chapter 4: Shedding of TMEFF2 by serine proteases and ADAMs over-expressed in prostate cancer

Chapter 5: Expression and purification of TMEFF2 ectodomain fragments in *E. coli*

Chapter 6: Expression and purification of TMEFF2 ectodomain fragments using mammalian cells

Chapter 7: The fate of TMEFF2 cytoplasmic domain following ectodomain shedding

List of Tables:

List of abbreviations:

4-NPP – 4-nitrophenol phosphate

ActRII – activin receptor type II

ADAM – a disintegrin and metalloprotease

AD – Alzheimer's disease

ALK - activin receptor-like kinase

AP – alkaline phosphatase

APH-1 – anterior pharynx-defective 1

APP – amyloid precursor protein

AR – androgen receptor

BSA – bovine serum albumin

BM-40 - basement-membrane protein 40

BMP – bone morphogenic factor

BTC - betacellulin

CD – cluster of differentiation

CHO – Chinese chamster ovary

CUB - Cls/Clr, urichin embryonic growth factor, bone morphogenic protein-1

DAG - diacylglycerol

DAPI - 2-(4-amidinophenyl)-1H -indole-6-carboxamidine

DAPT - N-[N-(3,5-Difluorophenacetyl)-L-alanyl]-S-phenylglycine t-butyl ester

DESC1 - differentially expressed in squamous cell carcinoma gene 1

DMSO - dimethyl sulfoxide

DMEM - Dulbecco's modified eagle's medium

ECD – ectodomain

ECM – extracellular matrix

EDTA - ethylenediaminetetraacetic acid

EGF – epidermal growth factor

EGFP – enhanced green fluorescent protein

EGFR – epidermal growth factor receptor

ENaC – epithelial sodium channel

EpCAM – epithelial cell adhesion molecule

Eph - ephrin

ERK – extracellular signal-regulated kinase

FBS – foetal bovine serum

FGFR – fibroblast growth factor receptor

FS – follistatin

GAPDH - glyceraldehyde 3-phosphate dehydrogenase

GDF – growth differentiation factor

GPI – glycophosphatidyloinositol

GPCR - G-protein coupled receptor

Grb2 - growth factor receptor-bound protein 2

HAI-1, 2 - hepatocyte growth factor activator *inhibitor* type 1, 2

HAT – human airway trypsin-like protease

HB-EGF – heparin-binding epidermal growth factor

HEK293 – human embryonic kidney-293

HER2/neu – human epidermal growth factor receptor 2

HGF – hepatocyte growth factor

hPLAP - human placental alkaline phosphatase

IgG – immunoglobulin G

IGF – insulin growth factor

IGFBP – insulin growth factor binding protein

IL – interleukin

IGF1 - insulin growth factor 1

IPTG - isopropyl β-D-1-thiogalactopyranoside

KGF – keratinocyte growth factor

LBD – ligand binding domain

Lck - leukocyte-specific protein tyrosine kinase

LDLA - low-density lipoprotein receptor class A

LMB – leptomycin B

MAM - merpin/A5 antigen/receptor antigen phospatase mu

MAPK – mitogenactivated protein kinase

MBP – maltose binding protein

MEKK1 - mitogen activated protein kinase kinase

MSP-1 - merozoite surface protein-1

MSPL – mosaic serine protease large-form

MT-SP1 - membrane-type serine protease 1

NFκB – nuclear factor κB

NRG – neuregulin

PAI-1 - plasminogen-activator inhibitor 1

PAR-2 – protease-activated receptor 2

PBS – phospate buffered saline

PDGF - platelet-derived growth factor

PEN2 – presenilin enhancer 2

PI3K – phosphoinositide 3 kinase

PIN - prostatic intraepithelial neoplasia

PKC – protein kinase C

PMA - phorbol 12-myristate 13-acetate

PMSF - phenylmethylsulfonyl fluoride

PN-1 – protease nexin-1

PNGase F - peptide-N-glycosidase F

PRSS8 – protease serine 8

PSA – prostate specific antigen

PTEN - phosphatase and tensin homolog deleted on chromosome ten

RIP – regulated intramembrane proteolysis

S1P - sphingosine-1-phosphate

S2P - site 2 proteases

SARDH – sarcosine dehydrogenase

SEA - sea urichin sperm protein/enteropeptidase/argin domain

SPARC - secreted protein acidic and rich in cysteine

SPP - signal-peptide peptidases

ST14 - suppression of tumorigenicity 14

TBS – Tris buffered saline

TBST – Tris buffered saline + Tween 20

TGF-β – transforming growth factor β

TIMP – tissue inhibitor of metalloproteinase

TβR-I - transforming growth factor β receptor I

TMEFF2 – transmembrane protein with epidermal growth factor and follistatin-like domains 2

TMPRSS – transmembrane protease/serine

TNF-α – tumour necrosis factor α

TPEF - transmembrane protein containing epidermal growth factor

TTSP – type II transmembrane serine protease

uPA – urokinase plasminogen activator

XTT - 2,3-bis-(2-methoxy-4-nitro-5-sulfophenyl)-2H-tetrazolium-5-carboxanilide

YFP – yellow fluorescent protein

Chapter 1:

Introduction

1.1 Prostate cancer

Prostate cancer is the most common type of cancer in men in the UK and the second most common cause of cancer death, after lung cancer. According to Cancer Research UK statistics, about 30,800 patients were diagnosed with prostate cancer in 2009 in the UK. Worldwide, this disease is diagnosed in more than 670,000 men every year, accounting for almost one in seven (14%) of all new cancer cases in males. Prostate cancer risk strongly correlates with age: around three-quarters of cases occur in men over 65 years old with the largest number of cases in those aged 70-74. It is estimated from post-mortem data that around a half of men in their fifties and 80% of men aged 80 have histological evidence of cancer in the prostate. In addition to age another important risk factor for prostate cancer is family history of this disease. Men with one or more first-degree relatives diagnosed with prostate cancer have an increased risk of prostate cancer, especially if the relative was diagnosed at an early age. In 1970s only 20% of men diagnosed with prostate cancer survived their disease for at least 10 years. Thanks to the improved diagnostic procedures allowing to detect prostate cancer at early stages the survival rate over 10 years increased to about 70% (data obtained from Cancer Research UK website, May 2013).

The prostate is the largest male accessory gland with round, elliptical or triangular shape, surrounding the urethra at the neck of the bladder. The prostate contains multiple acini and ductal structures producing components of the seminal fluid (Figure 1.1 A). This gland is composed of two major compartments - epithelium and stroma. Prostate epithelium consists of two distinct layers, named the luminal and basal layers (Figure 1.1 B). The luminal cell layer contains columnar cells responsible for the production of seminal fluid components. The basal layer is populated by morphologically distinct flattened cells called basal epithelial cells as well as rare neuroendocrine cells that are thought to release paracrine hormones necessary for luminal cells. Prostate stroma is composed of specialised smooth muscle cells and fibroblasts and accounts for about half of the volume of the prostate. Both epithelial and stromal cells are completely dependent on each other for their survival and produce the extracellular matrix proteins contributing to the basement membrane separating these two compartments (Kumar & Majumder 1995; Vasioukhin 2004).

A.

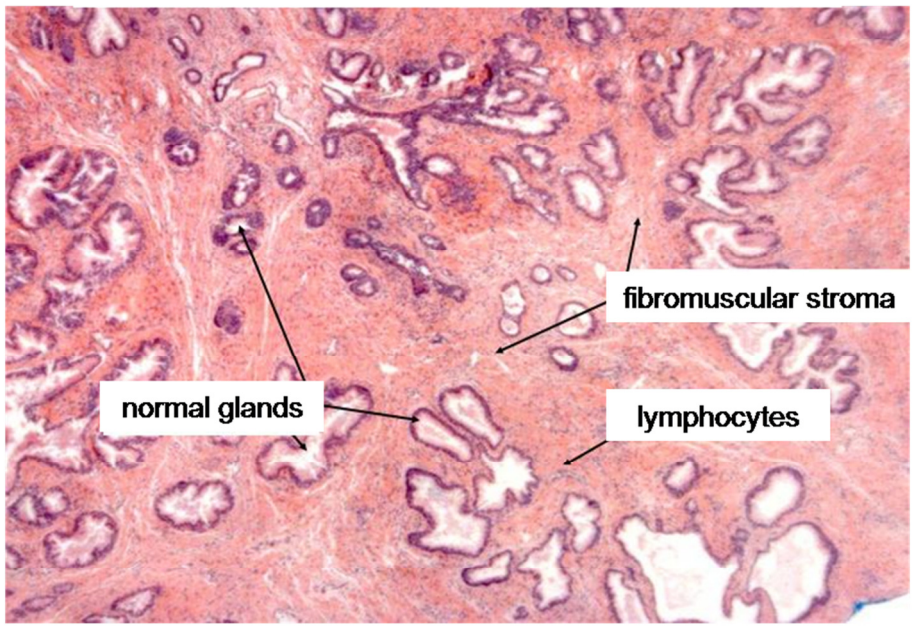

B.

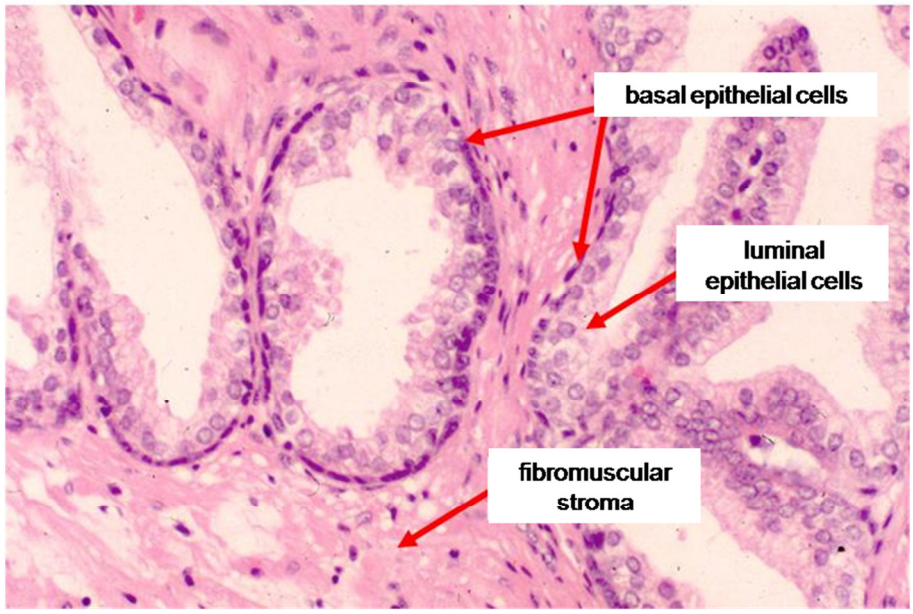

Figure 1.1 Hematoxylin and eosin staining of the normal human prostate gland, A. lower magnification, B. higher magnification(from SCGAP Urologic Epithelial Stem Cells Project, http://scgap.systemsbiology.net/ontology/).

Development of prostate cancer requires alterations in gene expression leading to specific morphological changes. Multiple genes have been implicated in the development of prostate cancer, including regulators of cell proliferation, apoptosis and response to stress factors (DeMarzo et al. 2003; De Marzo et al. 2004). A universally accepted precursor of prostate cancer is prostatic intraepithelial neoplasia (PIN), characterized by intra-acinar proliferation with cells often showing nuclear anaplasia. The basement membrane is intact and all the morphologic changes are confined to the epithelial layer within the prostate acini. The basal layer is usually present but the number of basal cells is decreased (Vasioukhin 2004). Most common genetic alterations observed in PIN lesions include chromosomal deletion in region 8p21 (occurs in 63% of PIN lesions) (De Marzo et al. 2004), loss of prostate-specific homeobox protein NKX3.1 expression (20% of PIN lesions) (Bowen et al. 2000) and down-regulation of reactive oxygen species scavenger GSTP1 (Lee et al. 1994). Transition from PIN to prostate carcinoma is characterized by the loss of basal cells and change in cellular morphology caused by the nuclear and nucleoli enlargement. The basement membrane is disrupted and the overall epithelial organization is lost with tumour progression, evolving from well differentiated to moderately and poorly differentiated (Vasioukhin 2004). The histological pattern of carcinoma cell arrangement is commonly used to determine the pathological stage of prostate cancer. The disorganization of prostate cells is classified using the Gleason grading system (Gleason 1966). There are five basic grades in the Gleason system, where grade 1 corresponds to the morphologically normal prostate tissue and grade 5 is given to poorly differentiated prostate gland (Figure 1.2). Analysing the prostate tissue biopsy, the pathologist assigns a primary grade to the most common tumour pattern and a secondary grade to the next most common tumour pattern. The two grades are added to obtain the Gleason score which is directly related to the pathological stage and is one of the most powerful predictors of prostate cancer clinical outcome. The Gleason score ranges from 2 to 10, with 10 having the worst clinical prognosis. For Gleason score 7, 4+3 is more aggressive than 3+4 and also there is no significant difference between the aggressiveness of Gleason score 9 and 10 tumours (Epstein 2010).

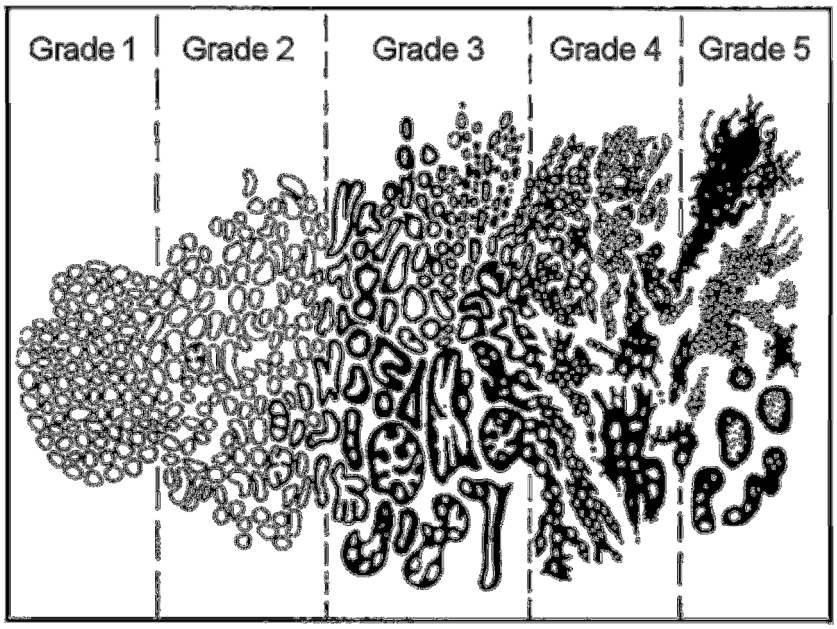

Figure 1.2 Gleason grading system, original drawing (from Gleason 1966).

In addition to the Gleason score, the diagnosis of prostate cancer includes also the description of cancer stage. The stage indicates certain aspects of the cancer such as the tumour size, depth of its penetration, extent to which the cancer has spread and to which organs it has metastasized. Determination of stage at the diagnosis of cancer determines the required therapy and is an important indicator of patient's survival (Madu & Lu 2010). One of the two most common staging systems is the TNM system, that describes the extend of the tumour size and grade (T), detection of the lymph nodes (N) and other metastases (M) by adding an appropriate number (X-4) to the letter. For example, T3N1M0 describes a prostate tumour that extended through the prostate capsule (T3), spread to one lymph node smaller than 2 cm (N1) and there are no distant metastases (M0) (Madu & Lu 2010).

The most important genetic changes associated with the transition of PIN to prostate carcinoma are inactivation of the transcription factor KLF6 (occurs in 55% of primary tumours) (Narla et al. 2001), loss of the negative regulator of the PI3K phosphatase PTEN (10-15% of primary tumours) (Wang et al. 1998) and inactivating mutations of the tyrosine kinase receptor EphB2 (12% of primary tumours) (Huusko et al. 2004). Additionally, advanced, poorly differentiated prostate tumours often display loss of adhesion proteins such as E-cadherin, CD44 and integrins $\alpha_6\beta_4$ and $\alpha_6\beta_1$ as well as basement membrane proteins laminin-332 and collagen VII (Umbas et al. 1994; Nagle et al. 1995; Gao et al. 1997). As these proteins play important roles in mediating cell-cell and cell-matrix interactions their loss is responsible for tissue disorganization and invasion of

the primary tumour. A further hallmark of prostate cancer progression is spreading of the tumour cells through the lymphatic system and blood vessels to the distant organs. Metastatic lesions of prostate cancer usually appear in lymph nodes and bones but it can also metastasize to lung and liver. Spreading of prostate cancer is crucial in the development of the disease because while the prostate-defined tumour is curable, the advanced metastatic cancer is usually lethal (Vasioukhin 2004). The genetic changes associated with prostate cancer metastasis include further inactivation of PTEN (30-43% of metastatic lesions) and amplification of the *c-myc* gene (21% of metastatic lesions) (Cairns et al. 1997; Jenkins et al. 1997).

Normal prostate epithelial cells as well as majority of prostate carcinomas require androgens for growth and survival (Colombel et al. 1992). Androgens belong to steroid hormones that act through the androgen receptor (AR), a steroid hormone-binding protein composed of N-terminal transcriptional regulatory region, central DNA-binding domain and C-terminal ligand-binding domain (LBD). In the absence of ligand binding, AR resides in the cytoplasm in complex with chaperones that prevent its interaction with DNA. Binding of androgen facilitates conformational changes in the AR protein and leads to the dissociation of AR-chaperone complex. The androgen-AR complexes form homodimers and translocate to the nucleus where they bind to specific DNA regions termed androgen-responsive elements and stimulate the transcription of androgen-regulated genes (Evans 1988; Edwards & Bartlett 2005). Growth and survival of prostate cancer cells, at least at the initial stages of the disease, are also regulated by androgens. For that reason ablation of androgens is usually the most effective treatment of prostate cancer. However, while most of the prostate cancer cases initially regress in response to androgen deprivation, in most cases the tumour stops responding to this treatment, due to becoming androgen independent. The molecular mechanisms allowing prostate cancer cells to proliferate and survive in the absence of androgens are diverse. Normal expression of AR and androgen-dependent genes in androgen-independent prostate cancer tissue suggest that AR signalling is inappropriately restored, allowing the cells to proliferate and survive. Apparently, although this type of prostate cancer is androgen-independent it remains dependent on AR signalling. Activation of AR in androgen-independent cancer cells may be achieved through several mechanisms. Amplification of AR gene or mutations causing AR hypersensitivity allow prostate cancer cells to survive in the presence of minimal concentrations of androgens (Visakorpi et al. 1995; Gregory et al. 2001). Expression of constitutively active AR variant that lacks he ligand-binding domain cause constant transcription of AR-dependent genes (Guo et al. 2009). Finally, mutations of the LBD may change AR specificity and enable its activation by other hormones such as estrogens (Tilley et al. 1996; Fenton et al. 1997) or non-steroidal growth factors as shown for insulin growth factor 1 (IGF1), keratinocyte growth factor (KGF) and EGF (Culig et al. 1994). However, it is more likely that there is no single mechanism responsible for the survival

and proliferation of androgen-independent cells in every tumour and for that reason individual characterization of each prostate cancer case seems to be the future of prostate cancer therapy (Vis & Schröder 2009).

In recent years the number of patients diagnosed with prostate cancer increased significantly, mostly due to the improvement of prostate cancer diagnostic procedures. The most widely used biomarker for screening and early detection of prostate cancer is prostate specific antigen (PSA, also known as kallikrein-3), a serine protease secreted by prostate cancer cells as well as normal prostate secretory epithelial cells (Lilja 1985). High levels of PSA are directly associated with the risk of cancer and high grade disease as well as with tumour stage. The biological function of PSA is liquefaction of the seminal fluid and the expression of PSA gene is under the control of AR. In addition to semen, PSA can also be detected in the serum. Although prostate cancer cells produce less PSA than normal prostate epithelial cells, it is thought that the disruption of the prostate gland structure observed in tumours results in the leakage of PSA into the blood and raises the PSA serum levels up to 10^5 fold. Serum PSA levels higher than 4 ng/ml prompt a recommendation that the patient should undergo prostate biopsy (Lilja et al. 2008). However, the level of PSA in the serum rise not only in prostate cancer but also in a number of non-malignant conditions such as benign prostate hyperplasia, infection or chronic inflammation (Pienta 2009). Serum PSA levels are also influenced by ejaculation, body weight, intake of carbohydrates and insulin resistance (Parekh et al. 2008). In some of these circumstances patients with primary prostate cancer might have serum PSA levels below 4 ng/ml, which do not classify them for further biopsy and cause misdiagnosis of the disease. On the other hand, PSA concentrations higher than 4 ng/ml might also be measured in healthy men, subjecting them to undergo unnecessary biopsies. To improve PSA testing several modifications have been introduced like the change of PSA ratio in time (PSA velocity) or the ratio of PSA to prostate volume (PSA density) (Benson et al. 1992; Carter et al. 1992).

In addition to the search for prognostic and diagnostic biomarkers of prostate cancer much attention is paid to the development of novel therapies targeting prostate cancer. Whereas the androgen ablation therapy is quite successful in treatment of primary, androgen-dependent prostate tumours, there is no efficient therapy for hormone-insensitive metastatic prostate cancer which is usually lethal. For that reason every newly identified protein expressed by prostate cancer cells is carefully investigated in order to better understand the mechanisms responsible for the development of an aggressive prostate cancer phenotype. One of these novel proteins, potentially involved in the development and progression of prostate cancer and thus being a promising targets for new anti-prostate cancer therapies is TMEFF2.

1.2 TMEFF2 – a novel protein expressed in prostate cancer

1.2.1 TMEFF2 protein structure

TMEFF2 (a transmembrane protein with EGF-like and two follistatin-like domains 2) is also known in literature as tomoregulin-2, TENB2, HPP1 or TPF. It is a type I transmembrane protein composed of two follistatin-like (FS) domains, an EGF-like domain, transmembrane (TM) domain and short cytoplasmic tail (Figure 1.3). Analysis of TMEFF2 protein sequence revealed the presence of potential G-protein activating motifs within the TMEFF2 cytoplasmic domain, defined as at least two basic residues in the N-terminus and BBxB at the C-terminus, where B stands for basic residue. The extracellular domain of TMEFF2 contains two sites for N-glycosylation and two potential glycosaminoglycan attachment sites but no heparin-binding region (Uchida et al. 1999).

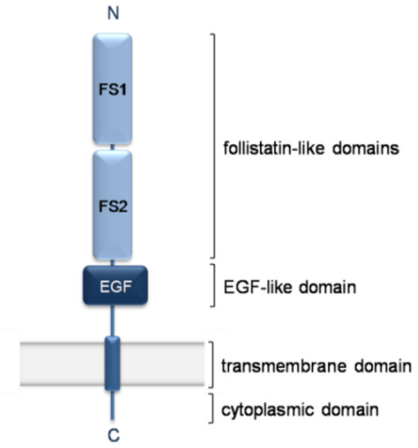

Figure 1.3 Schematic structure of TMEFF2.

1.2.2 Expression of TMEFF2

Despite the fact that the *Tmeff2* gene was isolated for the first time from stomach fibroblasts (Uchida et al. 1999) the highest expression of the TMEFF2 protein was detected in two organs: brain and prostate (Liang et al. 2000; Horie et al. 2000). Elevated expression of TMEFF2 was also found in prostate cancer cell lines and clinical samples (Glynne-Jones et al. 2001; Gery et al. 2002; Afar et al. 2004), indicating that TMEFF2 could play a significant role in prostate cancer progression. High TMEFF2 expression was also recently reported in human primary oocytes (Markholt et al. 2012), suggesting that TMEFF2 could be involved in embryonic development.

1.2.3 Regulation of *Tmeff2* gene expression

The expression of the *Tmeff2* gene is under the control of the androgen receptor. Gery and co-workers shown that TMEFF2 expression in the LNCaP cells increased following treatment with dihydrotestosterone (DHT) in a dose- and time-dependent manner. Moreover, TMEFF2 mRNA levels in CWR22R xenografts propagated in male mice decreased following castration. *In vitro* studies on LNCaP cell line showed that TMEFF2 expression is also up-regulated in response to treatment with 17b-estradiol (E2) and 1,25-dihydroxyvitamin D3 (VD3) (Gery et al. 2002) which can activate the androgen receptor (Veldscholte et al. 1990; Hsieh et al. 1996).

1.2.4 TMEFF2 null mice

In 2012 Chen and co-workers generated TMEFF2 null mouse in order to gain more insight into the physiological function of TMEFF2 in the prostate and nervous system. Inactivation of the *Tmeff2 gene* was achieved by replacing the first coding exon of *Tmeff2* with cDNA encoding human placental alkaline phosphatase (hPLAP). *Tmeff2*$^{hPLAP/hPLAP}$ animals did not express TMEFF2 as confirmed by in-situ hybridization and were used to examine TMEFF2 expression within the body by performing simple AP-staining of tissue sections. The first observation about the TMEFF2 null mice was that they were born normal with a Mendelian ratio but failed to gain weight and appeared smaller in size when compared with heterozygous or wild type littermates. Moreover, all TMEFF2 null mice died around weaning time (about 3 weeks old). As TMEFF2 expression was found predominantly in the prostate and brain it was suspected that some abnormalities in these two organs might cause TMEFF2 null mice death. However, the histology of the prostate gland as well as central, peripheral and enteric nervous systems appeared normal. There were also no differences in neuronal differentiation markers expression between TMEFF2 null and wild type mice and no spontaneous tumors were developed in aged TMEFF2 heterozygous mice. The only significant difference between TMEFF2 null and wild type mice was reduction of the white adipose tissue (WAT) in the body. Subsequently, the AP-staining revealed that TMEFF2 is expressed strongly in WAT. However, the *in vitro* adipocyte differentiation is not affected by TMEFF2 deficiency (Chen et al. 2012). So far, the characterization of the TMEFF2 null mice did not answer the question about the biological role of TMEFF2 due to premature death. Transgenic mice bearing organ-specific deletions of Tmeff2 gene would be a better *in vivo* model to study physiological role of TMEFF2 and could potentially explain its role in the brain and prostate.

1.2.5 The role of TMEFF2 in the central nervous system

As mentioned previously, TMEFF2 is abundantly expressed not only in the prostate but also in the brain (Horie et al. 2000). The biological role of TMEFF2 in the central

nervous system was studied less extensively than TMEFF2 involvement in prostate cancer but it was shown that TMEFF2 is a survival factor for primary cultured neurons (Horie et al. 2000). Interestingly, TMEFF2 was also found in β-amyloid Alzheimer plaques; however, not all plaques contain TMEFF2. The biological significance of TMEFF2 expression in some plaques is unknown (Siegel et al. 2006).

1.2.6 Controversial role of TMEFF2 in normal prostate and prostate cancer

Due to the almost exclusive expression of TMEFF2 in two organs - brain and prostate as well as its up-regulation in primary prostate cancer and metastatic lesions from lymph nodes and bones (Uchida et al. 1999; Horie et al. 2000; Afar et al. 2004) TMEFF2 was intensively studied as a potential target for novel anti-cancer therapies. Afar and co-workers generated monoclonal antibody recognizing the extracellular part of TMEFF2 that was internalized upon TMEFF2 binding and was used to deliver toxic agents to prostate cancer cells. The side effects of this toxin-conjugated antibody would be minimized due to the low expression of TMEFF2 in other organs and the inability of antibody complexes to cross the blood-brain barrier (Afar et al. 2004). Several studies showed significant reduction of cancer growth in LNCaP tumor xenograft model following treatment with monoclonal anti-TMEFF2 antibody conjugated with radioactive isotopes (Zhao et al. 2005) or toxins (Afar et al. 2004). However, the current knowledge about TMEFF2 ectodomain shedding and possible presence of TMEFF2-ECD in the circulation must be considered in designing future anti-cancer therapies. It is also important to better understand the biology of this protein before using it as a target in prostate cancer treatment.

The data published to date regarding TMEFF2 involvement in the development and progression of prostate cancer is controversial. Some publications indicate that TMEFF2 has cancer-promoting activity while others suggest that TMEFF2 inhibits progression of cancer. Analysis of TMEFF2 expression pattern in biopsies from prostate cancer patients showed elevated expression of TMEFF2 in the malignant compartments of the tumor compared to the surrounding benign tissue (Glynne-Jones et al. 2001). These data suggest that TMEFF2 expression correlates with prostate cancer malignancy. Moreover, recombinant TMEFF2-ECD promoted proliferation of HEK293 cells (Ali & Knäuper 2007; Chen et al. 2011). However, data from *in vitro* experiments indicate that TMEFF2 is down-regulated upon prostate cancer progression. TMEFF2 was found in androgen-dependent prostate cancer cell line LNCaP but not in more invasive, androgen-independent DU145 and PC3 cells. Additionally, forced expression of TMEFF2 in DU145 and PC3 cells reduced their growth by 34-66% when compared to empty vector controls (Gery et al. 2002). A similar conclusion came from the study on a colon cancer model. Over-expression of TMEFF2 in colon cancer cell line HCT116 reduced their proliferation rate and tumorigenic potential when implanted in nude mice. Comparison of gene expression between parental cell line and TMEFF2 expressing HCT116 cells revealed that TMEFF2

over-expression increase expression of STAT1 (Elahi et al. 2008), a tumor suppressor gene that impairs angiogenesis, growth and metastasis of cancer cells (Huang et al. 2002). All this information suggests that TMEFF2 inhibits growth of more advanced cancer and is down-regulated during cancer progression.

The hypothesis that TMEFF2 inhibits growth of cancer is also supported by the fact that the *Tmeff2 gene* is frequently hypermethylated in cancer cells. 5' hypermethylation and silencing of the *Tmeff2 gene* was detected in prostate, colon and bladder cancer cell lines (Liang et al. 2000) as well as samples obtained from patients suffering from oral squamous cell carcinoma, gastric, breast, bladder and colorectal cancer and gliomas (Nagata et al. 2012; Shibata et al. 2002; Park et al. 2011; Costa et al. 2010; Young et al. 2001; Sato et al. 2002; Lin et al. 2011). Additionally, *Tmeff2* gene expression can be repressed by c-Myc (Gery & Koeffler 2003). Moreover, the*Tmeff2 gene* is located on chromosome 2q33, where a high frequency of loss was associated with lung, colon, bladder, prostate, breast and esophageal squamous cell carcinoma (Liang et al. 2000).

1.2.7 Soluble TMEFF2 fragments

The ectodomain of TMEFF2 (TMEFF2-ECD) is shed from the cell surface by ADAM10 and ADAM17 and the membrane-retained fragment undergoes further processing by a large membrane enzymatic complex, called the γ-secretase (Ali & Knäuper 2007). Shedding of TMEFF2-ECD can be induced by pro-inflammatory cytokines TNFα and IL-1β and involves NF-κB signaling (Lin et al. 2003). Interestingly, in the conditioned medium of CHO cells stably transfected with TMEFF2 two soluble TMEFF2 fragments were detected – TMEFF2-ECD and a fragment composed of two FS domains only (Uchida et al. 1999). Moreover, in the conditioned medium of LNCaP cells that endogenously express TMEFF2 one more soluble TMEFF2 variant was found, composed of the first follistatin domain and a novel, C-terminal amino acid sequence that does not exist in the full length protein (Quayle & Sadar 2006). The three variants of TMEFF2 found in conditioned media are schematically presented in Figure 1.4. Whereas it is not known how the FS1-FS2 TMEFF2 fragment is generated, the form containing FS1 and the novel amino acid sequence is a secreted splice variant of TMEFF2, resulting from the transcription termination by a premature stop codon (Quayle & Sadar 2006).

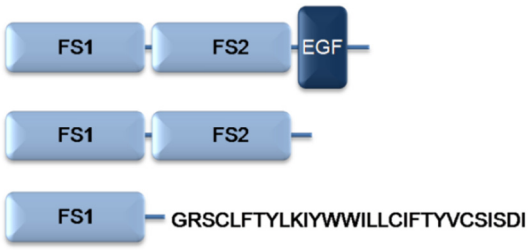

Figure 1.4 Schematic picture of soluble TMEFF2 variants isolated from the conditioned media of stably transected CHO cells and LNCaP cell that endogenously express TMEFF2; FS-follistatin domain, EGF-EGF-like domain (based on Quayle and Sadar 2006; Uchida et al. 1999).

The physiological role of TMEFF2 variants composed of the two FS domains and FS1 domain and a novel amino acid sequence is currently not known. The role of TMEFF2-ECD, which is generated by ADAM10 and ADAM17, remains controversial. Initial findings by Uchida and co-workers indicated that recombinant TMEFF2-ECD weakly induced phosphorylation of epidermal growth factor receptor ErbB-4 in MKN28 gastric cancer cells (Uchida et al. 1999). These data were supported by Ali and Knäuper who showed that TMEFF2-ECD treatment induced phosphorylation of ERK1/2 kinases in HEK293 cells (Ali & Knäuper 2007). However, a recently published analysis of recombinant TMEFF2-ECD binding to different growth factors and receptors did not show any interaction between TMEFF2 and ErbB receptors (Lin et al. 2011). The only known binding partner of TMEFF2-ECD is platelet-derived growth factor isoform AA (PDGF-AA), whereas other PDGF variants (AB, BB, CC and DD) do not interact with TMEFF2-ECD. The interaction between TMEFF2-ECD and PDGF-AA might be of biological significance as the pre-incubation of PDGF-AA with TMEFF2-ECD significantly reduced PDGF-AA-dependent proliferation of NR6 murine fibroblasts*in vitro*. The data indicate that TMEFF2-ECD and PDGR-AA receptor, PDGFRα, compete for PDGF-AA binding, leading to inhibition of cell growth through inactivation of PDGF-AA (Lin et al. 2011). However, several other studies showed that treatment of HEK293 cells with TMEFF2-ECD increased cell growth (Ali & Knäuper 2007; Chen et al. 2011), indicating that the biological activity of TMEFF2-ECD needs to be further investigated in order to explain the role of TMEFF2 and TMEFF2 shedding in the context of prostate cancer.

1.2.8 The role of TMEFF2 cytoplasmic domain

Processing by the γ-secretase complex produces a small C-terminal fragment of TMEFF2 that is released from the cell membrane into the cytoplasm. The biological role of this secondary cleavage as well as the activity of TMEFF2 cytoplasmic domain is very enigmatic. Immunoprecipitation of the TMEFF2 cytoplasmic tail from lysates of stably

transfected HEK293 helped to identify sarcosine dehydrogenase (SARDH) as a TMEFF2 C-terminus interaction partner (Chen et al. 2011). This enzyme is present mostly in mitochondria but also in the cytoplasm and catalyzes the conversion of sarcosine into glycine (Porter et al. 1985). Co-precipitation of TMEFF2 and SARDH was also observed in cell lysates of LNCaP that endogenously express TMEFF2. The biological role of TMEFF2-SARDH interaction is not clear, however it was shown that over-expression of TMEFF2 in HEK293 significantly reduces cytoplasmic sarcosine levels, suggesting that binding to TMEFF2 increased the activity of SARDH (Chen et al. 2011).

1.3 Differential processing of TMEFF2 – possible explanation of TMEFF2 controversial role in prostate cancer

1.3.1 Proteolysis on the cell surface – an important regulatory mechanism of protein function

The biological activity of many cell surface proteins depends on or is regulated by proteolysis. Proteolytic processing is responsible for activation of membrane-anchored protein precursors, removal of regulatory proteins when they are not needed or if they require cellular translocation, for example from the cell membrane to the nucleus. Proteolytic processing is involved in regulation of several signaling pathways, including EGFR and Notch signaling pathways (Blobel 2005; Groot & Vooijs 2012; Weber & Saftig 2012).

In many cases, membrane proteins are proteolytically modified by proteases that are also attached to the cell surface via specific membrane-anchoring domains. These enzymes are ideally positioned to interact with other cell surface molecules as well as soluble proteins, components of extracellular matrix and proteins on adjacent cells. Proteolysis on the cell surface can be mediated by at least three classes of enzymes (Seiki 1999; Edwards et al. 2008; Hooper et al. 2001):

- membrane-type matrix metalloproteinases (MT-MMPs),
- a disintegrin and metalloproteinases (ADAMs)
- membrane-anchored serine proteases.

Members of the membrane-anchored serine proteases can be divided further, depending on their membrane-anchoring unit into three groups (Netzel-Arnett et al. 2003):

- type I transmembrane serine proteases that are anchored in the membrane via their C-terminal transmembrane domain;

- type II transmembrane serine proteases (TTSPs), anchored via the N-terminal domain;
- serine proteases that do not contain a transmembrane domain and are attached to the outer leaflet of the plasma membrane through a glycophosphatidyloinositol (GPI) anchor.

The specificity of the mentioned proteases in identifying and processing their substrates depends on the structural properties of the protease active site, the accessibility of the potential cleavage sites within the substrate as well as localization of enzyme and substrate on the same cell or cellular compartment (Ehrmann & Clausen 2004).

1.3.1.1 Ectodomain shedding

ADAMs, MT-MMPs and membrane-anchored serine proteases are key mediators of the proteolytic process called ectodomain shedding in which the extracellular domain of membrane-anchored protein undergo regulated release from the cell surface. The ectodomain shedding of most of transmembrane proteins is usually low in basal conditions and increases dramatically upon cellular activation. The most common inducers of ectodomain shedding are phorbol esters which activate protein kinase C (PKC) due to their structural similarity to diacylglycerol (DAG), a naturally occurring PKC activator (Brose & Rosenmund 2002). Ectodomain shedding is also increased following treatment with G-protein coupled receptors (GPCRs) agonists, calcium ionophores, and ceramide as well as stress conditions such as UV radiation or hypertonic osmotic pressure. The data from *in vitro* experiments showed that ectodomain shedding decreases in the presence of protein tyrosine kinases (PTKs) and mitogen-activated protein kinases (MAPKs) inhibitors, indicating that this process is regulated by several intracellular signaling pathways. Consistently with this observation, ectodomain shedding is activated also by agonists of these signaling pathways such as cytokines, growth factors and bacterial toxins (Hayashida et al. 2010).

The list of membrane proteins undergoing ectodomain shedding is constantly expanding and includes precursors of tumor necrosis factor α (pro-TNFα) (Black et al. 1997), heparin-binding epidermal growth factor (pro-HB-EGF) (Suzuki 1997), epidermal growth factor (pro-EGF), amphiregulin, betacellulin, epiregulin, neuregulin (Sahin et al. 2004) and many others. The extracellular part of several cell surface receptors is also shed by membrane-bound proteases, reducing the amount of receptor present on the plasma membrane and causing the release of decoy receptors that bind and neutralize specific signaling molecules. Among several receptors undergoing ectodomain shedding are EGF receptors (Lin & Clinton 1991), interleukin-6 receptor (IL-6R) (Croucher et al. 1999), TNF receptors type I and type II (TNFRI, TNFRII) (Porteu & Nathan 1990) and CD23, a low affinity IgE receptor (Letellier et al. 1990). Proteolytic down-regulation of cell

surface proteins is also involved in modification of cellular adhesion properties. Extracellular domains of vascular adhesion molecule-1 (VCAM-1) and intracellular adhesion molecule 1 (ICAM-1) (Singh et al. 2005; Becker et al. 1991) and well as E-, L- and P-selectins (Wyble et al. 1997; Migaki 1995; Semenov et al. 1999) are shed from the cell surface and this process is an important regulatory mechanism for leukocyte homing. Ectodomain shedding of CD44, a receptor for hyaluronic acid that also binds collagens and matrix metalloproteinases affect cell-extracellular matrix interactions (Bazil & Strominger 1994). Finally, for some proteins ectodomain shedding is prerequisite step for further proteolytic processing called regulated intramembrane proteolysis (RIP), leading to the liberation of the cytoplasmic domain that can play several biological functions inside the cell.

1.3.1.2 Regulated intramembrane proteolysis (RIP)

RIP was described for the first time in 2000 by Brown *et al.* as a conserved mechanism observed from bacteria to higher eukaryotes, including humans (Brown et al. 2000) in which a membrane protein is proteolytically processed within the transmembrane domain, in a hydrophobic environment of the lipid bilayer. Proteolysis within the membrane can be catalyzed by four groups of enzymes:

- presenilins (aspartyl proteinases),
- site 2 proteases (S2P) (zinc dependent metalloproteinases),
- rhomboids (serine proteinases)
- Signal-peptide peptidases (SPP) (aspartyl proteinases).

Presenilins and rhomboids are able to proteolytically process only type I transmembrane proteins, containing a carboxy-terminal cytoplasmic domain whereas S2P and SPP cleave type II transmembrane proteins (Urban & Freeman 2002).

Most of the described RIP substrates in mammals are cleaved by presenilins (presenilin 1 and presenilin 2), ~50 kDa multiple membrane-spanning heterodimers, composed of N- and C-terminal fragments resulting from endoproteolytic auto activation (Li et al. 2009). Presenilins are present in the membrane as a part of a large protein complex called the γ-secretase complex, containing also three other essential components: APH-1, PEN2 and nicastrin (Figure 1.5 A) (Wolfe et al. 1999). APH-1 has seven transmembrane domains with a cytosolic carboxyl terminus (Fortna et al. 2004) whereas PEN-2 is a double-transmembrane hairpin-like protein with both ends located extracellularly (Crystal et al. 2003). APH-1 and PEN-2 are thought to play a structural role in assembly and maturation of the γ-secretase complex. Nicastrin is a type I transmembrane glycoprotein with a large extracellular part, that consists of about 45% of the calculated protein molecular mass of the entire γ-secretase complex (Herreman et al. 2003). Nicastrin plays a receptor function for the γ-secretase substrates – its extracellular domain recognizes the new amino-

terminus of type I transmembrane protein generated by ectodomain shedding. The recognized substrate is then recruited to the γ-secretase complex and cleaved by presenilin (Shah et al. 2005) (Figure 1.5 B).

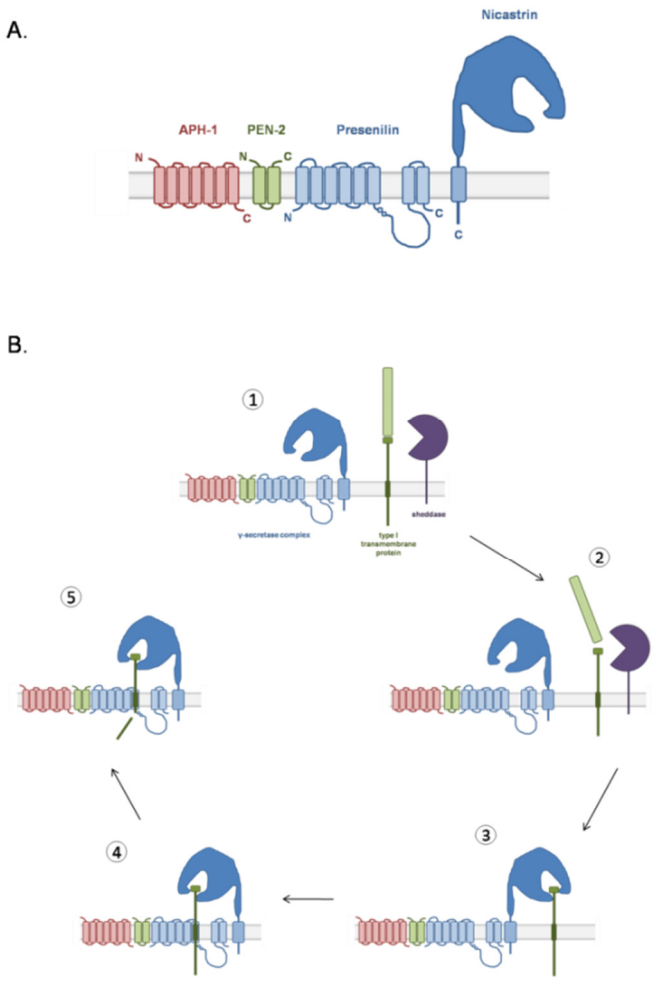

Figure 1.5 Schematic representation of the γ-secretase complex and its role in regulated intramembrane proteolysis (RIP).

(A) The γ-secretase complex consists of four transmembrane proteins: APH-1, PEN-2, presenilin and nicastrin and is involved in regulated intramembrane proteolysis (RIP). (B) In addition to the γ-secretase, RIP requires also a sheddase (1) that cleaves the extracellular part of the type I transmembrane substrate (2). Newly generated N-terminus of the substrate is then recognized by the large receptor ectodomain of nicastrin (3) and the protein is recruited into the γ-secretase complex (4). The intracellular domain of the substrate is then released into the cytoplasm by the catalytic unit of the γ-secretase complex, presenilin (5) (Shah et al. 2005).

The sequential proteolysis of transmembrane proteins (ectodomain shedding followed by RIP) generates two fragments with potentially distinct biological fate and function. The fate of several intracellular RIP products was already identified and includes regulation of gene transcription, induction of apoptosis, regulation of cytoplasmic kinases and proteosomal degradation (Figure 1.6).

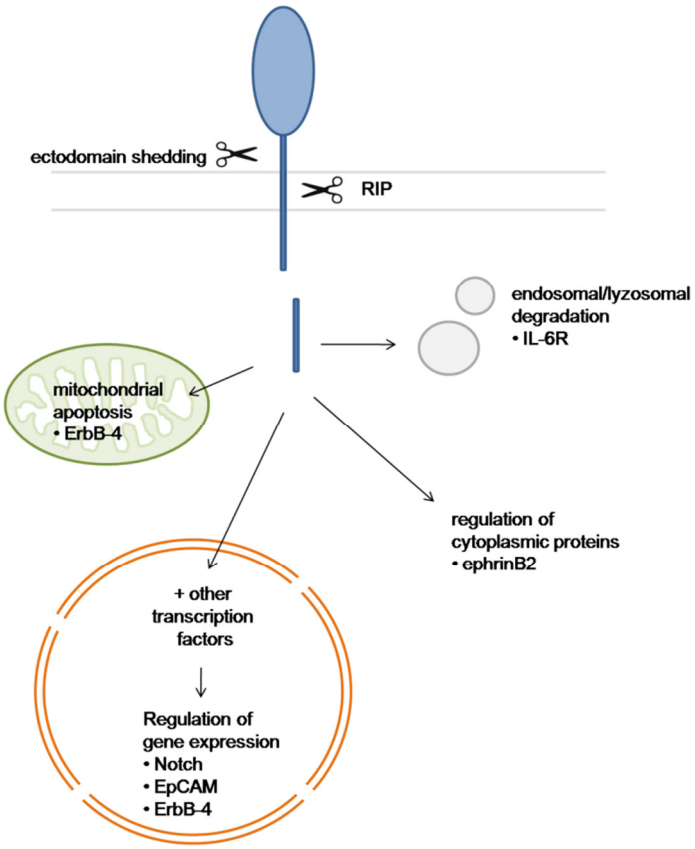

Figure 1.6 The fate of proteins' cytoplasmic domains following RIP.

1.3.1.2.1 RIP-dependent release of transcription factors

The most prominent example of the transmembrane protein that following ectodomain shedding and RIP releases cytoplasmic domain with transcription factor activity is Notch receptor, a type I transmembrane protein controlling development and tissue renewal. Deregulation or loss of the Notch signalling causes a wide range of pathologies, from developmental disorders to adult-onset diseases and cancer. The large extracellular domain of Notch is composed of 29-36 EGF-like repeats which participate in the interaction between Notch and its ligands, followed by unique negative regulatory region (NRR) that plays an important role in preventing receptor activation in the absence of the ligand. Notch ligands are type I transmembrane proteins which can be divided into two subclasses: the Delta and the Serrate/Jagged (Kopan & Ilagan 2009). Ligand binding leads to the cleavage of Notch ectodomain by ADAM10 or 17 at the cleavage site located ~12 amino acids before the transmembrane domain, within the NRR region. The shedding of the Notch ectodomain creates a membrane-tethered fragment called Notch extracellular truncation (NEXT) that is a substrate for the γ-secretase complex. Cleavage by presenilin releases free Notch intracellular domain (NICD) that translocates to the nucleus were it forms a complex the DNA-binding protein CSL (CBF1/RBPjK/Su(H)/Lag-1) and the transcriptional co-activator Mastermind (MAM). This tri-protein complex recruits additional co-activators and activate the transcription of Notch-targeted genes (Fortini & Bilder 2009; Kopan & Ilagan 2009; Wang 2011).

Another example of a transcription factor released by RIP is the cytoplasmic domain of epithelial cell adhesion molecule (EpCAM). EpCAM is a transmembrane glycoprotein frequently over-expressed in human cancers, considered to be a novel marker of cancer initiating cells of the colon, breast, pancreas and prostate carcinomas (Went et al. 2006; Al-Hajj et al. 2003; Ricci-Vitiani et al. 2007; O'Brien et al. 2007). Following ADAM17-mediated ectodomain shedding, EpCAM is further processed by the γ-secretase complex. The released 5 kDa intracellular domain (EpICD) binds to "four and a half LIM domain" protein 2 (FHL2), a nucleocytoplasmic protein that links intracellular EpCAM signaling with the components of the Wnt pathway: β-catenin and Lef-1. The EpICD/FHL2/β-catenin/Lef-1 complex translocates to the nucleus and binds to DNA at Lef-1 consensus sites, inducing transcription of targeted genes (Maetzel et al. 2009). EpICD signaling targets mostly genes regulating the cell cycle, like c-myc and cyclin D1 (Münz et al. 2004; Chaves-Pérez et al. 2012; Maaser & Borlak 2008) but also other genes, for example MMP7 (Denzel et al. 2012). In embryonic stem cells, EpICD is recruited to promoters of genes associated with stem cell features such as c-Myc, Oct-4, Sox2 and Nanog (Lu et al. 2010). Interestingly, the accumulation of EpICD in the cytoplasm and nucleus was associated with the development of human epithelial cancers (Ralhan et al. 2010).

The cytoplasmic domain of an EGF receptor ErbB-4 is also a transcription factor released by RIP. Processing of ErbB-4 by the γ-secretase produces a ~80 kDa cytoplasmic protein that can be found in the nucleus (Rio et al. 2000; Ni et al. 2001; Lee et al. 2002). Recent studies indicate that the intracellular ErbB-4 fragment (ErbB4-ICD) is a chaperone that facilitates the nuclear entry of transcription factor signal transducer and activator of transcription 5A (STAT5A), YES-associated protein 1 (YAP1) and Eto2, a transcriptional co-repressor involved in erythrocyte differentiation (Komuro et al. 2003; Williams et al. 2004; Linggi & Carpenter 2006). The ErbB4-ICD can be detected also in mitochondria where it is believed to induce cell death due to the presence of the BH3 domain within ErbB4-ICD. ErbB4-ICD pro-apoptotic activity is lost upon mutation of this domain. Moreover, the ErbB4-ICD interacts with an anti-apoptotic protein Bcl-2, which when over-expressed abrogates ErbB4-ICD induced cell death (Vidal et al. 2005; Naresh et al. 2006).

1.3.1.2.2 Regulation of cytoplasmic proteins by RIP products

In addition to acting as transcription regulators, liberated cytoplasmic domains generated by RIP can also remain in the cytoplasm. An interesting example is ephrinB2, a ligand for the tyrosine kinase receptor EphB (Tuzi & Gullick 1994). Since ephrins and Eph receptors are both membrane-bound proteins, activation of ephrin/Eph intracellular signalling pathways can only occur via direct cell-cell interaction. The unique property of ephrins is the capacity to generate a 'reverse' signal that is separate and distinct from the intracellular signal activated in Eph receptor-expressing cells. An early event that follows EphB-ephrin binding is phosphorylation of Src kinase (Boyd & Lackmann 2001). Binding of ephrinB2 by EphB receptor induces ectodomain shedding and RIP of ephrinB2, resulting in the release of ephrinB2 intracellular domain (ephrinB2-ICD). EphrinB2-ICD remains in the cytoplasm where it binds to Src kinase and prevents its association with the inhibitory kinase Csk, allowing auto phosphorylation of Src. Moreover, ephrinB2-ICD-activated Src phosphorylates ephrinB2 and inhibits its processing by γ-secretase, providing a mechanism controlling the level of phosphorylated Src and regulating sprouting of endothelial cells (Georgakopoulos et al. 2006).

1.3.1.2.3 Degradation of RIP products

The biological function of some transmembrane proteins depends entirely on their extracellular part and following ectodomain shedding the membrane-stub is no longer needed. An example of the involvement of RIP in the degradation process is removal of the interleukin-6 receptor (IL-6R) membrane stub. IL-6, a critical regulator of the immune system, signals through a complex of IL-6R and membrane protein gp130. Membrane-anchored IL-6R undergoes induced and constitutive shedding mediated by ADAM17 and 10 (Matthews et al. 2003). Unlike most of the soluble receptors, soluble IL-6R (sIL6R)

does not act as decoy receptor but as an agonist of IL-6 signaling. The sIL6-R/IL-6 complexes stimulate cells that express only gp130 on their surface and normally do not respond to IL-6 treatment (Rose-John & Heinrich 1994). Due to the involvement of IL-6 signaling in chronic inflammation (Rose-John et al. 2006), the fate of IL-6R membrane stub generated by ADAMs was also investigated. The work published by Chalaris and co-workers showed that the transmembrane fragment of IL-6R was processed by the γ-secretase but did not translocate to the nucleus. Labeling of cells expressing GFP-tagged IL-6R with antibody detecting the lysosomal marker LAMP1 showed co-localization of these two proteins, indicating that the cytoplasmic domain of IL-6R is rapidly degraded upon ectodomain shedding (Chalaris et al. 2010).

1.3.2 Biological consequences of dysregulated cell surface proteolysis

Deregulated proteolysis of cell surface proteins may result in severe pathological conditions, of which the most prominent example is Alzheimer's disease. For many years the progressive accumulation of amyloid plaques containing peptide derivate of amyloid precursor protein (APP) was recognized as a key feature of this incurable neurodegenerative disease. APP is a type I transmembrane protein composed of 770 amino acids with a large ectodomain, a transmembrane domain and short, 47 amino acids cytoplasmic domain. The extracellular domain of APP is released from the cell surface either by α-secretases such as ADAM9, ADAM10 and ADAM17 or β-secretases BACE1 and BACE2. In both α and β pathway the membrane-retained fragment is further processed by the γ-secretase complex. In the α pathway γ-secretase cleavage produces a small peptide p3, whereas in the β pathway this processing generates Aβ peptide that accumulates as plaques in brains of the Alzheimer's disease patients (Figure 1.7). Cleavage position heterogeneity for the γ-secretase complex produce Aβ peptides composed of 40 or 42 amino acids and called Aβ40 and Aβ42, respectively (Fortini 2002). Generation of the Aβ peptides is a physiological event (Pearson & Peers 2006), however their overproduction as well as high ratio of Aβ42 to Aβ40 peptide is responsible for development of Alzheimer's disease (Glenner & Wong 1984). Aβ peptides reduce the level of the neurotransmitter acetylcholine, disrupts ion channels essential for nerve excitation leading to progressive loss of signal transduction and severe impairment of neurological functions (Lichtenthaler 2006). Aβ42 shows greater neurotoxicity that Aβ40. The direct mechanism responsible for the imbalance of α and β secretase APP processing as well as accelerated production of more toxic Aβ42 are not known, however genetic studies of families suffering from early-onset Alzheimer's disease established that mutations of APP and presenilin genes are linked to early neurodegenerative disease progression. (Bertram et al. 2010).

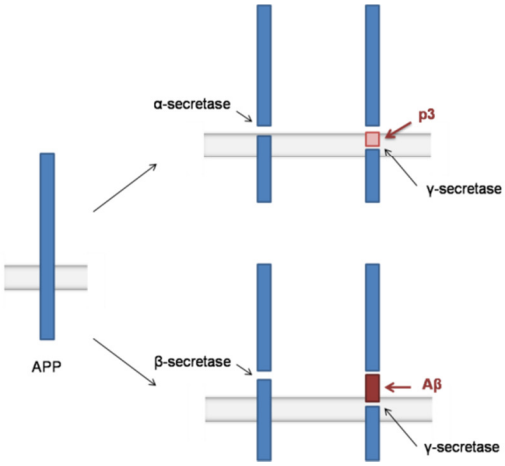

Figure 1.7 Processing of amyloid precursor protein (APP) by α, β and γ secretases.
APP is a type I transmembrane protein undergoing ectodomain shedding and RIP. The extracellular part of APP can be cleaved by α secretases ADAM9, 10 and 17 (upper panel) or β secretases BACE1 and BACE2 (bottom panel), releasing soluble ectodomain. In both the α and β pathways the membrane-remained fragment is further cleaved by the γ-secretase complex, resulting in generation of a small p3 peptide (α pathway) or larger Aβ peptide (β pathway). Accelerated production of the Aβ peptide leads to amyloid plaques formation and development of Alzheimer's disease.

1.3.3 The role of proteolysis in modulating TMEFF2 function

As a transmembrane protein TMEFF2 is exposed for proteolytic processing by membrane-anchored proteases, as showed already for ADAM10 and ADAM17 (Ali & Knäuper 2007). Examples of several other membrane-anchored proteins described in previous paragraphs indicate that proteolysis may significantly modulate protein function through the generation of several biologically active protein fragments from one transmembrane molecule. Based on this fact it was hypothesized that the controversial data about the role of TMEFF2 in prostate cancer result from proteolytic processing of TMEFF2 by different membrane-anchored proteases which are co-expressed with TMEFF2 in prostate cancer cells. Due to the failure of targeting MMPs in anti-cancer therapies in recent years more attention was paid to characterize the role of other proteases present in tumor cells, such as ADAMs and membrane-anchored serine proteases. Several members of these two families were found to be expressed in prostate cancer and their expression was shown to influence cancer cell behavior (Mochizuki & Okada 2007; Netzel-Arnett et al. 2003). For these reasons ADAMs and membrane-anchored serine proteases are proposed to be responsible for the regulation of TMEFF2 biological activity in prostate cancer.

1.4 Membrane-anchored proteases implicated in prostate cancer

1.4.1 ADAMs

The ADAMs (a disintegrin and metalloproteinases) are a family of membrane-associated proteins with functions in cell adhesion and proteolytic processing of several cell surface receptors and signaling molecules. There are 40 members of the ADAM family identified to date in the mammalian genome, of which 37 were found in mice and 22 are thought to be expressed in humans. The first ADAMs to be described, ADAM1 and ADAM2 are the two subunits of the sperm protein fertilin, known also as fertilin-α and fertilin-β, respectively (Wolfsberg et al. 1993; Wolfsberg et al. 1995).

1.4.1.1 Expression of ADAMs

Expression pattern of ADAMs vary considerably. Some ADAMs, including ADAM2, 7, 18, 20, 21, 29 and 30 are expressed predominantly in the testis as their main biological roles are regulation of spermatogenesis and sperm function. The expression of ADAM8 was found primarily in hematopoietic cell types, whereas other ADAMs show rather broad somatic tissues distribution (Seals & Courtneidge 2003; Edwards et al. 2008). Additionally, many ADAM genes undergo alternative splicing, giving rise to several protein variants. For example, there are two known variants of ADAM12 (Wewer et al. 2006), ADAM9 (Mazzocca et al. 2005) and ADAM28 (Fourie et al. 2003), whereas ADAM15 has about 13 splice variants identified to date (Kleino et al. 2007).

1.4.1.2 ADAM domain structure

A common characteristic of all ADAM family members is a complex multi-domain structure, usually containing a prodomain, a metalloproteinase domain, a disintegrin domain, a cysteine-rich domain, an EGF-like unit, a transmembrane domain and a cytoplasmic tail. The modular structure of a typical ADAM is schematically presented in Figure 1.8.

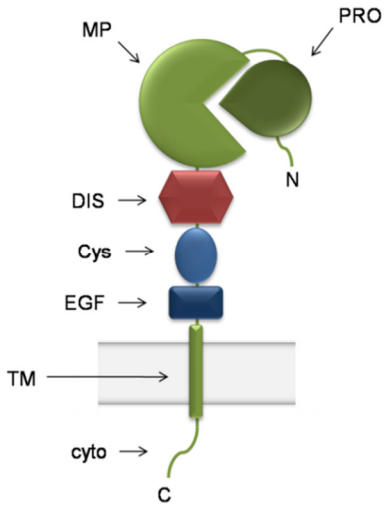

Figure 1.8 Schematic structure of a disintegrin and metalloproteinase (ADAM).
A typical ADAM molecule is composed of N-terminal signal sequence, prodomain (PRO), metalloproteinase domain (MP), disintegrin domain (DIS), cysteine-rich motif (Cys), EGF-like unit (EGF), transmembrane domain (TM) and C-terminal cytoplasmic domain (cyto).

The N-terminus of all ADAMs contains a signal sequence that directs them to the secretory pathway as a type I transmembrane protein. The signal sequence is followed by a prodomain that is responsible for keeping the catalytic domain of ADAMs in an inactive state. A conserved cysteine residue within the prodomain coordinates the zinc atom present in the metalloproteinase domain's active site, sequestering the catalytic domain in an inactive conformation. The prodomain is usually removed during transport through the Golgi system by the pro-protein convertases which cleave the consensus RX(R/K)K motif and release the prodomain from the enzyme (Edwards et al. 2008, Seals and Courtneidge 2003). In some cases ADAMs may undergo autocatalytic activation, as shown for ADAM8 and ADAM28 (Howard et al. 2000; Schlomann et al. 2002). Interestingly, the isolated prodomain of some ADAMs can act as potent, selective inhibitors of the mature forms of these enzymes as demonstrated for ADAM10, ADAM17 (Gonzales et al. 2004; Moss et al. 2007) and ADAM9 (Moss et al. 2011). The other function of the prodomain is to chaperone proper folding of ADAMs, particularly the metalloproteinase domain. It was demonstrated experimentally by several groups that the deletion of the prodomain from ADAMs expression constructs resulted in the synthesis of inactive, improperly folded proteins (Seals & Courtneidge 2003; Edwards et al. 2008).

The metalloproteinase domain of ADAMs has a globular structure divided into two subdomains with the active site cleft running between them which are characteristic for the metzincin family. The catalytic zinc atom is located at the bottom of the groove between the subdomains and is coordinated by three conserved histidine residues and a downstream methionine. The methionine lies in a Met turn motif that loops around and

faces the consensus HEXXHXXGXXH site, present within the metalloproteinase domain of catalytically active ADAMs: ADAM8, 9, 10, 12, 15, 17, 19, 20, 21, 28, 30 and 33. In contrast, ADAM2, 7, 11, 18, 22, 23, 29 and 32 lack one or more critical features within the Zn-binding active site and are thought to play non-proteolytic functions in the cell (Seals & Courtneidge 2003; Edwards et al. 2008; Weber & Saftig 2012).

The disintegrin domain is about 90 amino acids long and is named after its homology to the small proteins found in hemorrhagic snake venoms, SVMPs (snake venom metalloproteinases). SVMPs competitively inhibit integrin-mediated adhesion of platelets to RGD sequences in fibrinogen at the wound site through RGD or related sequences present at the end of an extended loop, known as a disintegrin loop. The disintegrin domains of the majority of ADAMs do not contain the RGD sequence, with an exception of human ADAM15. However, there is now considerable evidence that the disintegrin domains of many ADAMs are able to interact with integrins and modify cell adhesion and cell-cell interactions through the consensus CRXXXXXCDXXEXC motif within their disintegrin loops (Seals & Courtneidge 2003).

The disintegrin domain is followed by the cysteine-rich domain that seems to be involved in determining substrate specificity and/or regulation of catalytic activity (Weber & Saftig 2012). The cysteine-rich domain of ADAM12 mediates its interactions with syndecans, leading to engagement of integrins (Iba et al. 2000) whereas this domain in ADAM17 is required for shedding of IL-1 receptor-II (Reddy et al. 2000). Determination of the crystal structure of a conserved snake venom homolog of ADAMs, a vascular apoptosis-inducing factor-1 (VAP1) indicated that the metalloproteinase/disintegrin/cyteine-rich part of extracellular domain forms a C-shape, with part of the cysteine-rich domain being in close contact with the catalytic site of the metalloproteinase domain (Takeda et al. 2006).

Most of the ADAMs, with exception of ADAM10 and 17, contain an EGF-like unit between the cysteine-rich domain and the transmembrane region (Janes et al. 2005). The EGF-like domain is thought to participate in the substrate binding and in the interactions with cell surface proteoglycans (Weber & Saftig 2012). The corresponding membrane-proximal domain present in ADAM17 was found to be involved in protease multimerization and ligand recognition (Lorenzen et al. 2011; Lorenzen et al. 2012).

The hydrophobic membrane-spanning region of ADAMs is followed by a cytoplasmic domain that is considered to be the most variable domain of ADAMs. It varies extensively in length and sequence, ranging from 11 amino acids in ADAM11 to 231 residues in ADAM19. The cytoplasmic domain contains several specialized motifs that are involved in the inside-out regulation of ADAM activity, the outside-in regulation of cell signaling and the control of maturation and subcellular localization of ADAMs. The most

common motifs within the cytoplasmic domain are proline-rich sequences (PXXP) that act as docking sites for proteins containing Src-homology region 3 (SH3) domains. The cytoplasmic domains of several ADAMs contain potential phosphorylation sites for serine-threonine or tyrosine kinases. The phosphorylation of the cytoplasmic domain may directly regulate ADAM activity as well as serve as binding sites for proteins containing Src-homology 2 (SH2) domains (Seals & Courtneidge 2003; Edwards et al. 2008).

1.4.1.3 ADAMs proteolytic activity

As mentioned previously, twelve of known human ADAMs contain a consensus catalytic sequence HEXGHXXGXXHD within their metalloproteinase domain and are active metalloproteinases, classified to the adamalysin subfamily of metzincins (Edwards et al. 2008; Weber & Saftig 2012).The adamalysin subfamily includes also snake venom metalloproteinases and ADAM-TS (a disintegrin and metalloproteinase with thrombospondin motif) (Seals & Courtneidge 2003). The main function of proteolytically active ADAMs is shedding of various membrane-anchored proteins, including growth factor precursors, cytokines and their receptors as well as components of the extracellular matrix. ADAM-mediated shedding can occur constitutively or is induced by different stimuli such as ligands for G-protein coupled receptors (GPCRs), activators of protein kinase C (PKC) and calcium ionophores, as described in more details in the introduction to Chapter 4. The activity of ADAMs is naturally regulated by tissue inhibitors of metalloproteinases (TIMPs) which inhibit also MMPs. There are four TIMPs identified in mammals, named TIMP-1-4. Human TIMPs comprise of two domains - N-terminal inhibitory domain and C-terminal domain without inhibitory function, providing an additional site for protease-inhibitor interactions. TIMPs inhibit ADAMs and MMPs by forming tight complexes with a 1:1 molar ratio (Brew & Nagase 2010; Murphy 2011). In general, TIMPs display much greater selectivity towards ADAMs than MMPs. For example, several ADAMs are exclusively inhibited by TIMP-3 (Baker et al. 2002), whereas ADAM8, 9 and 19 are insensitive for TIMPs inhibition (Amour et al. 2002; Chesneau et al. 2003).

Due to the involvement of ADAMs in the regulation of various physiological processes aberrant expression or deregulated activity of ADAMs are implicated in many pathologies, including Alzheimer's disease, multiple sclerosis, rheumatoid arthritis, asthma and several types of cancers (Seals & Courtneidge 2003; Edwards et al. 2008). In the area of prostate cancer research increased attention was paid recently to three ADAM family members: ADAM9, ADAM12 and ADAM15 which are described below.

1.4.1.4 ADAM9

1.4.1.4.1 Expression of ADAM9

ADAM9, also known as meltrin-γ or MDC9 was originally cloned as a 84 kDa protein, widely expressed in mouse and human tissues (Weskamp et al. 1996). Alternative splicing of ADAM9 gene results in two variants of this metalloproteinase – a full length, transmembrane ADAM9-L and secreted ADAM9-S, that lacks transmembrane and cytoplasmic domains (Hotoda et al. 2002). Similarly to the full length ADAM9-L, ADAM9-S is catalytically active and is expressed in a wide range of human tissues, including brain, liver, lung, heart, kidney and trachea (Hotoda et al. 2002; Mazzocca et al. 2005).

1.4.1.4.2 ADAM9 substrates

The first described substrate processed by ADAM9 is the precursor of heparin-binding epidermal growth factor (pro-HB-EGF). ADAM9-mediated shedding of pro-HB-EGF is induced by TPA, a protein kinase C (PKC) activator and involves direct interaction between PKC and ADAM9 cytoplasmic domain (Izumi et al. 1998). The list of ADAM9 substrates includes amyloid precursor protein (APP) (Hotoda et al. 2002), insulin-like growth factor binding protein-5 (IGFBP-5) (Mohan et al. 2002), ADAM10 (Cissé et al. 2005), collagen XVII (Franzke et al. 2004), laminin (Mazzocca et al. 2005), precursor of epidermal growth factor (pro-EGF) and fibroblast growth factor receptor iiib (FGFRiiib) (Peduto et al. 2005). ADAM9 was also implicated in the processing of angiotensin-I converting enzyme (ACE), a zinc-dependent metallopeptidase regulating vasoactive peptide metabolism that is activated by shedding from the cell surface (Coates 2003). ADAM9-mediated shedding of ACE is induced by bacterial lipopolysaccharide (LPS) but not by TPA and does require membrane anchorage of ADAM9 (English et al. 2012). In contrast with most of the membrane-associated metalloproteinases, ADAM9 is insensitive to inhibition by TIMPs (Amour et al. 2002).

1.4.1.4.3 ADAM9 as an adhesion molecule

In addition to shedding of several membrane-anchored proteins, ADAM9 plays also an important role in the regulation of cell adhesion. The ADAM9 disintegrin domain is a ligand for specific integrin heterodimers, including multiple β_1 (Mahimkar et al. 2005; Zigrino et al. 2007), $\alpha_6\beta_4$ (Mazzocca et al. 2005), $\alpha_v\beta_5$ (Karadag et al. 2006) and $\alpha_V\beta_3$ (Cominetti et al. 2009). The biological significance of some of these ADAM9-integrins interactions in the context of cancer progression is described in paragraph 1.4.1.4.6

1.4.1.4.4. Cytoplasmic domain of ADAM9

The cytoplasmic domain of ADAM9 contains proline-rich motifs that are known to interact with proteins containing SH3-domain. Yeast two-hybrid screen and

immunoprecipitation from mammalian cells experiments identified two SH3 domain-containing binding partners of ADAM9 intracellular domain: endophilin I and SH3PX1. As these molecues binds preferentially with ADAM9 precursor but not with the mature, processed form it is hypothesized that they are involved in regulation of intracellular processing, transport and subcellular localization of ADAM9 (Howard et al. 1999).

1.4.1.4.5 ADAM9 null mice

Despite the ubiquitous expression pattern as well as high levels in some tissues, ADAM9-deficient mice are viable, fertile and do not display any obvious pathologies. Analysis of the constitutive and induced pro-HB-EGF shedding from embryonic fibroblasts isolated from ADAM9-deficient mice did not shown any reduction in HB-EGF release when compared with pro-HB-EGF shedding from wild type fibroblasts. Furthermore, there were no differences in the production of the APP α- and γ- secretase cleavage product (p3) and of β- and γ-secretase cleavage product (Aβ) in cultured hippocampal neurons from wild-type and ADAM9-deficient mice (Weskamp et al. 2002). The normal levels of HB-EGF and APP shedding in ADAM9-deficient animals may be explained by the compensation of ADAM9-mediated shedding by other members of the ADAM family. Interestingly, in 2009 Parry and co-workers identified that the mutation of ADAM9 gene is responsible for the development of a cone-rod dystrophy (CRD), an inherited progressive retinal dystrophy affecting the function of cone and rod photoreceptors. Studies on aged ADAM9-deficient mice confirmed that the lack of ADAM9 causes retinal degeneration. Here, retinal dysfunction in ADAM9-deficient mice and CRD patients results from impaired remodelling of the extracellular matrix (ECM) between the retinal pigment epithelium and photoreceptor outer segments or decreased shedding of factors essential for the maintenance of ECM (Parry et al. 2009)..

1.4.1.4.6 ADAM9 in cancer

ADAM9 is one of the ADAM family members that are intensively studied in the context of cancer development and progression as its expression is significantly elevated in various types of cancers, including renal (Fritzsche, Wassermann, et al. 2008), pancreatic (Grützmann et al. 2004), gastric (Carl-McGrath et al. 2005), breast (O'Shea et al. 2003) and prostate cancer (Sung et al. 2006). High levels of ADAM9 in these cancers correlate with tumor progression. ADAM9 is also present in non-small cell lung carcinoma where it was demonstrated to enhance cell adhesion and invasion via modulation of $\alpha_3\beta_1$ integrin and sensitivity to growth factors, and thus promote brain metastasis (Shintani et al. 2004).

In breast cancer ADAM9 over-expression was found in cell lines and clinical samples, with significantly higher expression in breast cancers with lymph node metastases (O'Shea et al. 2003; Lendeckel et al. 2005). Analysis of ADAM9 expression

using splice variant specific antibodies demonstrated that breast cancer cells express both forms of ADAM9 – transmembrane ADAM9-L and secreted ADAM9-S. Interestingly, these splice variants seem to have opposing effect on the breast cancer progression. ADAM9-S promotes migration of cancer cells that requires metalloproteinase activity, whereas ADAM9-L suppresses cell migration independently of its catalytic functions. Suppression of migration by ADAM9-L depends on disintegrin domain and involves integrin binding. Therefore, the relative levels of ADAM9-L and S may determine the aggressive migratory phenotype associated with breast cancer progression (Fry & Toker 2010). Human colon and breast cancer cell lines grown in the presence of ADAM9-S-containing medium were more invasive when tested in a Matrigel invasion assay. The induction of the invasive phenotype by ADAM9-S required its catalytic activity as well as the ability of the disintegrin domain to directly bind to $\alpha_6\beta_4$ and $\alpha_2\beta_1$ integrins on the surface of carcinoma cells. The same group investigated ADAM9 expression in sections from human liver metastases by immunohistochemistry. This analysis showed that ADAM9 is expressed by stromal liver myofibroblasts in close proximity of the invasive front of the tumour. These results emphasize the importance of tumour-stromal interactions in cancer invasion and metastasis and suggest that ADAM9-S can be an important determinant in the ability of cancer cells to invade and colonize the liver (Mazzocca et al. 2005).

ADAM9 over-expression is also associated with prostate cancer with higher ADAM9 levels found in malignant than in benign prostate tissue (Sung et al. 2006). Moreover, ADAM9 expression correlates with PSA relapse following prostatectomy and was proposed to be a novel prognostic marker for prostate cancer patients (Fritzsche, Jung, et al. 2008). *In vitro* studies showed that ADAM9 increases the therapeutic resistance of prostate cancer cells to radiation and chemotherapy, as the down-regulation of ADAM9 expression in C4-2 prostate cancer cell line significantly increases apoptosis following radiation and sensitizes them to treatment with chemotherapeutic agents. Moreover, knock-down of ADAM9 induces E-cadherin and integrin expression in C4-2 prostate cancer cell line and drives C4-2 cell transition to an epithelial phenotype, decreasing their invasive potential (Josson et al. 2011). Microarray analysis revealed that ADAM9 is one of the most up-regulated genes during the transition of LNCaP prostate cancer cells from an androgen-dependent to an androgen-independent and metastatic state. ADAM9 mRNA and protein levels in prostate cancer cells increase also on exposure to stress conditions such as cell crowding, hypoxia, and hydrogen peroxide (Sung et al. 2006).

The role of ADAM9 expression in the development of prostate cancer *in vivo* was investigated using W^{10} mouse model of prostate cancer, in which the SV40 large T antigen is expressed in prostate epithelium under control of the probasin promoter, a prostate-specific gene (Shaffer et al. 2005). In the absence of ADAM9 expression most

tumours in a W^{10} mouse were well differentiated, whereas the ADAM9-positive tumours were poorly differentiated and significantly larger. Moreover, ADAM9-positive tumours showed significant abnormalities, including intraepithelial hyperplasia and prostate intraepithelial neoplasia (PIN), a putative precursor lesion of prostate cancer. The tumour-promoting activity of ADAM9 can be explained by the ability of this metalloproteinase to shed two proteins with a pivotal function in the pathogenesis of prostate cancer – fibroblast growth factor receptor iiib (FGFRiiib) and epidermal growth factor (EGF) (Peduto et al. 2005). FGFR signalling was previously shown to regulate the pathogenesis of prostate cancer and the phenotype of the mice expressing a dominant-negative FGFRiiib resembles that seen in animals over-expressing ADAM9 (Jin et al. 2003). Another ADAM9 substrate, EGF, is known to be over-expressed in benign prostatic hyperplasia as well as in tumours (De Miguel et al. 1999) and was implicated in promoting tumour progression for example by increasing proliferation of epithelial and stromal prostate cells (Schuurmans et al. 1988), enhancing growth of androgen-independent prostate cancer by trans-activation of the androgen receptor (Culig et al. 1994; Gregory et al. 2004).

1.4.1.5 ADAM12

1.4.1.5.1 Expression of ADAM12

ADAM12, initially known as meltrin-α, was identified in 1995 as a transmembrane protein expressed by myoblasts and involved in muscle cell fusion (Yagami-Hiromasa et al. 1995). but was found also in other mesenchymal cell types, such as osteoblasts, chondroblasts, adipocytes, hepatic stellate cells and oligodendrocytes (Kveiborg et al. 2008). Alternative splicing of the ADAM12 gene results in the expression of two ADAM12 variants – a transmembrane, full length ADAM12-L and secreted ADAM12-S, in which the transmembrane and cytoplasmic domains are replaced by unique 33 amino acids sequence (Gilpin et al. 1998).The mechanisms regulating ADAM12 expression, in particular those that might be responsible for altered expression of this metalloproteinase in pathological conditions are poorly understood. The expression of ADAM12 is induced by TGF-β (Le Pabic et al. 2003), a multifunctional growth factor that acts through type I and type II receptors with serine/threonine activity and Smad proteins (Heldin & Moustakas 2012). The expression of ADAM12 decreases following stimulation with SnoN (Solomon et al. 2010), a negative regulator of TGF-β signaling, preventing transcription (Deheuninck & Luo 2009). Interestingly, the disintegrin and cysteine-rich domains of ADAM12 interacts with TGF-β receptor type II (TGFβRII), enhancing TGF-β-dependent activation of transcription (Atfi et al. 2007).

1.4.1.5.2 ADAM12 synthesis and activation

ADAM12 is synthesized in the rough ER and matures in the Golgi compartment. Activation of ADAM12 zymogen occurs during transit in the trans-Golgi network and

requires removal of the prodomain by furin-like pro-protein convertases (Loechel et al. 1999). Interestingly, following activation the prodomain remains non-covalently attached to the mature ADAM12 molecule, forming the shape of a four-leafed clover (Wewer et al. 2006). The biological function of the attached ADAM12 prodomain is not clear, there is however some evidence suggesting its involvement in regulation of ADAM12 proteolytic activity (Sørensen et al. 2008). Mature, catalytically active ADAM12 is stored intracellular and translocates to the cell surface in response to external cell stimulation by phorbol esters or integrin engagement (Hougaard et al. 2000). Transport of the ADAM12-containing vesicles to the plasma membrane is a dynamic process that involves activation of PKC (Sundberg et al. 2004), recruitment of receptor for activated PKC 1 (RACK1) to the ADAM12 cytoplasmic domain (Bourd-Boittin et al. 2008) and transient interaction with c-Src kinase (Stautz et al. 2010).

1.4.1.5.3 ADAM12 substrates

As an active metalloproteinase (Loechel et al. 1998), ADAM12 is involved in the processing of various substrates, including ligands for EGF receptors: HB-EGF, EGF and betacellulin (Asakura et al. 2002; Kurisaki et al. 2003; Horiuchi et al. 2007), a ligand for Notch receptor, Delta-like-1 (Dyczynska et al. 2007) and placental leucine aminopeptidase (Ito et al. 2004). Initial studies implicated ADAM12 in the proteolytic modification of the extracellular matrix components such as gelatin, type IV collagen and fibronectin (Roy et al. 2004), which were not confirmed later on, questioning the involvement of ADAM12 in matrix remodelling (Jacobsen et al. 2008). The secreted ADAM12-S variant is also catalytically active and cleaves insulin-like growth factor binding protein-3 (IGFBP-3) and IGFBP-5 (Loechel et al. 2000). Interestingly, ADAM12-S does not shed Delta-like 1 (Dyczynska et al. 2007), suggesting that the transmembrane and cytoplasmic domains of ADAM12 have an important influence on substrate specificity. The activity of ADAM12 variants is regulated by TIMPs. The most potent physiological inhibitors of ADAM12 are TIMP-3 (Loechel et al. 2000) and TIMP-2. TIMP-1 is also able to inhibit ADAM12 but with much lower affinity (Jacobsen et al. 2008).

1.4.1.5.4 The role of ADAM12 in cell adhesion

In addition to the proteolytic activity ADAM12 also modulates cell adhesive functions. The disintegrin and cysteine-rich domains of ADAM12 interact with $\alpha_9\beta_1$, $\alpha_7\beta_1$ and $\alpha_4\beta_1$ integrins (Eto et al. 2000; Zhao et al. 2004; Huang et al. 2005). The cysteine-rich domain binds cell surface proteoglycans, such as syndecans. The interaction of syndecan-4 with ADAM12 cysteine-rich domain promotes β_1 integrin-dependent cell spreading, stress fiber assembly and focal adhesion formation via signaling pathway involving protein kinase C (PKC) and RhoA protein (Thodeti et al. 2003).

1.4.1.5.5 Cytoplasmic domain of ADAM12

In addition to the extracellular domain, the cytoplasmic tail of ADAM12L splice variant is implicated in several signaling pathways. The cytoplasmic domain of ADAM12-L is relatively long and contains several motifs potentially involved in protein-protein interactions. The proline-rich regions of ADAM12-L bind SH3 domains of c-Src and Yes non-receptor tyrosine kinases, as well as Src-substrate and adaptor protein Grb2 (Kang et al. 2000). Other SH3 domain-containing proteins associating with the ADAM12-L cytoplasmic tail are Eve-1, a protein abundantly expressed in skeletal muscle, heart and several cancer cell lines and PACSIN3, a cytoplasmic molecule involved in endocytosis. The biological significance of these interactions is unclear; it is however hypothesized that they are required for ADAM12-mediated ectodomain shedding (Mori et al. 2003; Tanaka et al. 2004). The cytoplasmic domain of ADAM12-L binds the adaptor protein Tks5/FISH which is implicated in podosome formation and subsequent matrix degradation in human breast cancer cells (Abram et al. 2003; Seals et al. 2005).

1.4.1.5.6 ADAM12 deficiency in mice

Generation of transgenic mice lacking ADAM12 expression showed that these animals do not display any major histological abnormalities in muscles and bones. They are also fertile and the pups are born in a normal Mendelian ratio, however about 30% of new born ADAM12-deficient mice die in the first week after birth. Detailed characterization of the ADAM12-deficient mice revealed impaired formation of the neck and interscapular muscles and reduction of the interscapular brown adipose tissue (Kurisaki et al. 2003).

Characterization of the ADAM12-deficient mice as well as ADAM12 expression pattern suggests that this metalloproteinase regulates development and functions of muscles and adipose tissue. Endogenous ADAM12 expression in muscle tissue is up-regulated during regeneration (Borneman et al. 2000; Galliano et al. 2000) and increased expression of ADAM12 in mouse skeletal muscles improves muscle regeneration following mild freeze injury. Moreover, transgenic expression of ADAM12 alleviates the pathology of young dystrophin-deficient *mdx* mice, a model for Duchenne muscular dystrophy (Kronqvist et al. 2002), a severe musculoskeletal disease characterized by degradation and gradual replacement of the skeletal muscles by connective tissue and adipocytes (Emery 2002). ADAM12 is hypothesized to compensate for the lack of dystrophin through increasing the expression of dystrophin homologue utrophin, as well as α_7 integrin and dystroglycans (Moghadaszadeh et al. 2003). Interestingly, long-term effect of ADAM12 over-expression in *mdx* mice caused decreased skeletal muscles mass with accelerated fibrosis and adipogenesis, indicating that the ADAM12-mediated therapeutic effect is not sufficient to provide protection during prolonged disease (Jørgensen et al. 2007).

1.4.1.5.7 ADAM12 in cancer

As previously mentioned, ADAM12 is implicated in the development and progression of various carcinomas, with high expression in breast, prostate, liver, stomach, colon, bladder and brain cancers. In contrast, its expression is almost undetectable in normal breast, prostate, colon and liver epithelium (Kveiborg et al. 2005; Peduto et al. 2006; Le Pabic et al. 2003; Carl-McGrath et al. 2005; Fröhlich et al. 2006). Most of the reports describing elevated levels of ADAM12 in cancer samples do not distinguish between ADAM12-L and ADAM12-S variants. However, the soluble ADAM12-S variant was found in the urine of patients suffering from bladder or breast cancers and high levels of ADAM12-S correlates with the advanced stage of disease (Roy et al. 2004; Fröhlich et al. 2006). The levels of ADAM12-S in the urine of bladder cancer patients decrease following surgical removal of the tumor and increase upon recurrence of the disease (Fröhlich et al. 2006), indicating that ADAM12-S is a potential biomarker for bladder and breast cancer diagnosis.

The data obtained from mouse models of prostate and breast cancers indicate that ADAM12 has cancer promoting activity. As described previously, ADAM12 has proteolytic activity as well as the ability to module cellular adhesion and probably both of these functions are involved in cancer progression. Elevated ADAM12 levels correlate with increased proliferation of human glioblastoma cells, as well as the amount of shed HB-EGF, suggesting that the increased proliferation is mediated through HB-EGF signalling (Kodama et al. 2004). This finding is in agreement with *in vitro* results, showing decreased proliferation of various cancer cell lines following treatment with anti-ADAM12 antibodies (Carl-McGrath et al. 2005; Lendeckel et al. 2005).

The most extensive data explaining the role of ADAM12 in cancer progression derive from studies on PyMT mice model of breast carcinoma. PyMT animals develop breast tumour due to the expression of the polyoma virus middle T oncogene under the control of mouse mammary tumour virus. Over-expression of ADAM12 in mammary gland of PyMT mice increase cancer aggressiveness, tumour grade and metastasis to the lungs (Kveiborg et al. 2005). On the other hand, ADAM12 deficiency reduces tumour progression in PyMT mouse breast cancer model. Interestingly, endogenous expression of ADAM12 by the tumour-associated stroma in the PyMT model does not influence tumour progression and the presence of ADAM12 in tumour cells is necessary for cancer development in these mice.

In human breast carcinoma ADAM12 localizes almost exclusively in tumour cells and is only rarely detected in the tumour-associated stroma (Fröhlich et al. 2011). The stromal cells are known to release TGF-β (Massagué 2008) that up-regulates ADAM12 expression. It could be hypothesized that tumour stroma is responsible for increased

ADAM12 levels in breast tumour cells (Ray et al. 2010; Fröhlich et al. 2011). Whereas both ADAM12 variants are over-expressed in breast cancer tissue, recently published data indicate that only the secreted ADAM12-S variant has cancer-promoting activity. Increased expression of ADAM12-S in breast cancer cells enhances migration and invasion *in vitro* and promotes development of distant metastases *in vivo* (Roy et al. 2011).

ADAM12 was also implicated in the progression of triple-negative breast cancer, an aggressive form of this disease, with poor prognosis and limited treatment options. Triple-negative breast cancer is characterized by the absence of estrogen receptor (ER) and progesterone receptor (PR) as well as the lack of human epidermal growth factor receptor 2 (HER2) over-expression (Carey et al. 2010). Proliferation of triple-negative breast cancer cells rely on signaling through EGFR (HER1) and the ligand-mediated activation of EGFR1 become critical for tumor progression (Wilson et al. 2009). ADAM12 was shown to be involved in the shedding of at least two EGFR ligands, EGF and betacellulin (Horiuchi et al. 2007) and ADAM12-L is responsible for activation of EGFR in early stage, lymph-node negative triple-negative breast cancer (Li et al. 2012).

In contrast, some studies showed inactivation of ADAM12 in the breast cancer cells. A genome-wide analysis of somatic mutations in human genes in breast and colorectal cancers identified three ADAM12 mutations to be associated with breast cancer: D301H mutation within the metalloprotease domain, G479E in the disintegrin domain, and L792F in the cytoplasmic tail (Sjöblom et al. 2006). Two of these mutations (D301H and G479E) were found to prevent ADAM12 maturation, leading to ER retention and loss of ADAM12 function at the cell surface (Dyczynska et al. 2008). The third mutation (L792F) that was localized in one of two di-leucine motifs within ADAM12 cytoplasmic domain does not affect protein maturation, trafficking and internalization. There are also no significant differences in proliferation or ectodomain shedding between cells expressing wild-type ADAM12 and ADAM12 L792F mutant (Stautz et al. 2012). Therefore the L792F mutation does not contribute to the development of breast cancer phenotype. The influence of D301H and G479E mutations on breast cancer progression as well as their potential use in therapy and diagnosis of breast cancer requires additional verification.

The role of ADAM12 in the development and progression of prostate cancer is poorly understood. Evaluation of ADAM12 expression in normal prostate tissue, as well as well-differentiated and poorly-differentiated prostate tumours from W^{10} mice model of prostate carcinoma showed that ADAM12 is not expressed in normal prostate but it is up-regulated in prostate cancer. Moreover, the expression of ADAM12 in well-differentiated prostate tumours localizes in a subpopulation of α-smooth muscle actin-positive stromal cells, adjacent to cancer cells. In poorly-differentiated tumours, which lack glandular

epithelial structures, ADAM12 expression was more widespread but still limited to certain areas of the tumour. Comparison of the prostate tumours from W^{10} mice lacking ADAM12 expression and W^{10} animals expressing normal levels of ADAM12 indicate that inactivation of ADAM12 significantly reduces tumour size and the progression of well-differentiated tumours to the poorly-differentiated phenotype (Peduto et al. 2006). These data suggest that the over-expression of ADAM12 in tumour-associated stromal cells plays an important role in prostate cancer progression *in vivo*. However, these findings as well as ADAM12 expression pattern in human prostate tumours require further experimental verification.

1.4.1.6 ADAM15

1.4.1.6.1 ADAM15 expression

ADAM15 has quite ubiquitous expression pattern, however the highest levels of this metalloproteinase are present in vascular cells, the endocardium, and hypertrophic cells in developing bone as well as specific areas of the hippocampus and cerebellum. During mouse embryonic development prominent ADAM15 expression was found from embryonic day 9.5 in the developing vasculature, suggesting its critical role in vascularisation (Horiuchi et al. 2003).

1.4.1.6.2 The role of ADAM15 in adhesion

Human ADAM15 is the only known member of the ADAM family that contains a consensus RGD integrin-binding sequence in its disintegrin domain. For that reason an alternative name of ADAM15 is metargidin, for metalloprotease-RGD-disintegrin (Krätzschmar et al. 1996). Interestingly, mouse ADAM15 does not contain this sequence and has a TDD motif instead (Lum et al. 1998). The RGD sequence indicates that ADAM15 plays a role in mediating cell-cell interaction through binding of integrins. Several experimental data show that ADAM15 interacts with $\alpha_v\beta_3$ and $\alpha_5\beta_1$ integrins through the RGD sequence (Zhang et al. 1998; Nath et al. 1999). Additionally, ADAM15 interacts with integrins in a RGD-independent manner, for example with integrin $\alpha_9\beta_1$ (Eto et al. 2000). The involvement of ADAM15 in modulating cell adhesion is supported by the co-localization of this metalloproteinase with vascular-endothelial (VE)-cadherin, an adhesion molecule involved in endothelial cell adherens junction formation (Ham et al. 2002).

The ability of ADAM15 to interact with integrins is thought to contribute to the development of atherosclerosis, as elevated expression of ADAM15 was detected in developing atherosclerotic lesions (Herren et al. 1997). Interestingly, $\alpha_v\beta_3$ and $\alpha_5\beta_1$ integrins which interact with the ADAM15 disintegrin domain are also up-regulated in arteriosclerotic arteries and immunohistochemical analysis showed their co-localization with ADAM15 in smooth muscle cells (SMCs) present in vessel walls. *In vitro* stimulation

of human arterial or venous SMCs with platelet-derived growth factor (PDGF) induces up-regulation of $\alpha_v\beta_3$ and $\alpha_5\beta_1$ integrin's followed by up-regulation of ADAM15 expression. Therefore it is thought that ADAM15 expression is up-regulated in response to increased integrin expression in order to modulate integrin-matrix interactions (Al-Fakhri et al. 2003).

1.4.1.6.3 ADAM15 proteolytic activity

ADAM15 is an active metalloproteinase, involved in proteolytic processing of several cell surface proteins such as the pro-forms of TNFα, HB-EGF and amphiregulin (Schäfer et al. 2004; Hart et al. 2005), the low-affinity IgE receptor CD23 (Fourie et al. 2003), fibroblast growth factor receptor 2iiib (FGFR2iiib) (Maretzky, Yang, et al. 2009), as well as extracellular matrix molecules, for example collagen type VII and gelatin (Martin et al. 2002). ADAM15-mediated shedding is not induced by phorbol esters or calcium ionophores and is inhibited by TIMP-3 but not by TIMP-1 and only weakly by TIMP-2 (Maretzky, Yang, et al. 2009).

It is important to notice that due to its integrin-binding and proteolytic activities ADAM15 can either support or inhibit cell migration. Proteolytic modification of extracellular matrix components such as collagen type VII and gelatin by ADAM15 disrupts cell-matrix bonds and supports cell migration as shown in glomerular mesengial cells (Martin et al. 2002). Binding of ADAM15 to $\alpha_V\beta3$ integrin favors cell migration by competing with $\alpha_V\beta3$ integrin-vitronectin interaction that suppresses cell migration (Beck et. al. 2005). On the other hand, over-expression of ADAM15 inhibits cell migration though enhancing cell-cell interactions as shown for ADAM15 over-expressing NIH3T3 fibroblastic cell line (Herren et al. 2001).

1.4.1.6.4 ADAM15 cytoplasmic domain

Alternative splicing of ADAM15 gene is much more complicated than in other ADAMs. The 23 exons present in the ADAM15 gene give rise to at least 13 different ADAM15 protein variants, all of which arise from differential use of exons 18 to 23, encoding the cytoplasmic domain. Analysis of tissue distribution of ADAM15 isoforms showed that the relative ADAM15 variant levels varied from 1-59%, with the least diverse variant profile found in the placenta and the most diverse in spleen and peripheral leukocytes (Kleino et al. 2007). The cytoplasmic domains of ADAM15 variants contain proline-rich sequences binding SH3 domain-containing proteins, tyrosine phosphorylation sites involved in the interactions with proteins containing SH2 domain and potential serine/threonine phosphorylation motifs (Krätzschmar et al. 1996; Poghosyan et al. 2002; Charrier et al. 2005), suggesting the involvement of ADAM15 cytoplasmic tail in cell signaling. Initial experiments using yeast two-hybrid screening and immunoprecipitation of mammalian cell lysates identified binding partners of the ADAM15 cytoplasmic tail: endophilin I and SH3PX1. These proteins also interact with the intracellular domain of

ADAM9. Due to their role in intracellular protein transport, as well as preferential binding of ADAM15 precursor over the mature form it is hypothesized that these proteins regulate ADAM15 processing and trafficking(Howard et al. 1999).

The cytoplasmic domain of ADAM15 is able to specifically bind to Src family protein-tyrosine kinases, such as Src, Lck, Fyn and Abl and to the adaptor protein Grb2 in various hematopoietic cell lines. The intracellular domain of ADAM15 is phosphorylated by Hck and Lck kinases and the phosphorylation of ADAM15 is required for ADAM15 interactions with Src family protein-tyrosine kinases (Poghosyan et al. 2002). The differences in the cytoplasmic domains of ADAM15 isoforms is determined by the number of proline-rich regions, as well as other motifs involved in the interaction of ADAM15 intracellular domain with cytoplasmic proteins. Thus, it could be concluded that alternative splicing provides a regulatory mechanism of ADAM15 intracellular signaling and activity (Kleino et al. 2009).

1.4.1.6.5 ADAM15 null mice

Despite a ubiquitous expression pattern and significant levels in some tissues ADAM15-deficient mice do not display any obvious developmental defects or pathological phenotypes (Horiuchi et al. 2003), similarly to ADAM9- and ADAM12-deficient animals (Weskamp et al. 2002; Kurisaki et al. 2003). Moreover, double knock-out mice lacking ADAM9/15 expression or triple ADAM9/12/15 knock-out mice are viable, fertile and do not display any obvious pathologies. The lack of developmental and phenotypic defects was explained by the compensatory effect of other ADAM family members, as most of the ADAM9, 12 and 15 substrates were shown to be processed by other ADAM family members. Of the six EGFR ligands (EGF, HB-EGF, TFGα, amphiregulin, betacellulin, epiregulin) only epiregulin shedding was significantly reduced in ADAM9/12/15-deficient mice. These results suggest that ADAM9, 12 and 15 are not major sheddases of EGFR ligands, they can however contribute their release in the cells with high ADAM9, 12 and 15 expression (Sahin et al. 2004)..

1.4.1.6.6 ADAM15 in cancer

The expression of ADAM15 is often deregulated in pathological conditions and there is a growing evidence linking ADAM15 with arteriosclerosis, chronic inflammatory diseases such as rheumatoid arthritis (RA) and inflammatory bowel disease (IBD) (Charrier-Hisamuddin et al. 2008). ADAM15 is also aberrantly expressed in several types of cancer, including breast, stomach, lung, prostate and pancreas carcinomas (Mochizuki & Okada 2007; Yamada et al. 2007) and increased ADAM15 is generally associated with aggressive phenotype of the tumor (Kuefer et al. 2006). ADAM15 likely supports cancer progression differentially through the action of its various functional domains. ADAM15 may down-regulate adhesion of tumour cells to the extracellular matrix, reduce cell-cell

adhesion, and promote metastasis through the activity of its disintegrin and metalloproteinase domains. ADAM15 can influence cell signalling by shedding membrane-bound growth factors and other proteins that interact with receptor tyrosine kinases, leading to receptor activation.

There is also some evidence supporting a role for ADAM15 in angiogenesis that is critical for tumour growth and metastatic spread (Lucas & Day 2009). Due to the particularly high expression of ADAM15 in vascular cells, the biological role of ADAM15 in neovascularization was investigated in a mouse model of proliferative retinopathy. Young mice were placed for several days in high oxygen (75%) conditions and then returned to normal air. The drop of oxygen concentration triggered a strong angiogenic stimulus, resulting in pathological neovascularization in the retina. ADAM15-deficient mice had a 64% lower angiogenic response than wild-type controls. Analysis of ADAM15 expression in the retina of wild type mice following hypoxia showed increased ADAM15 protein levels, whereas ADAM15 protein expression did not change in untreated age-matched controls (Horiuchi et al. 2003). Based on these data it was concluded that ADAM15 plays a significant role in blood vessel formation.

Due to its cancer-supporting activity ADAM15 is a potential target for anti-cancer therapy. Anti-ADAM15 antibodies were successfully used *in vitro* to reduce proliferation of breast and gastric carcinoma cells (Lendeckel et al. 2005; Carl-McGrath et al. 2005).

The influence of ADAM15 expression on tumor growth was initially assessed by implanting B16F0 mouse melanoma cells into ADAM15-deficient or wild type mice. The tumors developed in animals lacking ADAM15 were significantly smaller than in wild-type controls (Horiuchi et al. 2003). The influence of recombinant disintegrin domain (RDD) of human ADAM15 on progression, metastasis and angiogenesis in a mouse model of breast cancer was also assessed. RDD treatment decreased the growth of the tumor from inoculated breast cancer cells by 78%. Morphological analysis of the RDD-treated tumors reveled 53% fewer blood vessels in comparison with tumors from non-treated controls (Trochon-Joseph et al. 2004).The ADAM15 disintegrin domain is also involved in tumor progression through regulation of cancer cell migration and invasion. Over-expression of ADAM15-RGD in human ovarian OV-MZ-6 cancer cells reduced their $\alpha_v\beta_3$ integrin-mediated adhesion to vitronectin and impaired tumour cell adhesion to the extracellular matrix (Beck et al. 2005). In breast cancer cell lines, ADAM15-mediated cancer-promoting activity depends on the ability to shed the extracellular part of E-cadherin following deprivation of growth factors. The cleaved E-cadherin binds and activates HER2/HER3 receptor dimers, resulting in increased migration and cell proliferation (Najy et al. 2008b). This result suggests that ADAM15 can contribute to the cancer progression through enhancing HER2/HER3 signaling.

In prostate cancer ADAM15 expression is elevated at the mRNA and protein levels which correlates with metastatic progression (Lucas & Day 2009).The reduction of ADAM15 expression using shRNA in malignant prostate cancer cell line PC3 attenuates cell migration and their ability to adhere to fibronectin, laminin, and vitronectin impairing the malignant characteristics of this cell line *in vitro* as well as *in vivo.* This is associated with alterations of metastatic-associated cell surface proteins, such as E-cadherin, α_V integrin and CD44 receptor (Najy et al. 2008a).

It was also investigated if the expression of ADAM15 splice variants changes in cancer and if the presence of particular ADAM15 isoforms may be associated with malignant phenotype of the tumor. Analysis of four ADAM15 variants, named ADAM15A, B, C and D in human breast cancer tissue samples revealed that the expression pattern of these isoforms is different than in normal breast tissue. The expression of the individual isoforms did not correlate with patient's age, tumor size, grade and nodal status but the presence of two isoforms, ADAM15A and ADAM15B was associated with poor outcome in node-negative patients. On the other hand, elevated levels of ADAM15C variant correlated with better relapse-free survival only in node-positive patients. Over-expression of ADAM15A or B in MDA-MB-435 breast cancer cell line significantly influenced cell morphology. Whereas ADAM15A-expressing cells were well spread and displayed prominent actin stress fibers, the cells transfected with ADAM15B appeared smaller with fewer and shorter actin fibers. These morphological differences influence the migratory properties of the ADAM15A and B-expressing cells. The expression of ADAM15A enhanced adhesion, migration and invasion of MDA-MB-435 cells in *in vitro* assays, whereas the presence of ADAM15B reduced adhesion. ADAM15 variants display also isoform-specific association with intracellular signaling proteins. ADAM15A, B and C equivalently bind to extracellular signal-regulated kinases 1 and 2 (ERK1/2) and the adaptor molecules Grb2 and Tks5/Fish, but associate in an isoform-specific fashion with adaptor protein Nck and tyrosine kinases Src and Brk (breast tumor tyrosine kinase). Nck and Src interact strongly with ADAM15B and C but weakly with ADAM15A whereas Brk strongly binds to ADAM15A and B but not C (Zhong et al. 2008). Further experiments showed that the interaction of ADAM15B that is associated with aggressive breast cancer phenotype with Src increases ADAM15B catalytic activity, providing insight into the mechanism of how the selective expression of ADAM15 variants in breast cancers determine tumor aggressiveness (Maretzky, Le Gall, et al. 2009).

1.4.2 Type II transmembrane serine proteases (TTSPs)

Serine proteases, with 175 predicted members in the human genome, are the oldest and one of the largest of protease families (Lander et al. 2001). Since the discovery of the first members of the serine protease family, trypsin and enteropeptidase, serine proteases were found to regulate number of physiological processes, including blood coagulation, digestion, and regulation of blood pressure and wound healing. They are also implicated in several pathologies related to these systems. Recent advances in deciphering the mammalian genome helped to identify novel serine proteases, as well as expanded the knowledge about those already known. One of the most interesting, recently separated subfamilies of these enzymes are type II transmembrane serine proteases (TTSPs), which contain a characteristic N-terminal transmembrane domain that anchors them in the plasma membrane (Hooper et al. 2001).

1.4.2.1 The structure of TTSPs

The TTSPs share a number of common structural features including a C-terminal proteolytic domain, a transmembrane domain, a short cytoplasmic domain and a variable length stem region containing modular structural domains, linking the transmembrane and catalytic domains (Hooper et al. 2001).

The catalytic domain present in all TTSPs is highly conserved and can be classified as chymotrypsin-like serine protease (Hooper et al. 2001). The activity of this domain depends on the presence of the catalytic triad residues, histidine, aspartate, and serine, within the substrate binding pocket, which is a major determinant of substrate specificity (Szabo & Bugge 2008). The serine protease domains are approximately 225-250 amino acids in size and are oriented at the terminus of an extracellular region that is directly exposed to the pericellular environment. All TTSPs show a preference for cleavage of substrates with basic amino acids (lysine or arginine) in the P1 position, although each enzyme displays different substrate specificity. For example, matriptase and hepsin prefer basic residues in the P4-P1 positions (Antalis et al. 2010).

The cytoplasmic domains of TTSPs consist of 20-160 amino acids and often contain consensus sites for serine, threonine or tyrosine phosphorylation that may participate in communication between the cell and extracellular environment. Whether these domains are able to interact with cytoskeletal proteins and signalling molecules is not known but it is hypothesized that cytoplasmic domains of TTSPs contribute to the targeting of these enzymes to particular areas of the cell membrane (Netzel-Arnett et al. 2003).

The most complex part of the TTSP structure is the stem region that may contain 1-11 domains of six different types, as indicated below (Hooper et al. 2001; Netzel-Arnett et al. 2003; Antalis et al. 2010):

- The **LDLA** (low density lipoprotein receptor class A) domain is the most common domain in TTSPs. The function of this domain in TTSPs was not described, however, in other proteins this Ca2+ binding domain mediates internalization of macromolecules, such as lipoproteins or protease-inhibitor complexes;
- the **group A scavenger receptor** domain may function as a mediator of TTSP binding to polyanionic molecules, including modified lipoproteins, cell surface lipids and sulfated polysaccharides;
- The **Frizzled** domain, is only present in one member of TTSP family, corin. Frizzled domains function as receptors for Wnt proteins during development;
- the **CUB** (Cls/Clr, urchin embryonic growth factor and bone morphogenic protein 1) domain is present in the stem region of matriptase, matriptase-2 and matriptase-3 as well as enteropeptidase;
- the **SEA** (sea urchin sperm protein, enterokinase, agrin) domain, present in all proteases from the HAT/DESC subfamily (see below), as well as enteropeptidase and three matriptases;
- The **MAM** (a meprin, A5 antigen, and receptor protein phosphatase μ) domain is only found in enteropeptidase.

The stem region of TTSPs contributes to their cell surface orientation and modulates proteolysis by regulating enzyme activation, substrate binding and interactions with other proteins (Hooper et al. 2001; Netzel-Arnett et al. 2003; Antalis et al. 2010). For example, the stem region of enteropeptidase is required for efficient cleavage of its substrate trypsinogen (Lu et al. 1997).

1.4.2.2 Classification of TTSPs

To date 19 members of the TTSP family were identified in mouse and humans. They are organized into four subfamilies, based on the homology of the catalytic domain and the structure of the stem region (Szabo et al. 2003; Bugge et al. 2009):

- the **HAT/DESC** (human airway trypsin-like protease/ differentially expressed in squamous cell carcinoma) subfamily consists of 7 members: HAT, DESC1, TMPRSS11A (transmembrane protease/serine 11A), HAT-like 2, HAT-like 3, HAT-like 4, HAT-like 5, with the simplest stem region of all TTSPs, composed of a single SEA domain.
- the **hepsin/TMPRSS** (transmembrane protease/serine) subfamily includes hepsin, MSPL (mosaic serine protease, large form), TMPRSS2, TMPRSS3, TMPRSS4, spinesin and enteropeptidase. All members of this subfamily have a group A scavenger receptor domain in their stem regions. In TMPRSS2, 3, 4 and MSPL this domain is preceded by a single LDLA domain. The stem region of

enteropeptidase is more complex and contains an array of SEA, LDLA, CUB and MEM domains.

- the **matriptase** subfamily contains three highly homologous proteases: matriptase, matriptase-2, matriptase-3 and one with a rather unique and atypical structure - polyserase-1. Polyserase-2 and polyserase-3 were recently identified in murine and human tissues, but both lack the transmembrane domain and therefore cannot be classified as TTSPs (Cal et al. 2005; Cal et al. 2006). All matriptases have a SEA domain, two CUB domains, and three to four LDLA domains in their stem region, whereas polyserase-1 stem region consists of one LDLA domain and two active and one catalytically inactive serine protease domains.
- **Corin** subfamily with a single member corin that displays a complex stem region, not found in any other TTSP which is composed of two frizzled domains, eight LDLA domains, and one group A scavenger receptor domain.

Schematic structures of all known TTSPs are presented in Figure 1.9

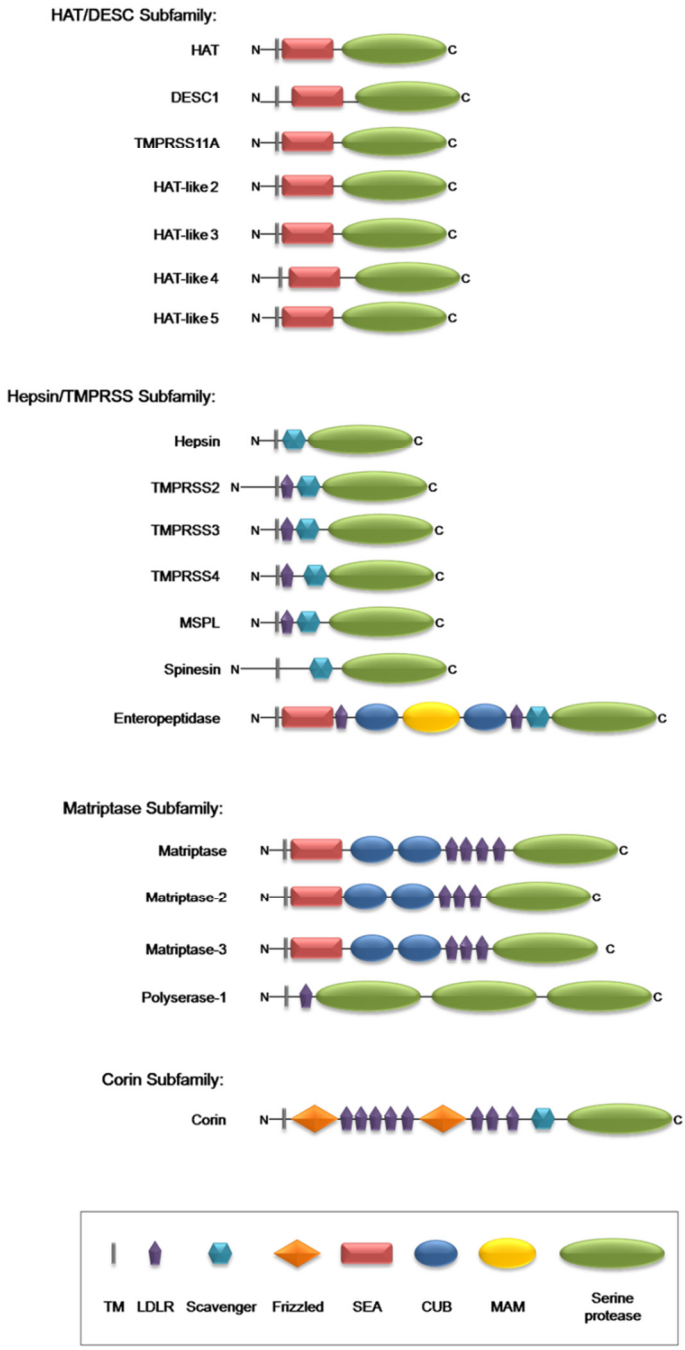

Figure 1.9 Subfamilies of type II transmembrane serine proteases.

The 19 described to date type II transmembrane serine proteases (TTSPs) are divided into four subfamilies: HAT/DESC, Hepsin/TMPRSS, Matriptase and Corin. Each TTSP consist of an N-terminal transmembrane domain (TM), stem region and C-terminal extracellular serine protease domain. The stem region may contain six different types of domains: SEA (sea urichin sperm protein/enteropeptidase/argin domain), LDLA (low-density lipoprotein receptor class A), Scavenger (group A scavenger receptor domain), Frizzled, CUB (Cls/Clr, urichin embryonic growth factor, bone morphogenic protein-1) and MAM (merpin/A5 antigen/receptor antigen phospatase μ) (from Bugge et al. 2009).

1.4.2.3 Activation of TTSPs

All TTSPs are synthesized as single-chain inactive zymogens with an N-terminal propeptide and require proteolytic cleavage following an arginine or lysine present in a highly conserved activation motif to generate the active enzyme. Activation results in a two-chain form of the enzyme that remains attached to the membrane due to the presence of a disulphide bridge, linking the pro- and catalytic domains (Hooper et al. 2001). An unusual feature of several TTSPs, including matriptase (Takeuchi et al. 2000), matriptase-2 (Velasco et al. 2002), hepsin (Qiu et al. 2007), TMPRSS2 (Afar et al. 2001) and TMPRSS3 (Guipponi et al. 2002) is their ability to undergo autocatalytic activation. In addition to the activating cleavage, at least some of the TTSPs undergo processing within their SEA domains. This additional cleavage severs the covalent link between the catalytic domain and the membrane anchor, allowing shedding of the protease from the cell surface (Szabo & Bugge 2008). Indeed, soluble forms of enteropeptidase (Fonseca & Light 1983), HAT (Yasuoka et al. 1997), TMPRSS2 (Afar et al. 2001) and matriptase (Lin, Anders, Johnson & Dickson 1999) were detected *in vivo*, presenting a novel, interesting aspect of regulation of the TTSPs function by shedding.

1.4.2.4 Expression of TTSPs

Although a few of the TTSPs are expressed across several tissues and cell types, in general these enzymes show relatively restricted expression patterns, indicating that they have tissue-specific functions. For example, the expression of enteropeptidase is restricted in normal tissues to enterocytes of the proximal small intestine (Yuan et al. 1998), whereas corin is present almost exclusively in the heart (Yan et al. 1999) and HAT is expressed predominantly in trachea (Yamaoka et al. 1998). Similarly to ADAMs, many TTSPs are aberrantly expressed in cancers and are considered novel biomarkers predicting the stage of the disease. In most cases serine proteases are over-expressed in tumor cells and are implicated in promoting tumor development and progression. Up-regulation of hepsin expression occurs in ovarian (Tanimoto et al. 1997) and prostate tumors (Magee et al. 2001). TMPRSS3 is strongly over-expressed in pancreatic cancer (Wallrapp et al. 2000) and significantly elevated levels of matriptase were found in ovarian and breast tumors (Oberst et al. 2002; C. M. Benaud et al. 2002). TTSPs promote progression of cancer by activating growth factors that stimulate proliferation of tumor cells or processing of extracellular matrix or basement membrane components and modulating metastasis (Netzel-Arnett et al. 2003; Antalis et al. 2010). In contrast, the expression of several TTSPs can be down-regulated in malignancy. For example, DESC1 is expressed in normal epithelial cells of prostate, skin, testis, head and neck but not in cancer cells derived from these tissues (Lang & Schuller 2001).

1.4.2.5 Regulation of TTSPs activity

The involvement of membrane-anchored serine proteases in many physiological processes and their frequent association with cancer and other diseases indicate that the activity of these enzymes must be tightly regulated. A part of this regulatory system are their endogenous inhibitors, including serpins and Kunitz-type inhibitors. Serpins interact with serine proteases via their reactive centre loop that mimics serine protease substrates and upon cleavage covalently traps the protease by undergoing an irreversible conformational rearrangement. The nature of serpin inhibition is an effective strategy for regulation of proteolytic activity by removal of unwanted proteases via membrane-bound endocytic receptors. Secreted serpins, like anti-thrombin III, α_2-antiplasmin or plasminogen-activator inhibitor 1 (PAI-1) were found to form complexes with matriptase and DESC1. Kunitz-type inhibitors regulate the activity of serine proteases by forming very tight but reversible complexes with target proteases. In contrast, Kunitz-type inhibitors compete with physiological substrates to reduce the availability of the protease. The transmembrane Kunitz-type inhibitors HAI-1 (hepatocyte growth factor activator inhibitor type 1) and HAI-2 regulate the activity of matriptase and hepsin (Antalis et al. 2010).

1.4.2.6 TTSPs implicated in prostate cancer.

1.4.2.6.1 Matriptase

Matriptase, also known as epithrin, suppression of tumorigenicity 14 (ST14) or membrane-type serine protease 1 (MT-SP1), was described for the first time as a gelatinolytic enzyme released by cultured breast cancer cells (Shi et al. 1993) . In the healthy organism matriptase expression is not restricted to any particular organ, but rather to the epithelial compartments of many embryonic and adult tissues (Oberst, Singh, et al. 2003). In addition to epithelia, matriptase was found in monocytes, macrophages (Kilpatrick et al. 2006) and neural progenitor cells (Fang et al. 2011). Matriptase expression during mouse embryo development is detected from embryonic day 10 (E10) in the epithelial lining of several tissues and from E14-16 matriptase can be found in developing hair follicles and the interfollicular epidermis. Matriptase was also detected in the mouse and human placenta (List, Szabo, et al. 2006; Fan et al. 2007; Szabo et al. 2007). As presented in Figure 1.3, matriptase stem region consists of four LDLR and two CUB domains. The first CUB domain contains an RGD integrin binding motif (Lin, Anders, Johnson, Sang, et al. 1999). Similarly to other TTSPs, matriptase cleaves substrates with Lys or Arg in P1 position and prefers small side chain amino acids such as Gly or Ala in position P2. The list of matriptase substrates is constantly expanding and includes pro-hepatocyte growth factor (pro-HGF) and pro-urokinase plasminogen activator (pro-uPA) (Lee et al. 2000) as well as several adhesion molecules, matrix proteins, growth factors and receptors. Additionally, matriptase activates other proteases that are unable to

undergo autocatalytic activation, such as GPI-anchored serine protease prostasin (Chen et al. 2008).

Matriptase is synthesized as an inactive, single-chain zymogen and requires cleavage at the canonical activation motif resulting in two-chain active protease which remains linked to the cell surface via a disulphide bond between the pro- and catalytic domains. The activation of matriptase is unique among other proteases, it requires two sequential endoproteolytic cleavages and transient interaction with matriptase inhibitor HAI-1 (Karin List, Thomas H Bugge, et al. 2006, Figure 1.4). The first cleavage occurs after Gly present in the conserved GSVI motif within the SEA domain and is mediated by an unknown protease. The cleaved fragment remains attached to the rest of the molecule, possibly through noncovalent interactions within the SEA domain (Kojima & Inouye 2011). This cleavage is thought to occur in the secretory pathway, as only the SEA-domain cleaved matriptase zymogens reach the cell surface (Cho et al. 2001). Subsequently, matriptase undergoes secondary cleavage after Arg in the RVVGG activation cleavage site within the serine protease domain and is converted into its active, two-chain form. This is an autocatalytic event as the mutation of amino acids in the catalytic triad prevents matriptase activation. It is hypothesized that activation of matriptase is mediated through a transactivation mechanism in which the SEA domain-cleaved matriptase zymogen is cleaved by weak proteolytic activity of another SEA domain-cleaved zymogen molecule. (List, Bugge, et al. 2006; Kojima & Inouye 2011). As mentioned previously, HAI-1 inhibitor is necessary for the activation of matriptase. In the absence of active HAI-1 matriptase processing is suppressed and matriptase zymogen accumulates in the Golgi apparatus (Oberst, Williams, et al. 2003; Oberst et al. 2005). The lack of matriptase activation in the absence of HAI-1 is considered to protect cells from the uncontrolled, harmful activity of matriptase.

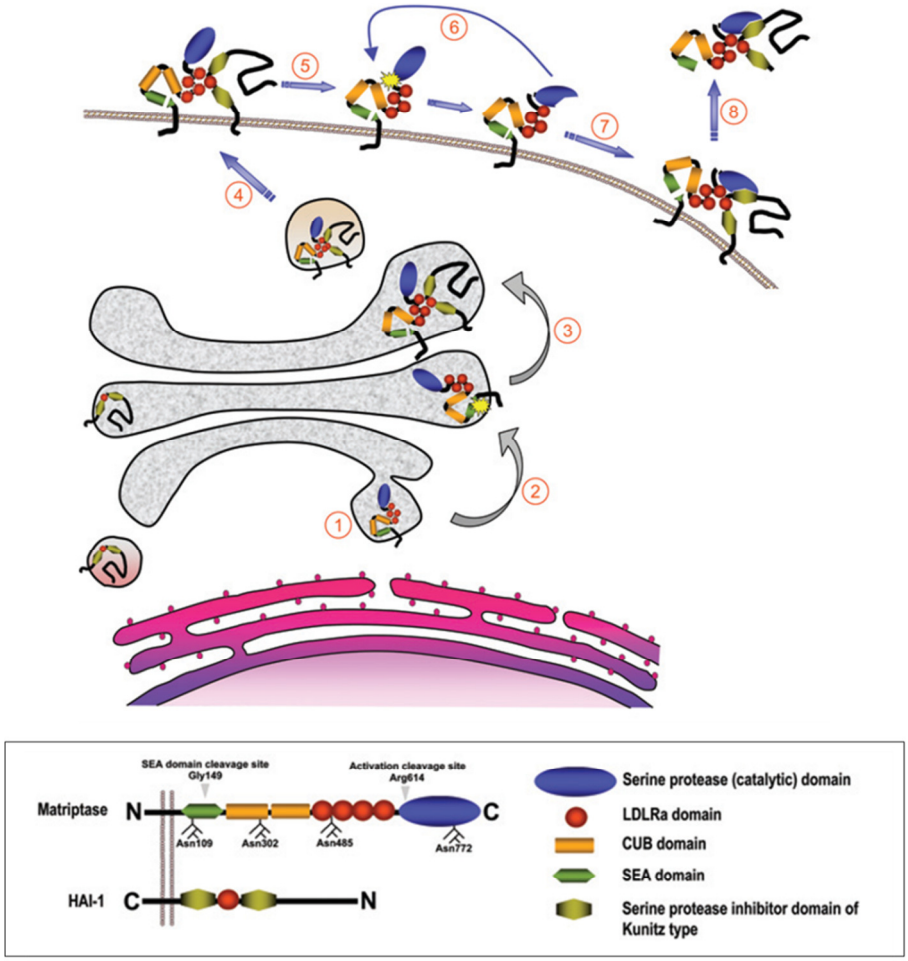

Figure 1.10 Proposed model of matriptase activation.

Matriptase zymogen is synthesized on the rough endoplasmic reticulum as a single-span type II transmembrane protein (1). The activation of matriptase begins already in the secretory pathway with the endoproteolytic cleavage after Gly within the SEA domain (2). SEA domain-cleaved matriptase associates with HAI-1 (3) and the matriptase-HAi-1 complex is transported to the plasma membrane (4) where the second autocatalytic cleavage occurs (5). Activated matriptase is rapidly inhibited by HAI-1 (6) and the matriptase-HAI-1 complex may be shed from the cell surface (8) (List, Bugge, et al. 2006).

The matriptase activation occurs in response to several factors which can be cell-type or organ specific. In mammary epithelial cells matriptase is activated by sphingosine 1-phosphate (S1P), a phospholipid present in the blood (C. Benaud et al. 2002). In the LNCaP prostate cancer cell line matriptase undergoes activation in response to androgen treatment through AR-dependent signaling pathway (Kiyomiya et al. 2006). In contrast, breast cancer cells respond to neither S1P nor androgens as they activate matriptase constitutively (C. M. Benaud et al. 2002). Exposure of matriptase-expressing epithelial cells from various organs to mildly acidic pH (pH 5.2-6.8, with the optimum at pH 6.0) resulted in rapid activation of matriptase zymogen (Tseng et al. 2010).

As for other TTSPs, the activity of matriptase is strictly regulated by the two Kunitz-type serine protease inhibitors – hepatocyte growth factor activator inhibitor 1 (HAI-1) and HAI-2 (Lin, Anders, Johnson & Dickson 1999; Kataoka et al. 2003). HAI-1 is co-expressed with matriptase in many embryonic and adult tissues and forms complexes with soluble matriptase which can be found in human milk or conditioned medium from some cancer cells (Shi et al. 1993; Lin, Anders, Johnson & Dickson 1999; Oberst et al. 2001). Formation of matriptase-HAI-1 complex requires interactions between Kunitz domain-1 and LDLR domain of HAI-1 and serine protease and second CUB domain of matriptase (Denda et al. 2002; Oberst, Williams, et al. 2003; Inouye et al. 2010).

In addition to HAI-1 and HAI-2 inhibition, the activity of matriptase is also regulated by glycosylation. The addition of β 1-6 *N*-acetylglucosamine (GlcNAc) branching mediated by N- acetylglucosaminyltransferase (GnT-V) protects matriptase from degradation (Ihara et al. 2002).

The isolation of soluble matriptase in complex with HAI-1 or serpin inhibitors from human milk led to the discovery that activated matriptase may be shed from the cell surface (Lin, Anders, Johnson & Dickson 1999). The shedding of matriptase can occur constitutively as a result of zymogen activation and HAI-I-mediated inhibition (Wang et al. 2009) or can be induced with phorbol esters, such as by phorbol 12-myristate 13-acetate (PMA). Interaction of the matriptase cytoplasmic domain with the cytoskeletal linker protein filamin is essential for shedding. PMA-induced shedding is inhibited by the metalloproteinase inhibitor GM6001, implicating the involvement of metalloproteinases in the shedding process (C. Kim et al. 2005).

Better understanding of the role of matriptase in embryonic development and normal physiology has come from the study of transgenic matriptase-null mice. These animals develop to term but uniformly die within 48 hours after birth, due to severe dehydration that results from impaired epidermal barrier function. The newborn matriptase-null animals display dry, red, shiny and wrinkled skin, hair follicle hypoplasia, lack of whiskers as well as accelerated apoptosis of immature T cells in the thymus (List et al. 2002).

Immunohistochemistry studies showed that the defective epidermal function in matriptase-null mice is caused by impaired processing of profilaggrin, a large epidermal polyprotein composed of multiple filaggrin monomers and Ca^{2+}-binding regulatory N-terminal S-100 protein. In the absence of matriptase-mediated processing profilaggrin accumulates in the stratum corneum, leading to a defective epidermal structure (List et al. 2003). Aberrant profilaggrin processing can also be responsible for hair follicle hypoplasia and thymocyte depletion in matriptase-deficient mice as profilaggrin is expressed in hair follicle and thymic epithelium (Dale et al. 1985; Favre 1989).

The lack of proteolytically active matriptase was recently linked with a rare form of skin disease, an autosomal recessive ichthyosis with hypotrichosis (ARIH). Patients suffering from ARIH display ichthyosis and hair follicle hypoplasia associated with fragile, dry, and slow-growing scalp hair. Based on recent reports, describing a single amino acid mutation within a highly conserved region of the catalytic domain of matriptase in ARIH patients it could be hypothesized that ARIH phenotype results from aberrant processing of profilaggrin (Basel-Vanagaite et al. 2007).

Matriptase is abundantly expressed in various tumors of epithelial origin, including breast, prostate, ovarian, cervical, gastric, colon, and renal cell, esophageal and oral squamous cell carcinoma. In most cancers, over-expression of matriptase mRNA and protein correlates with the disease progression (reviewed by Uhland 2006). In addition, the ratio of matriptase to its inhibitor HAI-1 is frequently shifted towards matriptase in the late stage tumors, indicating that the loss of matriptase inhibition might be involved in cancer progression and correlates with poor clinical outcome. The matriptase/HAI-1 ratio is considered as a good informative marker of cervical, prostate and colorectal carcinoma (Oberst et al. 2002; Saleem et al. 2006; Vogel et al. 2006).

The oncogenic potential of matriptase was evaluated using transgenic mice over-expressing this protease in skin. Increased levels of matriptase caused severe hyper proliferation of epidermal keratinocytes, leading to spontaneous skin squamous cell carcinoma (List et al. 2005). The pro-oncogenic potential of matriptase may result from the fact that matriptase activates several growth factors associated with tumor progression, such as pro-HGF, pro-uPA, pro-MSP-1 (pro-macrophage stimulating protein-1) or IGFBP-rP1 (iinsulin-like growth factor binding protein-related protein-1) (Lee et al. 2000; Bhatt et al. 2005; Ahmed et al. 2006). Matriptase may also promote invasion of epithelial-derived tumor cells through cleavage of desmoglein-2, a desmosome protein participating in cell-cell adhesion (Wadhawan et al. 2012).

Analysis of matriptase levels in normal prostate glands and prostate cancer tissue revealed a several-fold increase of matriptase expression in malignant cells and positive correlation between the level of matriptase and the Gleason score of the tumor (Riddick et

al. 2005). Additionally, over-expression of matriptase in prostate cancer cells was associated with significant down-regulation of matriptase inhibitors, HAI-1 and HAI-2. These findings strongly indicate that the progression of prostate cancer depends on increased proteolytic activity of matriptase (Saleem et al. 2006; Bergum & List 2010). The cancer-promoting activity of matriptase was confirmed in *in vitro* studies using prostate cancer cell lines. Reduced expression of matriptase in PC3 and DU145 prostate cancer cell lines inhibited their growth, proliferation and invasion by 50% (Sanders et al. 2006). Moreover, down-regulation of HAI-1 expression in the same cells significantly increased their invasiveness and motility (Sanders et al. 2007). It is believed that the increased invasiveness of prostate cancer cells over-expressing matriptase results from proteolytic processing of laminin-332, a basement membrane protein found in many epithelia, including prostate. DU145 cells showed increased motility in transwell migration assay when plated on matriptase-cleaved laminin-332 and LNCaP cells over-expressing matriptase plated on laminin-332 migrated faster than normal LNCaP cells (Tripathi et al. 2011). In addition to laminin-332, matriptase cleaves other basement membrane components - collagen IV and fibronectin (Shi et al. 1993; Satomi et al. 2001), contributing to increased motility of cancer cells. Finally, matriptase activates platelet-derived growth factor DD (PDGF-DD), a ligand for PDGFR- β (platelet-derived growth factor receptor β), which is frequently over-expressed in prostate cancer cells (Singh et al. 2002).

1.4.2.6.2 Matriptase-2

Matriptase-2 (TMPRSS6) was named after its structural homology to matriptase (Velasco et al. 2002). Similarly to matriptase, matriptase-2 contains two CUB domains within the stem region but has only three LDLR domains. Active matriptase-2 is a two chain protease generated from a single chain zymogen. Proteolytically activated matriptase-2 remains attached to the cell surface via disulphide bond linkage between the pro- and catalytic domains, however the soluble form of matriptase-2 can also be detected (Silvestri et al. 2008; Ramsay, Quesada, et al. 2009). Recent reports showed that the soluble form of matriptase-2 corresponds mainly to the two chains, highly active variant whereas membrane-associated matriptase-2 is an inactive single chain zymogen. N-terminal sequencing of the shed matriptase revealed that matriptase-2 shedding occurs within the second CUB domain. Mutation of the Ser residue of the catalytic triad blocks shedding and activation of matriptase-2. These data suggest that matriptase-2 is proteolytically activated and shed from the cell surface by neighboring matriptase-2 molecules (Stirnberg et al. 2010). In contrast with matriptase, the activity of matriptase-2 is not controlled by HAI inhibitors but by endocytosis, which removes matriptase-2 from the cell surface, preventing matriptase-2 interaction with its substrates. Internalization of matriptase-2 depends on specific residues within its N-terminal cytoplasmic domain, as

site-directed mutagenesis of these amino acids abrogated internalization and maintained the enzyme at the cell surface (Béliveau et al. 2011).

In comparison with matriptase, matriptase-2 has a more restricted expression pattern. Human matriptase-2 was found predominantly in adult and fetal liver, although in mice matriptase-2 expression was also detected in kidney, uterus and nasal cavity (Velasco et al. 2002; Hooper et al. 2003).

Matriptase-2 degrades extracellular matrix and basement membrane components such as fibronectin, fibrinogen and collagen type I. Similarly to matriptase, matriptase-2 activates pro-uPA but with much lower efficiency (Velasco et al. 2002). Mutations of the *matriptase-2* gene in humans are linked to the iron metabolism disorder called IRIDA (iron-refractory iron deficiency anemia) and correlates with elevated hepcidin levels in the urine of IRIDA patients (Finberg et al. 2008; Guillem et al. 2008). The critical role of matriptase-2 in maintaining iron homeostasis was deciphered in further studies using two mouse models with reduced matriptase-2 expression – matriptase-2 KO mouse and *Mask* mouse, a recessive, chemically induced mutant mouse that expresses matriptase-2 lacking its serine protease domain. Both of these models of matriptase-2 deficiency are characterized by the gradual loss of body but not facial hair, resulting in a complete nudity of the trunk. This phenotype could be reversed by keeping *Mask* and matriptase-2 KO animals on a high-iron diet, indicating deregulated iron metabolism in these mice. Matriptase-2 KO and Mask mice display microcytic anemia, low iron plasma levels and depleted iron stores, caused by the over-expression of hepcidin (Du et al. 2008; Folgueras et al. 2008). Studies by Silvestri and colleagues showed that matriptase-2 negatively regulates hepcidin expression through proteolysis of hemojuvelin (Silvestri et al. 2008), a GPI-anchored membrane protein synthesized by hepatocytes that acts as a co-receptor for bone morphogenic factor-2 (BMP-2), BMP-4 and BMP-6 (Babitt et al. 2006). These members of the TGF-β superfamily of growth factors are primary activators of hepcidin expression in hepatocytes (Truksa et al. 2006; Andriopoulos et al. 2009). Cleavage of hemojuvelin by matriptase-2 prevents hepcidin expression directly by inactivating BMP signaling and indirectly by creating an imbalance in levels of BMP co-receptor and antagonist (Ramsay, Hooper, et al. 2009). The lack of matriptase-2 causes over-expression of hepcidin and leads to severe iron deficiency.

The expression of hepcidin in the liver was also found to be dramatically down-regulated in response to hypoxic conditions (Nicolas et al. 2002). Recent studies demonstrated that one of the transcription factors induced by the low oxygen levels, the hypoxia-inducible factor (HIF) up-regulates expression of matriptase-2 through direct binding to the hypoxia responsive element (HRE) in *matriptase-2* gene promoter (Lakhal et al. 2011; Maurer et al. 2012). These data confirm the central role of matriptase-2 in the regulation of iron metabolism.

In healthy humans and mice matriptase-2 is expressed almost exclusively in the liver. Significant levels of this serine protease are also found in some types of cancers. Matriptase-2 mRNA expression was detected in Leydig tumor cells (Odet et al. 2006) as well as in prostate cell lines with low invasive potential, like P2HPV-7 and PNT2-C2. No matriptase-2 was detected in more invasive DU145 and PC3 cells (Sanders et al. 2008). Matriptase-2 seems to suppress growth of cancer cells and its expression in the tumors correlates with good clinical prognosis, as concluded from studies on breast and prostate cancers. For example, low levels of matriptase-2 correlate with overall poor prognosis for breast cancer patients. Transfection of the highly invasive breast cancer cell line MDA-MB231 with matriptase-2 significantly reduced its tumorigenic potential following administration into CD1 athymic mice as well as invasion and migration in *in vitro* experiments (Parr et al. 2007). Over-expression of matriptase-2 in PC3 prostate cancer cells impaired their invasiveness and migration rates *in vitro* and reduced their growth and survival following administration into CD1 nude mice. To explain the impaired migration rates of matriptase-2 over-expressing PC3 cell line, the cells were immune labelled for paxillin and focal adhesion kinase (FAK), revealing increased expression of these adhesion molecules, especially within the focal adhesion complexes. Therefore matriptase-2 may have anti-metastatic functions in cancer cells (Sanders et al. 2008).

1.4.2.6.3 Hepsin

Hepsin was named due to its significant expression in hepatocytes (Leytus et al. 1988). In addition to the liver cells, hepsin is present also in a number of other tissues including thymus, thyroid, lung, pancreas, pituitary gland, prostate, and kidney (Tsuji et al. 1991; Szabo & Bugge 2008). The most prominent hepsin substrate is pro-uPA. The catalytic efficiency of pro-uPA activation by hepsin is similar to that of plasmin which is considered to be the most potent pro-uPA activator and is about six fold higher than that of matriptase (Moran et al. 2006). Other substrates cleaved by hepsin include laminin-332 (Tripathi et al. 2008), prostasin (M. Chen et al. 2010) and pro-macrophage stimulating protein (pro-MSP), a plasminogen-related growth factor, implicated in promoting wound healing and tumor invasion and suppressing pro-inflammatory immune response (Ganesan et al. 2011). Similarly to matriptase, hepsin was shown to release the extracellular part of EGFR, however hepsin-mediated processing occurs in a different position than cleavage by matriptase (M. Chen et al. 2010). Hepsin converts the single-chain hepatocyte growth factor (pro-HGF) into biologically active two-chain HGF (Herter et al. 2005; Kirchhofer et al. 2005) and activates zymogen factor VII to factor VIIa (Kazama et al. 1995).

Hepsin is synthesized as inactive zymogen and undergoes autocatalytic activation (Qiu et al. 2007), however the detailed mechanism of this process has not been described

to date. The activity of mature hepsin is regulated by HAI-1B and HAI-2 (Kirchhofer et al. 2005).

Hepsin-deficient mice develop and breed normally, have no histological abnormalities in major organs, including liver and display no defects in blood coagulation (Wu et al. 1998). The only exhibited defect in these animals is severe hearing loss caused by abnormal cochlear tectorial membrane and defective compaction of spiral ganglion neurons (Guipponi et al. 2007).

As for many other TTSPs, hepsin is implicated in several types of cancer. Hepsin expression is markedly elevated in ovarian (Tanimoto et al. 1997), renal cell (Zacharski et al. 1998), endometrial (Matsuo et al. 2008), breast (Xing et al. 2011) and prostate carcinomas. Hepsin mRNA is over-expressed in 90% of prostate tumors and this up-regulation is accompanied by an increase in protein level. Moreover, expression of hepsin localizes to the cancer cells rather than to the stroma (Dhanasekaran et al. 2001; Jun Luo et al. 2001; Magee et al. 2001; Chen et al. 2003; Stephan et al. 2004; Riddick et al. 2005). Elevated levels of hepsin correlate with high Gleason score and serum PSA levels and were indicative of poor clinical outcome and disease relapse following radical prostatectomy (Dhanasekaran et al. 2001; Magee et al. 2001; Chen et al. 2003; Stephan et al. 2004; Goel et al. 2011). Significant up-regulation of hepsin in prostate cancer as well as the correlation between hepsin and the clinical outcome suggests that hepsin could be a potential target for anti-cancer therapy. Recently two groups described allosteric anti-hepsin inhibitory antibodies which can be potentially tested as a new treatment for prostate cancer patients (Ganesan et al. 2012; Koschubs et al. 2012). Several groups are also proposing to use hepsin as a prognostic marker that can be used alone or in combination with PSA testing. The lack of detectable hepsin in blood or urine allows to measure its levels only in prostate biopsies (Dhanasekaran et al. 2001; Stephan et al. 2004; Kelly et al. 2008; Pace et al. 2012).

To better understand the role of hepsin in prostate epithelium *in vivo* transgenic mice over-expressing hepsin under the control of the probasin promoter (PB-hepsin mice) were generated. Immunofluorescent staining and electron microscopic analysis revealed that over-expression of hepsin causes weakening of epithelial-stromal adhesion and disorganization of the basement membrane in the prostate gland. To investigate the influence of hepsin on prostate cancer progression PB-hepsin mice were then crossed with LBP-Tag mice, a transgenic model of prostate cancer. LBP-tag mice express SV40 large T antigen in the prostate epithelium and develop PIN and primary prostate carcinoma but do not develop metastases. Interestingly, 65% of double transgenic LBP-Tag/PB-hepsin mice developed metastatic lesion in bones, liver and lung by the 21 week of age (Klezovitch et al. 2004). Therefore hepsin promotes primary cancer progression and metastasis, possibly by direct disruption of the basement membrane through

degradation of extracellular matrix components. *In vitro* studies, showing enhanced motility of DU145 prostate cancer cells plated on hepsin-cleaved laminin-332 support this hypothesis (Tripathi et al. 2008). In another study investigating the role of hepsin in prostate cancer progression *in vivo*, PB-hepsin mice were crossed with the probasin directed *myc* mouse model of prostate carcinoma (*myc* mice). The double-transgenic animals (PB-hepsin/*myc*) progressed faster to carcinoma stage than the *myc* mice. Moreover, the PB-hepsin/*myc* mice developed a pathologically higher grade of tumour in comparison with the age-matched *myc* mice, confirming the cancer-promoting activity of hepsin (Ellwood-Yen et al. 2003; Nandana et al. 2010).

In contrast with hepsin over-expression in localized prostate tumors, hepsin is down-regulated in metastatic lesions (Dhanasekaran et al. 2001), suggesting that this serine protease is necessary only in the initial stages of tumorigenesis, mediating disruption of the epithelial organization. This activity of hepsin may not be needed when the metastasizing cells are establishing themselves at distant sites (Vasioukhin 2004). This presumption is supported by the finding that metastasis-derived prostate cancer cell lines DU145 and PC3 do not express hepsin (Srikantan et al. 2002; Wittig-Blaich et al. 2011). Furthermore, over-expression of hepsin in PC3 cells results in 75% growth inhibition and about 50% reduction of invasion in Matrigel migration assay (Srikantan et al. 2002). Hepsin-mediated loss of viability and adhesion of PC3 cells was linked to reduced phosphorylation of Akt kinase at Ser473 (Wittig-Blaich et al. 2011). Akt is an effector kinase of phosphatidylinositide 3-kinase (PI3K) signaling pathway that is the major regulatory mechanism of PC3 growth and viability (Bertram et al. 2006). Over-expression of hepsin was also shown to suppress growth and induce apoptosis in ovarian and endometrial cancer cell lines (Nakamura et al. 2006; Nakamura et al. 2008).

1.4.3 Prostasin – a GPI-anchored serine protease

The first isolated GPI-anchored serine protease was prostasin, also known as PRSS8 (Yu et al. 1994). Similarly to other GPI-anchored proteins, prostasin localizes in lipid rafts, cell membrane compartments enriched in cholesterol and glycolipids (Simons & Ikonen 1997; Verghese et al. 2006). Prostasin can also be isolated as a soluble protein from seminal fluid and at lower levels from urine. The highest expression of the GPI-anchored prostasin variant was found in prostate epithelium but it can also detected in colon, lung, liver, pancreas, kidney, salivary gland and bronchus (Yu et al. 1994; Yu et al. 1995). Prostasin is synthesized as an inactive zymogen that requires a site-specific proteolytic cleavage for activation. However, in contrast to some TTSPs prostasin is not able to undergo auto activation and requires processing by upstream proteases (Shipway et al. 2004). Among enzymes able to activate prostasin are matriptase and hepsin, indicating that membrane serine proteases may form catalytic cascades (Netzel-Arnett et al. 2006; M. Chen et al. 2010). The activity of prostasin following activation is regulated by

a serpin inhibitor, protease nexin-1 (PN-1) and HAI-1 which are co-expressed with prostasin in epithelial cells (Chen et al. 2004; Fan et al. 2005).

The soluble variant of prostasin is generated by cleavage at Arg323 (Arg322 in mouse prostasin) by trypsin-like proteases to remove the COOH-terminal hydrophobic domain (Yu et al. 1994). In contrast to prostate epithelium, prostasin is not efficiently released from the airway epithelial cells (Tong et al. 2004), indicating that the mechanism of soluble prostasin production is cell type specific. Indeed, analysis of various prostasin mutants expressed in kidney and lung epithelial cells showed that the secretion of prostasin in these cells is mediated by endogenous GPI-specific phospholipase D1 (Gpld1) (Verghese et al. 2006).

The first biological function of prostasin to be described was the activation of epithelial sodium channels (ENaC) (Adachi et al. 2001). ENaC are present in the distal segments of the kidney tubule, colon, urinary bladder, skin and airways and their function is critical for maintaining salt and fluid balance in these organs (Schild & Kellenberger 2001). Proteolytic cleavage has an important role in regulating ENaC activity as it increases the probability of an open channel conformation.

The other important function of prostasin is maintaining epithelial barrier function, as concluded from the observation of prostasin-deficient mice. Interestingly, the lack of prostasin in keratinized tissues results in the same phenotype as described previously in matriptase-deficient mice, including impaired stratum corneum formation, hair follicle defects, thymic abnormalities and postnatal lethality (Leyvraz et al. 2005). As mentioned previously, prostasin and matriptase are components of the same proteolytic cascade that regulates epidermal function, with matriptase acting upstream of prostasin (Netzel-Arnett et al. 2006). The matriptase-prostasin cascade is tightly regulated in differentiating epidermis by HAI-1, limiting the opportunity to act on substrates and at the same time protecting the tissue from uncontrolled proteolytic activity (Y.-W. Chen et al. 2010). The activation of prostasin by matriptase is additionally regulated by the spatial separation of the two serine proteases. In polarized epithelial cells matriptase is mainly located on the basolateral plasma membrane (Tsuzuki et al. 2005), whereas most of prostasin localizes on the apical plasma membrane (Chen et al. 2008; Selzer-Plon et al. 2009). These two compartments are separated by the tight junctions in order to prevent diffusion of membrane proteins between the two membranes. However, the proteolytic activation of prostasin by matriptase is possibly due to the brief co-localization of these two enzymes at the basolateral plasma membrane. A minor fraction of prostasin can be found on the basolateral plasma membrane where it undergoes matriptase-mediated activation, followed by endocytosis and transcytosis to the apical membrane where its long retention time causes the accumulation of active prostasin (Friis et al. 2011).

The molecular mechanisms of how the matriptase-prostasin axis regulates the differentiation of epidermis are not fully understood. One of the signaling pathways controlled by the matriptase-prostasin cascade is EGFR signaling. Co-expression of matriptase and prostasin in EGFR-expressing cells results in the generation of two truncated EGFR fragments, lacking the ligand binding domain and unresponsive to EGF stimulation (Chen et al. 2008). Recent experimental evidence suggests that the proteolysis-activated receptor-2 (PAR-2) is a major downstream effector of the matriptase-prostasin proteolytic cascade. Transgenic mice lacking prostasin and PAR-2 expression do not display any epidermal abnormalities, implicating PAR2 as a potential mediator of pathologies linked to loss of serine protease regulation in skin (Frateschi et al. 2011).

In the healthy organism the highest expression of prostasin is found in prostate epithelial cells but prostasin is also aberrantly expressed in some types of tumors. For example, high levels of prostasin are found in ovarian cancer (Mok et al. 2001), whereas the expression of prostasin decreases in prostate cancer. The levels of prostasin in biopsies from patients with hormone-refractory prostate cancer are about 6 times lower than in organ-confined tumors (Takahashi et al. 2003). Similar observation can be made from the analysis of prostasin expression in prostate cancer cell lines. Prostasin is expressed by LNCaP cells with low invasive potential but not by more invasive DU145 and PC3 cells (Yu et al. 1995; Chen, Hodge, et al. 2001). Down-regulation of prostasin in these cell lines is caused by hypermethylation of the prostasin gene promoter (Chen et al. 2004). Transfection of DU145 and PC3 cells with prostasin reduced their invasiveness in vitro by 68% and 42%, respectively (Chen, Hodge, et al. 2001).

To define the molecular mechanisms by which prostasin affects the behavior of prostate cancer cells, the PC3 cell line was transfected with prostasin followed by analysis of mRNA and protein levels of several molecules implicated in prostate cancer invasion. The molecular changes observed in cells over-expressing prostasin were down-regulation of EGFR mRNA and protein levels, inhibition of ERK1/2 phosphorylation in response to EGF treatment and decreased expression of uPA. Interestingly, both active and mutated prostasin caused significant down-regulation of the expression of two inflammation-induced genes, cyclooxygenase-2 (COX-2) and inducible nitric oxide synthase (iNOS) (Chen et al. 2007). The protease-dependent changes partially explain the reduction of prostate cancer cell invasion by prostasin; however the relevance of protease-independent effects requires further investigation. Silencing of prostasin expression in human benign prostatic hyperplasia cell line BPH-1 using siRNA resulted in up-regulation of iNOS, intracellular adhesion molecule-1(ICAM-1), interleukin-6 and interleukin-8, as well as down-regulation of cyclin D1 leading to reduced proliferation and invasion. Further experiments showed that prostasin is a negative regulator of PAR-2-mediated signalling and this function of prostasin is critical for inhibition of prostate cancer cells invasiveness

(Chen et al. 2009). Prostasin in also present in normal human mammary epithelial cells, poorly invasive breast carcinoma cell line MCF-7 and the non-metastatic breast carcinoma cell line MDA-MB-453, while highly invasive and metastatic breast carcinoma cell lines MDA-MB-231 and MDA-MB-435 lack prostasin expression. Similarly to invasive prostate cancer cell lines, the lack of prostasin expression in MDA-MB-231 and MDA-MB-435 is caused by methylation of the prostasin gene promoter. Enforced expression of prostasin in these cells reduced their invasiveness *in vitro* by 50% (Chen & Chai 2002).Expression of prostasin is breast cancer cell lines and clinical samples strongly correlated with the expression of matriptase, suggesting the involvement of matriptase-prostasin cascade is the progression of breast cancer (Bergum et al. 2012).

1.5 Aims of the thesis.

TMEFF2 is novel transmembrane protein implicated in the development and progression of prostate cancer. However, the literature data describing the role of TMEFF2 in prostate cancer are controversial, indicating that this protein might be involved in both enhancement and suppression of prostate cancer growth and progression. Based on these findings it was hypothesized that the dual action of TMEFF2 in prostate cancer results from differential processing of the full-length, transmembrane TMEFF2 by membrane-anchored proteases over-expressed by normal prostate epithelium and prostate cancer cells. To verify this hypothesis the following experiments were performed and discussed in this thesis:

- analysis of the co-expression of TMEFF2 and membrane-anchored serine proteases in prostate cancer cell lines and clinical samples (Chapter 3);
- characterization of AP/V5 TMEFF2 and AP/V5$\Delta_{303\text{-}320}$TMEFF2 HEK293 cells as an *in vitro* model to study TMEFF2 shedding from the cell surface and generation of different C-terminal fragments (Chapter 4);
- analysis of TMEFF2 processing by serine proteases (matriptase, matriptase-2, hepsin, prostasin) and ADAMs (ADAM9, ADAM12, ADAM15A, ADAM15B, ADAM15C) implicated in prostate cancer (Chapter 4);
- production and purification of recombinant TMEFF2 fragments, corresponding to N-terminal products of serine protease and ADAM-mediated processing in *E. coli* and mammalian cells (Chapters 5 and 6);
- characterization of the biological activity of purified TMEFF2 fragments *in vitro*, using ERK1/2 phosphorylation and XTT proliferation assays (Chapters 5 and 6);
- investigation of the fate of TMEFF2 C-terminal fragments generated by serine proteases and ADAMs following ectodomain cleavage using fluorescent confocal microscopy and Western blotting (Chapter 7).

Chapter 2:

Materials and methods

The formulations of all used solutions are summarized in Appendix I. All chemical components were purchased from Fisher Scientific unless otherwise stated.

2.1 Cell culture

Cell lines were maintained at 37℃ in humidified air with 5% CO_2 and passaged upon confluency by washing once with PBS and incubating with 1-2 ml trypsin/EDTA (GIBCO) for 5 minutes at 37℃. The trypsin/EDTA solution was then neutralised by adding 6 ml of culture medium containing 10% foetal bovine serum (FBS) and the cell suspension was centrifuged to remove trypsin. Specific culture media formulations for each cell line are presented in Table 2.1. All media were purchased from Lonza, FBS from GIBCO and Hygromycin B solution from Invitrogen. Tissue culture plastic ware was obtained from Sarstedt unless otherwise stated.

To prepare aliquots for freezing, cells were suspended in freezing medium (50% FBS, 40% medium, 10% DMSO) following trypsinization and stored overnight at -80℃ before being transferred into liquid nitrogen.

Table 2.1. List of used cell lines.

Cell line	Growth medium:	Obtained from:
PNT2-C2	RPMI 1640 + 10% FBS	Dr Anne Collins, University of York, UK
LNCaP		
DU145	EMEM + 10% FBS	
PC3	Ham's F12 + 10% FBS	
CHO Flp-In	Ham's F12 + 10% FBS + 100 µg/ml Zeocin	Invitrogen
HEK293 Flp-In	DMEM + 10% FBS + 100 µg/ml Zeocin	
HA/V5 TMEFF2 CHO AP/V5 HB-EGF CHO	Ham's F12 + 10% FBS + 500 µg/ml Hygromycin B	Dr Vera Knäuper
HA/V5 TMEFF2 HEK293 HA/V5 $\Delta_{303\text{-}320}$TMEFF2 HEK293 AP/V5 TMEFF2 HEK293 AP/V5 $\Delta_{303\text{-}320}$TMEFF2 HEK293	DMEM + 10% FBS + 100 µg/ml Hygromycin B	

2.2 Immunolocalisation of TMEFF2 and $\Delta_{303-320}$TMEFF2 in HEK293

HA/V5 TMEFF2 and HA/V5 $\Delta_{303-320}$TMEFF2 HEK293 cells were seeded at the density of $5x10^5$ cells per well in a 6-well plate on poly-L-lysine (Sigma Aldrich) coated coverslips and grown overnight. In some experiments cells were treated with 5 µM DAPT, 25 µM GM6001 or 100 ng/ml PMA (all purchased from Enzo). After performing the experiment cells were washed once with PBS, fixed in 4% paraformaldehyde (Fisher Scientific) in PBS solution for 7 minutes and washed 3 x 5 minutes in PBS. Cells were permeabilised by incubation in 0.5% saponin (Sigma-Aldrich) in PBS for 10 minutes followed by 3 x 5 minutes washing in PBS. Cells were then blocked with 1% BSA (Sigma-Aldrich) in PBS solution for 30 minutes and incubated with primary antibody (mouse anti-V5 1:500, Invitrogen) for 2 hours in a humidified chamber. After 3 x 5 minutes washing in PBS coverslips were incubated with secondary antibody (goat anti-mouse AlexaFluor 596 1:500, Cell Signaling) for 1 hour in the dark. Following 3 x 5 minutes washing in PBS, coverslips were mounted in DAPI-containing Vectashield (Vector Labs) and analyzed using Leica SP5 Confocal Microscope.

2.3 Transient transfection of HEK293 cells

2.3.1 Transfection of HE293 cells for shedding experiments.

HEK293 cells were plated onto a 24-well plate at a density of $1x10^5$ cells per well and grown overnight. Next day medium was removed from the wells and replaced with 1 ml of DMEM supplemented with 10% FBS. To transiently transfect 4 wells of cells 6 µl of FuGENE 6 Transfection Reagent (Roche) were pre-incubated with 2 µg of plasmid DNA in serum-free DMEM to form the FuGENE:DNA complex. Following 30 minutes incubation the transfection mixture was added to the cells. For co-transfection experiments HEK293 cells were transfected with 6 µl of FuGENE, 1 µg of AP/V5 TMEFF2 pcDNA5 and 1 µg of plasmid encoding the appropriate protease.

2.3.2 Transfection of HEK293 cells with EGFP-TMEFF2 and TMEFF2-YFP.

HEK293 cells were plated at the density of $2.5 x10^5$ cells per well in a 6-well plate on poly-L-lysine (Sigma Aldrich) coated coverslips and grown overnight. Next day medium was removed and replaced with 2 ml of DMEM supplemented with 10% FBS. To transiently transfect 1 well of cells 6 µl of FuGENE 6 Transfection Reagent (Roche) were dissolved in 100 µl of serum-free DMEM and mixed 2 µg of plasmid DNA, encoding EGFP-TMEFF2 or TMEFF2-YFP. The transfection mixture was pre-incubated for 30 minutes to form FuGENE:DNA complex and added to the cells. Expression of EGFP-TMEFF2 and TMEFF2-YFP was analyzed 48 hours post-transfection.

2.4 Assay for alkaline phosphatase activity (AP assay)

48 hours post-transfection the conditioned medium from transfected cells was taken off. Cells were washed with 200 µl of warmed, gassed OptiMEM (GIBCO) and incubated for 1 or 3 hours in 250 µl of fresh OptiMEM at 37 ℃. In experiments with ADAM inhibitors transfected cells were incubated for 3 hours in 250 µl of OptiMEM containing 10 µM GI254023X and 10 µM GW280264X (GlaxoSmithKline). PMA-induced shedding of AP/V5 TMEFF2 and AP/V5 $\Delta_{303\text{-}320}$TMEFF2 was monitored after 1 hour treatment with different concentrations of PMA (Enzo) in 250 µl OptiMEM. An influence of PDGF-AA on AP/V5 TMEFF2 shedding was monitored after 1 hour or overnight incubation in 300 µl OptiMEM containing 10 or 100 ng/ml of recombinant human PDGF-AA (Peprotech). At the end of the incubation the culture medium was collected and centrifuged for 3 minutes at 13000 rpm. 100 µl of AP-TMEFF2 containing medium was placed in duplicates into a 96-well plate. 2 mg/ml 4-nitrophenyl phosphate (4-NPP) solution was prepared by dissolving appropriate amount of 4-NPP (Fisher Scientific) in AP buffer (100 mM This-HCl pH 9.5, 100 mM NaCl, 20 mM $MgCl_2$) and mixed at 1:1 ratio with culture medium on the plate. The accumulation of alkaline phosphatase product 4-nitrophenol (OD_{405}) was measured using FLUOstar Optima Microplate Reader (BMG Labtech) at the following time-points: 0h, 1h, 2h, 3h, 4h, 5h, 23h, 24h, 25h. Collected data were then analyzed using GraphPad Prism software by linear regression. The slope values were then used to calculate statistical significance between experimental conditions as described under each experiment.

2.5 Analysis of cell lysates by Western blotting

2.5.1 Cell lysis

Cells were lysed using RIPA lysis buffer (20 mM sodium phosphate pH 7.4, 150 mM NaCl, 1% v/v Triton-X-100) supplemented with protease inhibitor cocktail (Sigma-Aldrich, 10 µl per 1 ml of RIPA buffer), 10 mM 1,10-phenantroline (Sigma-Aldrich), 1.5 mM Na_3VO_4 (Sigma-Aldrich) and 5 mM NaF (Sigma-Aldrich). 35 µl (24-well plate) or 100 µl (6-well plate) of lysis buffer were added per well and incubated for 30 minutes on ice. Cell lysates were collected into eppendorf tubes and clarified by centrifugation for 3 minutes at 13000 rpm.

2.5.2 Protein concentration assay

Protein concentration in cell lysates was determined by the DC protein assay system (Bio-Rad) according to manufacturer's instructions. Briefly, bovine serum albumin (BSA) standards were prepared at concentrations ranging from 0-1.5 mg/ml in 0.15 M NaCl. 5 µl of BSA standard or sample were put onto 96-well plate in duplicates. 25 µl of reagent A' (20 µl of reagent S per 1 ml of reagent A) and 200 µl of reagent B were added to the plate. Following 15 min incubation at room temperature the absorbance was

measured at 570 nm. To determine the protein concentration readings were compared to the standard curve of known BSA standards and calculated using linear regression.

2.5.3 SDS-PAGE

The volume of cell lysate that contained required amount of protein was mixed with equal volume of 2x reducing sample buffer, denatured at 95℃ for 5 minutes and spun for 1 minute at 13000 rpm. Samples were separated on 4% stacking gel and appropriate resolving gel at 50 mA until the dye front reached the bottom.

2.5.4 Western blotting

Gels were equilibrated in Western blot transfer buffer and proteins were transferred to PVDF membrane (Amersham Biosciences) at 75 V for 1 hour using transfer tanks containing transfer buffer and cooling blocks. After the transfer, the membrane was blocked in 5% skimmed milk-TBST solution for 1 hour at room temperature. Primary antibodies were diluted in 5% skimmed milk-TBST solution and incubated with the membrane overnight at 4℃ on a rotating shaker. The list of primary and secondary antibodies used in this thesis is presented in Table II. Following 3x5 minutes washing with TBST, the membrane was incubated with secondary antibodies diluted in 5% skimmed milk-TBST for 1 hour at room temperature. The membrane was then washed with TBST for 15, 10 and 5 minutes followed by 5 minutes washing in TBS. Each membrane was incubated with 1 ml EZ-ECL Chemiluminescence Detection Reagent (Biological Industries, 1:1 Reagent A: Reagent B v/v) for 3 minutes and exposed to ECL™ Hyperfilm (Amersham Biosciences) for the appropriate amount of time. Films were developed using a CURIX 60 automated developer (AGFA – Healthcare N.V.).

2.5.5 Stripping for re-probing Western blots

To re-probe Western blot with another antibody the PVDF membrane was incubated for 30 minutes at 50℃ in a stripping buffer and then washed 3x 5 minutes in TBS followed by 1 hour blocking in 5% skimmed milk-TBST. Incubation with primary and secondary antibody was performed as described above.

Table 2.2. Primary and secondary antibodies used for Western blotting.

Antibody	Manufacturer	Catalogue number	Dilution	Working concentration
Primary antibody:				
mouse anti-V5	Invitrogen	R960-25	1:5000	20 ng/ml
mouse anti-GAPDH	Sigma-Aldrich	G8795	1:2500	25 ng/ml
rabbit anti-matriptase	Calbiochem	IM1014	1:1000	25 ng/ml
mouse anti-matriptase (M32)	-	-	1:2000	50 ng/ml
sheep anti-hepsin	R&D Systems	AF4776	1:1000	200 ng/ml
mouse anti-prostasin	Becton Dickinson	612173	1:1000	250 ng/ml
rabbit anti-ADAM9	R&D Systems	MAB939	1:1000	250 ng/ml
rabbit anti-ADAM15	Abcam	Ab4834	1:2000	250 ng/ml
mouse anti-FLAG	Sigma-Aldrich	F7425	1:5000	20 ng/ml
rabbit anti-pERK1/2	Cell Signaling	4370	1:5000	88 ng/ml
mouse anti-ERK1/2	Cell Signaling	9107	1:5000-1:1000	120-240 ng/ml
goat anti-PDGFRα	R&D Systems	AF-307-NA	1:4000	50 ng/ml
mouse anti-β-tubulin	Sigma-Aldrich	T4026	1:2000	200 ng/ml
goat anti-TMEFF2	R&D Systems	AF1867	1:4000	50 ng/ml
Secondary antibody:				
donkey anti-mouse F(ab')2 Fragment, HRP conjugated	Jackson ImmunoResearch	715-036-151	1:5000	16 ng/ml
donkey anti-rabbit, HRP conjugated	Jackson ImmunoResearch	711-005-152	1:5000	20 ng/ml
rabbit anti-goat, HRP conjugated	Jackson ImmunoResearch	305-035-045	1:5000	20 ng/ml
donkey anti-sheep, HRP conjugated	Jackson ImmunoResearch	713-005-147	1:5000	20 ng/ml

2.6 Coomassie Blue R-250 staining

Following electrophoresis polyacrylamide gels were incubated in Coomassie staining solution (3% Coomassie Brillinat Blue R-250, 10% acetic acid, 45% methanol) for 30 minutes and destained for required amount of time in Coomassie destain solution (10% acetic acid, 50% methanol).

2.7 Silver staining

To detect nanogram amounts of proteins present in the sample polyacrylamide gels were stained with silver according to the following steps (all reagents purchased from Sigma Aldrich except of ethanol and acetic acid purchased from Fisher Scientific):

Step:	Solution:	Incubation time:
1. Fix	ethanol/acetic acid/H_2O 50/12/38	minimum 1 hour
2. Wash	50% ethanol (v/v)	3x 5 minutes
3. Sensitize	0.02% $Na_2S_2O_3$	5 minutes
4. Wash	H_2O	2x 20 seconds
5. Impregnation	0.2% $AgNO_3$ + 0,015% formaldehyde	20 minutes
6. Wash	H_2O	2x 20 seconds
7. Develop	4% Na_2CO_3 + 0.015% formaldehyde	as required
8. Wash	H_2O	2x 20 seconds
9. Stop	ethanol/acetic acid/H_2O 50/12/38	

2.8 Construction of ^{HR}EGF TMEFF2 MBP-fusion expression vector

2.8.1 Overlap extension polymerase chain reaction (PCR)

The overlap extension PCR method was used in order to introduce a point mutation substituting the His39 codon (CAC) within the sequence of an EGF-like domain of TMEFF2 with the codon for Arg (CGC). This method enables the mutation of a single base pair as well as the incorporation of desired restriction sites flanking the sequence of interest by performing three PCR reactions. The sequences of primers used in these reactions are presented below:

	Sequence	Tm [°C]
Primer A	5' GTTATACTGGACAACGCTGTGAAAAAAAGGACTAC 3'	67.1
Primer B	5' GCAGCCGGATCAAGCTTAGACATACTGAAATCG 3'	69.5
Primer C	5' GCAGAATTCGGGCATTATGCAAGAACAGATTATGCA 3'	68.3
Primer D	5' ATGGTCCTTTTTTTCACAGCGTTGTCCAGTATAAC 3'	67.1

Primers A and D contained the designed point mutation (indicated in red) whereas primers B and C carried *HindIII* and *EcoRI* restriction sites, marked in the table above in green and blue, respectively. All primers were synthesised by MWG Operon (Germany).

First two PCR reaction (PCR1 and PCR2) were carried out using a 2ndFS+EGF TMEFF2 MAL pRSET B plasmid template and two primers – one carrying the point mutation (primer A or D) and one introducing the restriction site (primer C or D). Products of these reactions contained the point mutation (Both products) as well as *HindIII* (PCR1 product) or *EcoRI* (PCR2 product) restriction site and were partially complemented. PCR1 and PCR2 products were mixed with 5x loading buffer (QIAgen) and separated under constant voltage (100V) in 2% agarose gel containing ethidium bromide (Sigma-Aldrich) in 1xTEA buffer. The fragments were then extracted from the gel using QIAquick Gel Extraction Kit (QIAgen) according to manufacturer's instructions, mixed in appropriate ratio and used as a template in PCR3. PCR3 reaction was performed using primers A and D in order to amplify the whole ^{HR}EGF TMEFF2 fragment. The product of PCR3 (^{HR}EGF TMEFF2) was analyzed by electrophoresis using 1% agarose gel (1xTEA buffer, 100V) and purified using QIAquick Gel Extraction Kit (QIAgen).

The composition of each PCR master mix as well as programmes used to amplify DNA fragments are summarised in Table 2.5. All three PCR reactions were carried out using 96-well thermal cycler from VWR.

Table 2.3. Summary of overlap extension PCR reactions.

	Reaction components	PCR program
PCR 1	• 1 µl of plasmid template • 1 µl Herculase II DNA polymerase (Agilent) • 1x Herculase II buffer (Agilent) • 5 mM dNTP (Agilent) • 1 µl DMSO • 1 µl primer A • 1 µl primer B • 34 µl nuclease-free water	• Initialization step: 98℃ 2min • Denaturation: 98℃ 30 sec • Annealing: 60℃ 30 sec • Elongation step: 72℃ 3 min (20 cycles) • Final elongation: 72℃ 15 min • Store: 4℃
PCR 2	• 1 µl of plasmid template • 1 µl Herculase II DNA polymerase (Agilent) • 1x Herculase II buffer (Agilent) • 5 mM dNTP (Agilent) • 1 µl DMSO (NEB) • 1 µl primer C • 1 µl primer D • 34 µl nuclease-free water (GIBCO)	• Initialization step: 98℃ 2min • Denaturation: 98℃ 30 sec • Annealing: 60℃ 30 sec • Elongation step: 72℃ 3 min (20 cycles) • Final elongation: 72℃ 15 min • Store: 4℃
PCR 3	• 10 µl of PCR1 product • 1 µl of PCR2 product • 1 µl Herculase II DNA polymerase (Agilent) • 1x Herculase II buffer (Agilent) • 5 mM dNTP (Agilent) • 1 µl DMSO (NEB) • 1 µl primer A • 1 µl primer D • 24 µl nuclease-free water (GIBCO)	• Initialization step: 98℃ 2min • Denaturation: 98℃ 30 sec • Annealing: 60℃ 30 sec • Elongation step: 72℃ 1 min (20 cycles) • Final elongation: 72℃ 4 min • Store: 4℃

2.8.2 Restriction digest

Purified ^{HR}EGF TMEFF2 PCR fragment as well as MAL pRSET vector were digested for 1 hour at 37°C with *HindIII* and *EcoRI* restriction enzymes (New England Biolabs) in the presence of NEBuffer 2, separated in 1% agarose gel and extracted from the gel using QIAquick Gel Extraction Kit (QIAgen).

2.8.3 Ligation

1 µl of MAL pRSET vector and 3 µl of PCR3 product were used to perform ligation in the presence of 1 µl T4 DNA ligase and 5 µl of 2x T4 ligation buffer (Promega) for 1 hour at room temperature.

2.8.4 $^{H-R}$EGF TMEFF2 MAL pRSET amplification

5 µl of the ligation mixture were added to 50 µl of NovaBlue GigaSingles competent *E. coli* and incubated for 10 minutes on ice followed by 30 sec heat shock at 42°C in a water bath. Transformed cells were then plated in several dilutions on LB agar plates containing 50 µg/ml carbenicillin and grown overnight at 37°C. Next day single colonies were picked randomly, mixed with 3 ml of LB containing 50 µg/ml carbenicillin and grown for 6 hours at 37°C on a shaking platform. 1.5 ml of each culture was used to extract plasmid DNA using QIAprep Spin MiniPrep Kit. DNA was then cleaved with *HindIII* and *EcoRI* and analyzed in 1% agarose gel. *E. coli* clone containing an insert of the correct length was grown in 100 ml LB + 50 µg/ml carbenicillin and used to extract plasmid DNA with GenElute HP Plasmid DNA Midiprep Kit (Sigma-Aldrich).

2.9 Expression and purification of MBP-fusion proteins in *E.coli*

2.9.1 Transformation of bacteria

TMEFF2-ECD, 2xFS, 2ndFS+EGF and EGF TMEFF2 MAL pRSET vectors were cloned and purified by Dr Vera Knäuper. All plasmids were sequenced before they were used to transform bacteria. Sequences of all MBP-fusion proteins are included in Appendix II.

50-100 pg of plasmid DNA was mixed with Origami B(DE3)pLysS (Novagen) or SHuffle T7 Express *lysY* (New England Biolabs) competent *E. coli* and incubated on ice for 30 min. After 30 seconds heat shock at 42°C 500 µl of LB medium was added to the cells and the bacteria were grown for 1 hour at 37°C on a shaking platform. Transformed bacteria were then diluted and plated on LB agar plates containing the following antibiotics (Sigma-Aldrich):

- Origami B(DE3)pLysS: 50 µg/ml carbenicillin, 12.5 µg/ml tetracycline, 15 µg/ml kanamycin, 34 µg/ml chloramphenicol
- SHuffle T7 Express *lysY*: 50 µg/ml carbenicillin

Randomly picked single colonies were used to inoculate 10 ml liquid cultures and these were grown overnight at 37°C on a shaking platform. Glycerol stocks of transformed bacteria were prepared by mixing 0.5 ml of overnight culture with 0.5 ml of sterile 50% glycerol in LB solution and stored at -80°C.

2.9.2 Expression of recombinant proteins

10 ml of overnight Origami B(DE3)pLysS or Shuffle T7 Express *lysY* culture was added to 400 ml of rich broth containing the appropriate antibiotics and grown at 37°C until the OD_{600} reached the value 0.4-0.5. The OD was monitored using DU 800 Spectrophotometer (Beckman Coulter). At this point IPTG (Sigma-Aldrich) was added to the final concentration of 1 mM to induce protein expression and the culture was grown overnight at 16°C in a shaking incubator. The non-induced culture was maintained as a non-induced control.

2.9.3 Analysis of protein expression following IPTG induction

1 ml of the non-induced and induced culture was centrifuged for 15 minutes at 4000 rpm. The pellet was mixed with 200 µl of 2x reducing sample buffer and denatured for 5 minutes at 95°C. Expression of the MBP-fusion proteins was analyzed using SDS-PAGE electrophoresis using 4% stacking gel and 11% resolving gel. The gel was stained with Coomassie Brilliant Blue R-250 as described in the previous sections.

2.9.4 First step purification: affinity chromatography on amylose resin

500 ml of overnight bacteria culture were harvested by centrifugation for 20 minutes at 4000 rpm and resuspend in 50 ml of column buffer (20 mM Tris-HCl pH 7.4, 200 mM NaCl, 1 mM EDTA) containing a *Complete* protease inhibitor cocktail tablet (Roche, 1 tablet per 50 ml of buffer) and 1 mM PMSF (Sigma-Aldrich). Bacteria were stored frozen overnight, thawed and lysed by sonication. The extract was clarified by centrifugation for 30 minutes at 20000 rpm. 5 ml of amylose-resin (New England BioLabs) was equilibrated by incubating 2x10 minutes with 20 ml of column buffer at 4°C. The column buffer was removed and the amylose resin was incubated with bacterial extract overnight at 4°C on a rotating wheel. Next day the amylose-resin was loaded into the column and washed with column buffer until no protein was detected in the flow-through (OD_{280} of the flow-through = OD_{280} of the column buffer). The MBP fusion proteins were eluted with column buffer containing 10 mM maltose (Sigma-Aldrich). Elution of recombinant proteins was monitored by measuring OD_{280} on NanoVue Spectrophotometer

(GE Healthcare). Fractions containing the highest amount of protein were combined and dialysed overnight at 4°C into 20 mM sodium phosphate pH 6.4 containing 25 mM NaCl.

2.9.5 Second step purification: gel filtration

In order to further purify MBP-fusion proteins Superdex 200 10/300 GL column (GE Healthcare) was connected to ÄKTA*purifier* system (Amersham Pharmacia Biotech Inc.) and equilibrated with 20 mM sodium phosphate pH 6.4 containing 25 mM NaCl. 200 µl of recombinant protein sample was injected into the column and separated with the flow rate of 0.4 ml/min. Samples containing less than 1 mg/ml of MBP-fusion protein were concentrated using Vivaspin 500 centrifugal concentrators (Sartorius Stedim Biotech) by spinning at 13000rpm at 4°C for the required amount of time prior to loading into the column. Separation of the proteins present in the sample was monitored by measuring OD_{280} and eluted 0.5 ml fractions were collected.

2.9.6 Calculation of protein concentration using extinction coefficient factor

Concentration of separated EGF-like domains monomers and dimers was established by dividing the OD_{280} value of the fraction by the protein extionction coefficient factor. Extinction coefficient factors were calculated using Biology WorkBench 3.2 software based on the protein sequence and are presented below:

MBP-fusion protein	Extinction coefficient factor
EGF from HB-EGF	1.260
EGF from TMEFF2	1.270
^{HR}EGF from TMEFF2	1.349

2.10 Generation of N-protein A TMEFF2 expression plasmids

2.10.1 Amplification of TMEFF2 ectodomain fragments by PCR

DNA sequences encoding fragments of TMEFF2 ectodomain were amplified using AP/V5 TMEFF2 pcDNA5/FRT plasmid as a template and following primers:

	Sequence	Tm [℃]
Primer 1	5'-ATAGGATCCGCTTTCCCTACCTCCTTAAGTGACTGC-3'	71.7
Primer 2	5'-ATAGGATCCGGAGTCCATGAAGGCTCTGGAGAAACT-3‘	71.7
Primer 3	5'-ATAGGATCCAAGTCTGAAGATGGGCATTATGCAAGA-3‘	68.3
Primer 4	5'-TATCTCGAGTTATTCTCTGGCACTTTCTTCTAATTTGTTAGC-3‘	68.5
Primer 5	5'-ATACTCGAGTTAGACATACTGAAATCGTACAGGACC-3'	68.3

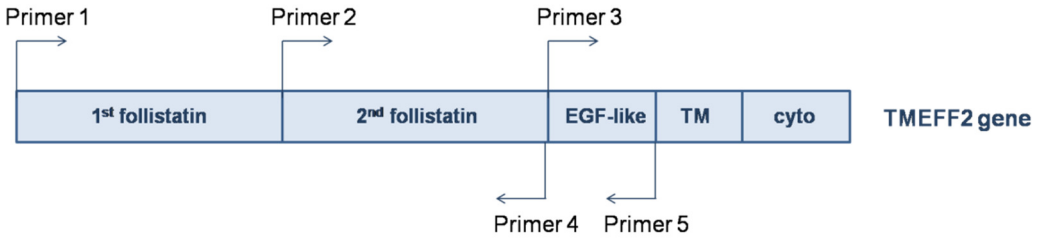

In order to clone amplified TMEFF2 fragments into the expression vector upstream of the IgG signal sequence-protein A fusion gene *BamHI* (marked in green) and *XhoI* (marked in blue) restriction sites were introduced in the primers.

PCR reactions were performed in the presence of Herculase II DNA polymerase, 1x Herculase II buffer, 5 mM dNTPs (Agilent), DMSO (New England BioLabs), nuclease-free water (GIBCO), AP/V5-TMEFF2 pcDNA5/FRT plasmid template and the pair of primers:

TMEFF2-ECD	Primer 1 Primer 5
TMEFF2 2xFS	Primer 1 Primer 4
TMEFF2 2ndFS+EGF	Primer 2 Primer 4
TMEFF2 EGF	Primer 3 Primer 5

PCR amplification was carried out using 96-well thermal cycler from VWR with the following settings:

- Initialization step: 98℃ 2min
- Denaturation: 98℃ 30 sec
- Annealing: 60℃ 30 sec
- Elongation step: 72℃ 2 min

(20 cycles)

- Final elongation: 72℃ 4 min
- Store: 4℃

Products of each PCR reaction were purified using QIAquick PCR Purification Kit (QIAgen) according to manufacturer's instruction.

2.10.2 Restriction digest

Purified PCR products were cleaved overnight at 37℃ with *BamHI* and *XhoI* in the presence of NEBuffer 2. pcDNA/FRT plasmid containing IgG signal sequence-protein A fusion gene, generated previously by Dr Vera Knäuper, was cleaved with the same enzymes for 1 hour at 37℃.

2.10.3 Ligation and plasmid amplification

BamHI and *XhoI*-cleaved inserts and vector were separated using 1% agarose gel and purified with Qiaquick Gel Extraction Kit (QIAgen). The appropriate amount of inserts and vector were then mixed and ligated for 1 hour at room temperature in the presence of 1 µl T4 DNA ligase and 5 µl of 2x T4 ligation buffer (Promega). The ligation mixture was used to transform NovaBlue GigaSingles *E. coli* as described is paragraph 2.8.5.

2.11 Generation of TMEFF2-ECD-Fc pcDNA5/FRT vector

2.11.1 Restriction digest

TMEFF2-ECD-Fc pcDNA5/FRT expression vector was generated using TMEFF2-ECD pcDNA4 and Fc-pcDNA5/FRT vectors, constructed previously by Dr Vera Knäuper. Both vectors were digested with *XhoI* and *HindIII* (Promega) for 1 hour at 37℃, in the presence of NEBuffer 2 (New England Biolabs). DNA fragment corresponding to TMEFF2-ECD as well as Fc-pcDNA5/FRT were separated using 1% agarose gel and extracted using QIAquick Gel Extraction Kit (QIAgen) according to manufacturer's instruction.

2.11.2 Ligation and plasmid amplification

1 µl of *XhoI* and *HindIII*-cleaved Fc-pcDNA5/FRT was mixed with 3 µl TMEFF2-ECD insert, 5 µl 2x T4 ligation buffer and 1 µl of T4 DNA ligase (Promega). The ligation mixture was then incubated for 1 hour at room temperature and used to transform NovaBlue GigaSingles competent *E. coli.* Single colonies were then analyzed for the presence of the TMEFF2-ECD-Fc insert. The plasmid was amplified as described previously in section 2.8.5.

2.12 Generation of CHO cell lines stably expressing Fc- and N-protein A fusion TMEFF2 fragments

Cell lines stably expressing Fc and N-protein A TMEFF2 fusion proteins were generated using the Flp-In System (Invitrogen), which is described in detail in Appendix III. $1x10^5$ CHO Flp-In cells were plated per well on a 6-well plate and grown overnight. Next day conditioned medium was replaced with 2 ml of Ham's F12 containing 10% FBS. To transfect one well of cells 1.8 µg pOG44 plasmid was mixed with 0.2 µg of TMEFF2 expression vector in serum free OptiMEM medium. 6 µl of FuGENE 6 Transfection Reagent (Roche) were diluted in OptiMEM and added to the DNA solution. The FuGENE-DNA mixture was incubated for 30 minutes in room temperature to allow the FuGENE:DNA complex to form. The transfection mixture as then added to the cells in a drop-wise manner. 24 hours post transfection conditioned medium was replaced with Ham's F12 supplemented with 10% FBS and 500 µg/ml hygromycin B. The selection medium was then replaced daily until the colonies of stably transfected cells were large enough to be transferred into a T25 tissue culture flask. The cells were subsequently grown in the present of 500 µg/ml hygromycin B and expanded to generate enough cells to perform the experiments and to produce stock aliquots for freezing.

2.13 Collection of conditioned medium

$3x10^6$ of stably transfected CHO cells were seeded in TripleFlasks 500cm^2 (Thermo Scientific Nunc) and grown in 200 ml of CHO-S-SFM II medium supplemented with 0.1 mM non-essential amino acids (GIBCO), nucleosides (26 µM adenosine, 25 µM guanosine, 27 µM uridine and 28 µM cytidine, Sigma-Aldrich) and 1% ultra low IgG FBS (Invitrogen) until confluent. Conditioned medium containing TMEFF2-ECD-Fc or N-protein A TMEFF2 fragments was collected, centrifuged for 5 min at 1500g to remove cell debris and transferred to a new tube. 1M Tris-HCl pH 7.4 was added to the medium to a final concentration of 5 mM Tris in order to prevent pH change during freezing. The medium was stored at -80℃.

2.14 Purification of N-protein A TMEFF2 fragments

2.14.1 Packing and equilibration of IgG Sepharose column

3 ml of IgG Sepharose 6 Fast Flow (GE Healthcare) were packed into a column, connected to an ÄKTA*prime* system (Amersham Pharmacia Biotech Inc.) and washed with 5 bed volumes of TST buffer (50 mM Tris-HCl pH 7.6, 150 mM NaCl, 0.05% Tween 20) to remove ethanol present in the storage solution. IgG Sepharose was then equilibrated with 3 bed volumes of the following solutions:

- 0.5 M acetic acid pH 3.4 (pH adjusted with 0.5 M ammonium acetate)
- TST
- 0.5 M acetic acid pH 3.4
- TST

2.14.2 Binding and elution of protein A fusion protein

500 ml of the conditioned medium containing N-protein A tagged TMEFF2-ECD was thawed overnight at 4℃ and the pH was adjusted to 7.0 with 100 mM HCl. The medium was filtered through 0.22 µm nitrocellulose filter membrane (Millipore) prior to applying to IgG Sepharose column at 4℃ with the flow rate of 1 ml/min. The column was then connected to ÄKTA*purifier* system (Amersham Pharmacia Biotech Inc.) and washed with 10 bed volumes of TST buffer and 2 bed volumes of 5 mM ammonium acetate pH 5.0. Protein A fusion protein was eluted with 0.1 M glycine-HCl pH 2.7 and 0.5 ml of eluted fractions were collected into tubes containing 80 µl of 1M Tris-HCl pH 9.0 to neutralise the pH.

2.14.3 Re-equilibration and storage of IgG Sepharose

IgG Sepharose column was washed with TST buffer until the pH of the eluate was around 7.0 followed by washing with 5 bed volumes of 20% ethanol in TST. The column material was then stored at 4°C.

2.15 Purification of Fc-TMEFF2 ectodomain

2.15.1 First step purification: affinity chromatography using protein G Sepharose

2.5 litres of thawed conditioned medium was dialysed overnight against 40 L of 20 mM sodium phosphate pH 7.0 and filtered through 0.45 µm nitrocellulose filter membrane (Millipore). The medium was then applied into a 1 ml Protein G Sepharose column (GE Healthcare) at 1 ml/min using ÄKTA*prime* system (Amersham Pharmacia Biotech Inc.). The column was washed with 20 mM sodium phosphate pH 7.0 until the OD_{280} of the eluate reached zero. The column was then connected to ÄKTA*purifier* system (Amersham Pharmacia Biotech Inc.) and the TMEFF2-ECD-Fc was eluted with 0.1 M glycine-HCl pH 2.7 with the flow rate of 0.5 ml/min. The change of the pH and OD_{280} were monitored during elution. Fractions were collected into tubes containing 1M Tris-HCl pH 9.0 to immediately neutralise the pH of eluted protein solution. Fractions containing the highest amount of protein were analyzed by SDS-PAGE and Coomassie Blue R-250 staining, silver staining or Western blotting according to previously described protocols.

2.15.2 Second step purification: HIS-Select HF Nickel Affinity Gel

Combined fractions containing TMEFF2-ECD-Fc purified using protein G Sepharose were mixed with 4M NaCl to a final NaCl concentration of 300 mM. 200 µl of HIS-Select HF Nickel Affinity Gel (Sigma-Aldrich) was washed 3 times with 1 ml of His-Select equilibration and wash buffer (50 mM Tris-HCl pH 8.0, 300 mM NaCl, 10 mM imidazole) and incubated with TMEFF2-ECD-Fc overnight at 4°C on a rotating wheel. Next day the medium was removed from the Nickel Affinity Gel by 5 minutes centrifugation at 1500g. The Nickel Affinity Gel was washed 5 times with 1 ml of wash and equilibration buffer. The elution of TMEFF2-ECD-Fc was performed 5 times with 200 µl of the elution buffer (50 mM Tris-HCl pH 8.0, 300 mM NaCl, 250 mM imidazole). The presence of TMEFF2-ECD-Fc in eluted fractions was analyzed by Western blotting and labelling with anti-TMEFF2-ECD antibody according to previously described protocol. The fractions containing TMEFF2-ECD-Fc were dialysed overnight at 4°C against 20 mM sodium phosphate buffer pH 7.4 to remove imidazole before being used in further experiments.

2.16 Analysis of ERK1/2 phosphorylation

2.16.1 Cell stimulation and sample analysis

HEK293 ($3x10^5$/well) or PNT2-C2 ($1x10^5$/well) cells were plated onto 24 well plate in medium containing 10% FBS. The next day medium was removed and 400 µl of serum free medium was added to the cells. PNT2-C2 cells were serum starved in the presence of 25 µM GM6001 inhibitor (Enzo) to reduce activation of endogenous ErbB ligands. Following serum starvation cells were treated for 5 or 15 minutes with 300 µl serum free medium containing recombinant MBP-fusion proteins. Medium with addition of buffer solvent or 10% FBS was used as negative and positive control, respectively. After treatment cells were lysed with 35 µl of RIPA buffer supplemented with protease inhibitor cocktail (Sigma-Aldrich, 10 µl/ 1 ml of RIPA buffer), phosSTOP phosphatase inhibitor cocktail (Roche, 25x solution prepared by dissolving 1 phosSTOP tablet in 1 ml of H_20), 1.5 mM Na_3VO_4 (Sigma-Aldrich) and 5 mM NaF. Cell lysates were then analyzed for pERK1/2 and total ERK1/2 by Western blotting as described in paragraph 2.5.

2.16.2 Quantification of the pERK1/2 to total ERK1/2 ratio using ImageJ

Intensities of the bands corresponding to pERK1/2 and total ERK1/2 were quantified using ImageJ software. Gel pictures were opened in the ImageJ and the pERK1/2 and total ERK1/2 bands were marked using the *Rectangular selection* tool. The *Plot lanes* option was used to draw profile plots of all bands which represented the relative density of the contents of the rectangle for each lane. The peaks were enclosed using the *Straight lane* tool by drawing a line across the base of the peak. The size of each peak was then quantified using the *Wand* tool and obtained values were copied into a Microsoft Office Excel spreadsheet. The pERK1/2 to total ERK1/2 ratio was calculated for each sample by dividing the size of the pERK1/2 peak by the size of the total ERK1/2 peak. In order to be able to compare pERK1/2 to total ERK1/2 values between experiments the pERK1/2 to totalERK1/2 value obtained for the positive control was set to 1 and used to calculate the relative pERK1/2 to totalERK1/2 ratios. The data was plotted as histograms using GraphPad Prism software.

2.17 Cell proliferation assay

Proliferation of cells grown in the presence of recombinant TMEFF2 fragments was assessed using Cell Proliferation Kit II (XTT) from Roche. In this assay cells are grown in 96-wells plates in the presence or absence of the tested molecule for the required amount of time followed by incubation with the XTT reagent to establish the number of viable cell in each well. The yellow XTT tetrazolium salt is reduced by succinate dehydrogenase system of the mitochondrial respiratory chain to form an orange formazan dye, as presented in Figure 2.1. Only living cells, possessing an intact mitochondrial and cellular membranes do have active dehydrogenase and are able to metabolize XTT to formazan. The amount of the soluble formazan salt can be quantified by measuring OD_{450} allowing to directly compare the number of viable cells between experimental conditions (Scudiero et al. 1988; Jost et al. 1992).

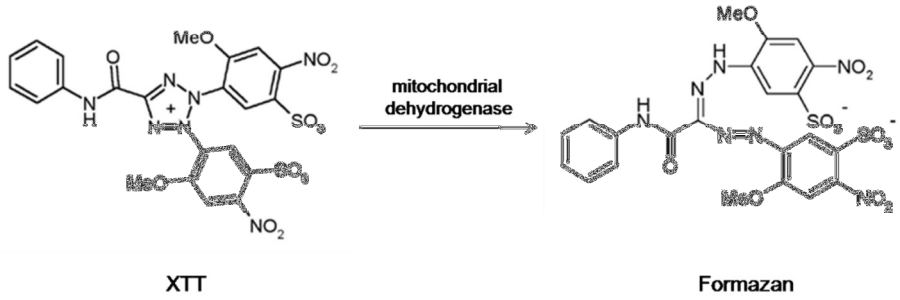

Figure 2.1 Reduction of XTT tetrazolium salt to formazan by dehydrogenases of the mitochondrial respiratory chain (from www.roche-applied-science.com).

2.17.1 Proliferation of CHO cells the presence of N-protein A TMEFF2 medium

CHO cells were plated into 96-well plates at a density of 600 cells per well in Ham's F12 medium containing 0.5% FBS. Next day medium was replaced with 100 µl of conditioned medium from CHO Flp-In parental cells or stable CHO cell lines expressing N-protein A TMEFF2 fragments. 24, 48 and 72 hours later the number of viable cells in each well was measured using the Cell Proliferation Kit II (XTT) according to manufacturer's instructions (Roche). Briefly, 50 µl of the XTT solution (XTT labeling reagent: electron coupling reagent 50:1) was added per well and the OD_{450} (absorbance of the soluble formazan salt) was measured after 4 hours incubation at 37°C. The obtained measurements were then corrected by the values of OD_{620}. The assay was performed using FLUOstar Optima Microplate Reader (BMG Labtech).

2.17.2 PNT2-C2 proliferation in the presence of TMEFF2-ECD-Fc

1000 of PNT2-C2 cells were seeded into 96-well plate in RPMI 1640 supplemented with 0.5% FBS. Following overnight growth conditioned medium was replaced with RPMI 1640 containing 0.5% FBS and different concentrations of TMEFF2-ECD-Fc. 72 or 96 hours later the number of valiable cells was measured in each well by Cell Proliferation Kit II (XTT) as described in section 2.17.1.

2.18 Preparation of nuclear and cytoplasmic extract

HEK293 cells were plated into poly-L-lysine coated 24-well plates at the density of $1x10^5$/well and transfected the next day with AP/V5 TMEFF2 or AP/V5 HB-EGF expression plasmids as described in section 2.3. In some experiments 48 hours post-transfection conditioned medium was replaced with serum free DMEM containing 10 ng/ml leptomycin B (Sigma-Aldrich) or carrier control and incubated for 2 hours at 37℃. At this point 100 ng/ml PMA was added to some wells. After 1 hour treatment medium was taken off the cells and 50 µl of cold Buffer C (10 mM HEPES pH 7.9, 10 mM KCl, 0.1mM EDTA, 1 mM DTT, 8 mM β-glycophosphate, 300 µM Na_3VO_4) supplemented with protease inhibitor cocktail (Sigma-Aldrich, 10 µl per 1ml of Buffer C) was added to each well. Following 15 minutes incubation on ice cell lysates were collected into eppendorf tubes, supplemented with 0.2% NP-40 (Fluka) and incubated on ice for further 20 minutes. Cell extract was then centrifuged for 1 min at 13000 rpm and the supernatant containing cytoplasmic extract was collected into a new eppendorf tube. Pellet containing cell nuclei was then washed once with 50 µl of Buffer C and resuspend in 60 µl of cold Buffer N (20 mM HEPES pH 7.9, 10% glycerol, 0.4M NaCl, 1mM EDTA, 1mM EGTA, 1 mM DTT, 8 mM β-glycophosphate, 300 µM Na_3VO_4) supplemented with protease inhibitor cocktail (Sigma-Aldrich, 10 µl per 1ml of Buffer N). After 30 minutes incubation at 4℃ on a rotating wheel the extract was centrifuged for 1 minute at 13000 rpm to obtain supernatant containing nuclear proteins.

2.19 Statistical analysis

Statistical analysis was assessed by one-way ANOVA and the differences of the means between samples were determined using Tukey test. P-values below 0.05 were considered significant. The number of independent experimental repeats is indicated in each figure caption.

Chapter 3:

Expression of TMEFF2 and serine proteases in prostate cancer

3.1 Introduction.

3.1.1 Expression of TMEFF2 in prostate cancer.

As described in the Introduction, TMEFF2 is expressed almost exclusively in two organs – brain and prostate (Liang et al. 2000, Horie et al. 2000). Elevated expression of TMEFF2 was detected in 74% of primary prostate cancer and 42% of metastatic lesions from lymph nodes and bone (Afar et al. 2004). Immunolocalization of TMEFF2 in biopsies obtained from prostate cancer patients revealed that TMEFF2 localizes in the malignant compartment of the tumour rather than within the surrounding benign tissue (Glynne-Jones et al. 2001). However, it is not known if TMEFF2 is expressed by all types of cells that are present in the tumor or whether it is restricted to some specialized cell subsets. These data suggest that TMEFF2 expression correlates with a more invasive phenotype of prostate cancer. However, analysis of TMEFF2 levels in prostate cancer cell lines revealed that this protein is present only in the androgen-sensitive cell line LNCaP and the expression of TMEFF2 is lost in more metastatic, androgen-independent DU-145 and PC3 cell lines (Gery et al. 2002). These observations suggest that TMEFF2 is expressed by prostate cancer cells in the initial stages of the disease when the growth is androgen-dependent and TMEFF2 expression decreases when the disease progresses to a more invasive, androgen-independent phenotype.

It is now known that TMEFF2 is shed from the cell surface by ADAM10 and ADAM17 resulting in the release of TMEFF2-ECD (Ali & Knäuper 2007) but the biological significance of TMEFF2 shedding is incompletely understood. Increased proteolysis resulting from dysregulated expression of proteolytic enzymes is one of the hallmarks of cancer cells (Lee et al. 2004; Netzel-Arnett et al. 2003; Mochizuki & Okada 2007). For that reason it was hypothesized that proteolysis might be involved in the regulation of TMEFF2 biological function and the analysis of TMEFF2 processing by proteases over-expressed in prostate cancer might help to understand the role of TMEFF2 in the development of cancer disease.

3.1.2 Dysregulated expression of potential TMEFF2 sheddases in prostate cancer.

To investigate the hypothesis that the function of TMEFF2 in the development of prostate cancer is regulated by processing mediated by different proteases, several proteolytic enzymes implicated in prostate cancer were considered as potential novel TMEFF2 sheddases.

The most interesting protease involved in the progression of prostate cancer is type II transmembrane serine protease hepsin. Hepsin is one of the highly over-expressed genes in prostate cancer, whereas its expression in normal prostate tissue and in benign prostate hyperplasia is minimal (J Luo et al. 2001). Hepsin mRNA was found to be elevated in 90% of prostate tumours with levels often increased by more than 10 fold

(Dhanasekaran et al. 2001). Interestingly, *in situ* hybridization showed that hepsin is expressed specifically by carcinoma cells themselves rather than by prostate stroma (Magee et al. 2001). Hepsin was also found in the prostate cancer cell line LNCaP (Srikantan et al. 2002). Expression of hepsin in prostate cancer significantly correlated with the poor clinical outcome of the disease. For that reason it was proposed by several research groups that expression of hepsin alone or in combination with other markers, for example UDP-N-Acetyl-alpha-D-galactosamine transferase (GalNAc-T3) will allow the diagnosis of prostate cancer by molecular profiling (Stephan et al. 2004; Landers et al. 2005; Kelly et al. 2008). It was described that patients with increased PSA levels following radical prostatectomy are likely to develop distant metastases and die due to prostate cancer. This medical condition is known as PSA failure (Pound et al. 1999). Analysis of hepsin levels in patients that developed PSA failure showed that high levels of PSA following radical prostatectomy were associated with loss or very weak hepsin expression (Dhanasekaran et al. 2001).

The other membrane serine protease that is significantly over-expressed in prostate cancer is matriptase. This member of the TTSP family was found in LNCaP, DU-145, CWR22Rv1 and PC-3 prostate cancer cell lines (Riddick et al. 2005; Saleem et al. 2006). As described in the Introduction, matriptase activity is tightly regulated by its inhibitor HAI-1 and the matriptase-HAI-1 ratio is often shifted towards matriptase in late stage tumour. This imbalance, resulting in increased matriptase activity was proposed to be a good prognostic marker for prostate cancer (Lin, Anders, Johnson & Dickson 1999; Saleem et al. 2006)

The expression of matriptase and hepsin is generally thought to increase with the progression of prostate cancer and indicate poor clinical outcome. In contrast, the inverse correlation was found for the GPI-anchored serine protease prostasin. Prostasin is present at high levels in normal prostate epithelial cells and in androgen-sensitive prostate cancer cell line LNCaP but its expression is lost in invasive DU-145 and PC3 cancer cell lines due to gene promoter hypermethylation (Chen, Skinner, et al. 2001; Chen et al. 2004). Decrease of prostasin was detected also in biopsies from patients with hormone-refractory prostate cancer (Takahashi et al. 2003).

The data described above indicated that the expression of membrane serine proteases significantly changes during the progression of prostate cancer. As TMEFF2 and serine proteases are likely to be expressed by the same type of cells in the tumour it was hypothesized that TMEFF2 is a novel substrate for serine protease processing.

3.1.3 Prostate cancer stem cells.

In recent years, most of the cancer research studies are based on the fact, that tumours are not simply a mass of identical cancer cells but rather they are composed of many cell types with different clonogenic and invasive potential. One of the facts arising from the discovery of tumour heterogeneity is the presence of a very specific population of cells within the tumour that can be described as cancer stem cells. This subpopulation is defined by high clonogenic and invasive potential, capacity to self-renew *in vivo* and initiate secondary tumour growth, as well as the ability to differentiate to reconstitute tumour heterogeneity (Heppner 1984; Hamburger & Salmon 1977; Maitland & Collins 2005). A growing body of evidence suggests that cancer stem cells are responsible for chemotherapy resistance as they express high levels of specific ATP-binding cassette (ABC) drug transporters. It has been hypothesized that these resistant cells may be the founder population that causes disease relapse and metastasis (Dean et al. 2005). To date the subpopulation of cancer cells with stem cell characteristics have been found in acute myeloid leukemia (Bonnet & Dick 1997), breast (Al-Hajj et al. 2003), brain (Singh et al. 2003), lung (C. F. B. Kim et al. 2005), pancreas (Li et al. 2007), skin (Fang et al. 2005) and prostate cancer (Collins et al. 2001).

Prostate cancer stem cells have been isolated for the first time from prostate cancer tissue obtained from patients undergoing radical prostatectomy and characterized by high expression of $\alpha_2\beta_1$ integrin together with the presence of CD44 and CD133 antigens ($CD44^+/ \alpha_2\beta_1^{hi}/CD133^+$). Integrin $\alpha_2\beta_1$ mediates adhesion of prostate cancer cells to bone marrow cells and thus probably contributes to the propensity of the prostate cancer to metastasize to bone. Prostate cancer stem cells represent only around 0.01% of tumor cells and display high proliferation rate *in vitro*, self-renewal and invasiveness. They are also able to differentiate into androgen receptor positive cells similar to prostate cancer cells *in situ* (Collins et al. 2005). Due to these properties $CD44^+/ \alpha_2\beta_1^{hi}/CD133^+$ stem cells are a very promising target for new prostate cancer therapy directed to eliminate the origin of the tumour resulting in a long-lasting therapeutic effect.

3.2 Aims.

Experiments described in this chapter were performed in order to examine the expression of TMEFF2 in prostate cancer cell lines using commercially available anti-TMEFF2-ECD antibody. The expression of TMEFF2 was analyzed also in clinical samples, containing lysed prostate cancer stem cells $CD44^+/ \alpha_2\beta_1^{hi}/CD133^+$. The same cell lines and patient samples were then examined for the expression of membrane-anchored serine proteases, implicated in prostate cancer progression: matriptase, hepsin and prostasin.

3.3 Results.

3.3.1 Expression of TMEFF2 in prostate cancer stem cells and cell lines.

The introduction part of this chapter indicated that in recent years more attention is paid to the fact that tumours are composed of different types of cells. Among the cells that form the tumour the subpopulation of cancer stem cells seems to be the most interesting as it is a promising target for novel anti-cancer therapies. Due to the collaboration with Professor Norman Maitland and Dr Annie Collins from the YCR Cancer Research Unit, University of York we have obtained lysates of $CD44^+/ \alpha_2\beta_1^{hi}/CD133^+$ prostate cancer stem cells isolated from 11 patients diagnosed with prostate cancer or benign prostate hyperplasia (BPH). The available details about each patient are summarized in Table 3.1.

Table 3.1 List of $CD44^+/\alpha_2\beta_1^{hi}/CD133^+$ prostate cancer stem cells clinical samples.

Sample ID	Gleason score	Age	Additional information
P1	3+3		
P2	7		
P3			no grade but cancer diagnosis
P4	BPH		
P5	5+5		anti-androgen treatment
P6	7	64	stage T2, PSA 6.1 ng/ml
P7	7	70	stage T2, PSA 6.5 ng/ml
P8	6		stage T2a, previously on hormone therapy
P9	5+4	61	receiving hormone therapy
P10	BPH	85	
P11	6	58	stage T3a, PSA 9.5 ng/ml

The prostate cancer stem cells were isolated fairly recently (Collins et al. 2001) and the data regarding the characterization of this subpopulation are still incomplete. For that reason the expression of TMEFF2 was examined in this cell subpopulation by Western blotting. Equal volumes of the obtained lysates were separated in 11% resolving gel, blotted and labeled using commercially available anti-TMEFF2 polyclonal antibody, that recognize the extracellular part of this protein. Due to the very limited amount of available material, the loading control labeling of this Western blot could not be performed, making this analysis qualitative but not quantitative. The Western blot analysis presented in Figure 3.1 showed that several bands were detected in each sample. Based on the data published previously by Glynne-Jones and colleagues it was concluded that the ~54 kDa band detected in some samples corresponded to the TMEFF2 core protein (Glynne-

Jones et al. 2001). Two bands with the apparent molecular sizes of ~75 kDa and ~100kDa, detected in samples P6, P7 and P10 potentially correspond to glycosylated variants of TMEFF2 (Glynne-Jones et al. 2001). Additionally, in all analyzed samples a ~28 kDa band was recognized by anti-TMEFF2-ECD antibody. This band was not described in the literature before as at this stage of the analysis it was hypothesized that it corresponds to some unknown product of TMEFF2 processing, containing at least a part of TMEFF2 extracellular fragment as it was detected by anti-TMEFF2-ECD antibody.

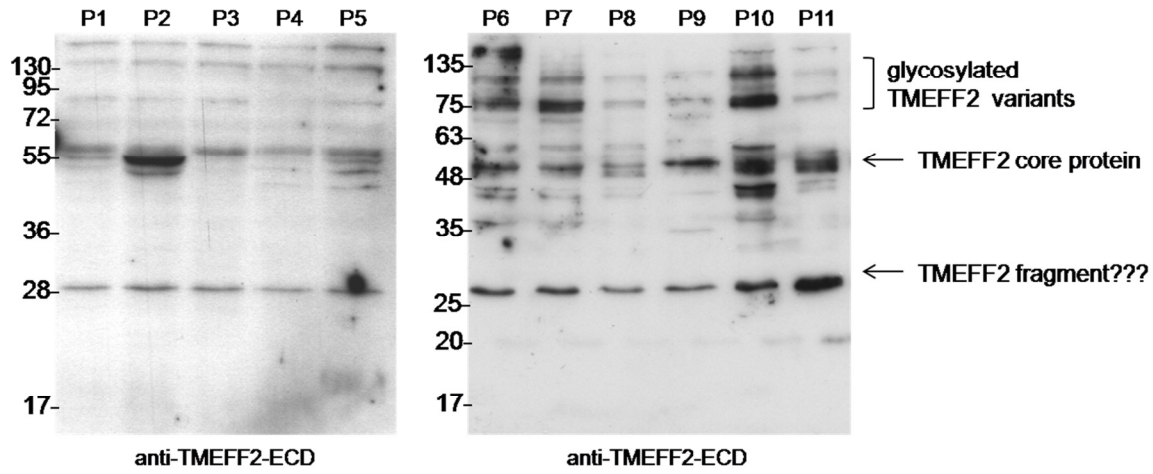

Figure 3.1 Expression of TMEFF2 in CD44^{+}/$\alpha_2\beta_1^{hi}$/CD133^{+} prostate cancer stem cells.

Equal volumes of the lysates obtained from prostate cancer cells isolated from 11 patients (P1-P11) were separated in 11% resolving gel, blotted and labeled with anti-TMEFF2-ECD polyclonal antibody. In some of the samples a ~54 kDa band corresponding to TMEFF2 core protein or ~75-100 kDa bands corresponding to glycosylated TMEFF2 variants were detected. A ~28 kDa band present in all samples is proposed to be a novel TMEFF2 fragment, not described in the literature to date.

Expression of TMEFF2 was also examined in different cell lines. Normal prostatic epithelial cells PNT2-C2, androgen dependent prostate cancer cell line isolated from lymph node metastases LNCaP, as well as androgen-independent DU145 and PC3 prostate cancer cell lines derived from brain (DU145) and bone (PC3) metastases are commonly used as *in vitro* models in prostate cancer studies. HEK293 cells and HEK293 cell line stably expressing HA/V5 TMEFF2 were included in this analysis as negative and positive controls, respectively. 50 µg of total cell lysates were separated as previously in 11% resolving gel, blotted and labeled using polyclonal anti-TMEFF2-ECD antibody. As presented in Figure 3.2 A, the highest amount of TMEFF2 was detected in LNCaP cells that expressed ~75 kDa and ~100 kDa glycosylated forms of TMEFF2 whereas no bands corresponding to TMEFF2 were detected in the lysates from HEK293 cells. In the lysate from DU145 cells weak bands corresponding to glycosylated TMEFF2 were detected and in the PC3 cells lysate the glycosylated TMEFF2 as well TMEFF2 core protein were detected. Figure 3.2 B showed anti-TMEFF2-ECD labeling of the lysate from HA/V5 HEK293 cells, indicating the main form of TMEFF2 in these cells is HA/V5 TMEFF2 core protein. The unknown ~28 kDa band was also present in some of the samples, including the lysate from PNT2-C2 and HA/V5 TMEFF2 HEK293 cells.

Detection of TMEFF2 expression in androgen-independent prostate cancer cell lines DU15 and PC3 is in disagreement with previously published data (Gery et al. 2002). This discrepancy could be explained by the use of a different method to analyze TMEFF2 expression. Gery and co-workers analyzed TMEFF2 expression by isolation of total RNA and performing northern blot analysis using a radiolabeled TMEFF2 probe. If the used probe was not complementary to the whole TMEFF2 sequence (information not included in the paper), some TMEFF2 variants might not be detected using this technique.

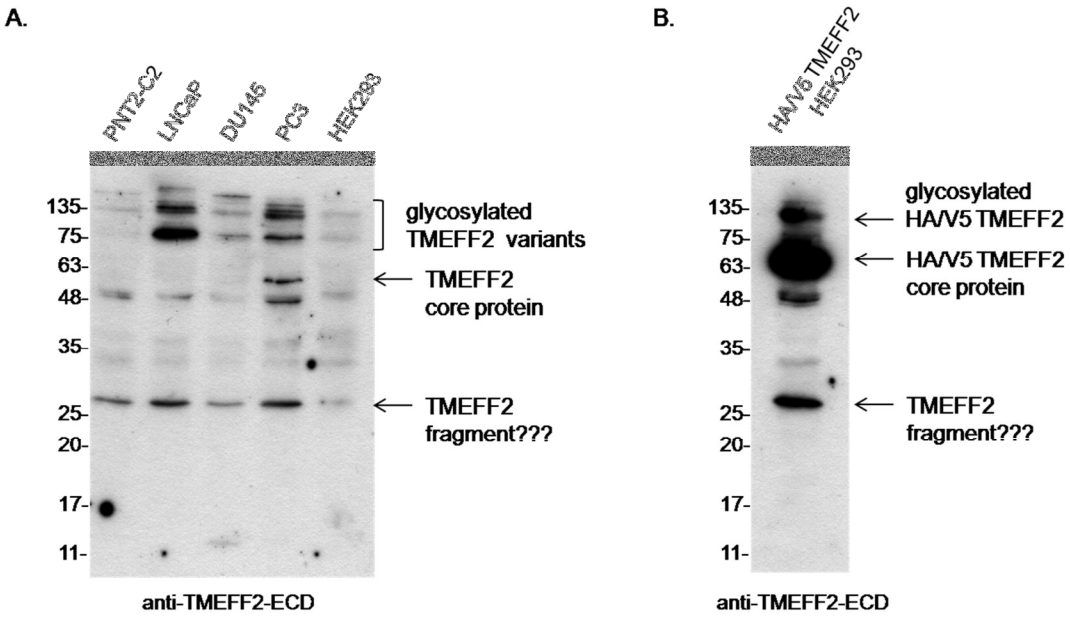

Figure 3.2 Expression of TMEFF2 in different cell lines.

50 µg of lysates from PNT2-C2, LNCaP, DU145, PC3 and HEK293 cell lines (A) as well as HEK293 cells stably expressing HA/V5 TMEFF2 (B) were separated in 11% resolving gel, blotted and labeled with anti-TMEFF2-ECD polyclonal antibody to examine TMEFF2 expression. The highest expression of TMEFF2 was detected in LNCaP cell (~75 kDa and ~100 kDa glycosylated forms) and weak bands corresponding to TMEFF2 were also observed in DU145 and PC3 cells. In the lysate from PNT2-C cells only a ~28 kDa band potentially corresponding to TMEFF2 degradation fragment was found, whereas no TMEFF2 was detected in HEK293 cells. Analysis of HA/V5 TMEFF2 HEK293 lysate indicated that the main form of TMEFF2 present in these cells is HA/V5 TMEFF2 core protein.

.

3.3.2 Expression of serine proteases in prostate cancer cells.

To investigate if TMEFF2 could be a substrate not only for ADAMs but also for membrane-bound serine proteases the expression of matriptase, prostasin and hepsin was tested in prostate cancer clinical samples and cell lines which were previously examined for TMEFF2 expression.

Lysates from $CD44^{+}/\alpha_2\beta_1^{hi}/CD133^{+}$ prostate cancer stem cells were loaded in equal volumes into a 11% resolving gel, separated and blotted followed by labeling with monoclonal anti-matriptase antibody M32 or monoclonal anti-prostasin antibodies (Figure 3.3). Anti-matriptase antibody M32 recognizes the third LDLR domain of matriptase and detected a band at ~70 kDa corresponding to the latent matriptase zymogen (Wu et al. 2010) in samples P6-P9 and P11 (Figure 3.3 A). Labeling with anti-prostasin antibody revealed the presence of ~40 kDa prostasin (Yu et al. 1994) in the same patient samples (Figure 3.3 B). The expression of hepsin was also analyzed in the prostate cancer stem cells samples, however due to the very limited amount of the lysates left for this analysis as well as the detection limit of the anti-hepsin antibody, hepsin could not be detected on the blot (data not shown).

The expression of matriptase, prostasin and hepsin was then analyzed in different cell lines. 50 µg of cell lysates were separated in 11% resolving gel, blotted and labeled with anti-matriptase M32, anti-prostasin or anti-hepsin antibodies. The Western blot presented in Figure 3.4 A showes that matriptase is expressed by all prostate cancer cell lines, but not by HEK293 cells. On the other hand, prostasin was present only in LNCaP cells but not in HEK293, PNT2-C2, DU145 and PC3 cells (Figure 3.4 B). Examination of hepsin expression presented in Figure 3.4 C showed the ~51 kDa band corresponding to mature form of hepsin (Tsuji et al. 1991) in the lysates from HEK293, LNCaP and PC3 cells.

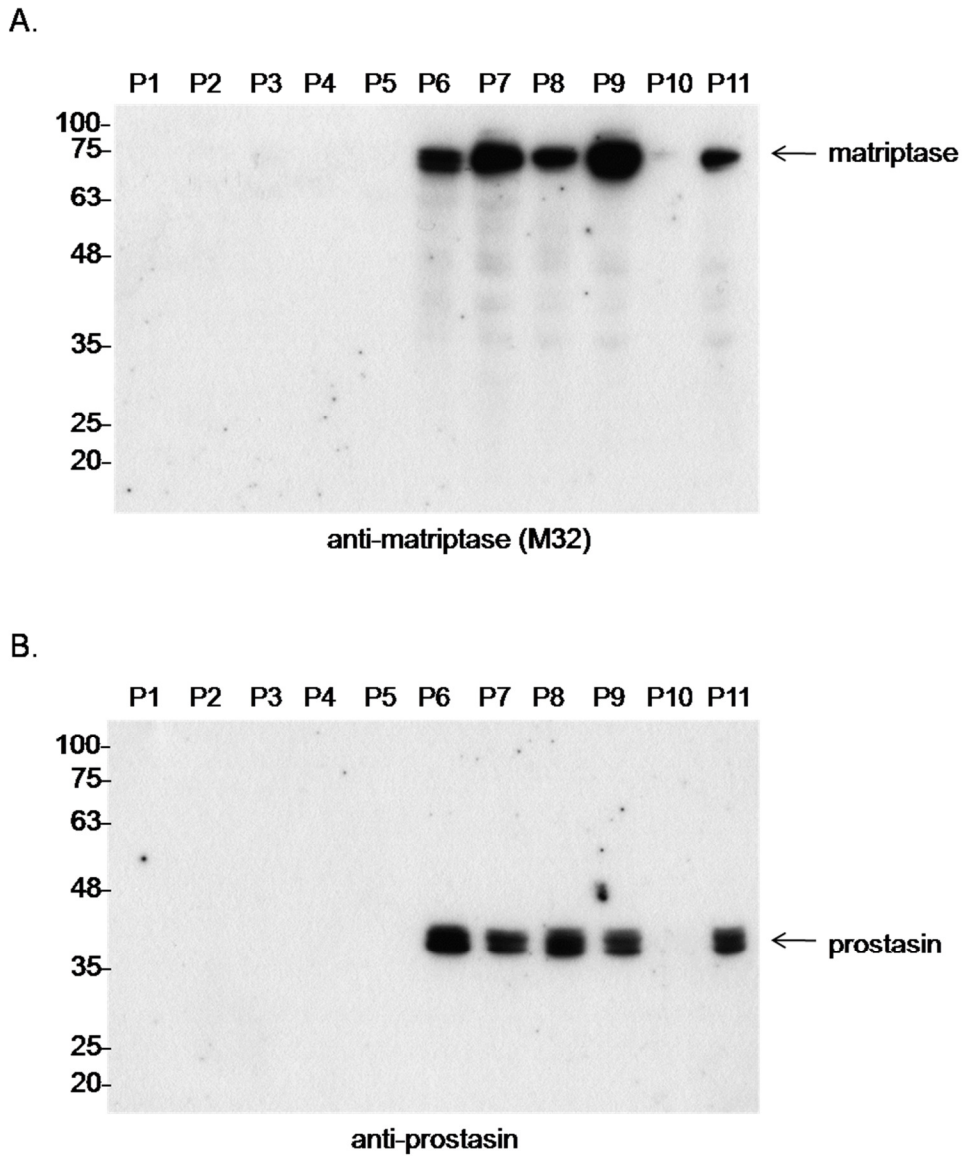

Figure 3.3 Expression of matriptase and prostasin in of $CD44^{+}/\alpha_2\beta_1^{hi}/CD133^{+}$ prostate cancer stem cells.

Equal volumes of the lysates from prostate cancer stem cells were separated in 11% resolving gel, blotted and labeled using monoclonal M32 anti-matriptase (A) or monoclonal anti-prostasin (B) antibodies. The ~70 kDa band corresponding to matriptase (A) and a ~40 kDa prostasin band (B) were detected in samples P6-P9 and P11. Arrows indicate specific bands corresponding to matriptase or prostasin.

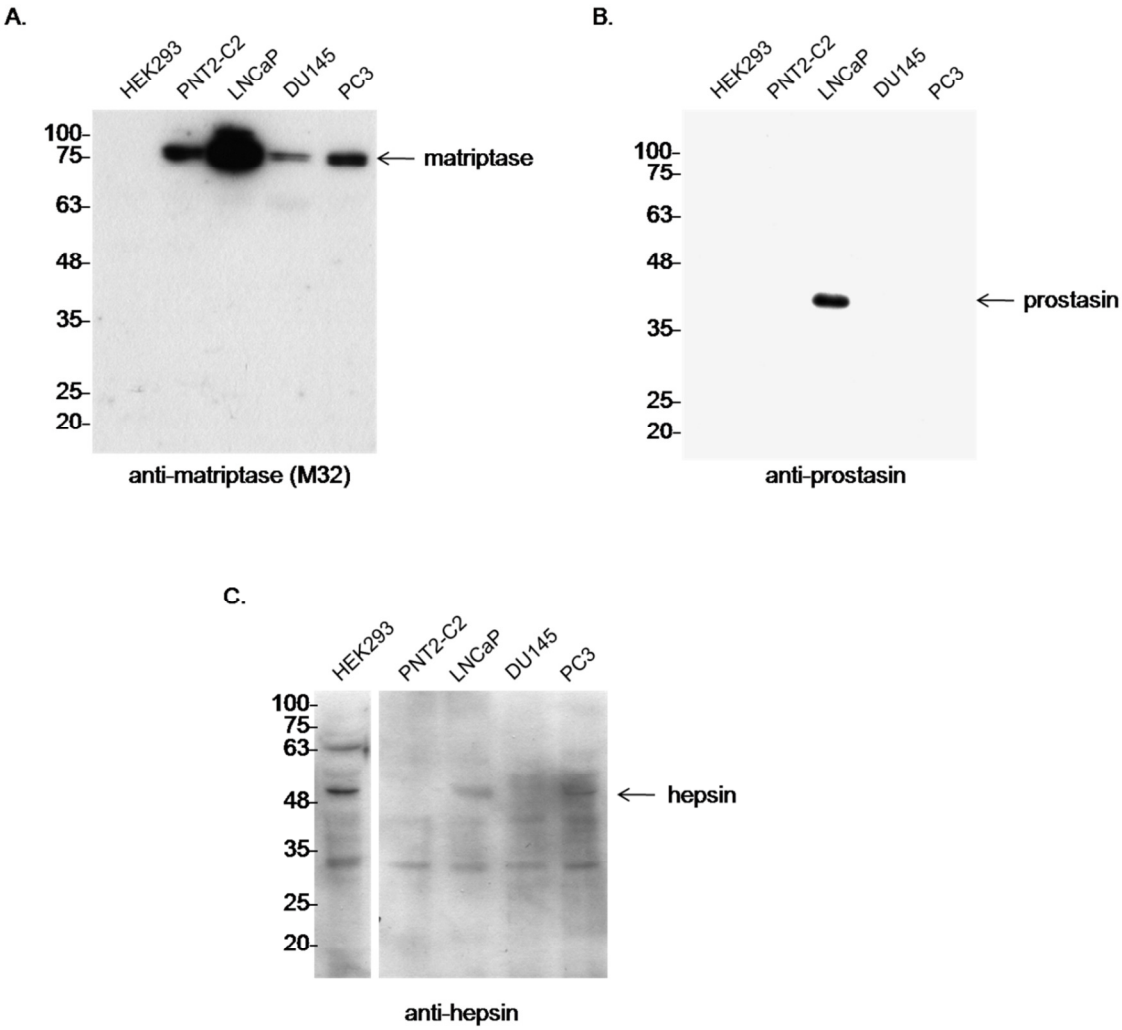

Figure 3.4 Expression of membrane serine proteases in cell lines.

50 µg of total cell lysates obtained from HEK293, PNt2-C2, LNCaP, DU145 and PC3 cell lines were analyzed by separation in 11% resolving gel, blotting and labeling with monoclonal M32 anti-matriptase (A), monoclonal anti-prostasin (B) and polyclonal anti-hepsin (C) antibodies. This analysis revelaed that matriptase is expressed by all tested cell lines except of HEK293 cells (A), prostasin is present only in LNCaP cells (B) and hepsin is found in HEK293, LNCaP and PC3 cell lines (C). Arrows indicate specific bands corresponding to serine proteases.

3.4 Chapter summary.

To address the hypothesis that the biological role of TMEFF2 in prostate cancer depends on its processing by different proteases, the expression of TMEFF2 and serine proteases was examined in prostate cancer clinical samples and cell lines, broadly used as *in vitro* models in prostate cancer studies. The summary of obtained data is presented in Table 3.2 below.

Table 3.2 Summary of TMEFF2 and serine protease expression in prostate cancer cell lines and clinical samples; na – not analyzed.

	TMEFF2	**Matriptase**	**Hepsin**	**Prostasin**
Cell lines:				
HEK293	**-**	**-**	**+**	**-**
PNT2-C2	**-**	**+**	**-**	**-**
LNCaP	**+**	**+**	**+/-**	**+**
DU145	**-**	**+**	**-**	**-**
PC3	**+**	**+**	**+/-**	**-**
Patient samples:				
P1	**-**	**-**	**na**	**-**
P2	**+**	**-**	**na**	**-**
P3	**-**	**-**	**na**	**-**
P4	**-**	**-**	**na**	**-**
P5	**+/-**	**-**	**na**	**-**
P6	**+**	**+**	**na**	**+**
P7	**+**	**+**	**na**	**+**
P8	**-**	**+**	**na**	**+**
P9	**+**	**+**	**na**	**+**
P10	**+**	**-**	**na**	**-**
P11	**+**	**+**	**na**	**+**

The expression of TMEFF2 was analyzed by Western blotting and labeling with commercially available polyclonal anti-TMEFF2 antibody, recognizing the extracellular part of TMEFF2 (TMEFF2-ECD). The expression of TMEFF2 was analyzed in the lysates from $CD44^+/\alpha_2\beta_1^{hi}/CD133^+$ cells isolated from 11 prostate cancer patients (Table 3.1), corresponding to the subpopulation of prostate cancer stem cells (Collins et al. 2001). These lysates were obtained due to the collaboration with Professor Norman Maitland and Dr Annie Collins from the University of York, UK. Prostate cancer stem cells are potentially very interesting target for future prostate cancer therapies as they display high proliferation rate, self-renewal and are able to differentiate into androgen receptor positive cells similar to prostate cancer cells *in situ* (Collins et al. 2005). The expression of TMEFF2 was never examined in this subpopulation before and for that reason the lysates were tested for TMEFF2 expression by Western blotting. As presented in Figure 3.1, the analysis using anti-TMEFF2-ECD antibody revealed the presence of multiple bands in all tested samples. According to Glynne-Jones and colleagues, the ~54 kDa band present for example in samples P2, P10 and P11 was identified as TMEFF2 core protein and the ~75 kDa and ~100 kDa bands corresponded to glycosylated variants of TMEFF2 (Glynne-Jones et al. 2001). Additionally, in all analyzed samples a ~28 kDa band was recognized by anti-TMEFF2-ECD antibody that was not described in the literature before. At this stage of the study in was hypothesized that this band corresponded to a novel product of TMEFF2 processing that contains some part of TMEFF2-ECD.

Due to the small number of available samples no conclusion could be made about the correlation of TMEFF2 expression and the stage of prostate cancer. Moreover, the detection of TMEFF2 in some samples could not be possible due to prolonged staorage of prostate cancer cell lysates and degradation of lysate components. However, TMEFF2 was found in cells isolated from both benign prostatic hyperplasia (sample P10) and prostate cancer with high Gleason score (samples P2, P6, P7). This analysis showed that TMEFF2 is present in some lysates from prostate cancer stem cells, raising a question about the functional difference between $CD44^+/\alpha_2\beta_1^{hi}/CD133^+/TMEFF2^+$ and $CD44^+/\alpha_2\beta_1^{hi}/CD133^+/TMEFF2^-$ prostate cancer stem cells that should be investigated in the future experiments.

TMEFF2 expression was also analyzed in different cell lines like normal prostate epithelial cells PNT2-C2, prostate cancer cell lines LNCaP, DU145 and PC3 as well as HEK293 and HEK293 transfected with HA/V5 TMEFF2 as negative and positive controls, respectively (Figure 3.2). The highest expression of TMEFF2 was found in LNCaP cells (~75 kDa and ~100 kDa bands corresponding to glycosylated TMEFF2 variants) but low levels of glycosylated TMEFF2 and the core protein were found also in DU145 and PC3 cells. This result is in disagreement with the findings published by Gery and co-workers, indicating that DU145 and PC3 cells do not express TMEFF2 (Gery et al. 2002). This

discrepancy could be explained by the different method used for TMEFF2 detection as Gery et al. analyzed TMEFF2 expression by Northern blotting.

The lysates from prostate cancer stem cells and cell lines were then analyzed for the expression of serine proteases implicated in prostate cancer progression – matriptase, prostasin and hepsin. Western blot analysis shown in Figure 3.3 revealed that matriptase and prostasin are expressed in some of the prostate cancer clinical samples. The expression of hepsin was also analyzed in these samples but due to the small amount of lysates available for this analysis as well as the detection limit of the anti-hepsin antibody, no hepsin could be detected in the samples (data not shown). The presence of matriptase, prostasin and hepsin was then assessed in the lysates from various cell lines. As shown in Figure 3.4 A), matriptase was present in all tested cell lines except of HEK293 cells, with the highest expression in LNCaP. On the other hand, prostasin was detected only in LNCaP cell line (Figure 3.4 B). Expression of hepsin was found in HEK293, LNCaP and PC3 cells (Figure 3.4 C).

Due to the very limited amount of prostate cancer clinical samples the labeling of the blots for the loading control protein could not be performed. For that reason presented analysis is qualitative but not quantitative and more precise examination of TMEFF2 expression levels in prostate cancer stem cells, for example by real-time PCR should be performed in the future. However, presented results indicated that TMEFF2 and serine proteases are expressed by the same prostate cancer cells (for example in samples P6, P7, P9 and P11) as well as cell lines (LNCaP) and thus TMEFF2 could be a novel substrate for this membrane-attached enzymes.

Chapter 4:

Shedding of TMEFF2 by serine proteases and ADAMs over-expressed in prostate cancer

4.1 Introduction.

Shedding of membrane proteins is a very important posttranscriptional modification that regulates their function. Precursors of many growth factors, pro-inflammatory cytokines and adhesion molecules are activated through ectodomain shedding. It is also important to remember that during shedding not only the soluble ectodomain is generated but also the membrane-retained stub that in many cases has its own biological role in the cell. Major mediators of ectodomain shedding are metalloproteases from the ADAM family but many transmembrane proteins are cleaved also by membrane-anchored serine proteases.

4.1.1 ADAM-mediated ectodomain shedding.

Shedding of protein ectodomain by ADAMs occurs constitutively by activated forms of these enzymes that are present on the cell surface or it can be induced by different stimuli. The most effective activators of ADAM-dependent shedding are phorbol esters which activate members of the protein kinase C (PKC) family (Brose and Rosenmund 2002). In research, the most commonly used phorbol ester is phorbol 12-myristate 13-acetate (PMA). Its PKC activating potential results from the structural similarity to the naturally occurring PKC activator – diacylglycerol (DAG). Shedding of many ADAM substrates is regulated by specific PKC izoenzymes. For example, PKCε is required for TNFα shedding (Wheeler et al. 2003), PKCδ is involved in shedding of pro-HB-EGF (Izumi et al. 1998) whereas PKCδ and PKCη regulate shedding of IL-6 receptor ectodomain (Thabard et al. 2001). Several studies indicate that ectodomain shedding is also positively regulated by protein tyrosine kinases (PTKs). Moreover, treatment with pervanadate, a potent inhibitor of protein tyrosine phosphatases enhance shedding of several membrane proteins, including L-selectin and syndecan-1 (Subramanian et al. 1997; Phong et al. 2003). It is not known how PKC and PTK kinases regulate ectodomain shedding but the current data suggest that these kinases do not enhance shedding by phosphorylating the substrate. For example, the deletion the cytoplasmic domains of IL-6R and TNFα receptor II does not reduce shedding of their ectodomains, despite the fact that the cytoplasmic domains of these receptors are phosphorylated upon PMA stimulation (Müllberg et al. 1994; Crowe et al. 1993). Furthermore, PMA and other activators of pro-HB-EGF shedding cause phosphorylation of Ser residue within pro-HB-EGF cytoplasmic domain but the mutation of this Ser residue do not impair pro-HB-EGF shedding (Wang et al. 2006). These results suggest that PTKs and PKCs enhance ectodomain shedding by phosphorylation of cytoplasmic proteins other than the substrate. However, the cytoplasmic domain of the substrate can affect ectodomain shedding through binding of intracellular modifiers. For example, interaction of a calcium-binding protein calmudulin with cytoplasmic domain of L-selectin down-regulates shedding (Kahn et al. 1998) whereas binding of L-selectin cytoplasmic tail to proteins from the

Ezrin/Radixin/Moesin (ERM) family is required for ectodomain shedding (Ivetic et al. 2004).

Alternatively, metalloproteases were also shown to undergo activation following PMA treatment through generation of reactive oxygen species (ROS). ADAM proforms are kept inactive by the cysteine switch that can be disrupted by ROS-mediated oxidation of the electrophilic thiol groups and allow activation of the ADAM catalytic domains (Meada et al. 1998, Fu et al. 2003, Ilbert et al. 2006). ROS are known to activate ADAM17 (Zhang et al. 2000, Zhang et al. 2000, Siegel et al. 2006) and ADAM9 (Sung et al 2006) and the ROS-dependent mechanism of ADAM-activation is involved in HB-EGF shedding (Kim et al. 2005).

In addition to phorbol esters and ROS, ADAM-dependent shedding of membrane proteins can be facilitated by UV radiation and hypertonic osmotic pressure as shown for HB-EGF, TGFα, and neuregulins (Takenobu et al. 2003; Montero et al. 2002). ADAM-mediated cleavage can also be induced by cytokines, like IL-1β and TNFα which induce shedding of TMEFF2 (Lin et al. 2003) and IL-8 that stimulates release of pro-HB-EGF in gastric cancer cells (Tanida et al. 2004). In addition to growth factors and cytokines ADAM-mediated shedding can be stimulated also by GPCR agonists. GPCR stimulation by lysophosphatidic acid, endothelin, thrombin, bombesin or carbachol was shown to induce HB-EGF shedding and subsequent transactivation of EGFR (Prenzel et al. 1999).

Ectodomain shedding mediated by some ADAMs can be also controlled by the regulation of their cell surface location. For example, ADAM12 is activated by the furin-peptidase during maturation within the trans-Golgi network and is stored intracellulary until translocation to the cell surface as a constitutively active protease. Transport of the ADAM12-containing vesicles to the cell surface can be induced with PMA through activation of a PKCε (Sundberg et al. 2004). On the other hand, Doedens and Black showed that following activation ADAM17 rapidly disappears from the cell surface by endocytosis which represents another potential control mechanism for ADAM-mediated ectodomain shedding (Doedens & Black 2000).

ADAMs usually cleave membrane proteins that are present on the surface of the same cell (*cis* orientation). However, as shown by Janes and co-workers for ADAM10 and ephrin, ADAM-mediated shedding of substrate expressed by the adjacent cell (*trans* orientation) is also possible (Janes et al. 2005).

4.1.2 Cleavage of transmembrane proteins by serine proteases.

In addition to metalloproteases, transmembrane proteins can also be released by membrane-anchored serine proteases. Similarly to ADAM-mediated cleavage, this process occurs constitutively or upon treatment with different shedding inducers. The

mechanisms of serine protease activation are often dependent on the cell type by which the enzyme is expressed. For example, matriptase is activated in breast cancer cells by the blood-derived phospholipid sphingosine-1-phosphate (S1P) (Bernaud et al. 2005) but in androgen-sensitive prostate cancer cells matriptase undergoes activation in response to androgens (Kiyomiya et al. 2006).

Most of the membrane serine proteases are transported to the plasma membrane as inactive pro-forms and require endoproteolytic cleavage to become fully active. This activation can be mediated by the enzyme itself as shown for matriptase, matriptase-2 and hepsin (Takeuchi et al. 2000; Oberst, Williams, et al. 2003; Velasco et al. 2002; Qiu et al. 2007). Some serine proteases require cleavage by additional enzymes. For example, a GPI-anchored prostasin can be activated by matriptase and hepsin and this serine protease catalytic cascade was found to be involved in the shedding of EGF receptor (Chen et al. 2008, 2010; Netzel-Arnett et al. 2006).

4.1.3 TMEFF2 as a potential substrate for serine proteases.

TMEFF2 undergoes ectodomain shedding mediated by ADAM10 and ADAM17 (Ali & Knäuper 2007). There is also a strong possibility that TMEFF2 can be cleaved by the serine proteases matriptase, matriptase-2, hepsin and prostasin, as they are expressed by the same cells. Moreover, it was shown by Ge and co-workers that TMEFF2 homologue, TMEFF1 interacts through its EGF-like domain with matriptase forming a complex on the cell surface. GST pull down assays showed binding of TMEFF1 to a fragment containing two CUB domains of matriptase (GST-CUB1-CUB2) whereas the fragment containing the first CUB domain alone (GST-CUB1) was not sufficient to interact with TMEFF1. This suggests that the interaction between TMEFF1 and matriptase requires the second CUB domain (CUB2) or both CUB domains (Ge et al. 2006). However, it is not known if this interaction results in TMEFF1 cleavage. Two CUB domains that can potentially interact with TMEFF2 are also present in the stem region of matriptase-2 (Velasco et al. 2002). TMEFF2 can also be a substrate for hepsin as most of the proteins cleaved by matriptase are also processed by hepsin, for example pro-uPA (Lee et al. 2000; Moran et al. 2006), pro-MSP (Bhatt et al. 2005; Ganesan et al. 2011), laminin-332 (Tripathi et al. 2008; Tripathi et al. 2011) and prostasin (Chen et al. 2008; M. Chen et al. 2010) .

4.2 Aims:

Experiments described in Chapter 4 were performed in order to:

- characterize the cellular model to study TMEFF2 ectodomain shedding and generation of C-terminal cleavage products;
- optimise shedding assay conditions;
- analyze TMEFF2 shedding by serine proteases implicated in prostate cancer: matriptase, matriptase-2, hepsin and prostasin;
- assess TMEFF2 shedding by ADAMs over-expressed in prostate cancer cells;
- analyze TMEFF2 release upon stimulation with its binding partner PDGF-AA.

4.3 Results.

4.3.1 Characterization of the cellular model to study TMEFF2 shedding.

Due to the restricted expression of TMEFF2 there is a very limited number of cellular models to study the biology of this protein. As reported by Gery and co-workers (Gery et al. 2002) and confirmed in Chapter 3, one of the few cell lines that endogenously express TMEFF2 and can be used to study shedding of this protein is the androgen-sensitive prostate cancer cell line LNCaP. Shedding of TMEFF2 ectodomain can be monitored in these cells by Western blotting of cell conditioned medium and labelling with a commercially available anti-TMEFF2 polyclonal antibody that recognises the extracellular part of this protein. However, this approach can be challenging due to the small amounts of TMEFF2-ECD in the conditioned medium and the limited sensitivity of Western blot analysis. The detection of the intracellular TMEFF2 cleavage products in LNCaP cell lysates would be also difficult due to the lack of an antibody recognizing the TMEFF2 cytoplasmic domain. Another limitation of the study of TMEFF2 shedding in LNCaP cells is the fact that this cell line is prone to undergo apoptosis upon treatment with phorbol esters such as PMA (Tanaka et al. 2003), which is the most commonly used inductor of PKC-dependent shedding (Brose & Rosenmund 2002). For these reasons shedding of TMEFF2 was examined in HEK293 cells stably transfected with TMEFF2 tagged on the N-terminus with alkaline phosphatase (AP) and on the C-terminus with a V5 epitope tag. The AP-tag enables the sensitive detection of TMEFF2-ECD release from the cell surface into the conditioned medium. The small V5 epitope at the carboxy-terminus allows the investigation of TMEFF2 C-terminal cleavage products, without interfering with TMEFF2 trafficking inside the cell.

ADAM-mediated shedding of TMEFF2 ectodomain occurs within the sequence adjacent to the transmembrane domain, as described by Ali and Knäuper (Ali & Knäuper 2007). In order to investigate if TMEFF2 cleavage can be mediated by membrane serine proteases and if it occurs within the same position as ADAM-dependent processing, HEK293 cells stably expressing AP/V5 $\Delta_{303\text{-}320}$TMEFF2 mutant were also used in shedding experiments. $\Delta_{303\text{-}320}$ TMEFF2 mutant lacks 17 amino acids in the membrane-proximal region and is resistant to ADAM-mediated cleavage (Ali & Knäuper 2007). Schematic pictures of AP/V5 TMEFF2 and AP/V5 $\Delta_{303\text{-}320}$ TMEFF2 are presented in Figure 4.1. HEK293 cells lines expressing AP/V5 TMEFF2 and AP/V5 $\Delta_{303\text{-}320}$ TMEFF2 were generated previously by Dr Vera Knäuper using Flp-In System from Invitrogen (see Appendix III).

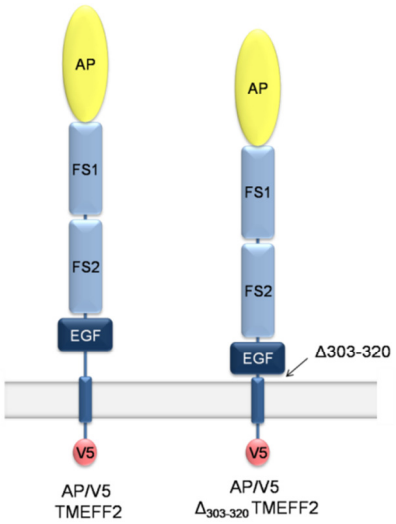

Figure 4.1 Schematic diagrams of AP/V5 TMEFF2 and AP/V5 $\Delta_{303-320}$TMEFF2 mutant; AP- alkaline phosphatase, FS - follistatin-like module, EGF – EGF-like domain

Generation of the stable cell lines may result in significant differences in the expression levels of recombinant proteins, even when the same Flp-In host cell line and the same type of expression vector were used. To compare shedding of AP/V5 TMEFF2 and AP/V5 $\Delta_{303-320}$ TMEFF2 it is very important to be sure that the levels of these proteins in stable HEK293 cell lines are similar. Significantly lower expression of one of these proteins may influence the outcome of the experiment and make the interpretation of the data difficult. For that reason the same amounts (10 µg) of lysates from AP/V5 TMEFF2 and AP/V5 $\Delta_{303-320}$ TMEFF2 HEK293 cells were analyzed by Western blotting and labelling with anti-V5 antibody to compare the total levels of AP/V5 TMEFF2 and AP/V5 $\Delta_{303-320}$ TMEFF2 (Figure 4.2). Labelling with anti-GAPDH antibody served as a loading control. This analysis detected similar amounts of 135-133 kDa proteins in lysates from stable HEK293 cell lines, corresponding to AP/V5 TMEFF2 and AP/V5 $\Delta_{303-320}$ TMEFF2. The molecular masses of AP/V5 TMEFF2 and AP/V5 $\Delta_{303-320}$ TMEFF2 calculated from the protein sequence are 65.6 kDa and 63.5 kDa, respectively and are much smaller than the apparent sizes on the Western blot but are in agreement with previously published data (Ali & Knäuper 2007). The discrepancy between calculated and detected sizes of these proteins is thought to be due to the heavy glycosylation of TMEFF2. As mentioned previously, the lack of 17 amino acids within the sequence of AP/V5 $\Delta_{303-320}$ TMEFF2 result in 2.1 kDa difference in calculated molecular mass compared to AP/V5 TMEFF2. This small difference in size causes a slight increase of the electrophoretic mobility of AP/V5 $\Delta_{303-320}$ TMEFF2 as shown in Figure 4.2, where samples were separated using a 8% resolving gel.

Interpretation of the shedding experiments would be impossible if the deletion of the 17 amino acid sequence from the membrane proximal region of $\Delta_{303-320}$TMEFF2 would impair its plasma membrane location. To investigate if TMEFF2 and $\Delta_{303-320}$TMEFF2 are both present on the cell surface, HA/V5 TMEFF2 and HA/V5 $\Delta_{303-320}$TMEFF2 HEK293 cells were grown on coverslips, fixed, permeabilised and labelled with mouse-anti-V5 and anti-mouse AlexaFluor®596 antibodies. To visualise cell nuclei, the coverslips were mounted using DAPI-containing solution. As presented in Figure 4.3, confocal microscope analysis of labelled cells revealed the presence of HA/V5 TMEFF2 and HA/V5 $\Delta_{303-320}$TMEFF2 on the plasma membrane. Anti-V5 labelling of TMEFF2 intracellular domain was also found in the perinuclear region and within the cytoplasmic structures that probably correspond to the endoplasmic reticulum (ER). This analysis indicated a similar expression pattern for both HA/V5 TMEFF2 and HA/V5 $\Delta_{303-320}$TMEFF2 in HEK293 cells which allowed to use these cell lines to investigate shedding by membrane proteases.

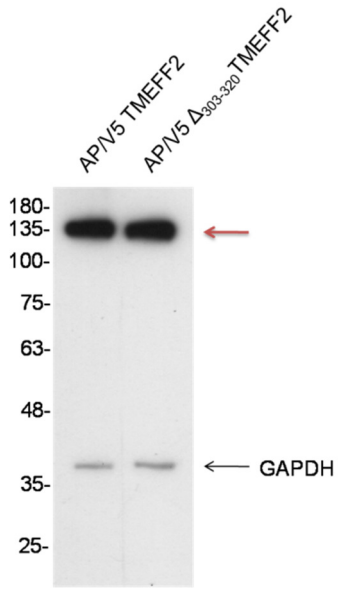

Figure 4.2 Expression of TMEFF2 and $\Delta_{303-320}$TMEFF2 in stably transfected HEK293 cells.

10 µg of total cell lysates from AP/V5 TMEFF2 and AP/V5 $\Delta_{303-320}$TMEFF2 HEK293 were analyzed by SDS-PAGE in 8% resolving gel and Western blotting. Membrane was labelled with anti-V5 antibody. Anti-GAPDH labelling was used as a loading control. Arrows indicate 135-133 kDa bands corresponding to glycosylated AP/V5 TMEFF2 and AP/V5 $\Delta_{303-320}$TMEFF2.

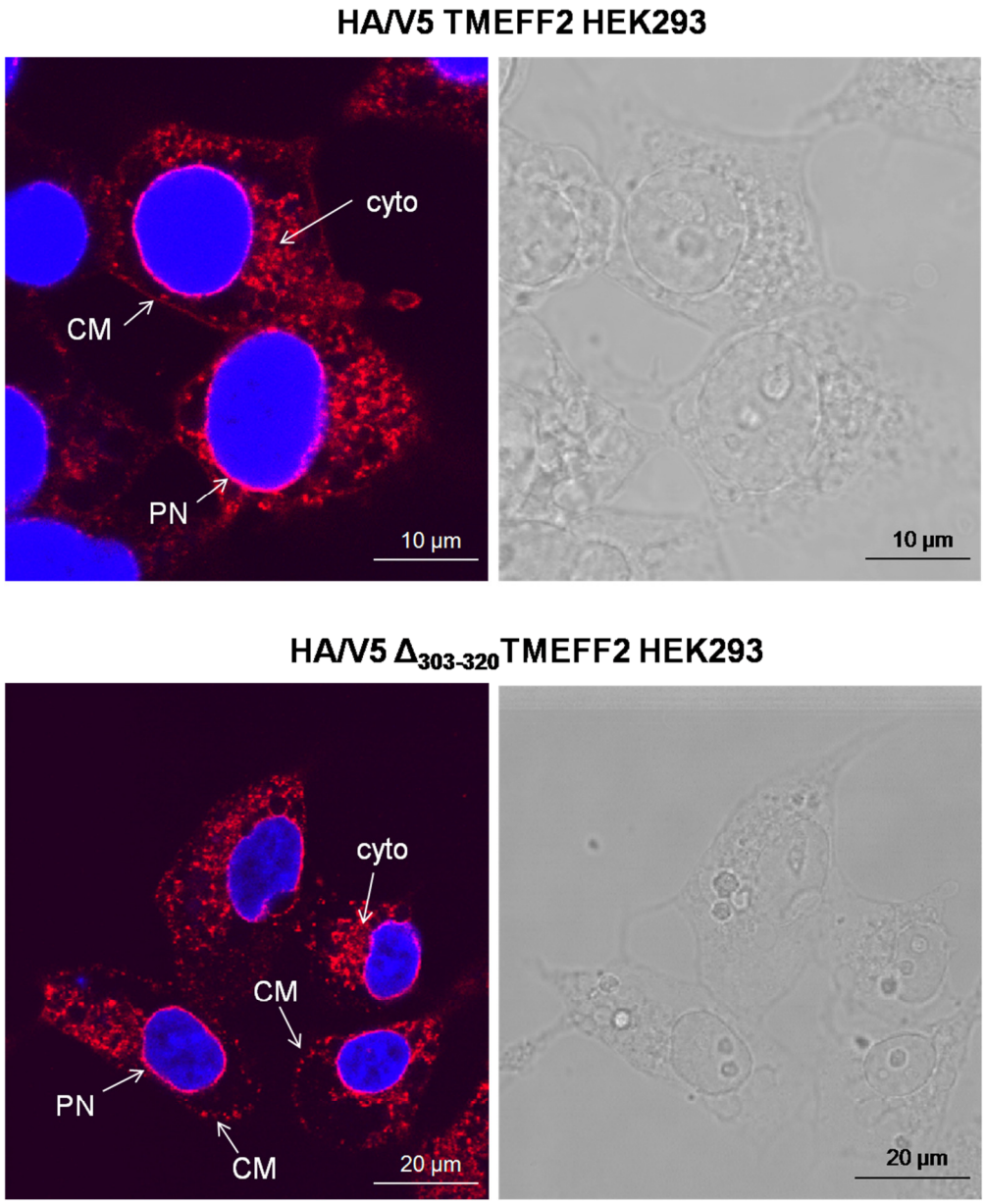

Figure 4.3 Immunolocalisation of HA/V5 TMEFF2 and HA/V5 $\Delta_{303\text{-}320}$TMEFF2 in stably transfected HEK293 cells.

HA/V5 TMEFF2 (upper panel) and HA/V5 $\Delta_{303\text{-}320}$TMEFF2 (bottom panel) HEK293 cells were grown on poly-L-lysine coated coverslips, fixed, permeabilised and labelled with mouse anti-V5 primary and donkey anti-mouse AlexaFluor®596 secondary antibody (red pseudocolor). Cell nuclei were visualised using DAPI (blue pseudocolor). Cellular localization of TMEFF2 was analyzed by confocal microscope. Positive staining for HA/V5 TMEFF2 and HA/V5 $\Delta_{303\text{-}320}$TMEFF2 detected on the cell membrane (CM), in the perinuclear region (PN) and in the cytoplasmic structures (cyto) is indicated with arrows.

As indicated previously, the lack of 17 amino acids within the membrane proximal region of $\Delta_{303-320}$ TMEFF2 mutant makes this protein resistant to ADAM-dependent cleavage (Ali & Knäuper 2007), reducing constitutive as well as induced release of the AP/V5 $\Delta_{303-320}$ TMEFF2 ectodomain. To compare shedding of AP/V5 TMEFF2 and AP/V5 $\Delta_{303-320}$ TMEFF2 from HEK293 cells in the basal conditions both cells lines were grown in 24-well plates until confluent and incubated for 3 hours in 250 µl of serum free OptiMEM. The levels of AP-tagged ectodomain were assessed in the collected medium using the alkaline phosphatase activity assay (AP assay), as described in Materials and methods. In the medium from AP/V5 TMEFF2 expressing cells high AP activity was detected, indicating constitutive shedding of AP/V5 TMEFF2 from HEK293 cells by endogenously expressed metalloproteases. Analysis of the conditioned medium from AP/V5 $\Delta_{303-320}$ TMEFF2 HEK293 cells showed minimal AP activity, confirming that the basal shedding of AP/V5 $\Delta_{303-320}$ TMEFF2 is strongly reduced (Figure 4.4).

The release of AP/V5 TMEFF2 and AP/V5 $\Delta_{303-320}$ TMEFF2 from HEK293 cells upon ADAM activation was also compared. In this experiment, stable cell lines were grown in 24-well plates until confluent and treated for 1 hour with different concentrations of PMA in serum free OptiMEM. Cells treated with medium containing DMSO served as a control (Figure 4.5). The AP activity in the collected medium samples was measured as described previously. The shedding of AP/V5 TMEFF2 or AP/V5 $\Delta_{303-320}$ TMEFF2 from control cells was set to 1 and used as a reference point to determine the fold increase shedding of all samples. The results obtained showed that treatment of AP/V5 TMEFF2 HEK293 cells with PMA increased shedding by about 1.8 fold in comparison to cells treated with DMSO. Interestingly, the shedding did not increase further when the cells were treated with higher concentrations of PMA (Figure 4.5 A), indicating that 100 ng/ml PMA caused complete shedding of cell surface AP/V5 TMEFF2. Incubation of AP/V5 $\Delta_{303-320}$ TMEFF2 HEK293 cells in medium containing PMA did not induce ectodomain shedding, even following treatment with high concentrations (up to 500 ng/ml) of PMA (Figure 4.5 B). These results confirmed, that AP/V5 TMEFF2 shedding is induced by PMA, whereas AP/V5 $\Delta_{303-320}$ TMEFF2 is resistant to PMA-induced shedding.

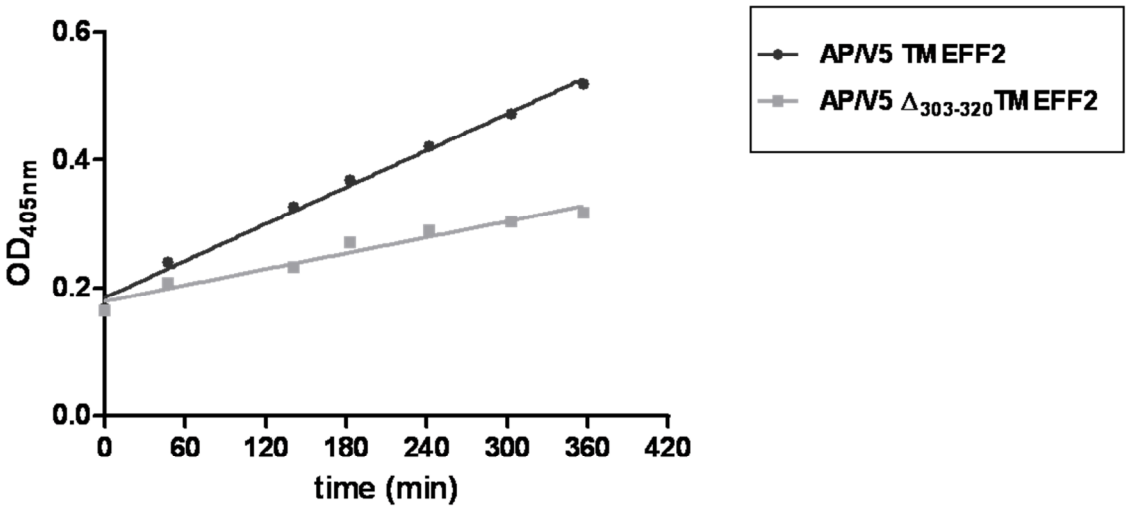

Figure 4.4 Comparison of the constitutive AP/V5 TMEFF2 and AP/V5 $\Delta_{303-320}$TMEFF2 shedding from HEK293 cells.

HEK293 cells stably expressing AP/V5 TMEFF2 and AP/V5 $\Delta_{303-320}$TMEFF2 were grown until confluent and incubated for 3 hours in serum free OptiMEM. After incubation, serum free medium was collected, clarified by centrifugation and assayed for AP activity as described in Materials and methods. The graph presents the linear regression analysis of the mean values from one experiment with four replicates.

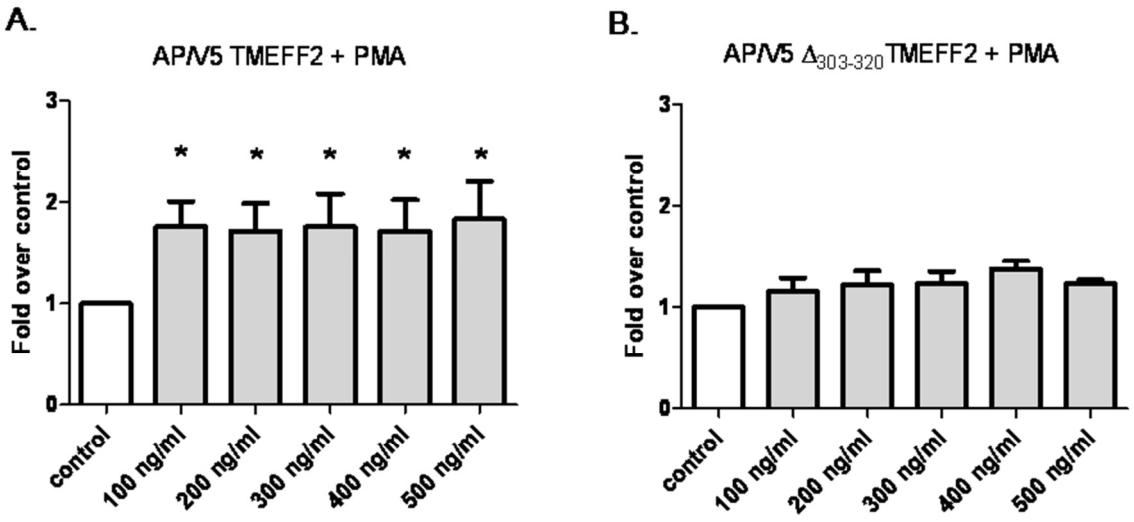

Figure 4.5 Comparison of PMA-induced shedding of AP/V5 TMEFF2 and AP/V5 $\Delta_{303-320}$TMEFF2 from HEK293 cells.

HEK293 cells stably expressing AP/V5 TMEFF2 (A) and AP/V5 $\Delta_{303-320}$TMEFF2 (B) were incubated for 1 hour in serum free OptiMEM with different concentrations of PMA or DMSO as a control. The amount of released AP-tagged ectodomain of AP/V5 TMEFF2 and AP/V5 $\Delta_{303-320}$TMEFF2 was measured using the AP assay. The release of AP/V5 TMEFF2 or AP/V5 $\Delta_{303-320}$TMEFF2 from control cells was set to 1 and used as a reference point to determine the fold increase shedding of PMA-treated samples. Release of AP/V5 TMEFF2 was induced by PMA (A) but AP/V5 $\Delta_{303-320}$TMEFF2 was resistant to PMA-induced shedding (B). Histograms show mean shedding values from three independent experiments ±SEM, *$p<0.05$.

Shedding of AP/V5 TMEFF2 and AP/V5 $\Delta_{303-320}$ TMEFF2 from the cells incubated with or without PMA was also analyzed by Western blotting. Labelling with anti-V5 antibody visualised C-terminal cleavage products of these proteins. According to the literature, AP/V5 TMEFF2 cleavage by ADAM10 and ADAM17 results in generation of ~19 kDa and ~10 kDa C-terminal fragments, corresponding to the ADAM-generated stump and the γ-secretase product, respectively (Ali & Knäuper 2007). To obtain the best separation of these small fragments lysates were analyzed using a 12.5% resolving gel. Figure 4.6 A presents analysis of the lysates from AP/V5 TMEFF2 HEK293 cells treated with increasing concentrations of PMA for 1 hour. In all samples a ~135 kDa band corresponding to the full length AP/V5 TMEFF2 was detected as well as a 17 kDa fragment corresponding to the ADAM-generated stump. This fragment was found also in the lysate from DMSO-treated control cells, indicating that AP/V5 TMEFF2 shedding occurs also in the absence of PMA treatment, which is in agreement with the data presented in Figure 4.4. No accumulation of the 17 kDa fragment was observed in cells treated with PMA, indicating that the AP assay is more sensitive method to analyze AP/V5 TMEFF2 shedding and gives more accurate information about the ratio of shed AP/V5 TMEFF2 than Western blot analysis of cell lysates. The lack of the ~10kDa γ-secretase product in analyzed samples can be explained by further processing or degradation of this small fragment. In the samples from AP/V5 $\Delta_{303-320}$TMEFF2 HEK293 (Figure 4.6 B) only the full length AP/V5 $\Delta_{303-320}$TMEFF2 was detected, even in the lysates from cells treated with high PMA dose. These data confirm again that AP/V5 $\Delta_{303-320}$TMEFF2 mutant is resistant to ADAM-dependent processing.

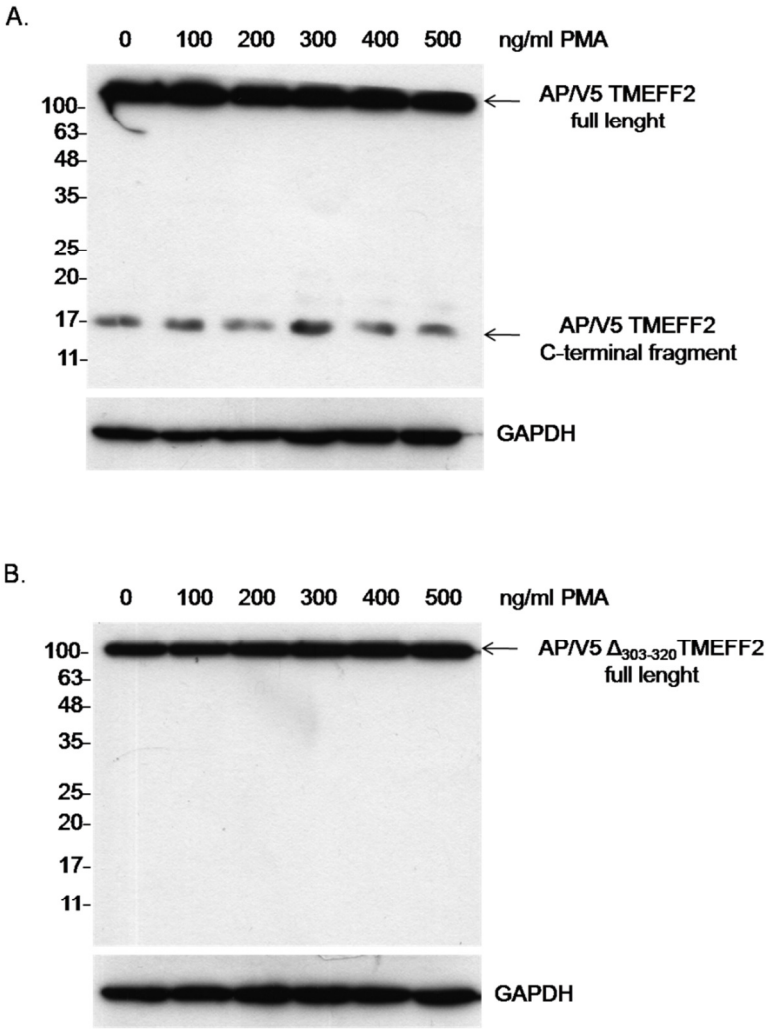

Figure 4.6 PMA-induced cleavage of AP/V5 TMEFF2 and AP/V5 $\Delta_{303-320}$TMEFF2 in HEK293 cells.

50 µg of total cell lysates from AP/V5-TMEFF2 (A) and AP/V5 $\Delta_{303-320}$TMEFF2 (B) HEK293 cells treated for 1 hour with different concentrations of PMA were analyzed by Western blotting and labelled with anti-V5 antibody. Anti-GAPDH antibody was used as a loading control. In the lysates from cells expressing AP/V5 TMEFF2 in addition to full length protein a 17 kDa V5-tagged C-terminal cleavage product was detected, whereas in lysates from AP/V5 $\Delta_{303-320}$TMEFF2 HEK293 cells only the full length AP/V5 $\Delta_{303-320}$TMEFF2 was present. Data are representative of three independent experiments.

4.3.2 Optimisation of TMEFF2 shedding assay.

As described at the beginning of this chapter, AP/V5 TMEFF2 HEK293 cells are a useful tool to study shedding of this protein due to the possibility of a simple and sensitive detection of AP-tagged ectodomain in the conditioned medium. Moreover, HEK293 cells are relatively easy to transiently transfect and the release of AP/V5 TMEFF2 can be monitored in the cells over-expressing both the substrate (AP/V5 TMEFF2) and the protease. Shedding of some proteins, especially those that are constitutively released from the membrane at high ratios, is easier to monitor in cells transiently co-transfected with the substrate and the potential sheddase. This experimental setup enables the reduction of background shedding as the cleavage occurs only from the cells expressing both proteins - the substrate and the enzyme.

To optimize the conditions to monitor shedding of AP/V5 TMEFF2 by serine proteases HEK293 cells were transiently transfected with AP/V5 TMEFF2 and matriptase in a 1:1 DNA ratio. Control cells were co-transfected with AP/V5 TMEFF2 and matriptase S-A mutant in order to establish the level of endogenous AP/V5 TMEFF2 shedding. Substitution of the Ser residue from the His-Asp-Ser catalytic triad of matriptase with Ala leads to inactivation of this enzyme. 48 hours post-transfection cells were incubated for 1 hour in 250 µl of serum free OptiMEM and the AP activity in the conditioned medium was analyzed as previously. Results presented in Figure 4.7 showed that very low AP activity was detected in the medium from cells co-transfected with AP/V5 TMEFF2 and matriptase or AP/V5 TMEFF2 and matriptase S-A. The data presented previously (Figure 4.4) proved that AP/V5 TMEFF2 is released from AP/V5 TMEFF2 HEK293 cells without any stimulation. For that reason the minimal AP activity in conditioned medium from co-transfected cells can be explained by a very low co-transfection efficiency. It indicates that co-transfection of HEK293 cells with AP/V5 TMEFF2 and the protease is not a good model to study shedding of this protein.

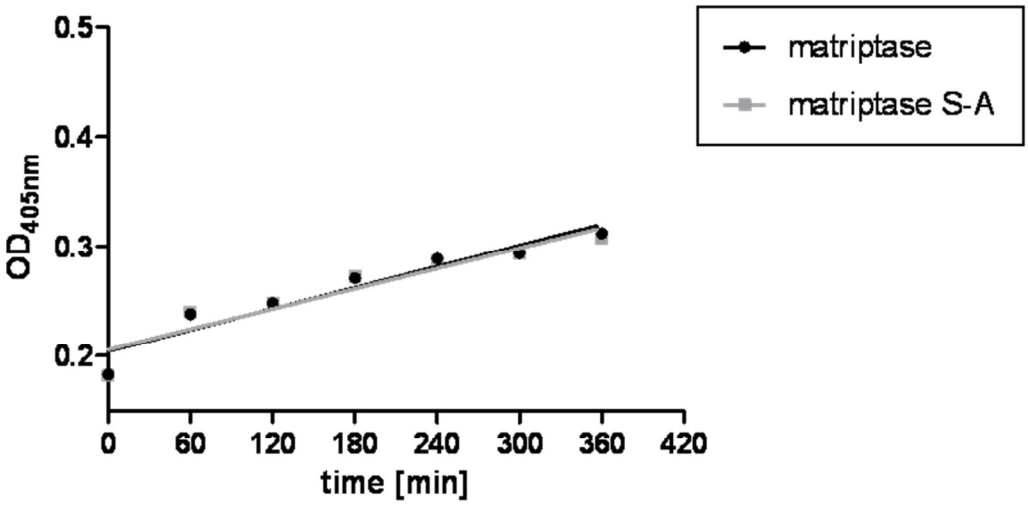

Figure 4.7 Optimisation of AP/V5 TMEFF2 shedding by matriptase in co-transfected HEK293 cells.

To optimise the experimental setup to monitor AP/V5 TMEFF2 shedding by serine proteases HEK293 cells were transiently co-transfected with AP/V5 TMEFF2 and matriptase in a 1:1 DNA ratio. Control cells were co-transfected with AP/V5 TMEFF2 and inactive matriptase S-A mutant. 48 hours post-transfection cells were grown for 1 hour in serum free OptiMEM and the conditioned medium was analyzed by AP assay as described in Materials and methods. Very low AP activity was detected in both samples, indicating low co-transfection efficiency. Graph shows linear regression analysis of the data from one representative experiment.

Further shedding optimisation experiments investigated AP/V5 TMEFF2 shedding from HEK293 cells stably expressing AP/V5 TMEFF2 which were transiently transfected with matriptase or inactive matriptase S-A. 48 hours post transfection cells were incubated for 1 hour or 3 hours in serum free OptiMEM followed by the AP assay. Figure 4.8 shows that in both experiments matriptase increases shedding of AP/V5 TMEFF2 as higher AP activity was detected in the medium from matriptase-transfected cells than from control cells transfected with matriptase S-A. However, more accurate data were obtained when transfected cells were grown in OptiMEM for 3 hours. The prolonged incubation time allowed accumulation of the AP/V5 TMEFF2 ectodomain shed by matriptase and the difference between cells transfected with matriptase and matriptase S-A is more pronounced. For this reason further shedding experiments were carried out using HEK293 cells stably expressing AP/V5 TMEFF2 or AP/V5 $\Delta_{303\text{-}320}$TMEFF2, transiently transfected with serine proteases or inactive S-A serine protease mutants and incubated with serum free OptiMEM for 3 hours prior to performing the AP assay.

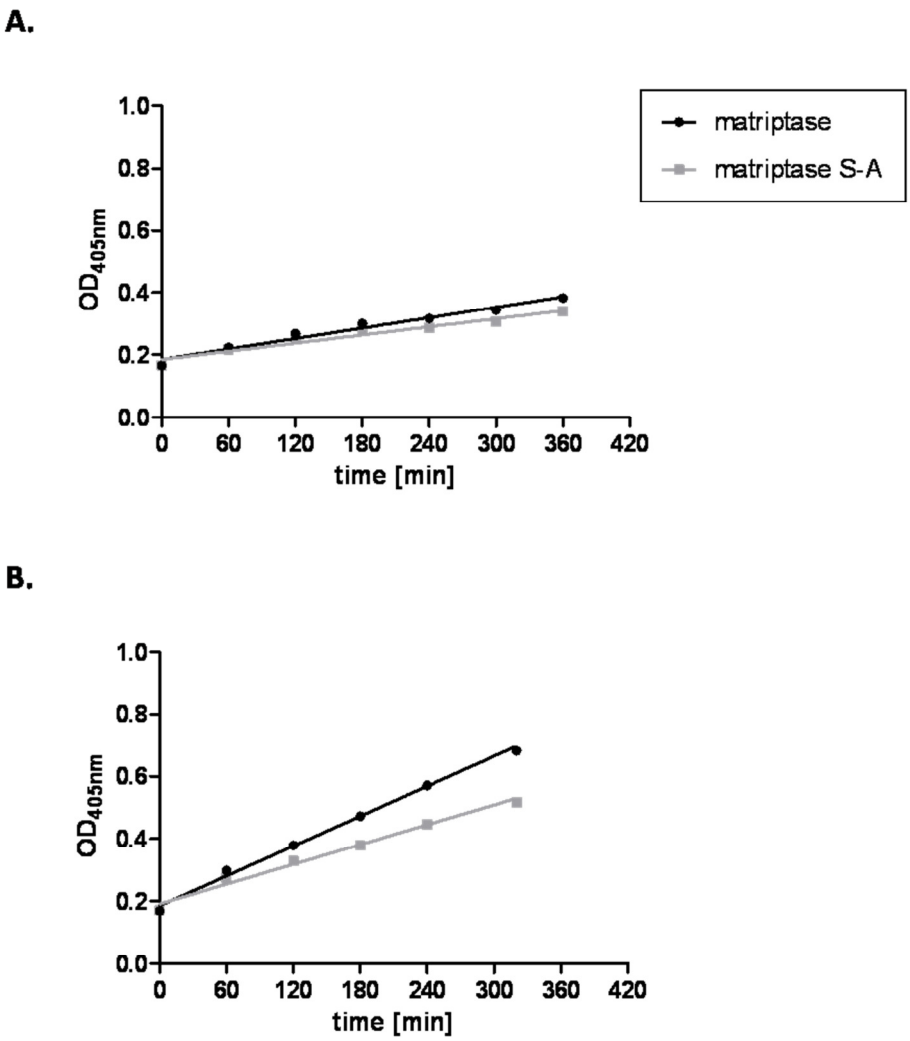

Figure 4.8 Optimisation of AP/V5 TMEFF2 shedding by matriptase in stable AP/V5 TMEFF2 HEK293 cell line transiently transfected with matriptase.

To optimise the detection of AP/V5 TMEFF2 shedding by serine proteases HEK293 cells stably expressing AP/V5 TMEFF2 were transiently transfected with matriptase or inactive S-A mutant, as a control. 48 hours post-transfection cells were incubated for 1 hour (A) or 3 hours (B) in serum free OptiMEM and the conditioned medium was analyzed by AP assay as described in Materials and methods. Both experiments showed increased AP/V5 TMEFF2 release from the cells transfected with matriptase. The increase was more pronounced in B as the 3 hours incubation period allowed the accumulation of AP-tagged ectodomain shed by matriptase in the conditioned medium. Graphs show linear regression analysis of the data from one representative experiment.

4.3.3 Shedding of TMEFF2 by membrane serine proteases expressed in prostate cancer.

The optimised shedding assay protocol was used to investigate if TMEFF2 is a novel substrate for membrane-anchored serine proteases that are implicated in the progression of prostate cancer. An expression plasmid for matriptase-2 was kindly provided by Dr Gloria Velasco from the University of Oviedo, Spain. Plasmids encoding matriptase, hepsin, prostasin as well as inactive SA serine protease mutants were generously supplied by Professor Vincent Ellis, University of East Anglia, UK. The expression of serine proteases in AP/V5 TMEFF2 HEK293 cells transiently transfected with the mentioned plasmids was confirmed by Western blotting and labelling with appropriate antibodies which were also provided by Professor Vincent Ellis (Figure 4.9). Matriptase was detected using rabbit polyclonal antibody recognizing the C-terminal part of this enzyme. This antibody should then detect all variants of matriptase: ~95 kDa full length protein, ~70 kDa processed matriptase and ~120 kDa complex of activate matriptase and its inhibitor HAI-1 (Oberst, Williams, et al. 2003). The detection of serine proteases was performed following separation of the samples in 12.5 % resolving gel, as the same Western blot membranes were then used to detect AP/V5 TMEFF2. For that reason the resolution between 120 kDa and 95 kDa forms of matriptase is not very clear. However, in cells transfected with matriptase and matriptase SA a dispersed ~95-130 kDa band containing one or both forms of this enzyme can be detected (Figure 4.9 A, *lane 1* and *3*). The ~ 70 kDa activated, uncomplexed matriptase was not detected in the samples. The ~40 kDa band detected in the lysates from matriptase-transfected cells as well as ~40-70 kDa bands seen in the matriptase SA sample are thought to be products of matriptase degradation as they do not correspond in size to any variant of matriptase described in the literature to date. The polyclonal anti-matriptase antibody does not recognize matriptase-2, as no bands were detected in the lysate from cells transfected with this enzyme (Figure 4.9 A, *lane 2*). Expression of hepsin in the transfected cells was analyzed using a sheep polyclonal antibody that recognizes a ~45 kDa band corresponding to active hepsin (Figure 4.9 B, *lane 1*). As the hepsin SA mutant is tagged with V5 epitope, the apparent size of this protein on the Western blot is ~47 kDa (Figure 4.9 B, *lane 2*).

The GPI-anchored serine protease prostasin was detected using a mouse monoclonal antibody that recognizes the prostasin zymogen (~40 kDa), activated prostasin (~38 kDa) and a prostasin complex with its inhibitor, protease nexin-1 (PN-1; ~84 kDa), as presented in Figure 4.9 C.

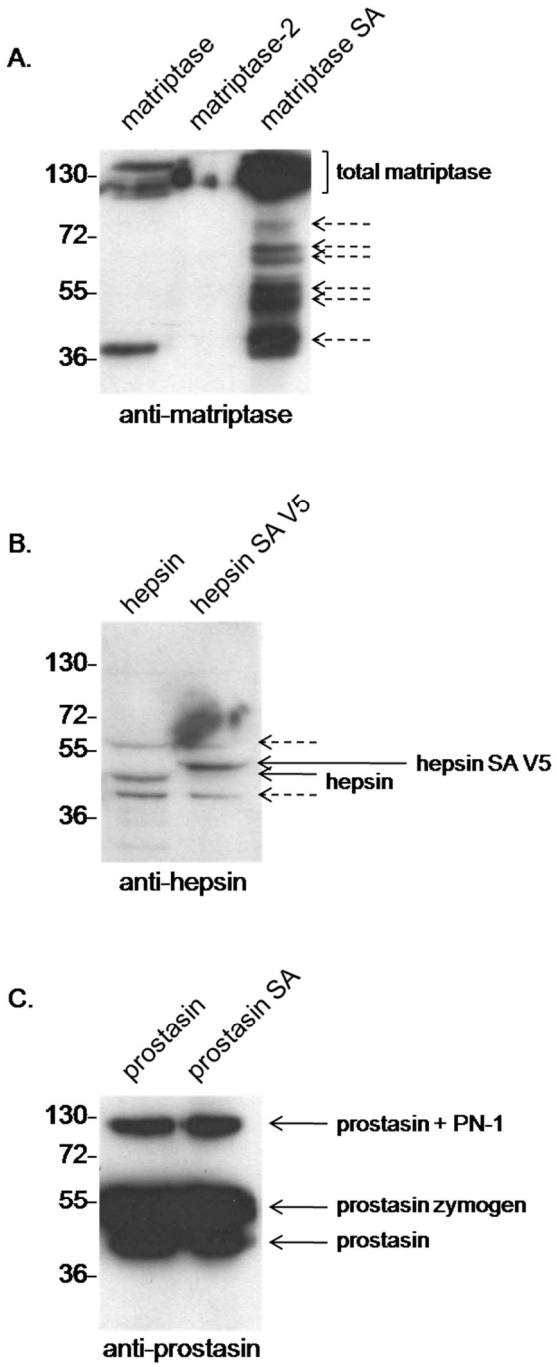

Figure 4.9 Expression of serine proteases in transiently transfected HEK293 cells.

50 µg of lysates from AP/V5 TMEFF2 HEK293 cells transiently transfected with serine proteases were analyzed by Western blotting and labelling with polyclonal anti-matriptase and anti-hepsin or monoclonal anti-prostasin antibodies. Full arrows show bands corresponding to serine proteases and dashed arrows indicate serine proteases degradation products and non specific bands.

In order to examine if TMEFF2 is a novel substrate for serine proteases over-expressed in prostate cancer, AP/V5 TMEFF2 HEK293 cells were transiently transfected with plasmids encoding matriptase, matriptase-2, hepsin and prostasin. To assess basal shedding of AP/V5 TMEFF2, control cells were transfected with inactive S-A serine protease mutants. 48 hours post transfection the cells were incubated for 3 hours in serum free OptiMEM followed by the analysis of AP activity in the collected conditioned medium. The AP activity in the medium from cells expressing inactive S-A serine protease was set to 1 and used as a reference point to determine the fold increase in shedding in response to over-expression of the appropriate active enzyme. Figure 4.10 A presents mean values from three independent experiments, showing that over-expression of matriptase, matriptase-2 and hepsin significantly increased shedding of AP/V5 TMEFF2 from HEK293 cells by 2.4, 1.5 and 3.2 folds, respectively. In contrast, over-expression of prostasin did not influence the release of AP/V5 TMEFF2, suggesting that AP/V5 TMEFF2 is not a substrate for prostasin.

Analogous experiments were performed using HEK293 cells stably expressing AP/V5 $\Delta_{303\text{-}320}$TMEFF2 mutant to investigate if cleavage mediated by serine proteases occurs with the membrane-proximal region. As shown in Figure 4.10 B, transfection with matriptase and hepsin increased shedding of AP/V5 $\Delta_{303\text{-}320}$TMEFF2, indicating that cleavage by these enzymes occurs in a different position than cleavage by ADAMs. Interestingly, transfection of AP/V5 $\Delta_{303\text{-}320}$TMEFF2 HEK293 with matriptase-2 did not increase AP activity in the analyzed conditioned medium. These results either suggest that the matriptase-2 cleavage site is located within 303-320 TMEFF2 region or that the matriptase-2 induces AP/V5 TMEFF2 shedding indirectly, for example through G-protein coupled receptor (GPCR)-dependent activation of ADAMs. One of the GPCRs that controls ADAMs activation, protease-activated receptor 2 (PAR-2) was shown before to be regulated by proteolytic processing by matriptase (Takeuchi et al. 2000). It is however not known if PAR-2 is activated by matriptase-2.

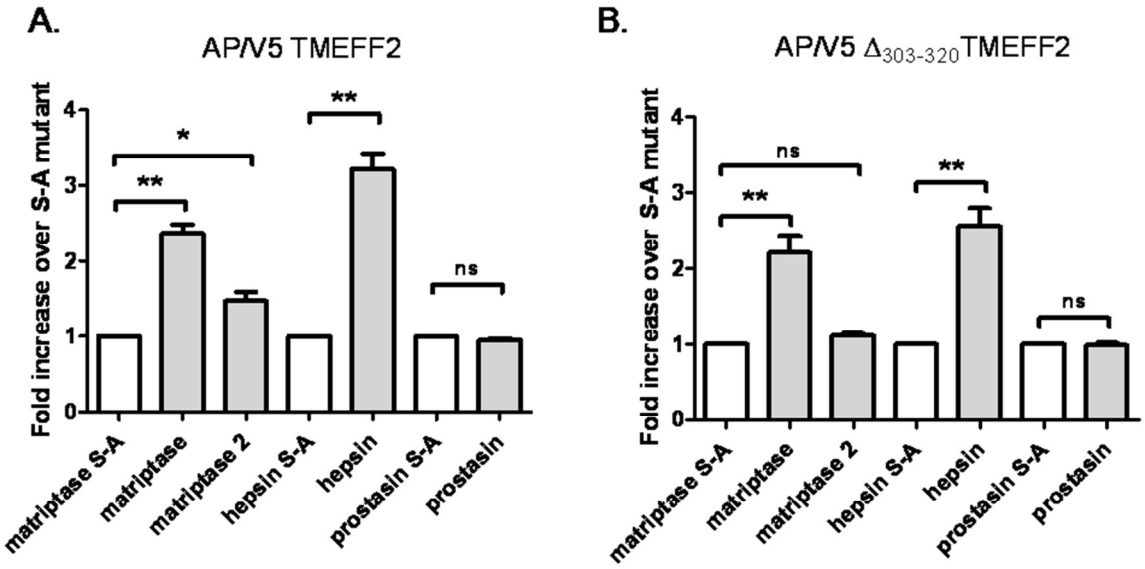

Figure 4.10 Shedding of AP/V5-TMEFF2 and AP/V5-$\Delta_{303-320}$TMEFF2 by membrane-anchored serine proteases.

HEK293 cells stably expressing AP/V5-TMEFF2 (A) or-AP/V5-$\Delta_{303-320}$TMEFF2 (B) were transiently transfected with matriptase, matriptase-2, hepsin and prostasin. As control, cells were transfected with inactive S-A mutants of serine proteases. Following 3 hours incubation in serum free OptiMEM AP activity was measured as described in Materials and methods. AP activity in the medium from cells transfected with inactive S-A serine proteases mutant was set to 1 (white bars) and used as a reference point to determine the shedding increase. Histograms show mean values ±SEM for three independent experiments, each with four repeats per condition. *p<0.05, **p<0.01, ns-not significant.

The lysates from shedding experiments were analyzed by Western blotting and anti-V5 labelling to detect C-terminal AP/V5 TMEFF2 (Figure 4.11 A) and AP/V5 $\Delta_{303-320}$TMEFF2 (Figure 4.11 B) cleavage products. Due to the small sizes of predicted C-terminal fragments samples were separated using 12.5 % resolving gels. As presented in Figure 4.11 A, in all lysates from AP/V5 TMEFF2-expressing cells a ~135 kDa full length AP/V5 TMEFF2 and ~17 kDa fragment generated by ADAMs were observed. In the lysate from matriptase-transfected cells two additional fragments with apparent molecular masses of ~22 kDa and ~27 kDa were seen, indicating that matriptase cleaves AP/V5 TMEFF2 in two positions that are different from the ADAM cleavage site. Transfection with hepsin also generated a novel C-terminal AP/V5 TMEFF2 fragment with the apparent molecular mass of ~19 kDa. A ~10 kDa band detected in the hepsin-transfected cells corresponds in size to the γ-secretase product of AP/V5 TMEFF2 processing (Ali & Knäuper 2007) and suggest that the 19 kDa fragment produced by hepsin can be further cleaved by the γ-secretase complex. No additional bands were observed in the lysates from cells transfected with matriptase-2, supporting the hypothesis that matriptase-2 cleaves AP/V5 TMEFF2 within the same region as ADAMs or enhances ADAM-dependent AP/V5 TMEFF2 shedding.

Analysis of the lysed AP/V5 $\Delta_{303-320}$TMEFF2 HEK293 cells transfected with serine proteases (Figure 4.11 B) revealed the presence of a ~133 kDa band corresponding to the full length AP/V5 $\Delta_{303-320}$TMEFF2 in all samples, whereas the amount of the ~17 kDa fragment was strongly reduced. In the lysate from matriptase-transfected cells a ~19 kDa cleavage product was observed. This fragments may correspond to the ~22 kDa band detected in the lysate from AP/V5 TMEFF2 cell transfected with matriptase, lacking the 17 amino acids (deleted 303-320 sequence). The lack of the second cleavage product can be explained by the different conformation of the AP/V5 $\Delta_{303-320}$TMEFF2 ectodomain that makes the second matriptase cleavage site inaccessible for the enzyme. The molecular size of the C-terminal AP/V5 $\Delta_{303-320}$TMEFF2 fragment generated by hepsin is bigger than in AP/V5 TMEFF2 HEK293 (~22 kDa). This suggests that AP/V5 $\Delta_{303-320}$TMEFF2 has a different conformation that exposes a novel cleavage site that is recognized by hepsin. Analysis of the lysates from AP/V5 TMEFF2 and AP/V5 $\Delta_{303-320}$TMEFF2 HEK293 cells over-expressing serine proteases is in agreement with the shedding assay results, indicating that matriptase and hepsin cleave AP/V5 TMEFF2 in a different position than ADAMs. Matriptase-2 sheds AP/V5 TMEFF2 within the same sequence as ADAMs or increases AP/V5 TMEFF2 indirectly. Transfection with prostasin does not influence AP/V5 TMEFF2 release.

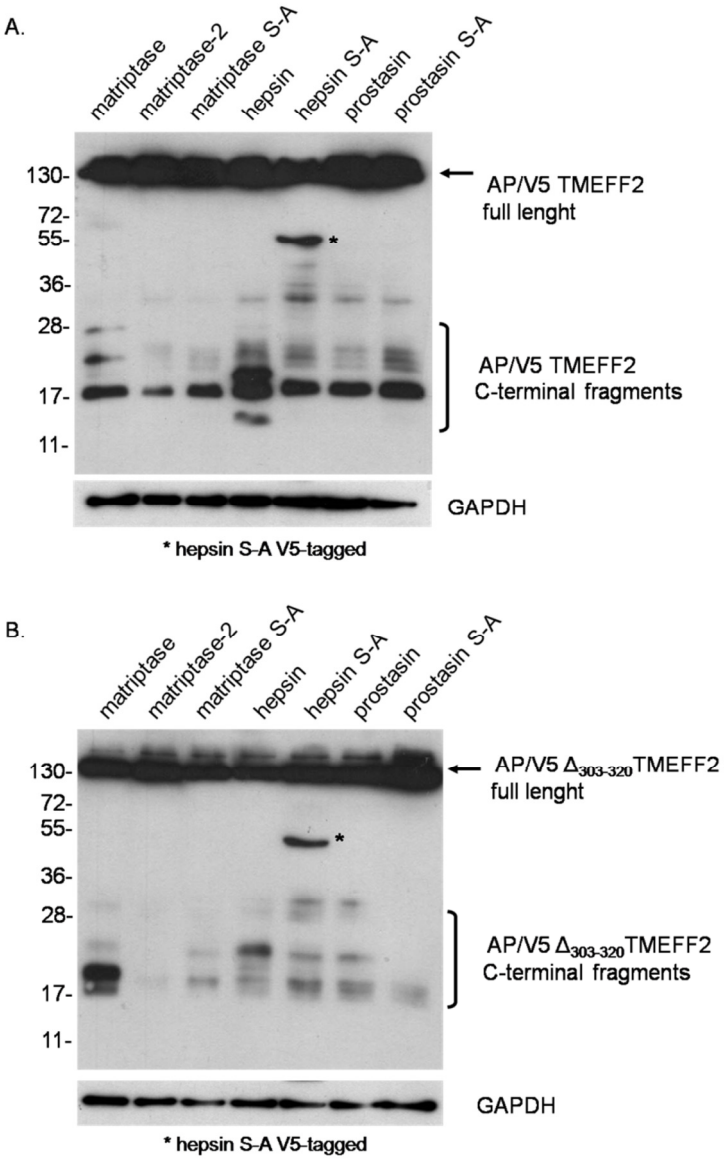

Figure 4.11 Analysis of AP/V5-TMEFF2 and AP/V5-$\Delta_{303-320}$TMEFF2 C-terminal fragments generated by membrane-anchored serine proteases.

Lysates from AP/V5 TMEFF2 (A) or AP/V5 $\Delta_{303-320}$TMEFF2 (B) HEK293 cells transfected with matriptase, matriptase-2, hepsin, prostasin or inactive S-A mutants were analyzed by Western blotting using anti-V5 antibody. 50 µg of total cell lysate was loaded per lane. Labelling with anti-GAPDH antibody served as a loading control. Data are representative for three experiments.

4.3.4 Analysis of AP/V5 TMEFF2 shedding by matriptase-2.

Data presented in the previous paragraph showed increased release of TMEFF2-ECD from AP/V5 TMEFF2 HEK293 cells upon transfection with matriptase-2 (Figure 4.10 A) but no additional C-terminal TMEFF2 cleavage products were detected in cell lysates (Figure 4.11 A, *lane 2*). Moreover, transfection of AP/V5 $\Delta_{303\text{-}320}$TMEFF2-expressing cells with matriptase-2 had no effect on AP/V5 $\Delta_{303\text{-}320}$TMEFF2 release. One of the two possible hypotheses that can explain these results is that matriptase-2 cleaves AP/V5 TMEFF2 in the same position as ADAMs. If this hypothesis is true, the C-terminal products generated by matriptase-2 and ADAMs have the same molecular size and cannot be distinguished by Western blotting. It is also possible, that matriptase-2 causes AP/V5 TMEFF2 shedding through an indirect mechanism, such as increasing activation of ADAMs. It was published recently, that some ADAM substrates are shed from the cell surface in response to agonists of G-protein coupled receptors, for example the proteinase-activated receptors (PARs) (Abdallah et al. 2010). PARs are a family of four transmembrane receptors that are activated upon enzymatic cleavage of their N-terminus by specific serine proteases resulting in the generation of a tethered ligand that activates the receptor (Macfarlane et al. 2001). A member of the PAR family, PAR-2 was shown to be a substrate for matriptase (Takeuchi et al. 2000). Based on this information it was hypothesized that matriptase-2 may increase AP/V5 TMEFF2 shedding through proteolytic processing of PARs and activation of ADAMs. These two hypotheses can be tested by performing AP/V5 TMEFF2 shedding assay in cells transfected with matriptase-2 in the presence or absence of metalloprotease inhibitors. If matriptase-2 cleaves AP/V5 TMEFF2 directly the metalloprotease inhibitor will have no effect on AP/V5 TMEFF2 release. In contrast, the shedding will be inhibited if matriptase-2 causes activation of ADAMs.

AP/V5 TMEFF2 is shed from the cell surface mostly by ADAM10 and ADAM17 (Ali & Knäuper 2007) and for that reason GW280264X (ADAM10 and ADAM17 inhibitor) and GI254023X (ADAM10 inhibitor) were used to test matriptase-2-dependent AP/V5 TMEFF2 shedding. AP/V5 TMEFF2-expressing cells were transiently transfected with matriptase, matriptase-2 and inactive matriptase S-A mutant and incubated for 3 hours in serum free OptiMEM containing 10 µM GW280264X and 10 µM GI254023X inhibitors or equal volume of DMSO as a solvent control. The AP activity in the collected medium was analyzed as described previously. The release of AP/V5 TMEFF2 from cells transfected with matriptase S-A and treated with DMSO was set to one and used to calculate the fold increase in shedding of other samples. As presented in Figure 4.12 A, treatment with GW280264X and GI245023X inhibitors significantly reduces shedding of AP/V5 TMEFF2 by endogenously expressed ADAMs in cells transfected with inactive matriptase S-A. Shedding of AP/V5 TMEFF2 was also reduced in cells expressing matriptase-2 and

treated with the mentioned inhibitors. The release of AP/V5 TMEFF2 was slightly decreased in cells transfected with matriptase and treated with inhibitors, but the difference was not significant. The data obtained from the shedding assay were further analyzed by calculating the percentage of shedding inhibition, according to the following formula:

$$100 - \frac{\text{shedding with inhibitor}}{\text{shedding without inhibitor}} \times 100\% = \% \text{ of shedding inhibition}$$

As shown in Figure 4.12 B, inhibitor treatment of AP/V5 TMEFF2 cells transfected with matriptase S-A reduced shedding by ~28%. A very similar level of shedding inhibition (25%) was calculated in cells transfected with matriptase-2, whereas treatment of AP/V5 TMEFF2 HEK293 cells expressing matriptase with GW280264X and GI245023X decreases shedding by only 12%. It indicates, that AP/V5 TMEFF2 release in cells over-expressing matriptase-2 is dependent on ADAMs, as it is inhibited by GW280264X and GI245023X at the same level as in cells over-expressing inactive matriptase S-A. Shedding of AP/V5 TMEFF2 by matriptase is ADAM-independent as the inhibitors reduce it only by 12%, suggesting that expression of matriptase 'overcome' the inhibitory effect of GW280264X and GI254023X. An analogous experiment was performed using AP/V5 $\Delta_{303-320}$TMEFF2-expressing cells. The results presented in Figure 4.13 show only slight reduction (4-10%) of AP/V5 $\Delta_{303-320}$TMEFF2 HEK293 upon treatment with GW280264X and GI245023X, as this TMEFF2 mutant is resistant to ADAM mediated shedding.

Cell lysates from the same experiments were analyzed by Western blotting and labelled with anti-V5 antibody to detect full length AP/V5 TMEFF2, AP/V5 $\Delta_{303-320}$TMEFF2 and C-terminal cleavage fragments (Figure 4.14). According to the shedding assay data treatment with GW280264X and GI245023X decreased shedding of AP/V5 TMEFF2 and should reduce the amount of ~17 kDa AP/V5 TMEFF2 fragment generated by ADAMs but not 22 kDa and 27 kDa fragments produced by matriptase. However, no reduction of the bands corresponding to AP/V5 TMEFF2 C-terminus was observed on the Western blot, probably due to the low sensitivity of Western blot and further proteolytic processing of this fragment.

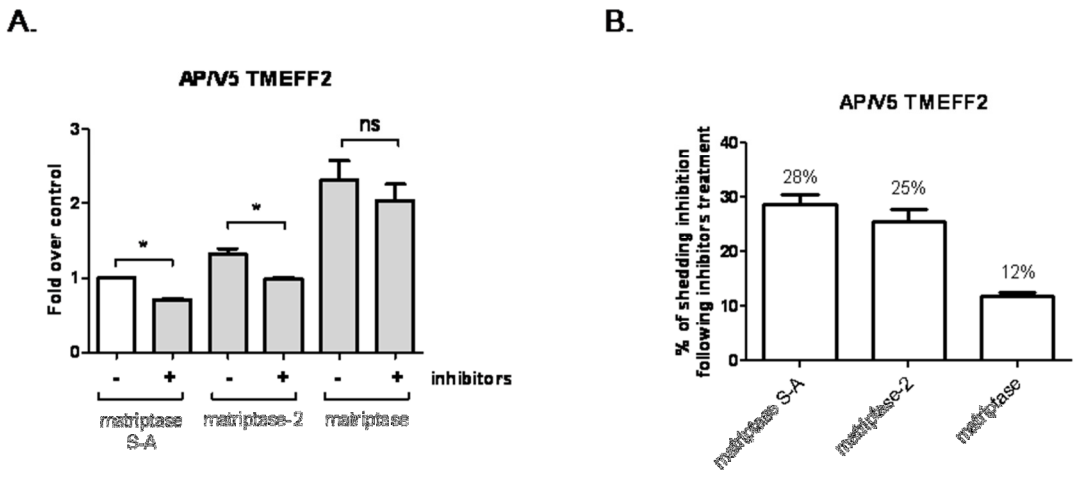

Figure 4.12 Shedding of AP/V5 TMEFF2 by matriptase and matriptase-2 in the presence of ADAM inhibitors.

AP/V5 TMEFF2 cells were transiently transfected with matriptase, matriptase-2 or matriptase S-A and treated for 3 hours with selective ADAM10 and ADAM17 inhibitors (10 µM GW280264X and 10 µM GI254023X) or DMSO as a control. (A) The AP activity of the medium from AP/V5 TMEFF2 cells transfected with inactive matriptase S-A and treated with DMSO was set to one (white bar) and used as a reference to calculate the fold increase in shedding of the remaining samples. Histogram shows mean values from three experiments ±SEM, ns-not significant, *$p<0.05$. (B) Shedding values were also used to calculate percentage of shedding inhibition based on the formula described in the text. Values displayed above bars correspond to mean percentage of shedding inhibition. Histogram shows data from three experiments ±SEM.

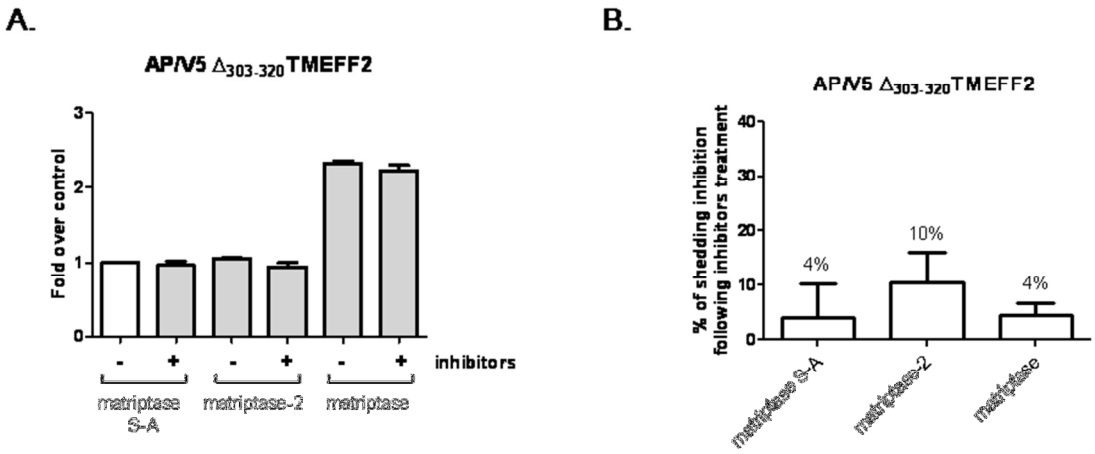

Figure 4.13 Shedding of AP/V5 $\Delta_{303-320}$TMEFF2 by matriptase and matriptase-2 in the presence of ADAM inhibitors.

AP/V5 $\Delta_{303-320}$TMEFF2 cells transfected with matriptase, matriptase-2 or matriptase S-A were treated for 3 hours with 10 µM GW280264X and GI254023X (ADAM10 and ADAM17 inhibitors) or DMSO as a control. (A) The AP activity of the medium from AP/V5 $\Delta_{303-320}$TMEFF2 cells transfected with inactive matriptase S-A and treated with DMSO was set to one (white bar) and used as a reference to calculate the fold increase in shedding of the remaining samples. Histogram shows mean values from three experiments ±SEM, ns-not significant, *$p<0.05$. (B) Shedding values were also used to calculate percentage of shedding inhibition based on the formula described in the text. Values displayed above bars correspond to mean percentage of shedding inhibition. Histogram shows data from three experiments ±SEM.

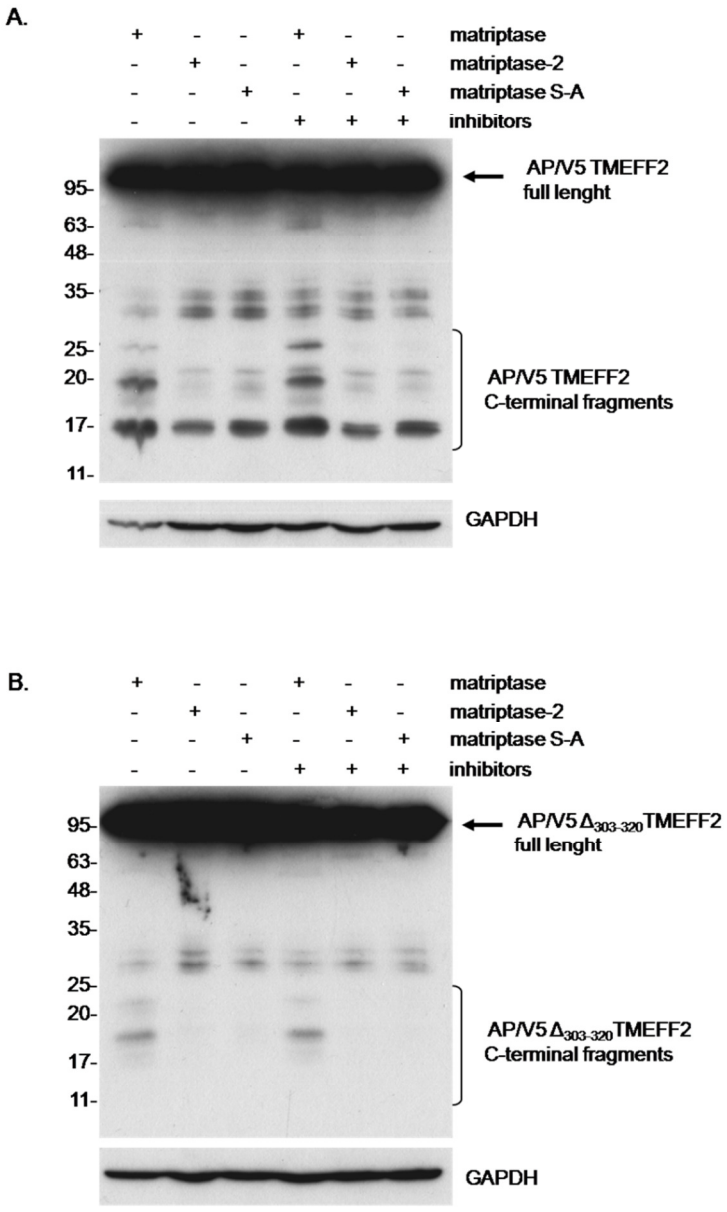

Figure 4.14 Analysis of AP/V5 TMEFF2 and AP/V5 $\Delta_{303-320}$TMEFF2 C-terminal cleavage products generated by matriptase and matriptase-2 in the presence of ADAM inhibitors.

Lysates from AP/V5 TMEFF2 (A) or AP/V5 $\Delta_{303-320}$TMEFF2-expressing cells transfected with matriptase, matriptase-2 or matriptase S-A and treated for 3 hours with 10µM GW280264X and 10µM GI254023X inhibitors were analyzed by Western blotting and labelling with anti-V5 antibody. Anti-GAPDH labelling served as a loading control. Data are representative for three independent experiments. No difference in bands intensity was observed between samples treated with and without inhibitors.

4.3.5 Shedding of TMEFF2 in the presence of matriptase-activated prostasin.

Most of the trypsin-like serine proteases are synthesized as inactive zymogens and require endoproteolytic cleavage to become active. The GPI-anchored serine protease prostasin is produced as an inactive pro-form and can be activated by other members of the serine proteases family, for example matriptase and hepsin (M. Chen et al. 2010; Netzel-Arnett et al. 2006). To assess if the lack of AP/V5 TMEFF2 cleavage from HEK293 cells transfected with prostasin is caused by the lack of prostasin zymogen activation AP/V5 TMEFF2 cells were co-transfected with prostasin and matriptase using a 1:1 DNA ratio.

Activation of the prostasin zymogen leads to the formation of the active enzyme that can be distinguished from the zymogen by a small increase in electrophoretic mobility (Netzel-Arnett et al. 2006). The ~40 kDa zymogen is a major form of prostasin detected in the lysates from cells co-transfected with prostasin or prostasin S-A and inactive matriptase S-A (Figure 4.15, *lanes 3 and 4*). Expression of prostasin or prostasin S-A together with active matriptase results in zymogen activation and only a ~38 kDa band of the activated enzyme was detected in these cells (Figure 4.15, *lanes 1 and 2*). In the lysate from cells expressing matriptase S-A and prostasin S-A a band corresponding to the complex of prostasin and its inhibitor, protease nexin-1 (PN-1) was seen. This result suggests that HEK293 cells are able to activate prostasin as PN-1 forms SDS-stable complexes only with activated prostasin but not with prostasin zymogen (Chen et al. 2006). This low level of prostasin activation may be mediated by endogenously expressed hepsin (see Chapter 3, Figure 3.4).

Co-transfection of AP/V5 TMEFF2 cells with matriptase and prostasin did not increase the release of AP-TMEFF2-ECD when compared with AP-TMEFF2 shedding from cells expressing inactive matriptase S-A and prostasin (Figure 4.16). This experiment confirms that TMEFF2 is not a substrate for prostasin.

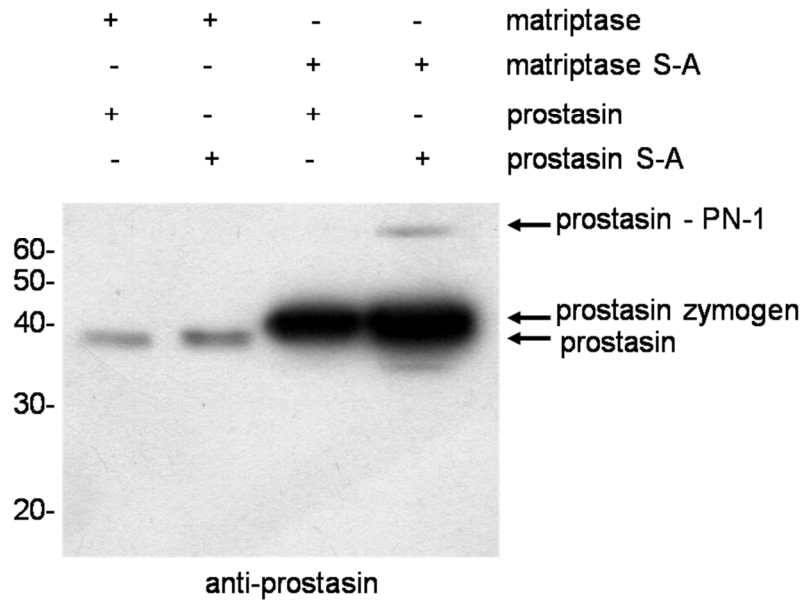

Figure 4.15 Activation of prostasin in HEK293 cells co-transfected with matriptase.

AP/V5-TMEFF2 HEK293 cells were transiently co-transfected with matriptase and prostasin or inactive S-A controls. Cell lysates were analyzed by Western blotting and labelling with anti-prostasin antibody to detect the presence of prostasin zymogen, activated prostasin and a complex of prostasin with its inhibitor, protease nexin-1 (PN-1). Data are representative for two experiments.

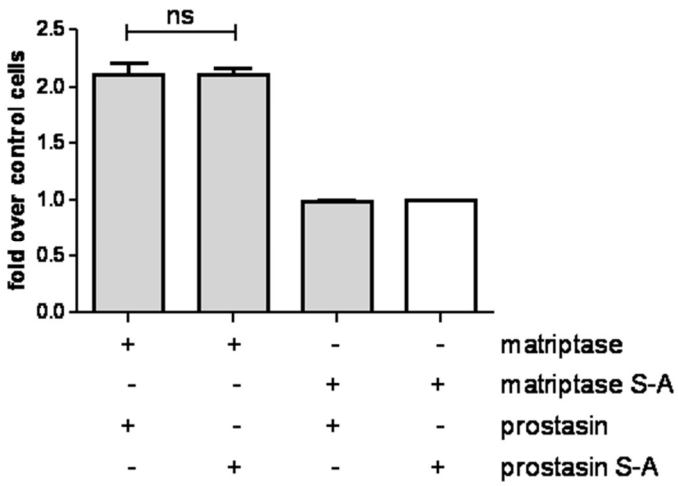

Figure 4.16 AP/V5 TMEFF2 shedding from HEK293 cells co-transfected with matriptase and prostasin.

AP/V5-TMEFF2 HEK293 cells were transiently co-transfected with matriptase and prostasin or inactive S-A controls. Release of AP-TMEFF2-ECD was monitored following 3 hours incubation in serum free OptiMEM. AP/V5 TMEFF2 shedding from control cells co-transfected with matriptase S-A and prostasin S-A mutants was set to 1 (white bar) and used as a reference point to determine the fold increase in shedding of all samples; ns – not significant, n=3, ±SEM.

4.3.6 Shedding of TMEFF2 by ADAMs involved in prostate cancer progression.

In addition to serine proteases also metalloproteases from the ADAM family are implicated in the progression of prostate cancer. The expression of ADAM9, ADAM12 or ADAM15 variants was found in prostate cancer cells and correlates with the disease progression, as described in Chapter 1. To investigate if these ADAMs are involved in TMEFF2 processing, AP/V5 TMEFF2-expressing cells were transiently transfected with plasmids encoding ADAM9, ADAM12 and ADAM15A, B and C variants. To assess the background shedding of AP/V5 TMEFF2 from HEK293 cells, mediated by endogenously expressed ADAMs, control cells were transfected with the inactive ADAM15B EA mutant. Expression vectors encoding ADAM9 and ADAM12 were obtained from Professor Carl Blobel, Hospital for Special Surgery, New York, US and the plasmids for FLAG-tagged ADAM15 variants were generously supplied by Dr Zaruhi Poghosyan, Cardiff University, UK. The construct endcoding ADAM12-V5 was generated by Dr Vera Knäuper.

Expression of ADAMs in transiently transfected HEK293 cells was confirmed by analysis of the lysates in 8% resolving gel and Western blotting (Figure 4.17). Labelling of the Western blot with anti-ADAM9 antibody revealed low endogenous expression of ADAM9 in these cells (Figure 4.17 A, *lane 1*) that significantly increased upon transfection with ADAM9 expression vector (Figure 4.17 A, *lane 2*). Due to the lack of specific high affinity antibodies recognizing ADAM12, the vector encoding V5-tagged ADAM12 was used in transient transfection. Anti-V5 labelling showed the presence of the latent proenzyme (~120 kDa) as well as the mature form (~90 kDa) of ADAM12 in transfected cells (Figure 4.17 B). Expression of ADAM15B EA was confirmed by labelling with anti-ADAM15 antibody (Figure 4.17 C) and FLAG-tagged active ADAM15A, B and C variants were detected using anti-FLAG antibody (Figure 4.17 D).

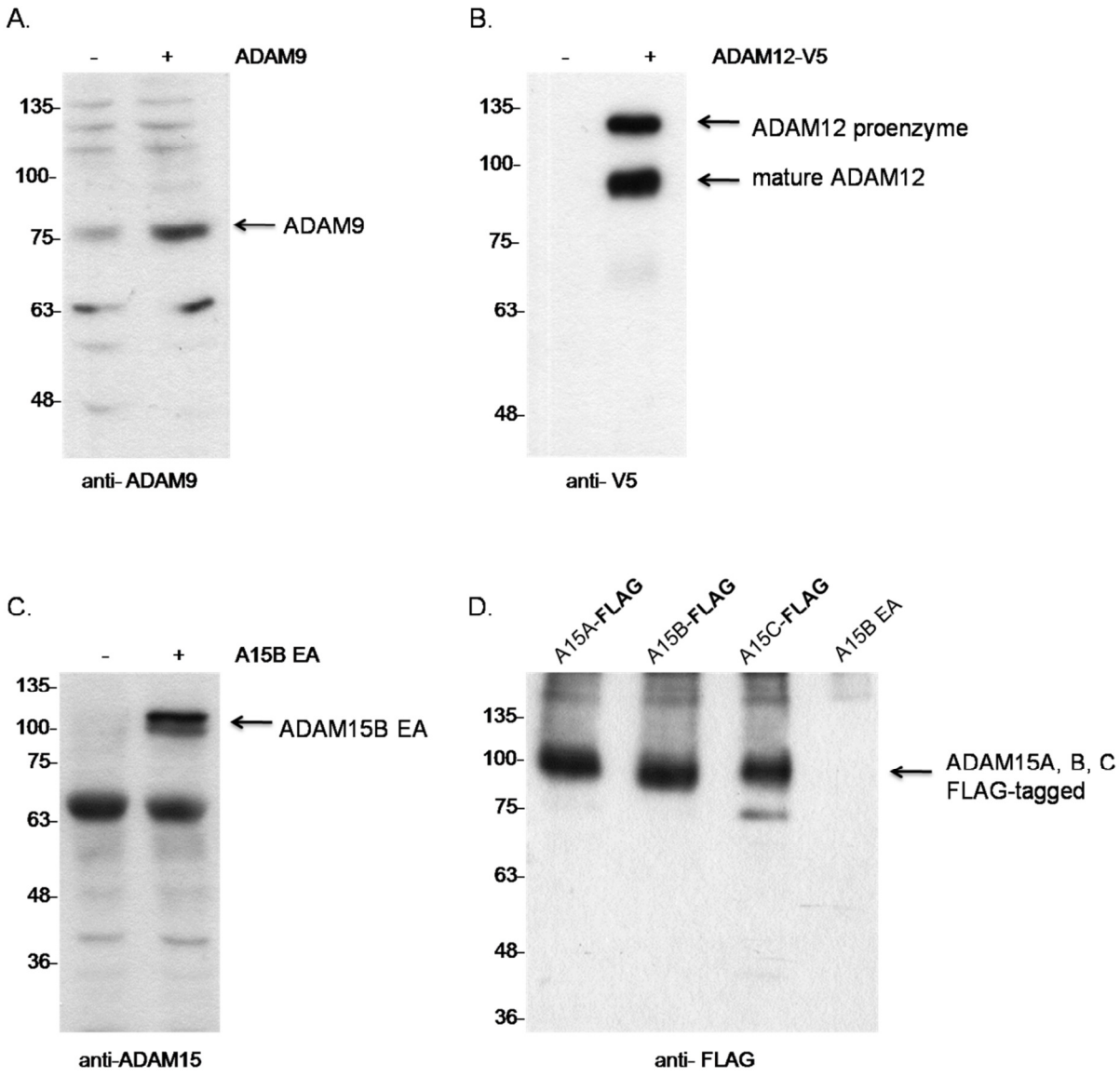

Figure 4.17 Expression of ADAM9,12 and 15 in transiently transfected HEK293 cells.

Lysates from HEK293 cells transiently transfected with vectors encoding ADAM9 (A), ADAM12-V5 (B), ADAM15B EA (C) and FLAG-tagged ADAM15A, B and C variants (D) were analyzed by Western blotting and labelled with appropriate antibodies. 50 µg of total lysate was loaded per lane and samples were separated using 8% resolving gels. Arrows indicate bands corresponding to specific ADAM labelling as described in the text.

Shedding of AP/V5 TMEFF2 by ADAMs implicated in the progression of prostate cancer was investigated similarly to serine protease-mediated cleavage. AP/V5 TMEFF2 cells were transfected with plasmids encoding ADAM9, ADAM12, ADAM15A, B, C or ADAM15B EA as inactive ADAM control and 48 hours post transfection cells were grown for 3 hours in serum free OptiMEM. The release of AP-tagged TMEFF2 ectodomain was measured in the collected medium by the AP assay. AP/V5 TMEFF2 shedding from cells transfected with ADAM9, 12, 15A, 15B and 15C was compared with the AP/V5 TMEFF2 release from ADAM15B EA-transfected cells. Results presented in Figure 18 A indicate, that AP/V5 TMEFF2 is a novel substrate for ADAM9 and ADAM12 but it is not cleaved by ADAM15A, B and C variants. Transfection of AP/V5 $\Delta_{303-320}$TMEFF2 HEK293 cells with ADAM9 and ADAM12, as well as ADAM15A, B and C variants did not increase shedding, as this TMEFF2 mutant lacks the ADAM cleavage sequence (Figure 4.18 B).

Processing of AP/V5 TMEFF2 by ADAMs expressed in prostate cancer cells was also analyzed by Western blotting and labelling with anti-V5 antibody (Figure 4.19 A). In the lysate from AP/V5 TMEFF2 HEK293 cells transfected with ADAM9 and ADAM12 an accumulation of the 17 kDa fragment was detected. The amount of this ADAM-generated stump in the samples from ADAM15A, B and C-transfected cells was comparable with the control cells, expressing ADAM15B EA. This result is in agreement with the shedding assay data and confirms that AP/V5 TMEFF2 is cleaved by ADAM9 and ADAM12 but not ADAM15A, B and C.

The lysates from AP/V5 $\Delta_{303-320}$TMEFF2 HEK293 cells transfected with ADAMs were also tested by Western blotting for the presence of V5-tagged C-terminal cleavage products (Figure 4.19 B). As this TMEFF2 mutant lacks the ADAM cleavage sequence, only the full length AP/V5 $\Delta_{303-320}$TMEFF2 was detected on the blot.

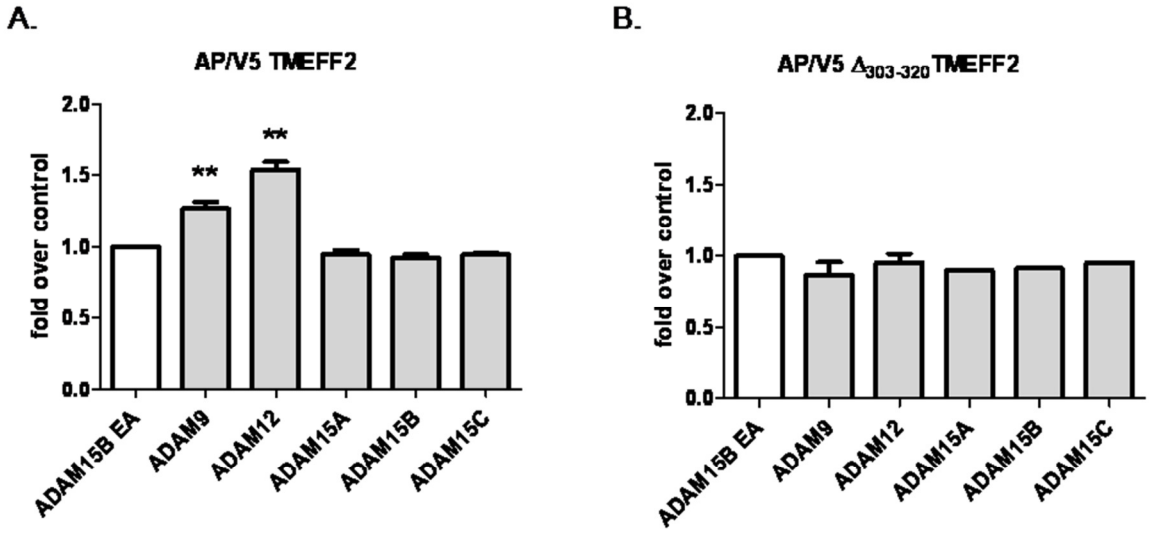

Figure 4.18 Shedding of AP/V5 TMEFF2 and AP/V5 $\Delta_{303-320}$TMEFF2 by ADAMs.

Cells expressing AP/V5 TMEFF2 (A) or AP/V5 $\Delta_{303-320}$TMEFF2 (B) were transfected with ADAM9, 12, 15A, 15B, 15C or inactive ADAM15B E-A as a control. The release of AP/V5 TMEFF2 and AP/V5 $\Delta_{303-320}$TMEFF2 was measured following 3 hours incubation in serum free OptiMEM using the AP assay. The AP activity in the medium from ADAM15B EA-transfected cells (white bars) was set to 1 and used as a reference point to determine the fold increase in shedding of all samples. The shedding of AP/V5 TMEFF2 was elevated in ADAM9 and ADAM12-transfected cells but not in cells expressing ADAM15 variants whereas AP/V5 $\Delta_{303-320}$TMEFF2 release was not increased in the presence of tested ADAMs. Histograms show mean values ±SEM for three independent experiments, each with four repeats per condition; **$p<0.01$.

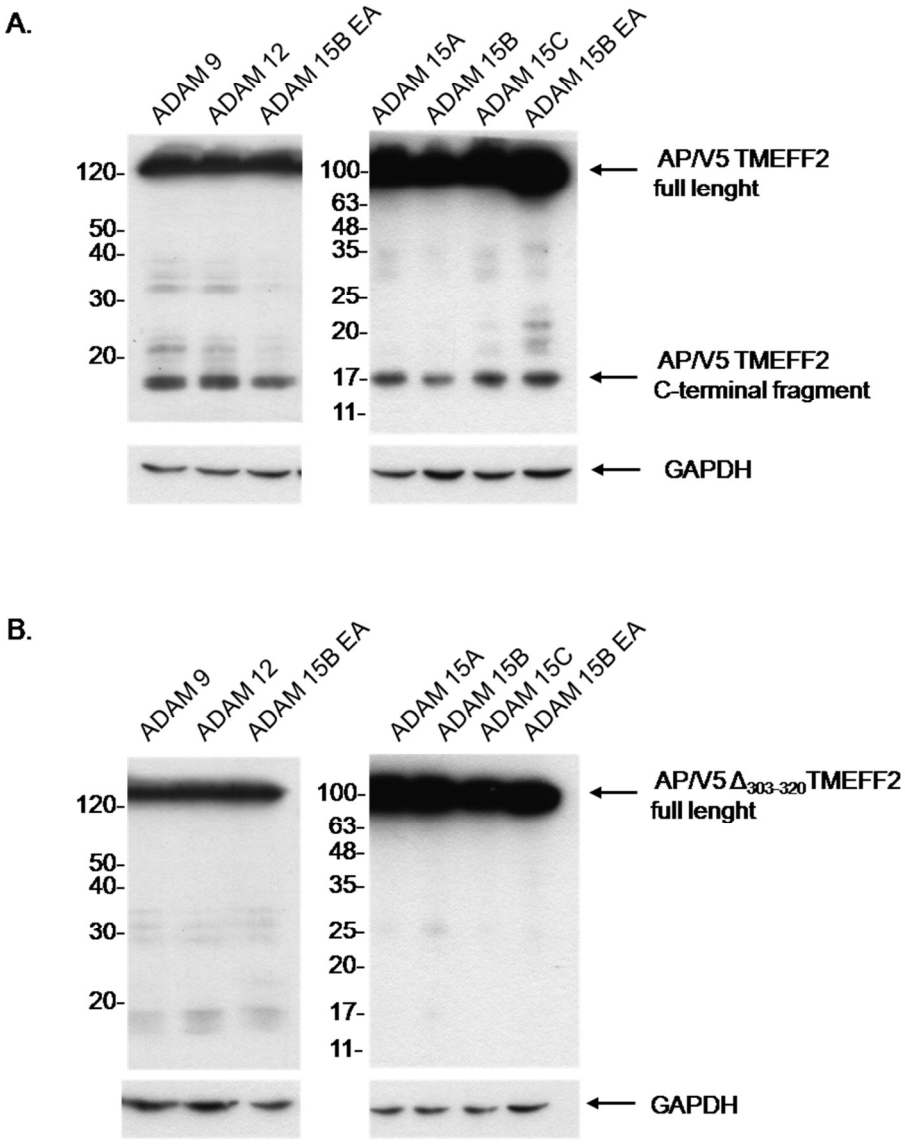

Figure 4.19 AP/V5-TMEFF2 and AP/V5-$\Delta_{303-320}$TMEFF2 C-terminal cleavage products generated by ADAMs.

Lysates from AP/V5-TMEFF2 (A) or AP/V5-$\Delta_{303-320}$TMEFF2 (B) cells transfected with ADAM 9, 12, 15A, 15B, 15C or inactive ADAM15B EA mutant were analyzed by Western blotting using anti-V5 antibody. 50 µg of total cell lysate was loaded per lane and samples were separated in 12.5% resolving gels. Labelling with anti-GAPDH antibody served as a loading control. Data are representative of three experiments.

4.3.7 Shedding of TMEFF2 in the presence of PDGF-AA.

TMEFF2 was recently reported to be an important regulatory factor of the PDGF signaling pathway. The ectodomain of TMEFF2 binds PDGF-AA and this interaction prevents PDGF-AA from activating its receptor, PDGFRα (Lin et al. 2011). It was shown previously by Lin and co-workers that the shedding of TMEFF2 ectodomain can be regulated by cytokines, for example IL-1β and TNF-α and involves the activation of the NF-KB transcription factor (Lin et al. 2003). Based on these data it was hypothesized that PDGF-AA may also influence TMEFF2 shedding. To examine this hypothesis AP/V5 TMEFF2 cells were transfected with human PDGFRα (hPDGFRα), as this receptor is not endogenously expressed by HEK293 cells. The expression of PDGFRα in transfected cells was confirmed by Western blotting and labelling with anti-PDGFRα antibody, which detected a ~110 kDa band corresponding to the human PDGFRα (Figure 4.20). In previous reports TMEFF2 shedding in response to cytokine treatment was detected following overnight stimulation (Lin et al. 2003). For that reason AP/V5 TMEFF2 cells transfected with hPDGFRα or empty vector were incubated overnight in serum free OptiMEM containing 10 ng/ml and 100 ng/ml of recombinant human PDGF-AA (rhPDGF-AA) or solvent control and the AP activity in the medium was measured. Results presented in Figure 4.21 show that PDGF-AA had no effect on AP/V5 TMEFF2 release following overnight treatment of cells in the presence (Figure 4.21 A) or absence (Figure 4.21 B) of hPDGFRα expression.

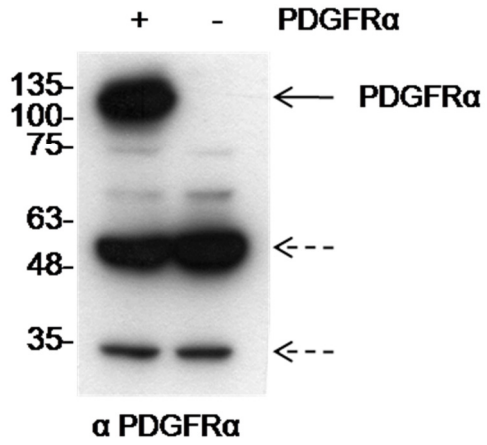

Figure 4.20 Expression of PDGFRα in transfected AP/V5 TMEFF2 HEK293 cells.

20 µg of lysates from AP/V5 TMEFF2-expressing cells transfected with human PDGFRα or empty vector were analyzed by Western blotting following separation using a 10% resolving gel. Labelling of the membrane with polyclonal anti-PDGFRα antibody showed the presence of a ~110 kDa band corresponding to human PDGFRα (full arrow) in the lysate from transfected cells and two non-specific bands (dashed arrows) in both samples.

A.

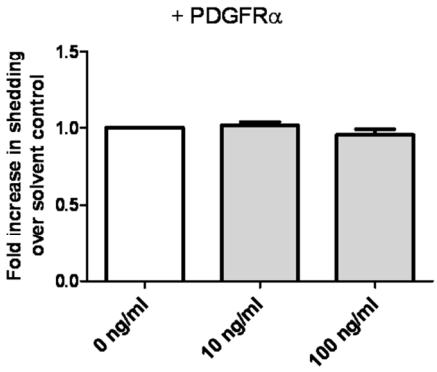

B.

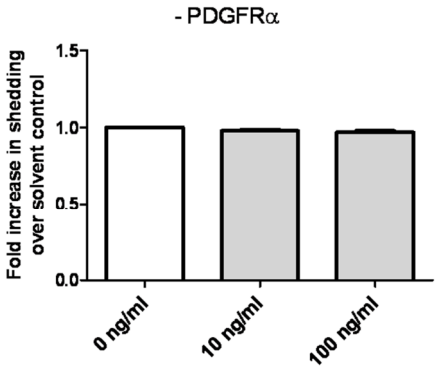

Figure 4.21 Shedding of AP/V5 TMEFF2 following overnight treatment with PDGF-AA.

AP/V5 TMEFF2 expressing cells were transiently transfected with hPDGFRα (A) or an empty vector (B) as a control. 36 hours post-transfection cells were treated overnight with 10 ng/ml, 100 ng/ml of rhPDGFR-AA or solvent control in serum free OptiMEM and the AP activity was measured in the collected medium. The AP/V5 TMEFF2 shedding from cells treated with solvent was set to one (white bars) and used as a reference point to asses fold increase shedding of PDGF-AA-treated samples. 24 hours treatment with PDGF-AA did not influence AP/V5 TMEFF2 shedding regardless of PDGFRα expression; n=3, ±SEM.

To further examine AP/V5 TMEFF2 shedding in response to PDGF-AA, AP/V5 TMEFF2 cells transfected with hPDGFRα or empty plasmid were serum-starved overnight followed by 1 hour treatment with 10 ng/ml or 100 ng/ml of rhPDGF-AA. Similarly to the previous experiment, the treatment with rhPDGF-AA had no impact on AP/V5 TMEFF2 shedding from PDGFRα-expressing cells (Figure 4.22 A). Surprisingly, 1 hour stimulation of AP/V5 TMEFF2 cells in the absence PDGFRα expression with rhPDGF-AA significantly reduced AP/V5 TMEFF2 release in a dose-dependent manner (Figure 4.22 B). As described by Lin and co-workers, the interaction between TMEFF2 and PDGF-AA occurs through the second follistatin domain of TMEFF2 and thus it is rather unlikely that PDGF-AA binding to TMEFF2 impaired its shedding by masking the ADAM cleavage site. The most possible explanation of this effect is the internalisation of the AP/V5 TMEFF2-PDGF-AA complex leading to decreased surface levels of AP/V5 TMEFF2 available for shedding. In the presence of PDGFRα, shedding of TMEFF2 was not impaired by PGDF-AA indicating higher affinity of this growth factor to its receptor than to TMEFF2. However, the suggested internalization of the TMEFF2-PDGF-AA complex as well as its cellular fate require further investigation.

A.

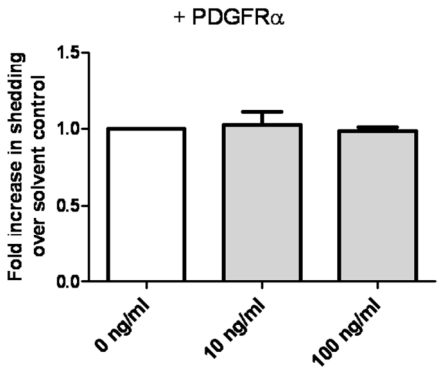

B.

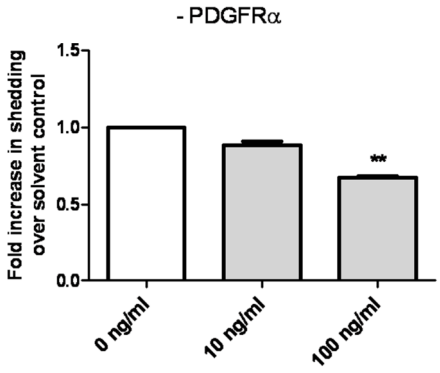

Figure 4.22 Shedding of AP/V5 TMEFF2 following 1 hour treatment with PDGF-AA.

AP/V5 TMEFF2 expressing cells were transiently transfected with hPDGFRα (A) or an empty plasmid (B) as a control. Following overnight serum starvation cells were treated for 1 hour with 10 ng/ml, 100 ng/ml of hPDGFR-AA or solvent control in serum free OptiMEM and the AP activity in the collected medium was measured. The AP/V5 TMEFF2 shedding from cells treated with solvent was set to one (white bars) and used as a reference point to asses fold increase shedding of PDGF-AA-treated samples. In the absence of PDGFRα 1 hour treatment with PDGF-AA significantly reduced AP/V5 TMEFF2 shedding; n=3, ±SEM, **<p0.01.

4.4 Chapter summary.

The main experimental question of this study is to investigate if TMEFF2 is a substrate for proteases over-expressed by the prostate cancer cells and if the proteolytic processing influences TMEFF2 biological function in prostate cancer. It was shown previously by Ali and Knäuper that TMEFF2 undergo ectodomain shedding mediated by abundantly expressed ADAM10 and ADAM17 (Ali & Knäuper 2007). There is also some indication that TMEFF2 may be a substrate for serine proteases as its homologue TMEFF1 forms a complex with the type II transmembrane serine protease matriptase (Ge et al. 2006), it is however not clear if TMEFF1 is cleaved by matriptase.

Investigating TMEFF2 shedding using prostate cancer cell lines that express TMEFF2 endogenously, for example LNCaP would be more difficult due to the low levels of TMEFF2 on the cell surface and TMEFF2-ECD in the conditioned medium, the lack of commercially available antibodies recognizing TMEFF2 C-terminal domain as well as the fact that LNCaP cells are prone to apoptosis following treatment with PMA, the most commonly used inducer of ADAM-mediated shedding (Tanaka et al. 2003). For these reasons the shedding of TMEFF2 was investigated using HEK293 cells stably transfected with human TMEFF2 tagged on the N-terminus with alkaline phosphatase (AP) and on the C-terminus with V5 epitope. The presence of the AP tag enabled easy and sensitive detection of the released TMEFF2 ectodomain in the conditioned medium and the small V5 tag allowed investigation of cytoplasmic products of TMEFF2 cleavage. It makes the AP/V5 TMEFF2 HEK293 cell line a useful model to monitor TMEFF2 processing by ADAMs and serine proteases. In order to establish if TMEFF2 shedding by serine proteases occurs within the same sequence as cleavage by ADAMs, HEK293 cells stably expressing AP/V5 $\Delta_{303\text{-}320}$TMEFF2 mutant were also used in the experiments. As described by Ali and Knäuper, $\Delta_{303\text{-}320}$TMEFF2 mutant is resistant to ADAM-mediated cleavage due to the deletion of the 17 amino acid sequence from the membrane proximal region (Ali & Knäuper 2007). Before performing the shedding study the total expression of AP/V5 TMEFF2 and AP/V5 $\Delta_{303\text{-}320}$TMEFF2 in both cell lines was compared by Western blotting (Figure 4.2) as significantly different expression levels would make the interpretation of the shedding data difficult. The cell membrane location of both recombinant proteins was confirmed by confocal microscopy (Figure 4.3), excluding the possibility that reduced shedding of AP/V5 $\Delta_{303\text{-}320}$TMEFF2 mutant results from the lack of the cell surface localization. The total expression levels as well as cellular location of AP/V5 TMEFF2 and AP/V5 $\Delta_{303\text{-}320}$TMEFF2 were very similar but the release of these two proteins from the cell surface was profoundly different. AP/V5 TMEFF2 was shed constitutively by endogenously expressed ADAMs and the shedding increased following PMA stimulation (Figure 4.4 and 4.5 A). As a result of shedding, a 17 kDa V5-tagged TMEFF2 C-terminal fragment was detected in lysates (Figure 4.6 A). AP/V5 $\Delta_{303\text{-}}$

$_{320}$TMEFF2 was not released from the cell surface, even upon treatment with high doses of PMA (Figures 4.4 and 4.5 B) and only the full length AP/V5 $\Delta_{303-320}$TMEFF2 was detected by Western blotting in cell lysates (Figure 4.6 B).

Following the characterization of the basal and PMA-induced release of AP/V5 TMEFF2 and AP/V5 $\Delta_{303-320}$TMEFF2 three experimental setups were tested to optimize the protocol allowing the sensitive detection of serine protease-mediated shedding (Figures 4.7 and 4.8). The most accurate results were obtained when HEK293 cells stably expressing AP/V5 TMEFF2 were transiently transfected with expression constructs for serine protease and incubated for 3 hours in serum free OptiMEM medium followed by AP activity assay of collected medium samples. This protocol was then used to investigate AP/V5 TMEFF2 and AP/V5 $\Delta_{303-320}$TMEFF2 shedding by serine proteases implicated in prostate cancer: matriptase, matriptase-2, hepsin and prostasin. The control cells were transfected with inactive S-A serine protease mutants and the release of AP/V5 TMEFF2 or AP/V5 $\Delta_{303-320}$TMEFF2 from these cells served as a reference values to calculate fold increase shedding. Data summarized in Figure 4.10 showed that both AP/V5 TMEFF2 as well as AP/V5 $\Delta_{303-320}$TMEFF2 were cleaved by matriptase and hepsin, indicating that serine proteases and ADAMs cleave TMEFF2 in different positions. Analysis of the intracellular cleavage products by Western blotting supported the data obtained from the AP activity assay as novel C-terminal fragments were detected in lysates from AP/V5 TMEFF2-expressing cells transfected with matriptase and hepsin (Figure 4.11). In addition to the ~17 kDa fragment generated by ADAM-mediated cleavage, ~22 kDa and ~27 kDa fragments were detected in the cells transfected with matriptase and ~19 kDa fragment was found in the lysate from cells transfected with hepsin. The apparent molecular sizes of these novel cleavage products as well as the fact, that serine protease cleave their substrate after Arg or Lys residues made possible to distinguish several cleavage sites which are potentially recognized by matriptase and hepsin. Analysis of the TMEFF2 3D structure, kindly modeled by Dr Konrad Beck using *3DPro* software and presented in Figure 4.23 revealed the compact structure of the follistatin-like modules and the EGF-like domain. Most of the Arg and Lys residues present in the follistatin-like and EGF-like modules are not solvent exposed and it is therefore unlikely that they would be accessible to matriptase or hepsin for cleavage. On that basis it was hypothesized that TMEFF2 shedding occurs within the linker sequences between the domains as they are situated on the surface of the molecule and are accessible for proteases.

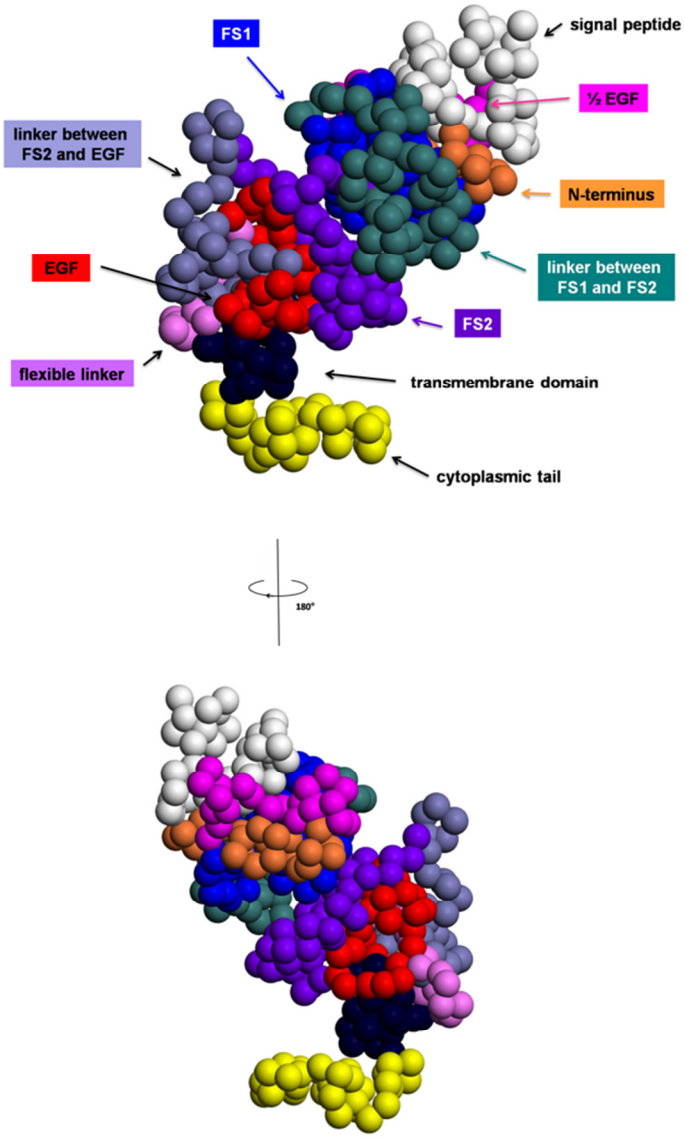

Figure 4.23 Human TMEFF2 modelled using 3DPro software.

TMEFF2 3D model generated by Dr Konrad Beck using 3DPro software. Each globule represents Cα position of residues.

Based on the analysis of TMEFF2 3D structure as well as the molecular masses of matriptase and hepsin cleavage products it was proposed that matriptase cleaves TMEFF2 within the linker between follistatin-like domains (~27 kDa C-terminal product) and between the second follistatin module and the EGF-like domain (~22 kDa fragment). The hepsin cleavage site is more likely located between the second follistatin module and the EGF-like domain but closer to the C-terminus of TMEFF2, as the molecular size (~19 kDa) is smaller than the matriptase-generated product. The proposed matriptase and hepsin cleavage sites are indicated by red arrows in the Figure 4.24.

Figure 4.24 Proposed matriptase (M) and hepsin (M) cleavage sites within the human TMEFF2 sequence.

The Arg and Lys residues that may serve as matriptase (M) or hepsin (H) cleavage sites are indicated by red arrows in the human TMEFF2 protein sequence. The two follistatin domains are marked in green and the EGF-like domain is indicated in blue.

The precise determination of the matriptase and hepsin cleavage sites could be investigated by N-terminal sequencing of the 19 kDa, 22 kDa and 27 kDa TMEFF2 fragments detected on the Western blot. The exact Arg and Lys residues that are recognized by matriptase and hepsin could be identified by performing shedding assays using cells expressing AP/V5 TMEFF2 mutants that contain R→A or K→A mutations within the proposed cleavage sites. Characterization of the N- and C-terminal TMEFF2 fragments generated by matriptase and hepsin would be a very interesting subject of the future experiments, however the data presented in this chapter are convincing enough to demonstrate that TMEFF2 is differentially processed by ADAMs and serine proteases. This processing results in the release of soluble TMEFF2-ECD as well as smaller fragments, containing for example two follistatin-like modules or the seconds follistatin-like module and the EGF-like domain. All of these soluble TMEFF2 fragments might have different biological activities that may significantly influence the behavior of prostate cancer cells.

The described shedding experiments investigated also the influence of matriptase-2 on TMEFF2-ECD release. Although matriptase-2 over-expression increased AP/V5 TMEFF2 release, no increase in shedding was observed when cells expressing AP/V5 $\Delta_{303\text{-}320}$TMEFF2 were transfected with matriptase-2 (Figure 4.10 B). These data together with the absence of novel TMEFF2 C-terminal cleavage products in the lysates of matriptase-2-transfected cells suggested that matriptase-2 cleaved TMEFF2 within the same region as ADAMs. The other hypothesis explaining the lack of AP/V5 $\Delta_{303\text{-}320}$TMEFF2 shedding from the cells expressing matriptase-2 is that matriptase-2 increases activation of ADAMs. It was recently published that ADAM-mediated shedding can be

regulated by activation of protease-activated receptors (PARs) and one of these receptors, PAR-2 was shown to be proteolytically activated by matriptase (Abdallah et al. 2010; Takeuchi et al. 2000). The results presented in this chapter indicated that the shedding of AP/V5 TMEFF2 in the cells expressing matriptase-2 may be regulated by a similar mechanism. To test the involvement of ADAMs in matriptase-2-dependent AP/V5 TMEFF2 release, the shedding was analyzed in the presence of selective ADAM10 and ADAM17 inhibitors - GW280264X and GI254023X. These experiments revealed that matriptase-2 increased AP/V5 TMEFF2 through activation of ADAMs, as treatment with ADAM inhibitors reduced the matriptase-2 effect. In contrast to matriptase-2, AP/V5 TMEFF2 release by matriptase is ADAM-independent as the GW280264X and GI254023X had much smaller effect on shedding from matriptase-transfected cells (Figure 4.12).

The last serine protease that was taken into consideration as a novel TMEFF2 sheddase was prostasin. Transfection of AP/V5 TMEFF2 and AP/V5 $\Delta_{303-320}$TMEFF2 HEK293 cells with this enzyme did not increase shedding (Figure 4.10). Prostasin is synthesized as an inactive zymogen and requires proteolytic cleavage to become activated. As it does not possess autocatalytic activity, prostasin need to be cleaved by other enzyme, for example matriptase or hepsin (M. Chen et al. 2010; Netzel-Arnett et al. 2006). To confirm that the lack of AP/V5 TMEFF2 shedding by prostasin does not result from insufficient prostasin activation, the release of AP/V5 TMEFF2 was monitored following co-transfection of prostasin with matriptase. This experiment confirmed that AP/V5 TMEFF2 is not processed by prostasin, even when activated prostasin is present in the cells (Figures 4.15 and 4.16). The lack of TMEFF2 processing by prostasin may be explained by the spatial separation of these two proteins on the cell surface. Prostasin is localized within lipid rafts (Verghese et al. 2006) whereas there is no indication that TMEFF2 is also present within these membrane compartments.

In addition to matriptase, matriptase-2, hepsin and prostasin shedding of TMEFF2 by ADAM9, ADAM12 and ADAM15A, B and C was also investigated. These ADAMs are expressed by the prostate cancer cells and their levels correlate with the progression of cancer disease (Sung et al. 2006; Peduto et al. 2006; Lucas & Day 2009). As shown in Figure 4.18 TMEFF2 shedding was elevated by ADAM9 and ADAM12 whereas tested ADAM15 splice variants (A, B and C) did not influence TMEFF2 release. Interestingly, ADAM9 and ADAM12 increased AP/V5 TMEFF2 release 1.2-1.5 times whereas shedding by matriptase and hepsin was elevated 2.5-3 times (Figure 4.10). These data suggest that serine proteases are more potent TMEFF2 sheddases than ADAMs.

To further investigate shedding of TMEFF2 and the factors that influence this process the release of AP/V5 TMEFF2 in the presence of PGDF-AA was tested. PDGF-AA is the only known binding partner of TMEFF2-ECD and it was proved that PDGF-AA-

TMEFF2 interaction prevents activation of PDGFRα (Lin et al. 2011). As it was shown before that TMEFF2 shedding is induced by cytokines (Lin et al. 2003), AP/V5 TMEFF2 HEK293 cells were treated overnight with different concentrations of recombinant PDGF-AA. This experiment did not show any change in AP/V5 TMEFF2 release, in the presence as well as absence of PDGFRα (Figure 4.21). Surprisingly, when AP/V5 TMEFF2 HEK293 cells were treated with PDGF-AA for 1 hour, the shedding was significantly reduced in a dose-dependent manner. This effect was however observed only in the cells without PDGFRα (Figure 4.22). The most possible explanation of this effect is the internalisation of the AP/V5 TMEFF2-PDGF-AA complex and decreased surface level of AP/V5 TMEFF2 available for shedding. It is also possible that PDGF-AA binding to TMEFF2 mask the ADAM cleavage site and prevent TMEFF2 ectodomain shedding, however both of these proposed scenarios require further investigation.

To summarize, the data presented in this chapter characterize the AP/V5 TMEFF2 and AP/V5 $\Delta_{303-320}$TMEFF2 HEK293 cell lines as useful model to study TMEFF2 processing with good specificity and sensitivity. The optimized shedding assay protocol allowed to demonstrate for the first time that TMEFF2 is processed not only by metalloproteases from ADAM family but also by serine proteases – matriptase and hepsin. Moreover, TMEFF2 cleavage mediated by these enzymes generated novel extracellular and cytoplasmic TMEFF2 fragments that could potentially have different biological functions or activities. The characterization of activity of these fragments may help to understand the role of TMEFF2 in the development and progression of prostate cancer and will be investigated in the following chapters.

Chapter 5:

Expression and purification of TMEFF2 ectodomain fragments in *E. coli*

5.1 Introduction.

The data presented in the previous chapter demonstrated that TMEFF2 is cleaved by proteases over-expressed in prostate cancer cells, specifically the type II transmembrane serine proteases matriptase and hepsin and the metalloproteases: ADAM9 and ADAM12. Moreover, serine proteases and ADAMs cleave TMEFF2 in different positions generating several soluble TMEFF2 fragments with potentially different biological functions. Deciphering the role of TMEFF2 cleavage products may help to understand the role of this transmembrane protein in the development of prostate cancer and explain how ADAMs and serine proteases regulate the biological activity of TMEFF2. The extracellular part of TMEFF2 is composed of two follistatin-like modules and an EGF-like domain which are found in many transmembrane proteins. Thus it was hypothesized that the biological activity of TMEFF2 ectodomain fragments may be similar to other proteins containing these structural modules.

5.1.1 The characterization of an EGF-like domain.

The EGF-like domain is an evolutionarily conserved structural motif, named after the epidermal growth factor (EGF) where it was first described. This protein domain was found singly or in tandem in many functionally diverse proteins including the epidermal growth factor (EGF) and neuregulin (NRG) family of growth factors, extracellular matrix proteins, cell adhesion molecules and plasma proteins. The characteristic structure of the EGF-like domain is defined by six cysteine residues spaced over a sequence of 30-40 amino acids in a characteristic pattern $X_nCX_7CX_{2-3}GXCX_{10-13}CXCX_3YXGXRCX_4LX_n$ and forming three disulphide bonds (Carpenter & Cohen 1990). The main structure of the EGF-like domain consist of two β-sheets, usually referred to as major (N-terminal) and minor (C-terminal) β-sheets (Wouters et al. 2005).

5.1.2 Signaling of EGF-like proteins through ErbB receptors.

The EGF-like domain is a characteristic structural motif present in several ligands activating the ErbB family of receptor tyrosine kinases. The ErbB family consist of four structurally related transmembrane receptors: EGFR (ErbB-1), ErbB-2, ErbB-3 and ErbB-4, also known as HER1-4. The first member of the family, EGFR was identified in 1975 (Carpenter et al. 1975) and since then the ErbB signaling pathway was studied intensively as the expression and signalling of these receptors as well as their ligands was found to be dysregulated in several pathological conditions, including cancer. The ErbB receptors are composed of a large extracellular ligand binding domain followed by a transmembrane domain, a small intracellular juxtamembrane domain preceding the kinase domain and the C-terminal tail containing docking sites for phosphotyrosine-binding effector molecules (Citri & Yarden 2006). The schematic structure of an ErbB receptor is presented in Figure 5.1.

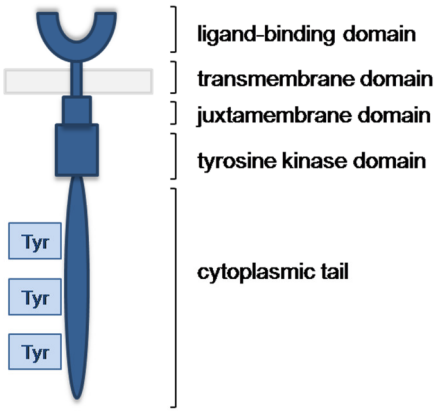

Figure 5.1 Schematic picture of an ErbB receptor.

Binding of a ligand containing the EGF-like domain to the appropriate ErbB results in dimerization of the receptor with another member of the ErbB family and leads to the activation of the tyrosine kinase. This results in phosphorylation of the tyrosine residues present within the cytoplasmic domain of the receptor. The phosphotyrosine residues are recognized by several adaptor proteins containing Src sequence homology (SH2/SH3) domains. These molecules subsequently activate intracellular signalling pathways, including the mitogen-activated-protein kinase (MAPK) pathway, phospholipase Cγ pathway and the phosphoinositide-3 kinase (PI3K) pathway (Figure 5.2) (Ratan et al. 2003).

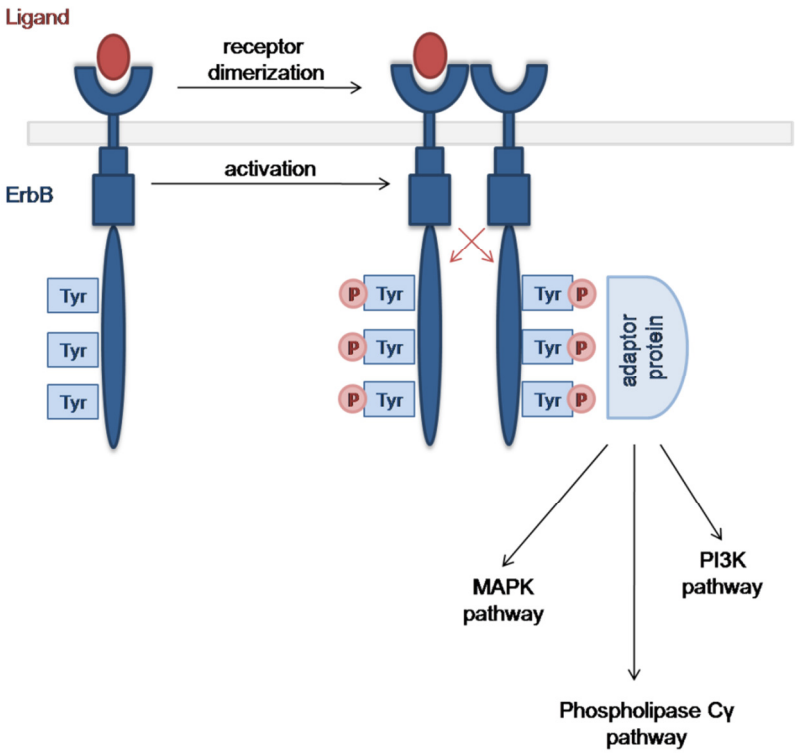

Figure 5.2. Signaling through ErbB receptors. Ligand binding to ErbB results in receptor dimerization and activation of the tyrosine kinase, causing phosphorylation of Tyr residues. Phosphotyrosine residues are recognize by several adaptor molecules that activate downstream signaling cascades, including the MAPK pathway, phospholipase Cγ pathway and PI3K pathway (Ratan et al. 2003).

Although the ErbBs are classified to the receptor tyrosine kinase family, two of these receptors: ErbB-2 and ErbB-3 are not able to signal autonomously. ErbB-2 lacks the capacity to interact with growth factor ligands whereas the kinase activity of ErbB-3 is defective. Despite this lack of autonomy ErbB-2 and ErbB-3 form heterodimers with two other ErbBs and are capable of generating intracellular signals (Citri & Yarden 2006).

The two autonomous ErbBs, EGFR and ErbB-4 share several recognition and signaling features as they are both activated by broad spectrum of EGF-like ligands and upon activation form homodimers as well as functional heterodimers (Citri & Yarden 2006). Phosphorylated EGFR and ErbB-4 interact with a number of adaptor proteins such as growth-factor-receptor bound-2 (Grb2) and Src-homology-2-containing (Shc) which are responsible for the recruitment of Ras and activation of the MAPK signaling cascade. Another protein that directly binds EGFR and ErbB-4 is the signal-transducer and activator of transcription 5 (STAT5) (Schulze et al. 2005).

As the main focus of this study is ectodomain shedding, it is important to mention, that one of the ErbB-4 splice variants, the JM isoform undergoes ADAM-mediated ectodomain shedding (Rio et al. 2000) followed by subsequent processing by γ-secretase and translocation of the cytoplasmic domain to the nucleus (Ni et al. 2001), as described in details in Chapter 1.

It was mentioned before that ErbB-2 (HER2/neu) does not interact with extracellular ligands but it binds to a much larger subset of adaptor molecules than other members of this receptor family. For that reason ErbB-2 is a preferred heterodimeric partner for the other three ErbBs. Furthermore, heterodimers containing ErbB-2 are characterized by a higher affinity and broader specifity to various ligands than other heterodimeric receptor complexes. Also, ErbB-2 containing heterodimers undergo endocytosis and are more frequently recycled to the cell surface (Citri & Yarden 2006).

Another not autonomous receptor, ErbB-3 has defective kinase activity and needs to form heterodimers with the other three ErbBs to participate in signaling. Following heterodimerization the intracellular domain of ErbB-3 undergoes phosphorylation and recruits PI3K to six distinct sites and Shc to one site although there is no binding site for Grb2. This segregation enables ErbB-3 to evade ligand-induced degradation, while strongly activating PI3K (Citri & Yarden 2006).

5.1.3 Non-signaling function of EGF-like domain.

Although several proteins which contain an EGF-like domain interact with ErbB receptors and act as growth factors, the EGF-like domain may have other, non-signaling functions. For example, EGF-like domains were found in components of the blood coagulation system, including factors VII, IX, X and thrombomodulin and are responsible for interactions between different components (Stenflo 1991). An EGF-like domain from neuregulin-1 (NRG-1) binds $\alpha_v\beta_3$ and $\alpha_6\beta_4$ integrins through direct interactions between three Lys residues located on the N-terminus of neuregulin-1 EGF-like domain. The NRG-1-integrin binding is required for NRG-1 signaling through ErbB-3 as NRG-1 mutants which lack one or three of these Lys residues display impaired ErbB-3 activation (Ieguchi et al. 2010). It was also shown that an EGF-like module is present in some adhesion molecules, for example selectins that are involved in leukocyte tethering and rolling on the endothelium. The function of the EGF-like domain in selectins may vary. As shown by Kansas and co-workers, an EGF-like domain in L-selectin does not participate in cellular adhesion whereas the EGF-like domain in P-selectin is important for ligand recognition and cell adhesion (Kansas et al. 1994). Finally, in many proteins EGF-like domains are combined with other domains in a mosaic fashion suggesting that these modules may play an important structural role as a spacer at the cellular level (Campbell & Bork 1993).

5.1.4 The atypical EGF-like domain from TMEFF2.

Alignment of EGF-like domains from TMEFF2 and other proteins containing this structural unit, like betacellulin (BTC), heparin-binding epidermal growth factor (HB-EGF), amphiregulin (AR), tumour necrosis factor α (TNFα) and epidermal growth factor (EGF) revealed several structural similarities. As presented in Figure 5.3, all these EGF-like domains contain the conserved 6 Cys residues in characteristic spacing as well as Gly13 and Gly37 that are essential for the backbone fold of the EGF-like structural unit. However, Arg39 that is involved in binding of EGF-like growth factors to ErbB receptors is replaced with His in TMEFF2 and TMEFF1 (Horie et al. 2000, Figure 5.3). This substitution may significantly affect TMEFF2 binding to ErbBs as the mutation of this Arg residue with Ala in the structure of EGF-like domain from EGF reduced the affinity to EGFR to less than 0.5% (D. a Engler et al. 1990). However, some reports suggest that the EGF-like domain from TMEFF2 has some signaling potential as it was able to activate ErbB-4 in gastric cancer cells (Uchida et al. 1999) and induce phosphorylation of ERK1/2 through EGFR in HEK293 cells (Ali & Knäuper 2007).

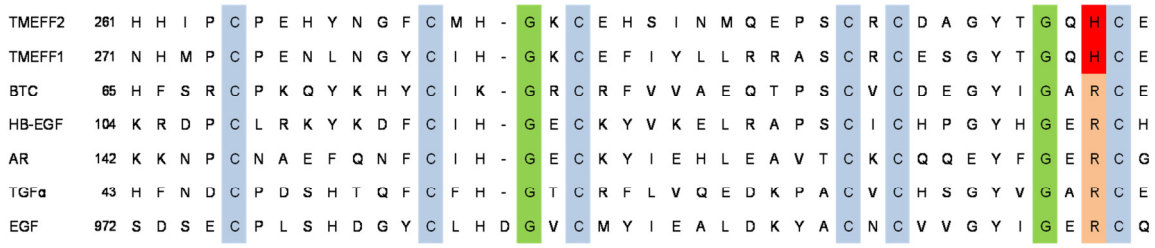

Figure 5.3 Alignment of EGF-like domains sequences from different human proteins: TMEFF2, TMEFF1, betacellulin (BTC), heparin-binding epidermal growth factor (HB-EGF), amphiregulin (AR), tumour necrosis factor α (TNFα) and epidermal growth factor (EGF) (Horie et al. 2000).

5.1.5 Characterization of the *E. coli* expression system chosen to produce TMEFF2 fragments.

To investigate the role of ADAM and serine protease processing in the regulation of TMEFF2 biological function, fragments corresponding to predicted N-terminal TMEFF2 cleavage products were expressed in *E. coli*. The prokaryotic expression system was chosen due to its low cost, fast growth rate of *E. coli* and high amount of recombinant proteins that can be obtained from a relatively small culture. The structure of the TMEFF2 ectodomain is stabilised by several disulphide bonds which makes this protein challenging to express in bacterial systems, since reductases present in the *E. coli* cytoplasm keep Cys residues in their reduced form. For that reason Origami B (DE3)pLysS and SHuffle T7

Express *lysY E. coli* strains were chosen to produce TMEFF2 fragments. The Origami B(DE3)pLysS strain has deletions in the genes for glutaredoxin reductase and thioredoxin reductase (*Δgor ΔtrxB*) which allows disulphide bonds to form in the cytoplasm. Combination of these two deletions is normally lethal, but in this strain the lethality is suppressed by a mutation in the peroxiredoxin enzyme (*ahpC*). In addition to *gor/trxB* mutations, SHuffle T7 Express *lysY* strain expresses in the chromosome a version of the periplasmic disulphide bond isomerase DsbC that lacks its signal sequence, retaining it in the cytoplasm. This enzyme was shown to correct mis-oxidized disulphide bonds and promote proper folding of proteins with multiple disulphide bonds (Lobstein et al. 2012).

Origami B (DE3)pLysS and SHuffle T7 Express *lysY E. coli* were transformed with MAL pRSET B vectors containing sequences encoding TMEFF2 fragments inserted downstream from the *malE* gene. The *malE* gene encodes a maltose binding protein (MBP), resulting in expression of N-terminally tagged MBP-TMEFF2 fusion proteins. Tagging proteins with MBP is a widely used method that gives high levels of expression, increased solubility and enhances proper folding of the targeted protein. Purification of MBP fusion proteins is carried out under physiological conditions and is based on the affinity of MBP to interact with amylose. Mild elution of MBP-tagged proteins from the column material can be achieved using maltose solution, which preserves the biological activity of the target protein and makes this system suitable for the purification of very unstable protein complexes (Kapust & Waugh 1999; Riggs 2000; Sun et al. 2011). Expression of the *malE* gene in MAL pRSET vector is under the control of a strong phage T7 promoter that is specifically recognised by T7 RNA polymerase. To induce the expression of the fusion protein it is necessary to deliver this polymerase to the cells. Origami B(DE3)pLysS or SHuffle T7 Express *lysY E. coli* strains are compatibile with the MAL pRSET B expression system as they both carry the T7 RNA polymerase gene under the control of the lac operon. In non-induced conditions expression of T7 polymerase is repressed in these strains by the *lac* repressor. Expression of the targeted protein is activated upon addition of the allolactose analogue isopropyl β-D-1-thiogalactopyranoside (IPTG) that binds and inactivates the *lac* repressor. The advantage of using IPTG to induce protein expression is that it is not metabolised by *E. coli* so its concentration is not variable during the experiment and the *lac* operon remains permanently activated (Hansen et al. 1998). However, there is always some basal expression level of T7 RNA polymerase which causes low background expression of the targeted gene in non-induced conditions. If the gene cloned downstream of the T7 promoter is toxic for the cells, basal expression of this gene may lead to reduced growth rates, cell death or plasmid instability. For that reason strains that are used to express recombinant proteins under the control of the T7 promoter produce also T7 lysozyme that binds T7 polymerase and inhibits transcription. The Origami B strain expresses T7 lysozyme from pLysS plasmid. This T7 lysozyme, in addition to its T7 RNA polymerase binding activity, cleaves also a specific

bond in the peptidoglycan layer of the *E. coli* cell wall. This makes the *E. coli* strains carrying pLysS plasmid more prone to lysis by freeze-thaw cycles and supports extraction of the recombinant protein. SHuffle T7 Express *lysY* strain produces modified variant of T7 lysozyme that lacks amidase activity and do not influence the structure of *E. coli* cell wall.

5.2 Aims.

The main aim of the experiments summarized in this chapter was to establish expression and purification methods allowing obtaining TMEFF2 fragments corresponding to the predicted N-terminal cleavage products. Recombinant proteins were expressed in two *E. coli* strains Origami B(DE3)pLysS and SHuffle T7 Express *lysY* as maltose-binding protein (MBP) fusion proteins and purified using affinity chromatography and gel filtration. To investigate if the presence of His39 instead of Arg 39 within the structure of EGF-like domain affect TMEFF2 binding to ErbB receptors, a vector encoding $^{H\text{-}R}$EGF-like TMEFF2 mutant was cloned and used to produce $^{H\text{-}R}$EGF-like TMEFF2 MBP-fusion protein. The potential of TMEFF2 EGF-like domain and $^{H\text{-}R}$EGF-like domain mutant to activate ErbB receptors was then compared in *in vitro* ERK1/2 phosphorylation assay.

5.3 Results.

5.3.1 Generation of TMEFF2 ^{HR}EGF-like domain mutant.

The EGF-like domain present within the structure of TMEFF2 ectodomain contains six characteristically distributed Cys residues as well as Gly16 and Gly37 which are required for correct folding and determine the biological activity of the EGF-like module. However, in contrast to other EGF-like proteins the EGF-like domain from TMEFF2 contains His39 instead of Arg39 and this substitution may significantly reduce TMEFF2 affinity to EGFR (Horie et al. 2000). To investigate if the substitution of Arg39 with His39 changes the potential of TMEFF2 EGF-like domain to activate ErbB receptors, an expression vector encoding $^{H\text{-}R}$EGF-like domain TMEFF2 mutant was generated. This TMEFF2 mutant contains a point mutation within the codon for His39 (CAC), changing this amino acid for Arg (CGC). The mutation within the TMEFF2 EGF-like domain was introduced using overlap extension polymerase chain reaction (PCR). This method enables the substitution of a single base pair within the DNA sequence, as well as the introduction of required restriction sites by performing three PCR reactions. A schematic diagram of the overlap extension PCR, designed to substitute His39 with Arg39 and to introduce *HindIII* and *EcoRI* restriction sites, flanking the TMEFF2 $^{H\text{-}R}$EGF-like domain sequence is shown in Figure 5.4.

The first two PCR reactions (PCR1 and PCR2) were performed using the 2ndFS-EGF TMEFF2 MAL pRSET B plasmid as the DNA template and a pair of primers – one carrying the designed point mutation (primers A and D in Figure 5.4) and one introducing required restriction site (primers B and C). Products of PCR1 and PCR2 contained the required mutation (both products) as well and *HindIII* (product of PCR1) or *EcoRI* (product of PCR2) restriction sites and were partially complementary. These products were then mixed in the appropriate ratio and used as a template in PCR3, where primers A and D were used to amplify the whole sequence of mutated TMEFF2 EGF-like domain. The final product of PCR3 corresponded to $^{H\text{-}R}$EGF-like domain from the TMEFF2 gene and was flanked with *HindIII* and *EcoRI* restriction sites at 5' and 3' end, respectively. This DNA fragment was then purified and cloned using *HindIII* and *EcoRI* into MAL pRSET B expression vector, sequenced (Figure 5.5) and used to express TMEFF2 $^{H\text{-}R}$EGF-like domain in *E. coli*.

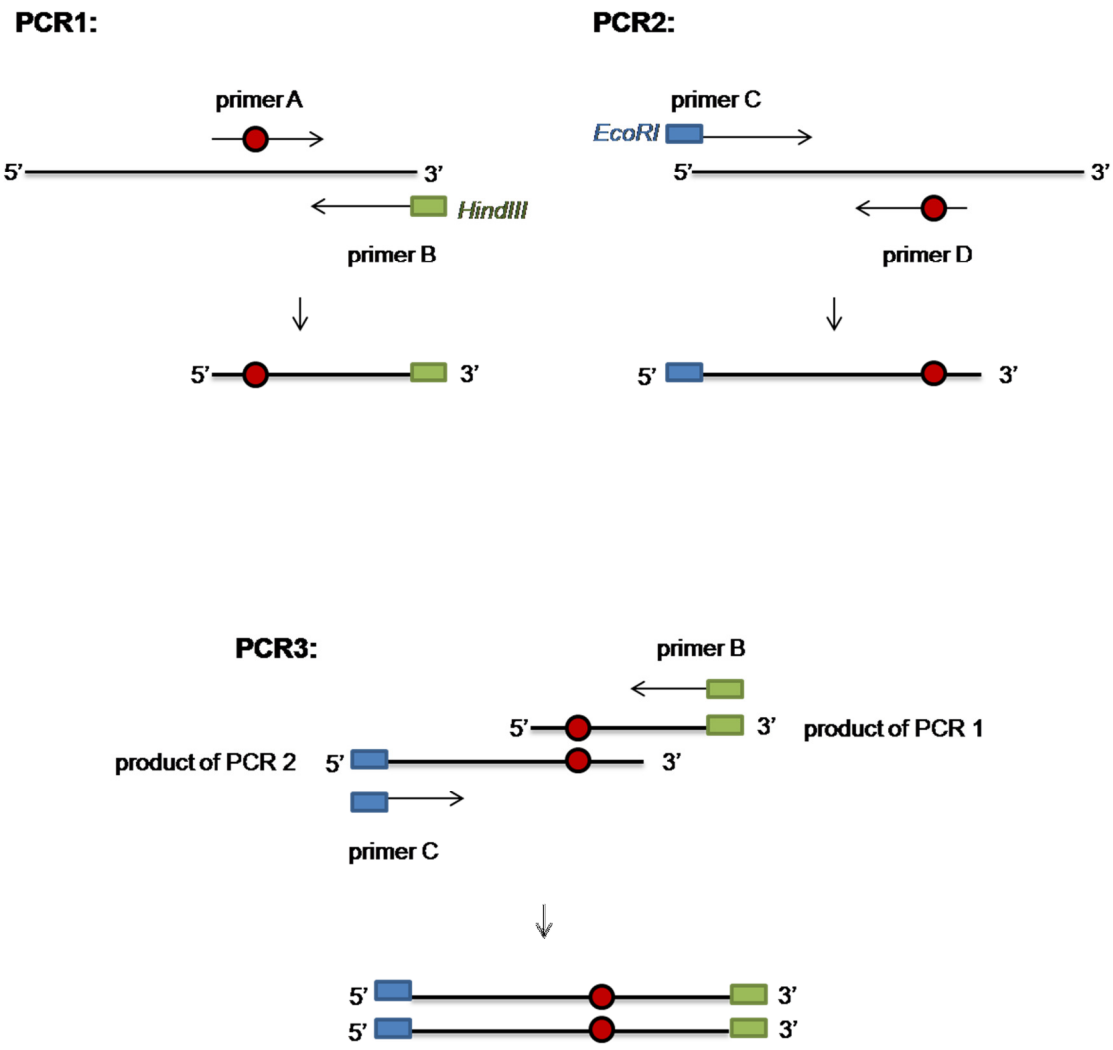

Figure 5.4 Schematic diagram of the overlap extension polymerase chain reaction (PCR) designed to substitute His39 with Arg39 within the sequence of TMEFF2 EGF-like domain.

The point mutation substituting His39 with Arg39 (CAC→CGC) within TMEFF2 EGF-like domain is indicated as a red dot and *HindIII* and *EcoRI* restriction sites are presented as green and blue boxes, respectively.

```
HREGF_TMEFF2    MKIKTGARILALSALTTMMFSASALAKIEEGKLVIWINGDKGYNGLAEVGKKFEKDTGIK
wtEGF_TMEFf2    ------------------------------------------------------------

HREGF_TMEFF2    VTVEHPDKLEEKFPQVAATGDGPDIIFWAHDRFGGYAQSGLLAEITPDKAFQDKLYPFTW
wtEGF_TMEFF2    ------------------------------------------------------------

HREGF_TMEFF2    DAVRYNGKLIAYPIAVEALSLIYNKDLLPNPPKTWEEIPALDKELKAKGKSALMFNLQEP
wtEGF_TMEFf2    ------------------------------------------------------------

HR_EGF_TMEFF2   YFTWPLIAADGGYAFKYENGKYDIKDVGVDNAGAKAGLTFLVDLIKNKHMNADTDYSIAE
wtEGF_TMEFf2    ------------------------------------------------------------

HR_EGF_TMEFF2   AAFNKGETAMTINGPWAWSNIDTSKVNYGVTVLPTFKGQPSKPFVGVLSAGINAASPNKE
wtEGF_TMEFF2    ------------------------------------------------------------

HR_EGF_TMEFF2   LAKEFLENYLLTDEGLEAVNKDKPLGAVALKSYEEELAKDPRIAATMENAQKGEIMPNIP
wtEGF_TMEFf2    ------------------------------------------------------------

HREGF_TMEFF2    QMSAFWYAVRTAVINAASGRQTVDEALKDAQTNSSSNNNNNNNNNNLGIEGRISEFGHYA
wtEGF_TMEFF2    ------------------------------------------------------------

HREGF_TMEFF2    RTDYAENANKLEESAREHHIPCPEHYNGFCMHGKCEHSINMQEPSCRCDAGYTGQRCEKK
                                :::::::::::::::::::::::::::::::::::.::
wtEGF_TMEFF2    -----------------HHIPCPEHYNGFCMHGKCEHSINMQEPSCRCDAGYTGQHCE--

HREGF_TMEFF2    DYSVLYVVPGPVRFQYV
wtEGF_TMEFF2    -----------------
```

Figure 5.5 Alignment of the protein sequence of full length TMEFF2 and ^{HR}EGF-like domain from TMEFF2 mutant.

Sequencing results of $^{H\text{-}R}$EGF TMEFF2 MAL pRSET B vector were translated and aligned with the wild type EGF-like domain from TMEFF2 (wtEGF_TMEFF2) protein sequence using Biology WorkBench 3.2 software. The EGF-like domain is marked in blue and the substituted amino acids ar indicated in red.

5.3.2 Expression of MBP-tagged TMEFF2 fragments in *E. coli*.

The Origami B (DE3)pLysS and SHuffle T7 Express *lysY* strains were transformed with MAL pRSET B vectors encoding MBP-tagged TMEFF2 fragments: the ectodomain (TMEFF2-ECD), two follistatin modules (2xFS), the second follistatin module and EGF-like domain (2^{nd}FS-EGF), the EGF-like domain alone (EGF) and the $^{H\text{-}R}$EGF-like domain TMEFF2 mutant. The MAL pRSET B vector encoding EGF-like domain from HB-EGF has also been used to transform bacteria in order to establish whether the chosen expression and purification protocol is appropriate to produce biologically active EGF-like proteins. MAL pRSET B plasmids used to express MBP-tagged TMEFF2 and HB-EGF fragments were generated by Dr Vera Knäuper based on the pMAL Protein Fusion & Purification System (New England BioLabs) and pRSET B vector (Invitrogen). Generation of $^{H\text{-}R}$EGF TMEFF2 MAL pRSET vector was described in the previous paragraph (5.3.1). The expression of recombinant proteins was induced with IPTG as described in Materials and Methods and small cultures grown without IPTG were kept as non-induced controls. Expression of the fusion protein by transformed bacteria upon IPTG treatment was analyzed by SDS-PAGE and Coomassie staining and presented in Figure 5.6. Addition of IPTG to SHuffle T7 Express *lysY* and Origami B (DE3)pLysS cells transformed with vector encoding MBP TMEFF2-ECD resulted in the accumulation of a 76 kDa TMEFF2-ECD MBP-fusion protein (Figure 5.6 A). Expression of a 65 kDa MBP-tagged 2^{nd}FS+EGF TMEFF2 fragment was also induced in both strains upon IPTG treatment (Figure 5.6 B). Production of 2xFS TMEFF2 MBP-fusion protein was detected as accumulation of a 72 kDa band only in extract from SHuffle T7 Express *lysY* strain but not in Origami B (DE3)pLysS *E. coli* (Figure 5.6 C), probably due to the toxicity of this protein for Origami B strain. Moreover, the level of MBP-2xFS TMEFF2 expression in SHuffle T7 was much lower than expression of ECD or 2^{nd}FS-EGF MBP-fusion proteins which also suggests that the 2xFS TMEFF2 fragment may be toxic for *E. coli* strains. The expression of MBP-EGF-like domains from TMEFF2 and HB-EGF as well as TMEFF2 $^{H\text{-}R}$EGF-like domain mutant was compared in Origami B (DE3)pLysS and SHuffle T7 Express *lysY* strains using a similar induction protocol (Figure 5.7). As shown in a schematic diagram in Figure 5.7 A, MBP-EGF TMEFF2 and MBP-EGF HB-EGF proteins contained an additional V5-His tag that slightly decreased their electrophoretic mobility. The expression of all three EGF-like domains was induced by IPTG in Origami B (DE3)pLysS *E. coli* (Figure 5.7 B). In SHuffle T7 Express *lysY* strain IPTG treatment caused production of MBP-EGF TMEFF2 and MBP-EGF HB-EGF proteins whereas expression of MBP $^{H\text{-}R}$EGF TMEFF2 mutant was not induced in this strain (Figure 5.7 C)..

A.

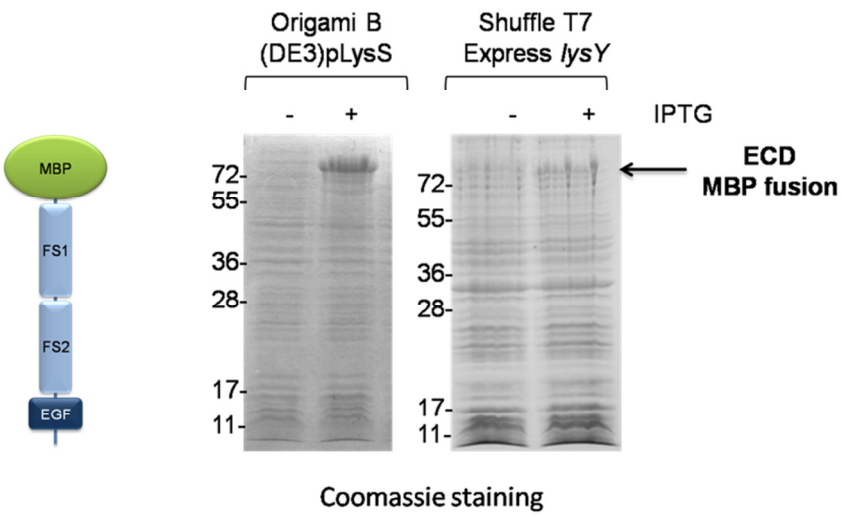

Coomassie staining

B.

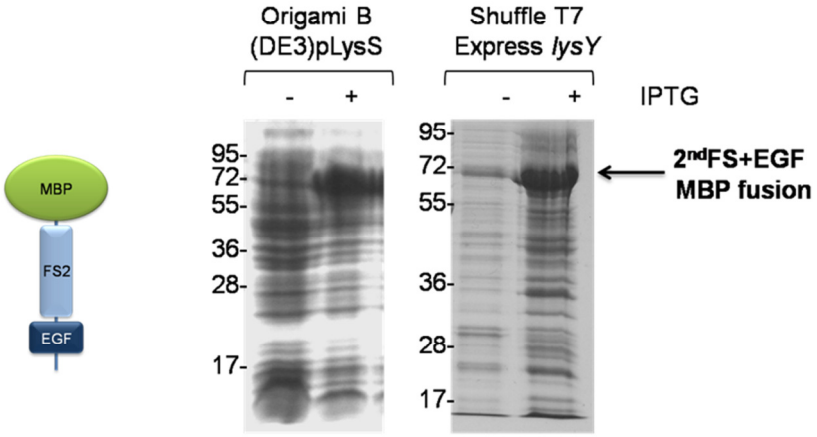

Coomassie staining

C.

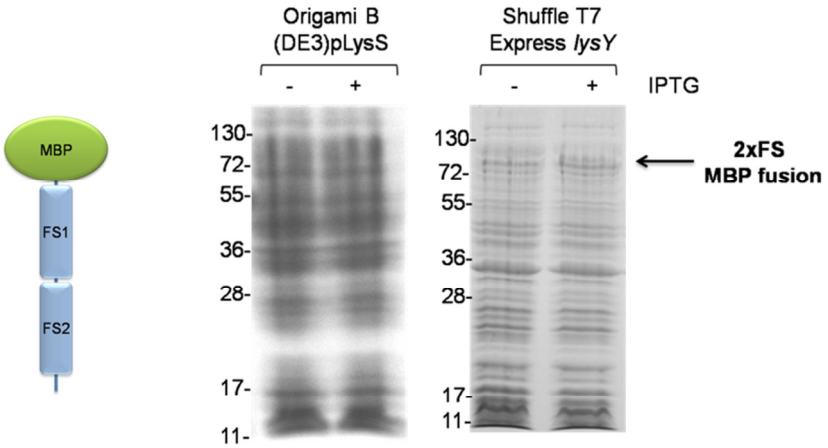

Coomassie staining

Figure 5.6 Expression of MBP-tagged TMEFF2 ECD, FS-EGF and 2xFS fragments in SHuffle T7 Express lysY and Origami B (DE3)pLysS E.coli.

SHuffle T7 Express *lysY* and Origami B (DE3)pLysS *E.coli* strains were transformed with plasmids encoding MBP-tagged TMEFF2 fragments and grown at 37℃ until OD_{600}=0.4-0.5. 1mM IPTG was added to the culture and bacteria were grown at 16℃ overnight. The expression of recombinant proteins was analyzed using cell extracts from induced and non-induced cultures. Proteins were separated by SDS-PAGE using 11% resolving gel and stained with Coomassie Brilliant Blue R-250. TMEFF2 ECD (A) and 2^{nd}FS+EGF (B) MBP-fusion proteins were detected in SHuffle T7 Express *lysY* as well as Origami B (DE3)pLysS *E.coli* induced with IPTG whereas a band corresponding to the 2xFS MBP fusion protein was detected only in extract from SHuffle T7 Express *lysY* strain (C). Schematic diagrams of expressed recombinant proteins are presented next to the gel pictures.

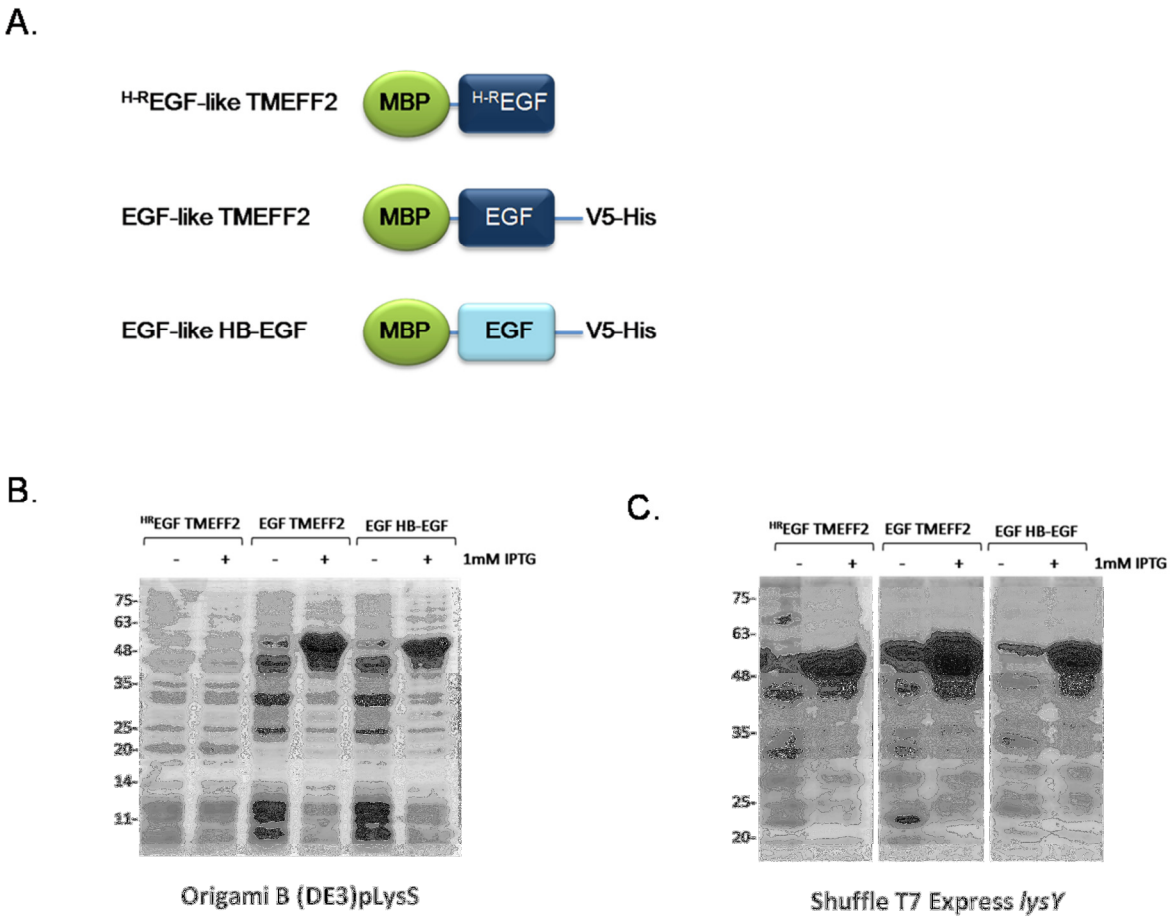

Figure 5.7 Expression of MBP-tagged EGF-like domains from ^{HR}TMEFF2, TMEFF2 and HB-EGF in Origami B (DE3)pLysS and SHuffle T7 Express lysY E. coli.

(A) Schematic diagrams of expressed EGF-like domains from TMEFF2 and HB-EGF and $^{H\text{-}R}$EGF-like domain from TMEFF2 mutant indicate the location of MBP as well as additional V5-His tag. The expression of mentioned EGF-like domains was compared in Origami B (DE3)pLysS (B) and SHuffle T7 Express *lysY* (C) *E.coli* strains. Transformed bacteria were grown at 37℃ until OD_{600}=0.4-0.5 and induced with 1mM IPTG. Following overnight growth at 16℃ samples from induced and non-induced cultures were analyzed by SDS-PAGE using a 11% resolving gel and stained with Coomassie Brilliant Blue R-250. Bands corresponding to MBP-tagged EGF-like domains from TMEFF2 and HB-EGF were observed in extracts from both SHuffle T7 Express *lysY* and Origami B (DE3)pLysS *E. coli* whereas MBP-fusion $^{H\text{-}R}$EGF-like domain from TMEFF2 was expressed only by the Origami B (DE3)pLysS strain.

5.3.3 Purification of TMEFF2 MBP-fusion proteins: affinity chromatography on amylose resin.

In order to purify MBP-tagged proteins the soluble extract from lysed bacteria was mixed with amylose-resin and incubated overnight to allow binding of MBP fusion proteins to amylose. After washing off non bound proteins, the MBP fusion proteins were eluted using 10 mM maltose solution. Due to the higher affinity of amylose to maltose than to MBP the proteins of interest were eluted as a consistent peak within the first 6-10 fractions as shown on Figure 5.8 for MBP-EGF-like domains.

The specificity of this purification method was confirmed by analysis of 1 µg of eluted fusion protein by Western blotting and labelling with anti-TMEFF2-ECD, anti-V5 and anti-MBP antibodies (Figure 5.9). Labelling with anti-TMEFF2-ECD polyclonal antibody enabled the detection of the EGF-like domains from TMEFF2 (wild type and mutated) but not EGF-like domain from HB-EGF (Figure 5.9, left blot). As indicated previously (Figure 5.7 A), the EGF-like domains from TMEFF2 and HB-EGF were tagged with a C-terminal V5-His tag in addition to the MBP protein and can be detected on Western blot using anti-V5 antibody, whereas the $^{H\text{-}R}$EGF-like TMEFF2 mutant lacks V5-His tag (Figure 5.9, middle blot). All three recombinant MBP-fusion proteins were detected using anti-MBP antibody (Figure 5.9, right blot). The apparent sizes observed for the EGF-like domains corresponded to calculated molecular masses of 54.8 kDa, 57.2 kDa and 56.7 kDa for $^{H\text{-}R}$EGF TMEFF2, EGF TMEFF2 and EGF HB-EGF, respectively (see Appendix II).

Additional bands of estimated molecular masses of 120 kDa were also seen when EGF-like domains from TMEFF2 and HB-EGF were analyzed using anti-V5 and anti-MBP antibody, suggesting that this recombinant proteins may form dimers that were not efficiently reduced during sample preparation (Figure 5.9, middle and right blots).

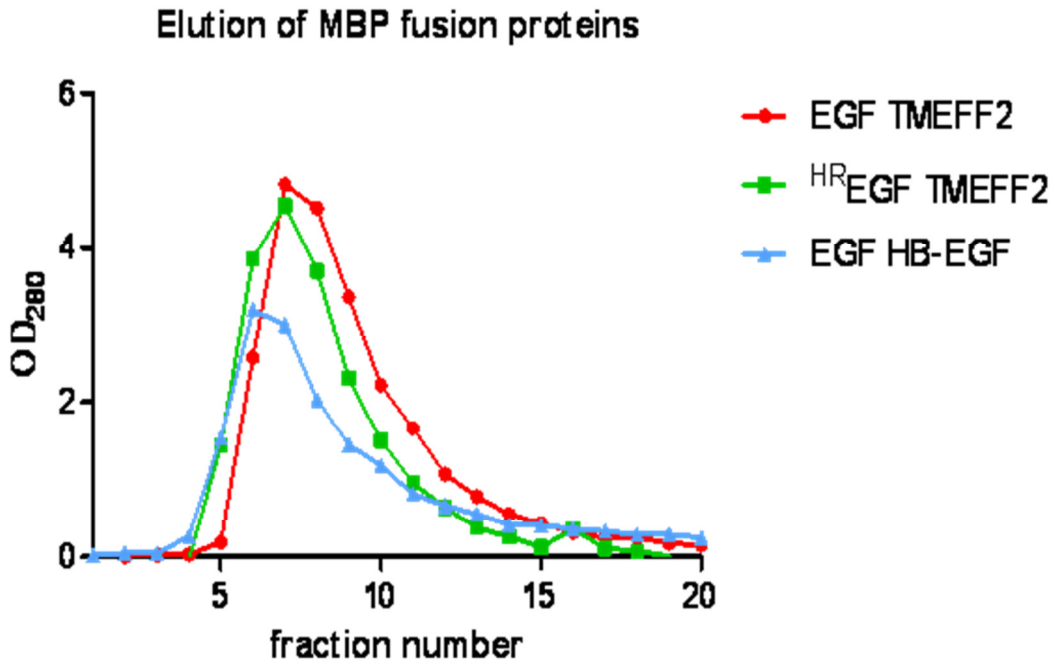

Figure 5.8 Elution of MBP-tagged EGF-like domains from the amylose resin column.

Recombinant EGF-like domains tagged with MBP were eluted from the amylose resin column with 10 mM maltose solution. OD_{280} of collected fractions was measured to monitor the elution of the MBP-fusion protein. All three recombinant proteins were eluted between fractions 6-10.

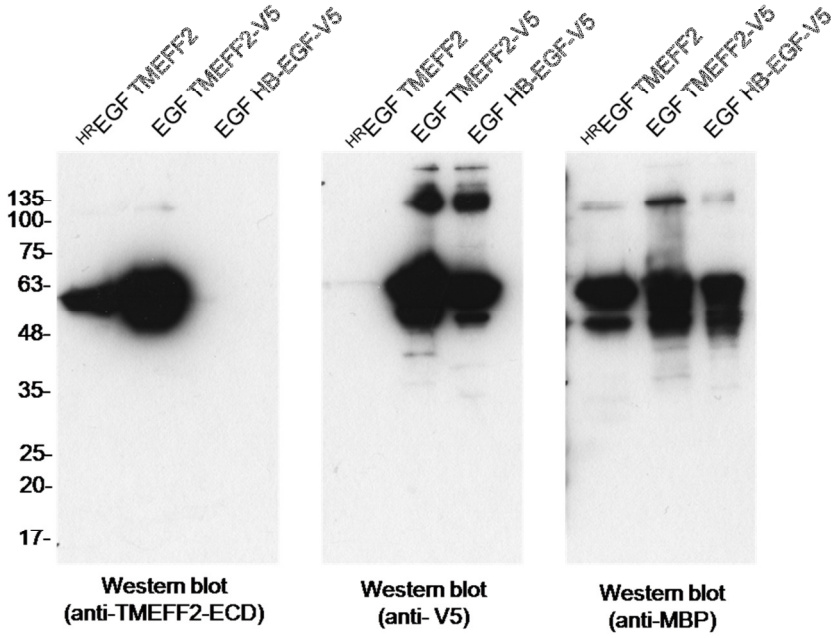

Figure 5.9 Analysis of recombinant EGF-like domains from TMEFF2, ^{HR}TMEFF2 and HB-EGF purified on amylose resin.

1 µg of purified EGF-like domains from TMEFF2 and HB-EGF as well as mutated ^{HR}EGF-like domain from TMEFF2 were analyzed by Western blotting and labelled with anti-TMEFF2-ECD, anti-V5 and anti-MBP antibodies.

5.3.4 Analysis of the folding of purified MBP-tagged EGF-like domains.

To further analyze the purity and folding of recombinant EGF-like domains from TMEFF2 and HB-EGF as well the as $^{H\text{-}R}$EGF-like domain from the TMEFF2 mutant, the same amounts of all three proteins were analyzed by SDS-PAGE in the presence or absence of β-mercaptoethanol (Figure 5.10). The lack of β-mercaptoethanol in the sample loading buffer prevents the reduction of disulphide bonds and enables the detection of dimers or larger complexes formed by purified MBP fusion proteins. Analysis of EGF-like domains by SDS-PAGE and staining with Coomassie Brilliant Blue in the presence of β-mercaptoethanol (Figure 5.10, A) confirmed high specificity of the amylose-resin purification method as no additional bands were detected in the three samples.

Analysis of the same samples in the absence of β-mercaptoethanol (Figure 5.10, B) revealed that the purified recombinant proteins are heterogeneous. The EGF-like domain from HB-EGF was present in the sample mostly as monomer (60 kDa) but also as large polymers (molecular mass above 250 kDa). $^{H\text{-}R}$EGF-like and EGF-like domains from TMEFF2 formed monomers (55-60 kDa), dimers (120-130 kDa) and polymers (>250 kDa). Since the proteins purified on the amylose resin were not homogeneous a second purification step was required to separate monomers and multimers of these proteins in order to be able to characterize and compare their biological activity.

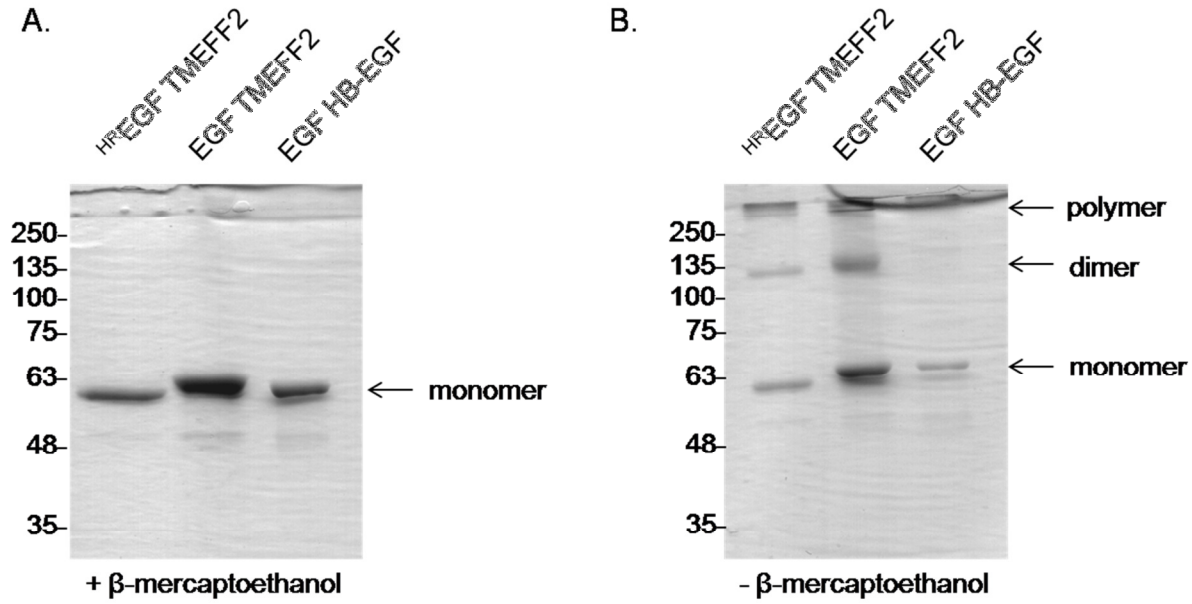

Figure 5.10 Analysis of the folding of MBP-tagged EGF-like domains from TMEFF2, $^{H\text{-}R}$TMEFF2 and HB-EGF in reducing and non-reducing conditions.

1 µg of recombinant EGF-like domains purified using amylose resin were analyzed by SDS-PAGE electrophoresis in 10% resolving gel in the presence (A) or absence (B) of β-mercaptoethanol. Proteins were visualised by Coomassie Brilliant Blue R-250 staining. Bands detected in the presence of β-mercaptoethanol in the loading buffer corresponded to monomers of MBP EGF-like domains. Analysis of the same samples in the absence of β-mercaptoethanol revealed that the recombinant EGF-like domains formed monomers (55-60 kDa), dimers (120-130 kDa) and polymers (>250 kDa), indicating that an additional purification step is required to obtain homogeneous proteins.

5.3.5 Further purification of MBP-EGF-like domains: gel filtration.

The analysis of MBP-tagged EGF-like domains by SDS-PAGE and Coomassie Brilliant Blue staining revealed that samples purified using amylose resin were not homogeneous and contained not only monomers of EGF-like domains but also dimers and polymers (Figure 5.10 B). In order to investigate the biological role of EGF-like and $^{H-R}$EGF-like TMEFF2 domains and compare their activity with the EGF-like domain from HB-EGF, the separation of monomers from dimers was required. A purification method employed to obtain homogeneous monomers and dimers fractions was gel filtration. This chromatography method separates proteins according to their molecular mass and is often used as a second, 'polishing' purification step after amylose resin affinity chromatography. Gel filtration can be performed in native conditions and for that reason does not influence the activity of purified proteins. The difference in size between monomers, dimers and polymers of EGF-like domains (Table 5.1) is significant enough to efficiently separate them by gel filtration using a Superdex 200 10/300 GL column, as this column material is suitable for separating proteins with molecular masses between 10-600 kDa (fractionation $1x10^4$-$1x10^6$).

Table 5.1 Calculated molecular masses of proteins separated by gel filtration.

Protein	Monomer	Dimer
MBP-EGF TMEFF2-V5-His	57.2 kDa	114.4 kDa
MBP-$^{H-R}$EGF TMEFF2	54.8 kDa	109.2 kDa
MBP-EGF HB-EGF-V5-His	56.7 kDa	113.4 kDa
BSA	66.5 kDa	133.0 kDa

To establish the expected elution volume for monomers and dimers of the MBP-fusion EGF-like domains, a sample containing BSA standard was analyzed first as the molecular masses of BSA monomer and dimer are similar to MBP-tagged EGF-like domains (Table 5.1). The elution profile for BSA presented in Figure 5.11 A shows that BSA dimer is eluted at 12 ml and monomer at 14 ml.

Separation of MBP-tagged EGF-like domains on Superdex 200 10/300 GL column confirmed heterogeneity of the samples. As presented in Figure 5.11 B, dimer and monomer of TMEFF2 EGF-like domain were separated at almost equal ratios. $^{H-R}$EGF-like domain from TMEFF2 formed mostly large polymers which were eluted early from the column (8-11 ml) but dimer and monomer were also detected and separated. 90% of

EGF-like domain from HB-EGF was present in the sample as a monomer, however small amounts of a dimer was also detected in eluted fractions.

The elution profiles of EGF-like domains obtained by gel filtration agree with analysis of the protein folding by SDS-PAGE under non-reducing conditions (Figure 5.10 B). This analysis showed that EGF and $^{H\text{-}R}$EGF-like domains from TMEFF2 form dimers whereas no dimer was detected in the sample containing the EGF-like domain from HB-EGF. Large polymers detected in the three EGF-like domains samples by Coomassie staining were probably removed from the samples by centrifugation prior to loading into Superdex column and for that reason were not seen on the elution profiles.

The gel filtration purification step enabled the efficient separation of monomers and dimers of recombinant EGF-like domains that were tested for their biological activity in *in vitro* experiments. The concentration of each monomer and dimer in collected fractions was calculated by dividing the OD_{280} of the fraction by the EGF-like domain extinction coefficient factor that was calculated based on the protein sequence, as described in detail in Materials and methods.

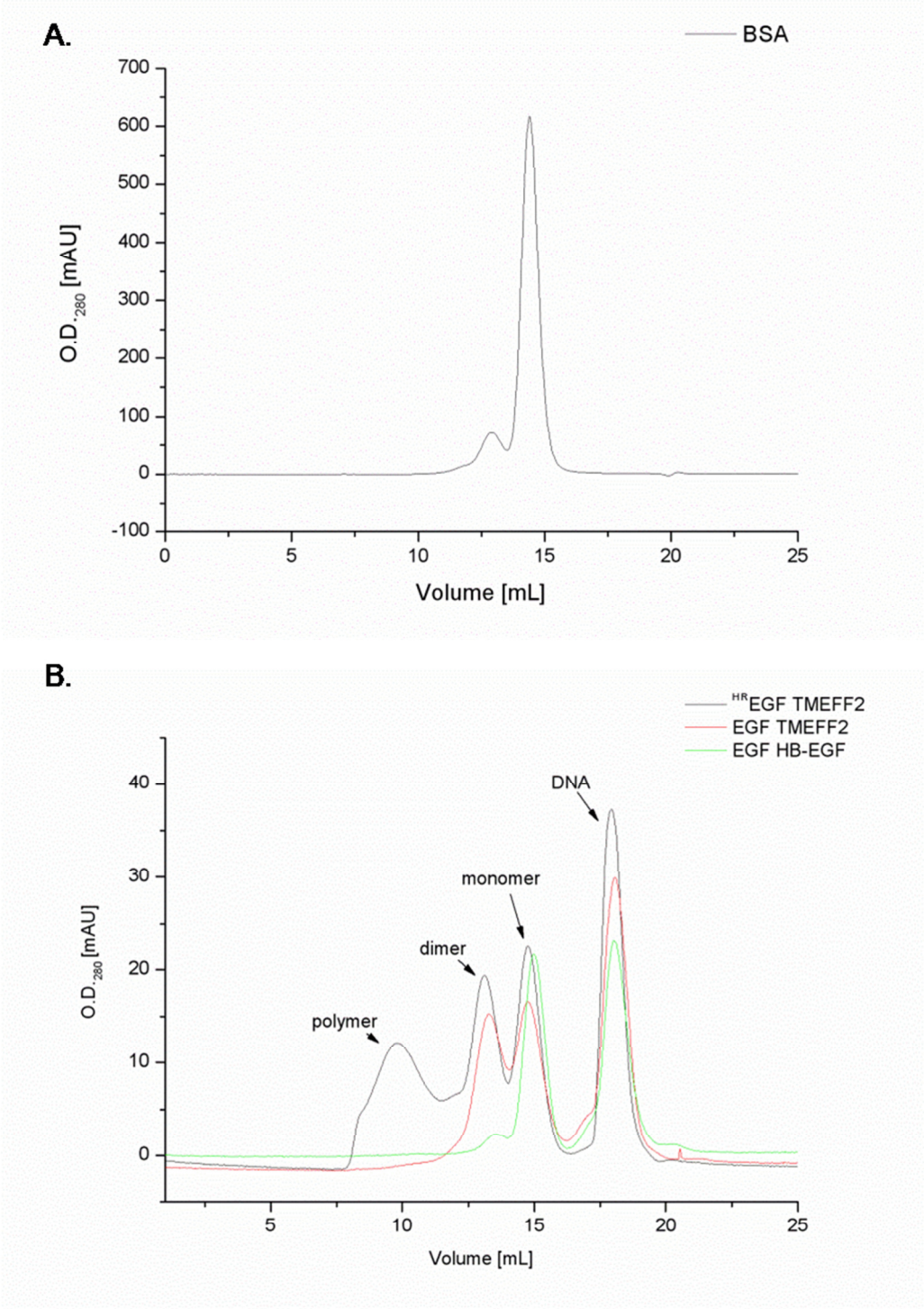

*Figure 5.11 Purification of MBP-tagged EGF-like domains by gel filtration***.**

Monomers, dimers and polymers of MBP-tagged EGF-like domains of ^{HR}TMEFF2, TMEFF2 and HB-EGF were separated by gel filtration on Superdex 200 10/300 GL column in native conditions (B). Elution profiles of recombinant proteins were compared with elution profile of a standard protein (BSA) with similar molecular weight (A).

5.3.6 Analysis of the biological activity of purified MBP-tagged EGF-like domains in ERK1/2 phosphorylation assay.

As described in the introduction to this chapter, several proteins containing EGF-like domains are able to interact with receptors from the ErbB family, leading to their dimerization and phosphorylation of Tyr residues present within the cytoplasmic domains of ErbBs. These phosphotyrosine residues serve as docking sites for cytoplasmic proteins that undergo phosphorylation and activate downstream signaling cascades. One of the downstream signaling pathways activated in response to ErbB stimulation is the MAPK/ERK pathway. Thus, activation of ErbBs can be measured by assessing the level of phosphorylated ERK1 and ERK2 (pERK1/2) in total cell lysates following treatment with EGF-like protein and compared with the total levels of ERK1/2 to correct for loading differences. As TMEFF2 is expressed predominantly in the prostate, activation of ErbB receptors by EGF-like domain from TMEFF2 was tested in normal prostatic epithelial cell line PNT2-C2. Prior to treatment with recombinant MBP-tagged EGF-like domains, PNT2-C2 cells were serum starved overnight in the presence of 25 µM metalloproteinase inhibitor GM6001 in order to reduce EGFR activation by endogenously released ligands. Positive control experiments were performed using PNT2-C2 cells treated for 5 and 15 minutes with different concentrations of MBP-EGF-like domain from HB-EGF (Figure 5.12). Total cell lysates, supplemented with protease and phosphatase inhibitors were then analyzed by Western blotting and labelled with anti-pERK1/2 antibody to detect the amount of phosphorylated ERK1/2. To establish the relative ratio of pERK1/2, membranes were stripped and re-probed for total ERK1/2. Cells treated with serum free medium containing control buffer or 10% FBS were used as negative and positive control, respectively. The intensity of bands corresponding to pERK1/2 and total ERK1/2 was quantified using ImageJ software (see paragraph 2.16.2 for details) and displayed as a histogram. MBP-EGF-like domain from HB-EGF significantly induces ERK1/2 phosphorylation in PNT2-C2 cells at all tested concentrations (0.5-2.0 µg/ml) (Figure 5.12). This result proves that biologically active EGF-like domains can be successfully expressed and purified from *E. coli* cultures and that PNT2-C2 cell line is a suitable model to study ErbB receptors activation.

The potential to induce ERK1/2 phosphorylation in PNT2-C2 by the MBP-EGF-like domain from TMEFF2 was tested using the same assay. As shown in Figure 5.13 neither the monomer nor the dimer of MBP-EGF-like domain from TMEFF2 increased phosphorylation of ERK1/2 in PNT2-C2 cells when used at concentrations from 1µg/ml to 5 µg/ml. However, the lack of ERK1/2 activation by MBP-EGF-like domain from TMEFF2 was not caused by the lack of Arg in the position 39, as neither the monomer nor the dimer of the MBP- $^{H\text{-}R}$EGF-like TMEFF2 were able to induce ERK1/2 phosphorylation (Figure 5.14).

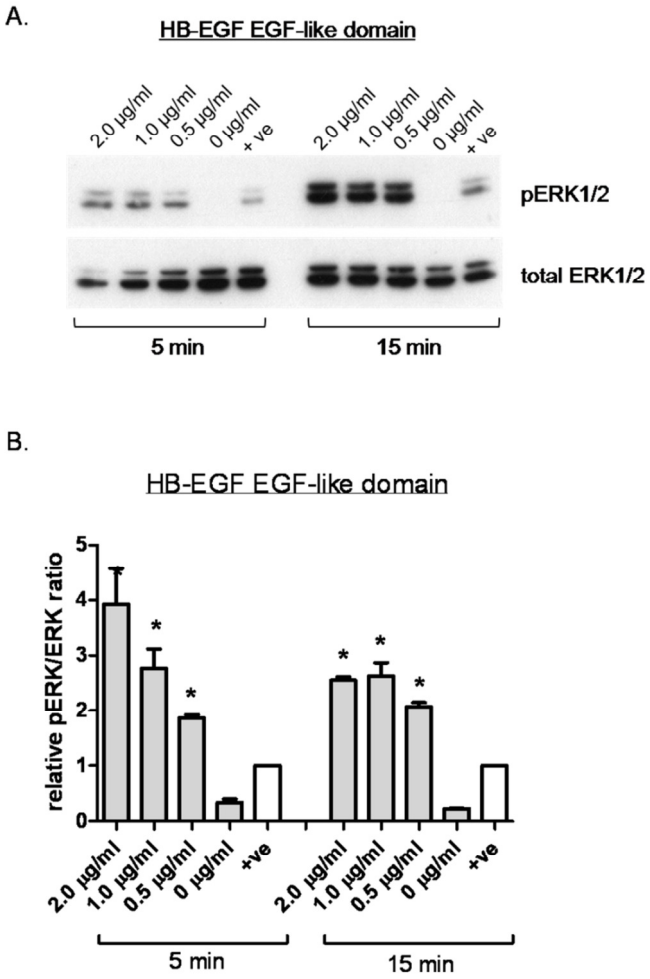

Figure 5.12 Phosphorylation of ERK1/2 in PNT2-C2 cells following treatment with MBP-tagged EGF-like domain from HB-EGF.

PNT2-C2 cell were serum starved overnight in the presence of 25 µM GM6001 followed by 5 and 15 minutes treatment with different concentrations of MBP-tagged EGF-like domain from HB-EGF. Serum free medium containing control buffer or 10% FBS was used as negative (0 µg/ml) and positive (+ve) control, respectively. Equal amounts of cell lysates were analyzed by Western blotting and labelling with anti-pERK1/2 and anti-ERK1/2 antibodies (A). The density of each band was quantified by ImageJ software and presented as a relative pERK/ERK ratio (B). The histogram shows mean values from three independent experiments ±SEM. *$p<0.05$ in comparison to negative control.

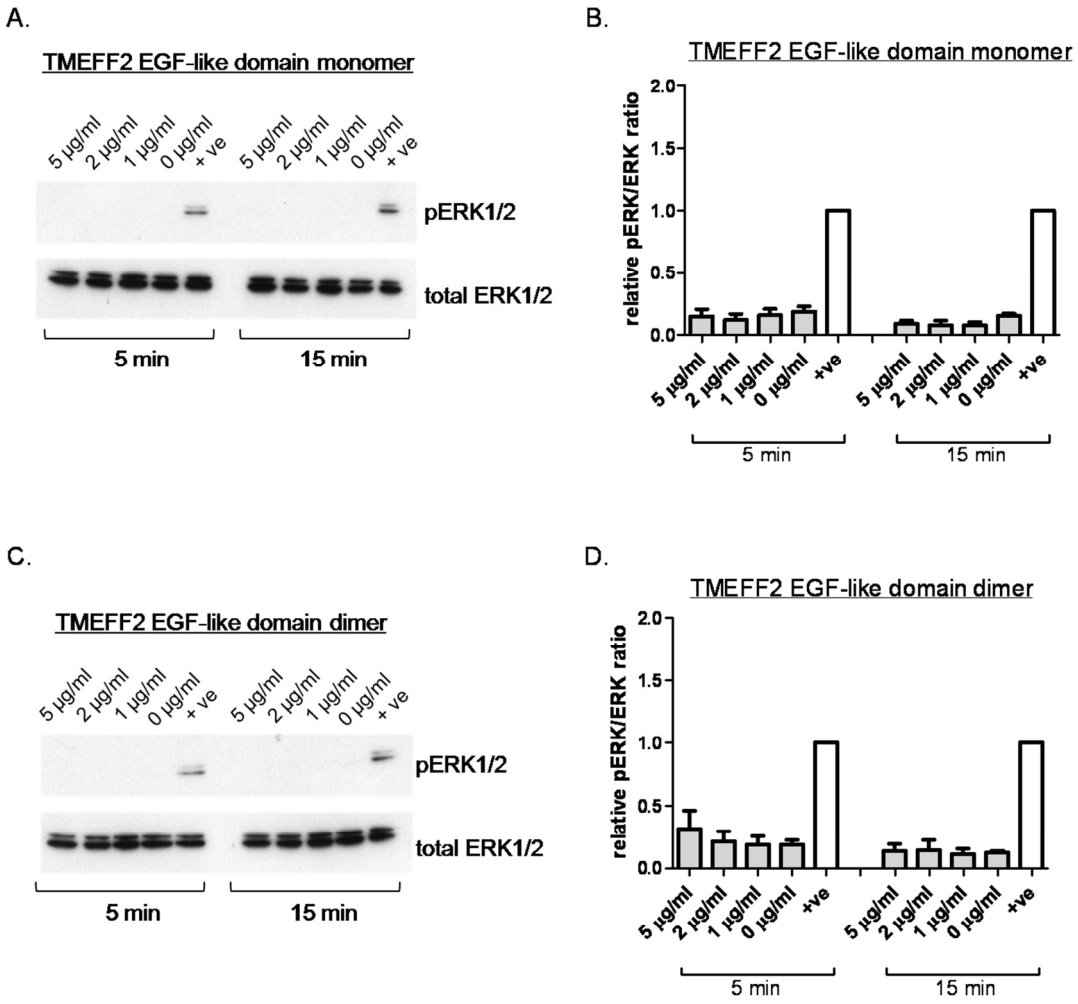

Figure 5.13 The TMEFF2 EGF-like domain did not induce ERK1/2 phosphorylation in PNT2-C2 cells.

PNT2-C2 cells were serum starved overnight in the presence of GM6001 and treated for 5 and 15 minutes with the monomer (A, B) or dimer (C, D) of MBP-tagged EGF-like domain from TMEFF2. Medium containing control buffer or 10% FBS was used as a negative (0 µg/ml) or positive (+ve) control, respectively. Total cell lysates were analyzed by Western blotting for pERK1/2 and total ERK1/2 (A, C). The density of bands was analyzed by ImageJ and presented as a relative pERK/ERK ratio (B, D). The histograms show mean values from three experiments ±SEM.

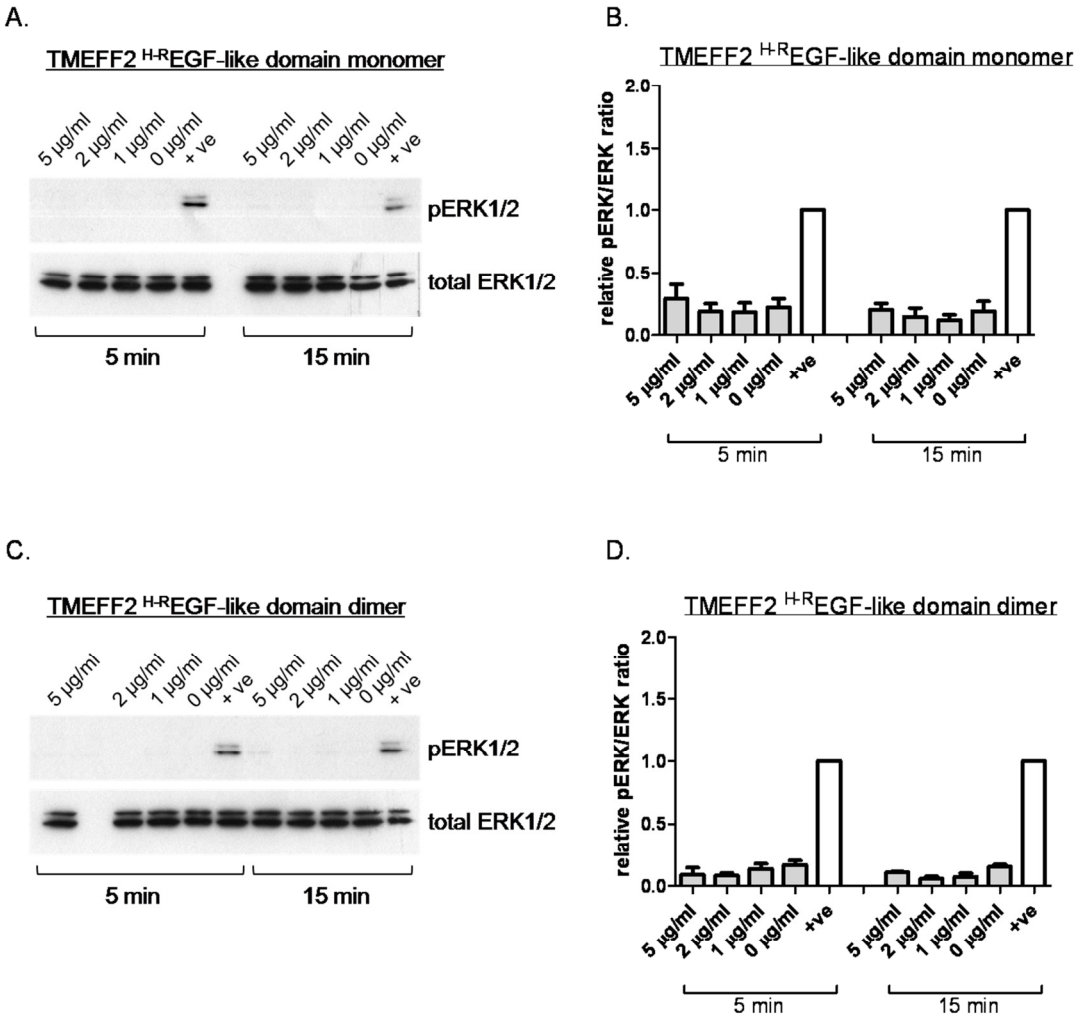

Figure 5.14 Substitution of His39 with Arg within the EGF-like domain from TMEFF2 did not increase pERK1/2 phosphorylation in PNT2-C2 cells.

Serum-starved PNT2-C2 cells were treated for 5 and 15 minutes with monomer (A, B) or dimer (C, D) of the MBP-tagged TMEFF2 $^{H\text{-}R}$EGF-like domain mutant. Medium containing control buffer or 10% FBS was used as negative (0 µg/ml) and positive (+ve) control, respectively. The ratio of pERK1/2 to total ERK1/2 was analyzed in total cell lysates by Western blotting (A, C) and ImageJ quantification (B, D). The histograms present mean values from three experiments ±SEM.

As the EGF-like domain from TMEFF2 did not activate ErbB signaling in PNT2-C2 cells, it was hypothesized that it may act as ErbB receptors antagonist and prevent their activation by other EGF-like proteins. To test this hypothesis, PNT2-C2 cells were serum starved overnight in the presence of GM6001 and 2 µg/ml of MBP EGF-like domain from TMEFF2 or buffer control. Next day, the cells were treated with 1 µg/ml of EGF-like domain HB-EGF or a mix of EGF-like domains from TMEFF2 (2 µg/ml) and HB-EGF (1 µg/ml) for 5 and 15 minutes and the levels of pERK1/2 and total ERK1/2 in cell lysates were assessed as described previously. As shown in Figure 5.15, the presence of EGF-like domain from TMEFF2 did not impair ErbB activation by the EGF-like domain from HB-EGF. This result suggests that TMEFF2 EGF-like domain is not involved in ErbB signaling as it did not activate nor antagonise ERK1/2 phosphorylation in PNT2-C2 cells.

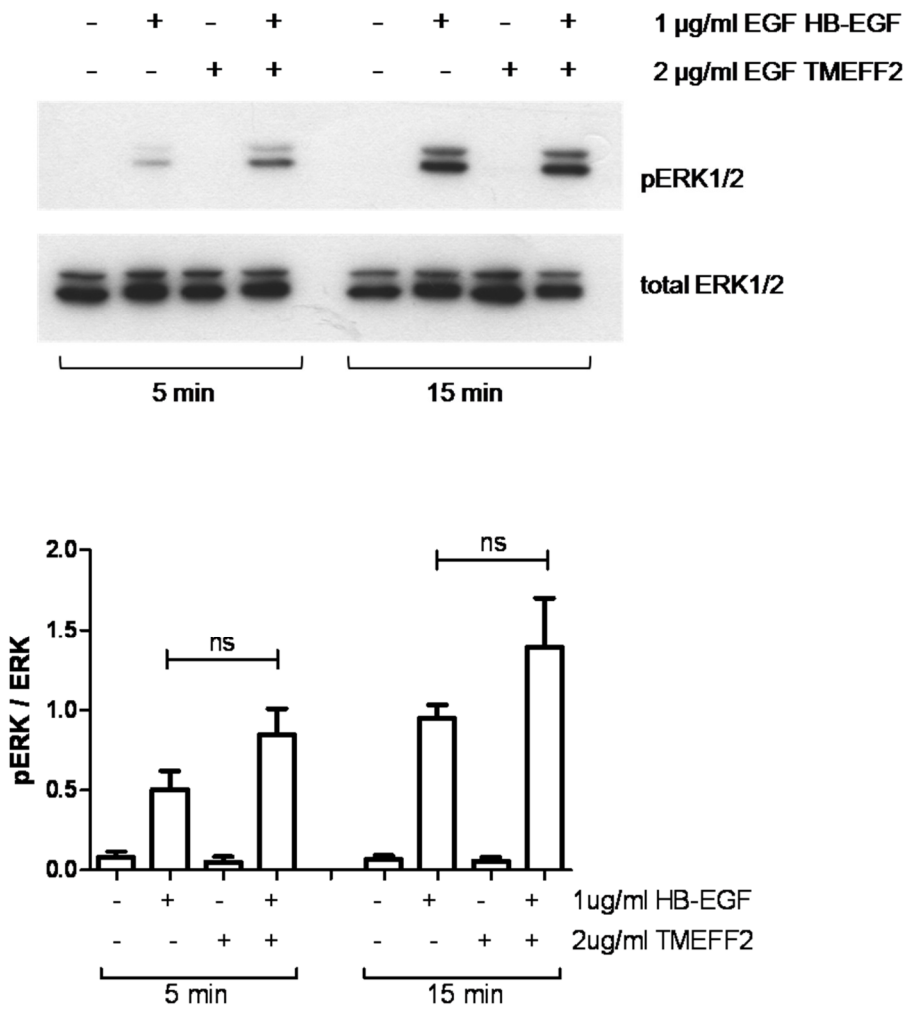

Figure 5.15 Phosphorylation of ERK1/2 in PNT2-C2 cells upon treatment with EGF-like domains from TMEFF2 and HB-EGF.

PNT2-C2 cells were grown overnight in serum free medium containing 25 µM GM6001 and 2 µg/ml of the MBP-tagged EGF-like domain from TMEFF2 (monomer). Phosphorylation of ERK1/2 was analyzed by Western blotting of the cell lysates following 5 and 15 minutes treatment with 1 µg/ml of HB-EGF EGF-like domain alone or together with 2 µg/ml TMEFF2 EGF-like domain. Density of the bands was quantified using ImageJ software; n=4 ± SEM; ns-not significant.

5.3.7 Purification on amylose resin and analysis of the folding of MBP-tagged TMEFF2-ECD, 2xFS and 2ndFS+EGF fragments.

In addition to the EGF-like domains larger TMEFF2 fragments: ECD, 2xFS and 2ndFS+EGF were expressed in SHuffle T7 Express *lysY E. coli* as MBP-fusion proteins and purified using amylose resin. The purity and folding of these fusion proteins were analyzed by SDS-PAGE in 11% resolving gel and stained with Coomassie Brilliant Blue in the presence or absence of β-mercaptoethanol (Figure 5.16). As calculated from the protein sequence the molecular sizes of MBP-fusion proteins are 76.4 kDa (ECD), 71.7 kDa (2xFS) and 65 kDa (2nd FS+EGF) (see Appendix II). Large amounts of all three proteins were successfully purified from bacterial extracts as single bands with expected molecular masses were detected by SDS-PAGE electrophoresis in reducing conditions (Figure 5.16 A). Analysis of ECD, 2xFS and 2nd FS+EGF TMEFF2 fragments in the absence of β-mercaptoethanol in the sample loading buffer revealed that most of these proteins formed large polymers with apparent molecular masses above 250 kDa (Figure 5.16 B). In samples containing 2xFS and 2nd FS+EGF MBP-fusion proteins weak bands corresponding to protein monomers were observed, as indicated by arrows on Figure 5.16 B. No monomer of the TMEFF2-ECD was detected in non-reducing conditions. These data indicated that larger TMEFF2 fragments (ECD, 2xFS, 2ndFS+EGF) fold incorrectly when expressed in *E. coli* and due to the small amount of monomers cannot be used to investigate the biological activity of TMEFF2 cleavage products.

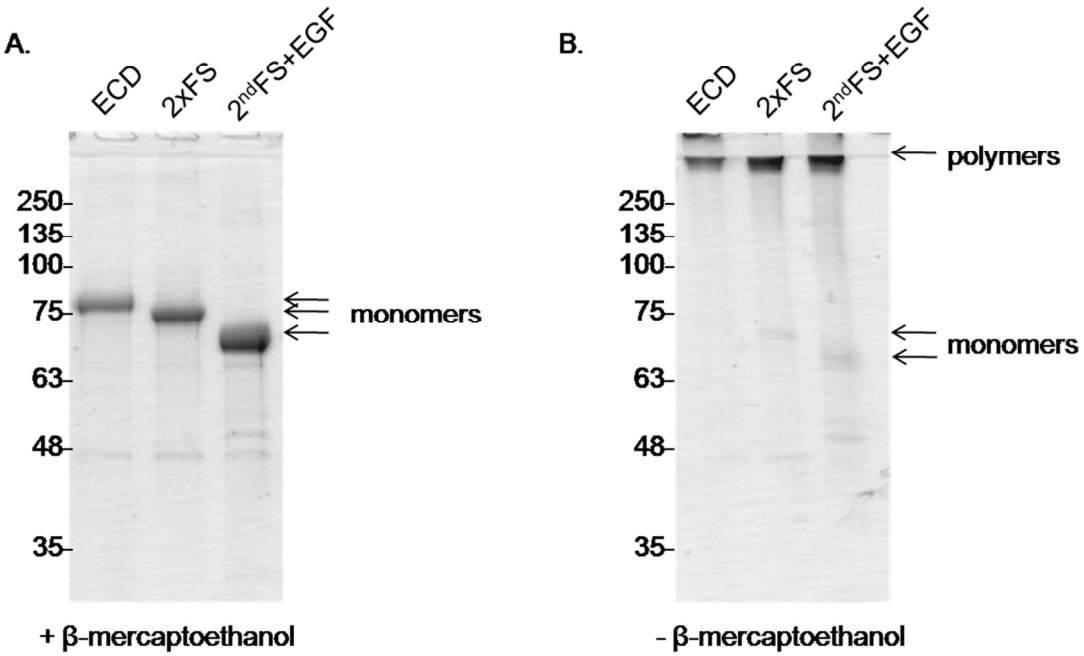

Figure 5.16 Analysis of the folding of MBP-tagged ECD, 2xFS and 2ndFS-EGF TMEFF2 fragments in reducing (A) and non-reducing (B) conditions..

MBP-tagged TMEFF2-ECD, 2ndFS-EGF and 2xFS fragments were purified using amylose resin, separated by SDS-PAGE and stained with Coomassie Brilliant Blue R-250 in the presence (A) or absence (B) of β-mercaptoethanol. Large amounts of the TMEFF2-ECD, 2ndFS-EGF and 2xFS fragments were successfully purified from bacterial extracts using amylose resin but most of the proteins formed large multimers (apparent molecular mass >250 kDa). Small amount of monomers can be observed only in samples containing 2xFS and 2ndFS+EGF MBP-fusion proteins, as indicated by arrows.

5.4 Chapter summary.

The aim of the experiments described in Chapter 5 was to express and purify recombinant proteins corresponding to N-terminal TMEFF2 cleavage products generated by ADAMs, matriptase and hepsin in order investigate their biological activity. The expression of the recombinant TMEFF2 fragments was performed in *E. coli* as this expression system generates high amounts of recombinant proteins from a low cost bacterial culture. The disadvantage of the prokaryotic expression system is the reducing environment of the *E. coli* cytoplasm that hinder proper folding of the proteins containing disulphide bonds. As the structure of TMEFF2 is stabilized by several disulphide bonds, TMEFF2 fragments were expressed in modified *E. coli* strains containing deletions in the genes for glutaredoxin reductase and thioredoxin reductase (*Δgor/ΔtrxB*), Origami B (DE3)pLysS and SHuffle T7 Express *lysY*. In addition to *Δgor/ΔtrxB* mutations, SHuffle T7 expresses also the periplasmic disulphide bond isomerase DsbC that helps to correct mis-oxidized bonds and promote proper folding of proteins with multiple disulphide bonds (Lobstein et al. 2012). The chosen *E. coli* strains were transformed with MAL pRSET B expression vectors containing sequences for TMEFF2 fragments inserted downstream of the gene for maltose-binding protein (MBP), resulting in the expression of N-terminally tagged MBP-fusion proteins. The MBP tag increases the solubility of recombinant protein, enhances proper folding and enables efficient purification due to the affinity of MBP to amylose. The elution of MBP-fusion proteins from the amylose resin is performed in mild, physiological conditions and helps to preserve their biological activity (Kapust & Waugh 1999; Riggs 2000; Sun et al. 2011).

The described expression and purification system was optimised in order to produce MBP-tagged EGF-like domain from TMEFF2. As indicated in the introduction to this chapter TMEFF2 contains atypical EGF-like domain that shares several structural similarities with other EGF-like proteins (characteristically located Cys and Gly residues) but is also significantly different due to the presence of His39 instead of conserved Arg39 (Figure 5.3). It was proposed that this substitution may reduce binding of TMEFF2 EGF-like domain to ErbB receptors (Horie et al. 2000), however some data suggest that TMEFF2 is able to activate ErbB-4 and EGFR (Uchida et al. 1999; Ali & Knäuper 2007). To investigate the influence of His39 on the activity of TMEFF2 EGF-like domain, a $^{H\text{-}R}$EGF-like TMEFF2 mutant was generated using overlap extension PCR method (Figure 5.4) and expressed in *E. coli* similarly to the wild-type TMEFF2 EGF-like domain. In order to examine if the *E. coli* expression system is suitable for production of biologically active EGF-like domains, MBP-tagged EGF-like domain from HB-EGF was expressed alongside EGF-like and $^{H\text{-}R}$EGF-like domains of TMEFF2. Analysis of the three EGF-like domains expression in lysates of transformed Origami B and SHuffle T7 *E. coli* revealed that all three recombinant proteins were expressed by the Origami B strain, whereas the SHuffle

T7 strain expressed the EGF-like domains from TMEFF2 and HB-EGF but did not express TMEFF2 $^{H\text{-}R}$EGF-like domain mutant (Figure 5.7). For that reason the Origami B strain was chosen for the large scale expression of all three EGF-like domains. Purification of the MBP-tagged EGF-like domains using affinity of MBP to amylose enabled to remove most of the unwanted proteins from the bacterial extract, as confirmed by Western blot analysis (Figure 5.9 B) and Coomassie Brilliant Blue R-250 staining (Figure 5.10 A). However, analysis of the folding of purified MBP-tagged EGF-like domains by SDS-PAGE in non-reducing conditions and Coomassie Brilliant Blue R-250 staining revealed that the samples containing EGF-like domains were not homogeneous (Figure 5.10 B). Enhanced disulphide bond formation in the cytoplasm of Origami B *E. coli* caused generation of the dimers and larger polymers of the MBP-tagged EGF-like domains. To directly compare the biological activity of the EGF-like domains *in vitro*, the heterogeneous samples required further purification, in order to obtain homogeneous monomers or dimers of the recombinant EGF-like domains. The purification method applied to achieve this goal was gel filtration using Superdex 200 10/300 GL column, as it is suitable to separate proteins with molecular masses between 10-600 kDa and can be performed in non-reducing conditions, allowing to preserve the protein structure. The monomers and dimers of the MBP-tagged EGF-like domains are very similar in molecular size to monomers and dimers of BSA (Table 5.1). For that reason BSA solution was separated on a gel filtration column prior to EGF-like domains samples in order to establish the expected elution volume of the MBP-EGF-like domains monomers and dimers (Figure 5.11 A). The collected fractions, containing homogeneous monomers or dimers of the EGF-like domains from HB-EGF, TMEFF2 and $^{H\text{-}R}$EGF-TMEFF mutant were suitable to analyze their physiological activity in *in vitro* assays.

As mentioned previously, the biological role of several proteins containing EGF-like domains is displayed through activation of the ErbB receptors that can be measured by assessing the relative levels of the phosphorylated downstream kinases ERK1 and ERK2 (Ratan et al. 2003). To examine if the EGF-like domain from TMEFF2 is able to activate ErbBs and induce ERK1/2 phosphorylation in prostate cells, the normal prostate epithelial cell line PNT2-C2 was treated with various concentrations of the recombinant TMEFF2 EGF-like domain for 5 or 15 minutes followed by analysis of the pERK1/2 and total ERK1/2 in the cell lysates. In order to reduce ErbBs activation by endogenously released ligands, PNT2-C2 cells were serum starved overnight in the presence of metalloproteinase inhibitor GM6001 prior to MBP-EGF-like domain treatment. This experiment demonstrated that stimulation of the prostate epithelial cells with 1-5 µg/ml of MBP-tagged TMEFF2 EGF-like domain monomer or dimer did not induce ERK1/2 phosphorylation (Figure 5.13). However, the lack of ErbB activation by the MBP-tagged EGF-like domain from TMEFF2 may result from the chosen protein expression method. The biological activity of some mammalian growth factors strongly depends on their

glycosylation and their expression in prokaryotic cells result in obtaining inactive proteins, as glycosylation does not occur in bacteria (Baneyx & Mujacic 2004). To exclude these possibility that the large MBP-tag prevents interaction of EGF-like domain with ErbBs, the MBP- EGF-like domain from HB-EGF was purified according to the same protocol was tested in the described *in vitro* ERK1/2 phosphorylation assay. As shown in Figure 5.12, 5 and 15 minutes treatment of PNT2-C2 cells with 0.5-2 µg/ml of the MBP-EGF-like domain from HB-EGF significantly increased the relative amount of pERK1/2. This result demonstrated, that the chosen expression and purification system is suitable to produce biologically active EGF-like domains. It was also hypothesized that EGF-like domain from TMEFF2 does not activate ErbB receptors due to the substitution of Arg39 with His39 (Horie et al. 2000). To test this hypothesis, prostate epithelial cells were treated with the MBP-tagged TMEFF2 $^{H\text{-}R}$EGF-like domain, however no increase in pERK1/2 phosphorylation was detected following 5 or 15 minutes treatment with 1-5 µg/ml of this mutant (Figure 5.14). As neither the EGF-like domain from TMEFF2 nor the $^{H\text{-}R}$EGF TMEFF2 mutant induced ERK1/2 phosphorylation it was hypothesized that TMEFF2 may be ErbBs antagonist and prevents their activation by EGF-like ligands. To test this hypothesis PNT2-C2 cells were pre-incubated with MBP-tagged TMEFF2 EGF-like domain following by treatment with MBP-EGF-like domain from HB-EGF. However, the pre-treatment with TMEFF2 EGF-like domain did not affect ERK1/2 phosphorylation in response to EGF-like domain from HB-EGF (Figure 5.15).

Based on the described results it was concluded that the EGF-like domain of TMEFF2 is not implicated in signaling and more likely plays another role in the prostate cancer environment. One of the possible functions of the EGF-like domain within the TMEFF2 structure is serving as a binding site for TMEFF2 interaction partners. This prediction is supported by the results published by Ge et al., showing that the EGF-like domain from TMEFF1 is involved in binding of matriptase (Ge et al. 2006).

In addition to the EGF-like domains, the described MBP-fusion proteins expression and purification protocol was applied to generate larger TMEFF2 fragemnts: ECD, 2xFS and 2ndFS+EGF. The three recombinant proteins were expressed in SHuffle T7 strain, as the transformation of the Origami B *E. coli* with 2xFS MAL pRSET B vector resulted in growth arrest and lack of recombinant protein expression, possibly due to the toxicity of 2xFS fragment (Figure 5.6). The MBP-tagged ECD, 2xFS and 2ndFS+EGF were efficiently purified from the bacterial extracts using amylose resin and analyzed for their folding by SDS-PAGE in the non-reducing conditions. The analysis showed that most of these proteins folded incorrectly when expressed in *E. coli* and are present in purified samples as large polymers, with the apparent molecular masses above 250 kDa. The separation of the ECD, 2xFS and 2ndFS+EGF monomers by gel filtration was not possible as only trace amounts of 2xFS and 2ndFS+EGF were detected in the samples (Figure 5.16 B). Based

on this observation it was concluded that the *E. coli* expression system is not suitable for production of larger TMEFF2 fragments and the expression of these proteins should be performed in mammalian cells in order to ensure proper folding and glycosylation of the TMEFF2-ECD, 2xFS and 2ndFS+EGF fragments.

Chapter 6:

Expression and purification of TMEFF2 ectodomain fragments using mammalian cells

6.1 Introduction.

The extracellular part of TMEFF2 is composed of two follistatin-like (FS) modules and a single EGF-like domain, leading to the hypothesis that the biological function of soluble TMEFF2 cleavage products depends on these structural motifs. The data described in Chapter 5 demonstrated that the TMEFF2 EGF-like domain is not involved in ErbB signaling as it failed to induce phosphorylation of downstream ERK1/2 kinases. On the other hand the EGF-like domain could be a structural motif, involved in the interaction of TMEFF2 with other molecules, for example membrane proteases responsible for TMEFF2 ectodomain cleavage. The biological function of soluble FS containing TMEFF2 fragments was not investigated in Chapter 5 due to incorrect folding. To circumvent problems with misfolding and lack of glycosylation associated with a prokaryotic expression system, soluble FS containing fragments of TMEFF2 (ECD, 2xFS and 2^{nd}FS+EGF) were expressed in mammalian cells. Chinese hamster ovary (CHO) cells are the most widely used mammalian cells for expression and large-scale production of recombinant proteins. CHO cells provide glycosylation that ensure proper post-transcriptional modification of produced recombinant protein (Sheeley et al. 1997; Werner 1998). To enable easy and efficient purification recombinant TMEFF2 fragments were tagged either with a C-terminal Fc-tag or N-terminal protein A tag. In order to exclude the possibility that the location of the tag influences the function of TMEFF2-ECD, the activity of C-terminally tagged TMEFF2-ECD-Fc and N-terminally tagged protein A-TMEFF2-ECD was compared using in vitro ERK1/2 phosphorylation and XTT proliferation assays

6.1.1 Expression of TMEFF2-ECD as a C-terminal Fc-fusion protein in CHO cells.

The first recombinant TMEFF2 fragment to be expressed in CHO cells was TMEFF2-ECD tagged on the C-terminus with the Fc-fragment of human IgG_1. The Fc-tagged proteins are secreted as disulphide-linked dimers (Figure 6.1) and could be purified from cell conditioned medium using the affinity of the Fc fragment to protein G. Similar purification method, based on the affinity chromatography, is commonly used to purify antibodies. Protein G, originally isolated from the cell wall of different streptococcal strains (Björck & Kronvall 1984), is an immunoglobulin-binding protein recognizing the constant region of IgG, called the Fc part as well as the Fab fragment that is responsible for antigen recognition. The Fc-IgG fragment interacts with the C-terminal domains of protein G whereas N-terminal domains of protein G are able to bind albumin (Akerström et al. 1987). However, because serum albumin is the major contaminant during antibody purification, the albumin-binding domain was removed from the recombinant forms of protein G, used for antibody or Fc-tagged protein purification. Elution of Fc-tagged proteins from the protein G Sepharose is performed with low pH and the eluted samples are mixed immediately with Tris-HCl pH 9.0 to neutralize the pH and preserve the activity of the purified protein.

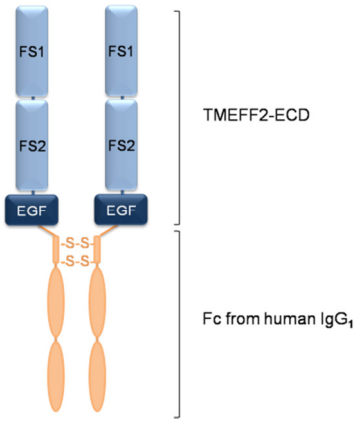

Figure 6.1 Schematic diagram of TMEFF2-ECD-Fc protein.

6.1.2 Expression of TMEFF2-ECD, 2xFS and 2ndFS+EGF fragments as N-terminal protein A fusion proteins.

An alternative system to produce recombinant TMEFF2 fragments was generation of stable CHO cell lines secreting TMEFF2-ECD, 2xFS and 2ndFS+EGF tagged N-terminally with protein A (Figure 6.2). Similarly to protein G, protein A is a commonly used fusion partner due to its strong and specific affinity to immunoglobulins (Ig). Originally found in the cell wall of a gram-positive bacterium *Staphylococcus aureus*, protein A contains five highly homologous domains: A, B, C, D and E. Each of these domains is able to bind the Fc and the Fab fragment of IgG. Disruption of protein A-IgG interactions in order to elute protein A-tagged recombinant proteins from IgG Sepharose is achieved at low pH, such as 0.1 M glycine-HCl pH 2.7. Eluted fractions are then immediately mixed with 1 M Tris-HCl pH 9.0 to prevent destruction of the protein structure caused by the low pH. In addition to its high affinity for IgG allowing efficient purification, protein A has also several other properties which make it a suitable fusion partner. For example high stability against proteolysis in various hosts and lack of Cys residues that could interfere with the disulphide bond formation within the fused targeted protein (Nilsson et al. 1997; Graille et al. 2000). Although protein A is used mostly to tag proteins expressed in *E coli*, several reports show that protein A fusions can be successfully expressed in mammalian cell, for example Chinese hamster ovary (CHO) cell line (Bierhuizen & Fukuda 1992; Zhang & Esko 1994; Maeda et al. 1996).

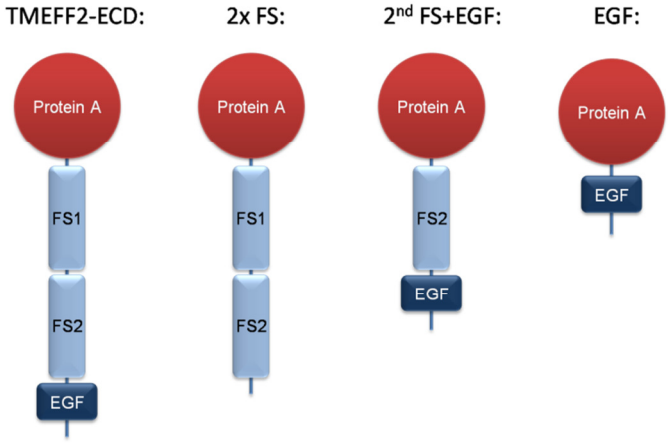

Figure 6.2 Schematic diagram of N-protein A TMEFF2 fusion proteins.

6.2 Aims.

Experiments summarized in Chapter 6 were performed in order to:

- generate stable CHO cell line secreting TMEFF2-ECD tagged on the C-terminus with Fc-tag
- optimize methods to purify TMEFF2-ECD-Fc
- analyze ERK1/2 phosphorylation in PNT2-C2 and HEK293 cells in response to TMEFF2-ECD-Fc treatment
- clone expression vectors encoding TMEFF2-ECD, 2xFS, 2ndFS+EGF and EGF-like domain tagged on the N-terminus with protein A
- generate CHO cell lines stably expressing N-protein A TMEFF2 fusion proteins
- purify N-protein A fusion TMEFF2 fragments from CHO conditioned medium
- analyze the influence of protein A-tagged TMEFF2 fragments on cell proliferation.

6.3 Results

6.3.1 Expression of Fc-tagged TMEFF2-ECD in CHO cells.

A stable CHO cell line expressing soluble TMEFF2-ECD tagged on the C-terminus with an Fc-tag was generated using the Flp-In System from Invitrogen (see Appendix III). The TMEFF2-ECD-Fc pcDNA5/FRT vector was cloned as described in Materials and Methods and sequenced (MWG Operon, Germany) before being used to stably transfect CHO Flp-In host cells. The amino acid sequence of TMEFF2-ECD-Fc is included in Appendix V. In addition to the Fc-tag, recombinant TMEFF2-ECD contained also a C-terminal 6xHis-tag which was used in additional purification steps (see below). For simplicity, the TMEFF2-ECD tagged with the Fc and His tags will be called TMEFF2-ECD-Fc.

The secretion of TMEFF2-ECD-Fc by stably transfected CHO cells was analyzed by Western blotting using 0.2 ml samples of conditioned medium containing 10% FBS, collected over a 5 day culture period (Figure 6.3). This analysis revealed the accumulation of a ~75 kDa band in cell culture medium that was specifically labeled with polyclonal anti-TMEFF2-ECD antibody. The molecular mass of the TMEFF2-ECD-Fc calculated using Biology WorkBench 3.2 software from the amino acid sequence is 61.7 kDa. The ~13.3 kDa difference between the calculated and apparent size of TMEFF2-ECD-Fc was thought to result from glycosylation of TMEFF2-ECD-Fc by CHO cells, as the extracellular part of TMEFF2 contains two N-linked glycosylation sites in its amino acid sequence and is known to be glycosylated (Uchida et al. 1999). Moreover, the detected band corresponded in size to recombinant TMEFF2-ECD-Fc previously described in the literature (Lin et al. 2011), confirming that generated stable CHO cell line released TMEFF2-ECD-Fc.

In addition to the ~75 kDa TMEFF2-ECD-Fc protein, two faint bands were also detected in this analysis (Figure 6.3). The >130 kDa band corresponded to the dimer of TMEFF2-ECD-Fc which was not efficiently reduced during Western blot sample preparation. The ~50 kDa band was likely a product of TMEFF2-ECD-Fc proteolytic processing, as it was shown in this thesis that TMEFF2 is a substrate for at least two groups of proteases, ADAMs and TTSPs (see Chapter 4).

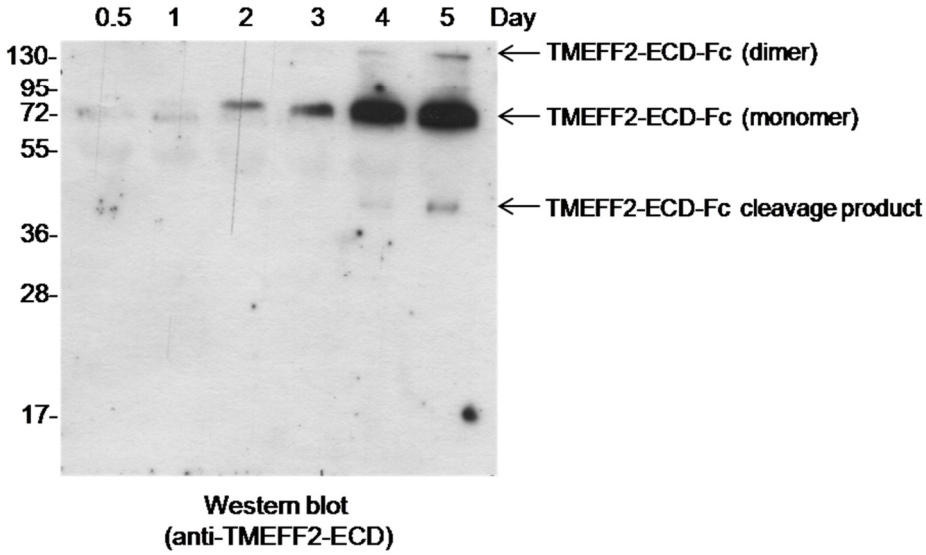

Figure 6.3 Western blot analysis of the TMEFF2-ECD-Fc release in conditioned medium of stably transfected CHO cells.

CHO cells stably expressing TMEFF2-ECD-Fc were grown in serum-containing medium for 5 days. 0.2 ml medium samples were collected every day, centrifuged to remove cell debris and analyzed by SDS-PAGE and Western blotting in reducing conditions. Labeling of the PVDF membrane with polyclonal anti-TMEFF2-ECD antibody revealed the accumulation of a ~75 kDa band corresponding to glycosylated TMEFF2-ECD-Fc monomer in the conditioned medium. The >130 kDa band detected in samples from Day 4 and Day 5 corresponded more likely to TMEFF2-ECD-Fc dimer and the ~50 kDa protein was thought to be a product of TMEFF2-ECD-Fc proteolytic processing.

6.3.2 Purification of TMEFF2-ECD-Fc from CHO conditioned medium using protein G Sepharose.

CHO cells expressing TMEFF2-ECD-Fc were cultured in medium supplemented with 1% low IgG FBS to minimize contamination of eluted TMEFF2-ECD-Fc with medium-derived IgG. In order to purify sufficient amounts of TMEFF2-ECD-Fc to test its biological activity *in vitro*, 2.5 litres of TMEFF2-ECD-Fc CHO conditioned medium was collected and centrifuged to remove cell debris. The medium was dialyzed overnight against 40 litres of column binding buffer (20 mM sodium phosphate pH 7.0) and filtered through 0.45 µm membrane to remove impurities that could block the protein G Sepharose column. TMEFF2-ECD-Fc containing medium was applied to previously equilibrated protein G Sepharose column and proteins which did not bind to the column material were removed by washing. TMEFF2-ECD-Fc was eluted with 0.1 M glycine-HCl pH 2.7 and the elution was monitored by measuring the pH and OD_{280} using the ÄKTA*purifier* system. As presented in Figure 6.4, the recombinant protein eluted as a sharp peak as soon as the pH of the buffer in the column began to decrease.

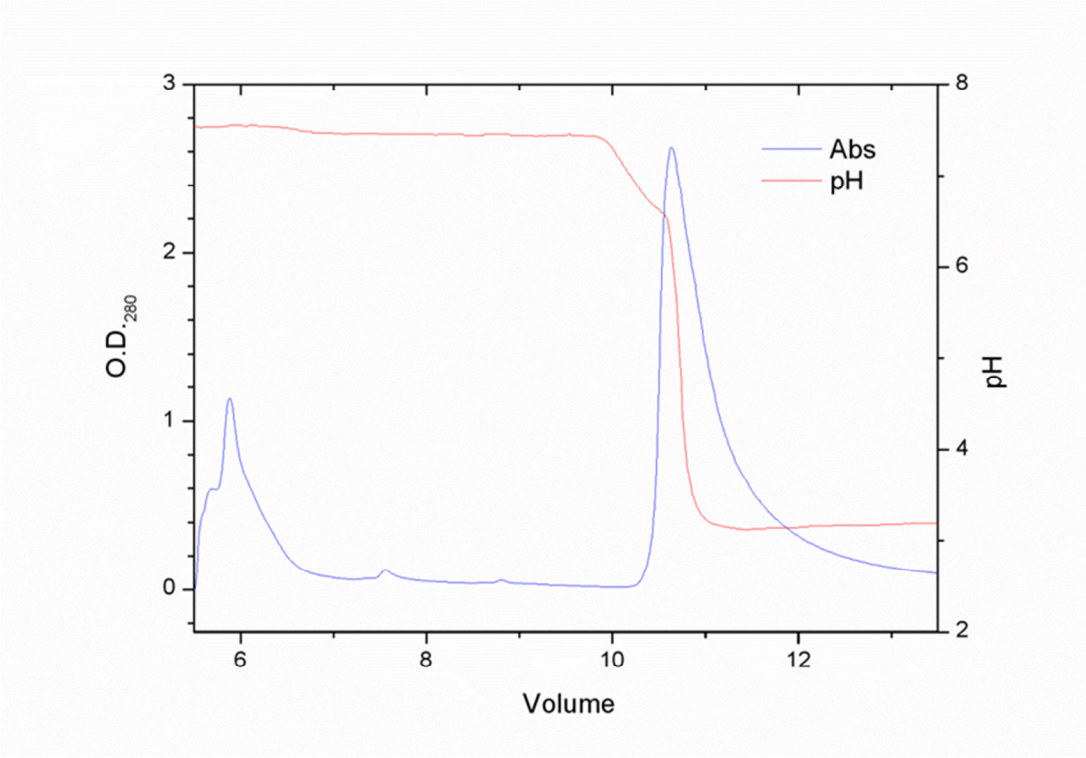

Figure 6.4 Elution profile of TMEFF2-ECD-Fc from protein G Sepharose

Conditioned medium from TMEFF2-ECD-Fc expressing CHO cells was applied onto protein G Sepharose column. Non-bound proteins were removed from the column material by washing and the TMEFF2-ECD-Fc was eluted using 0.1 M glycine-HCl pH 2.7. The decrease of pH as well as the elution of TMEFF2-ECD-Fc (OD_{280}) was monitored using ÄKTA*purifier* system.

The eluted samples were then analyzed by SDS-PAGE and Coomassie Brilliant Blue staining. As shown in Figure 6.5 A, two bands with apparent molecular masses of ~27 kDa and ~55 kDa were detected in all eluted samples. These bands corresponded to light and heavy chain of bovine IgG which were co-purified with TMEFF2-ECD-Fc due to their affinity to protein G Sepharose. The presence of the bovine IgG in eluted fractions indicated that a second purification step is required to purify TMEFF2-ECD-Fc for further experiments.

Western blot analysis of the same samples using anti-TMEFF2-ECD antibody showed the presence of two immunoreactive bands in the starting material as well as in fractions 2-8 (Figure 6.5 B). The ~75 kDa band was identified as the monomer of TMEFF2-ECD-Fc as it corresponded in size to the TMEFF2-ECD-Fc detected by Western blotting in Figure 6.3. The ~50 kDa protein in Figure 6.5 B was likely the product of TMEFF2-ECD-Fc proteolytic cleavage, also previously observed in Figure 6.3. However, the amount of the TMEFF2-ECD-Fc fragment in relation to the full length TMEFF2-ECD-Fc was much higher than observed previously. The increase of the TMEFF2-ECD-Fc cleavage product could be explained by the different culture conditions. Medium samples analyzed in Figure 6.3 were collected from cells grown in the presence of 10% FBS. In addition to several growth factors and hormones, bovine serum contains also protease inhibitors, such as alpha-1-antitrypsin (AAT), alpha-2-macroglobulin (α-2-M) and antithrombin (Gettins 2002; Armstrong & Quigley 1999). The presence of these inhibitors likely prevented proteolytic processing of TMEFF2-ECD-Fc. Conditioned medium collected for large-scale purification of TMEFF2-ECD-Fc contained only 1% low IgG FBS in order to reduce the contamination of recombinant protein with serum IgG. At the same time the amount of protease inhibitors in conditioned medium was reduced by 10 fold, resulting in increased amount of the ~50 kDa TMEFF2-ECD-Fc cleavage product.

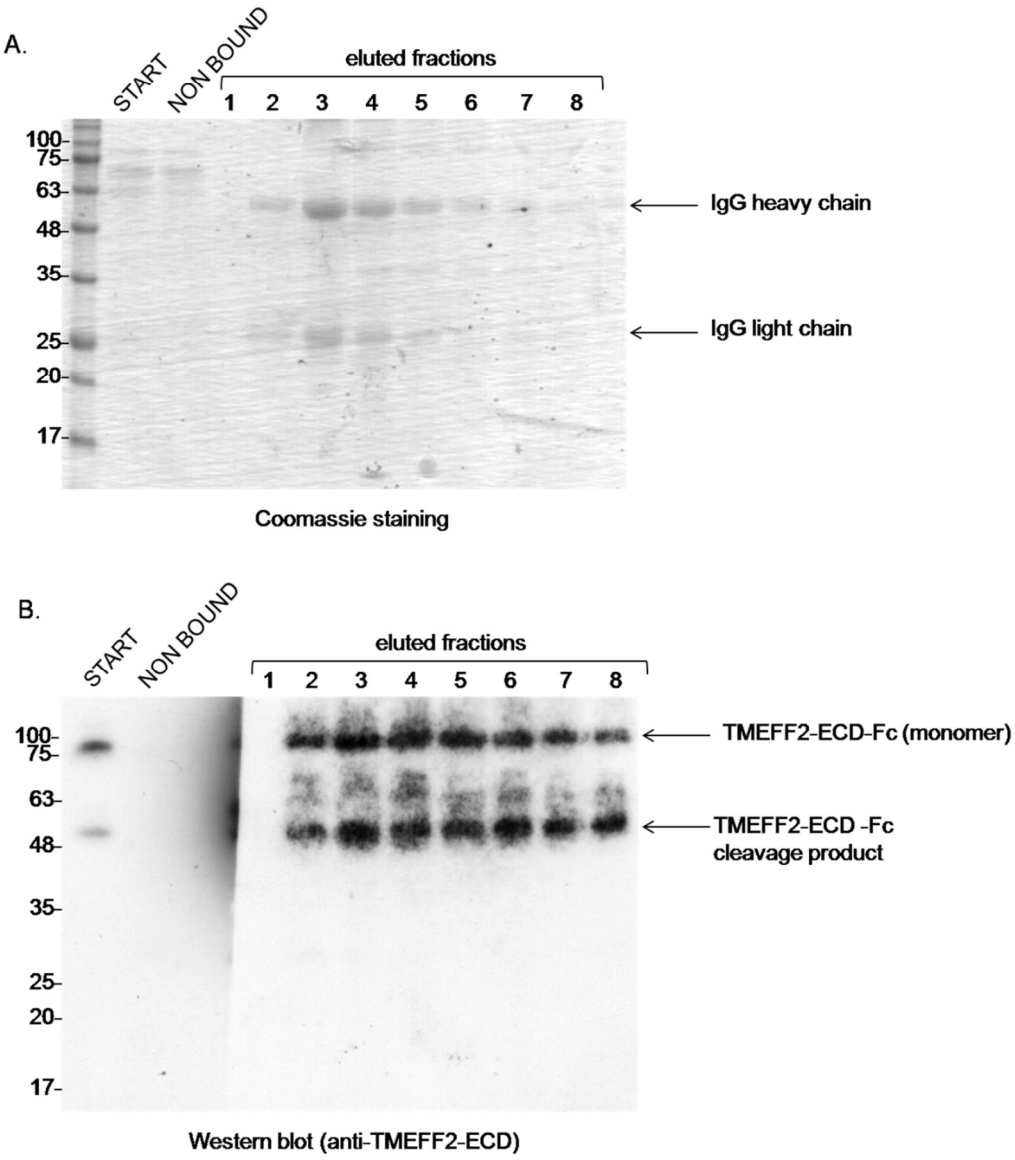

Figure 6.5 Analysis of TMEFF2-ECD-Fc fractions eluted from protein G Sepharose.

10 µl of CHO conditioned medium (START), flow-through medium (NON-BOUND) and fractions eluted from protein G Sepharose column (1-8) were separated using 11% resolving gels and stained with Coomassie Brilliant Blue (A) or blotted and labeled with polyclonal anti-TMEFF2-ECD antibody (B). Coomassie staining revealed the presence of bovine IgG contamination in the eluted fractions, indicating that a second purification step is required to obtain pure TMEFF2-ECD-Fc. Western blot analysis visualized a ~75 kDa band corresponding to TMEFF2-ECD-Fc monomer and ~50 kDa band corresponding to proteolytically cleaved TMEFF2-ECD-Fc dimer. Increased amount of ~50 kDa TMEFF2-ECD-Fc fragment resulted from reduced amount of serum in conditioned medium, leading to decreased serum protease inhibitors concentration.

6.3.3 Purification of the TMEFF2-ECD-Fc using HIS-Select HF Nickel Affinity Gel.

Purification of the TMEFF2-ECD-Fc using protein G Sepharose removed most medium proteins, however bovine IgG was co-purified with TMEFF2-ECD-Fc due to its affinity to protein G. In order to be able to use TMEFF2-ECD-Fc in *in vitro* experiment, the IgG impurities needed to be removed using an additional purification step. The TMEFF2-ECD-Fc construct contained also a C-terminal 6xHis-tag that allowed separation of TMEFF2-ECD-Fc from the IgG using the affinity of the fusion protein to nickel ions. Following washing, the 6xHis-tagged TMEFF2-ECD-Fc bound to the immobilized nickel was eluted using buffer containing imidazole that competes with the 6xHis-tagged protein for nickel binding.

Fractions 2-8 eluted from the protein G Sepharose were combined as they contained the highest amount of TMEFF2-ECD-Fc. Due to the small sample volume TMEFF2-ECD-Fc purification was performed in an Eppendorf tube using HIS-Select HF Nickel Affinity Gel. Before mixing with the affinity gel, NaCl solution was added to the TMEFF2-ECD-Fc sample to the final concentration of 300 mM NaCl in order to prevent non-specific binding to the affinity gel. The sample was mixed with the equilibrated affinity gel and incubated overnight on a rotating wheel at 4°C to allow the 6xHis-tagged TMEFF2-ECD-Fc to bind. The next day, the affinity gel was gently centrifuged (1 minute, 1000g) and washed with buffer containing 10 mM imidazole in order to elute non-specifically bound proteins. The TMEFF2-ECD-Fc was eluted by mixing the affinity gel 5 times with 200 µl of elution buffer, containing 250 mM imidazole. 10 µl of each eluted fraction, as well as the starting sample, the non-bound protein and washing solutions were analyzed by SDS-PAGE using 11 % resolving gel, followed by Western blotting (Figure 6.6) or silver staining (Figure 6.7).

Western blotting and anti-TMEFF2-ECD labeling demonstrated that the first eluted fraction (E1) contained a ~75 kDa band corresponding to TMEFF2-ECD-Fc monomer (Figure 6.6). A large amount of TMEFF2-ECD-Fc was also detected in the non-bound sample, indicating that the affinity gel was over-loaded and more HIS-Select gel needs to be used in future purifications of the TMEFF2-ECD-Fc. Sample E1 contained also a previously observed ~50 kDa proteolytically cleaved TMEFF2-ECD-Fc, whereas no TMEFF2-ECD-Fc was detected in fractions E2-E5 and in the sample collected after washing of the gel with buffer containing 10 mM imidazole (Figure 6.6, sample WASH), indicating strong and specific binding of TMEFF2-ECD-Fc to the Nickel affinity gel.

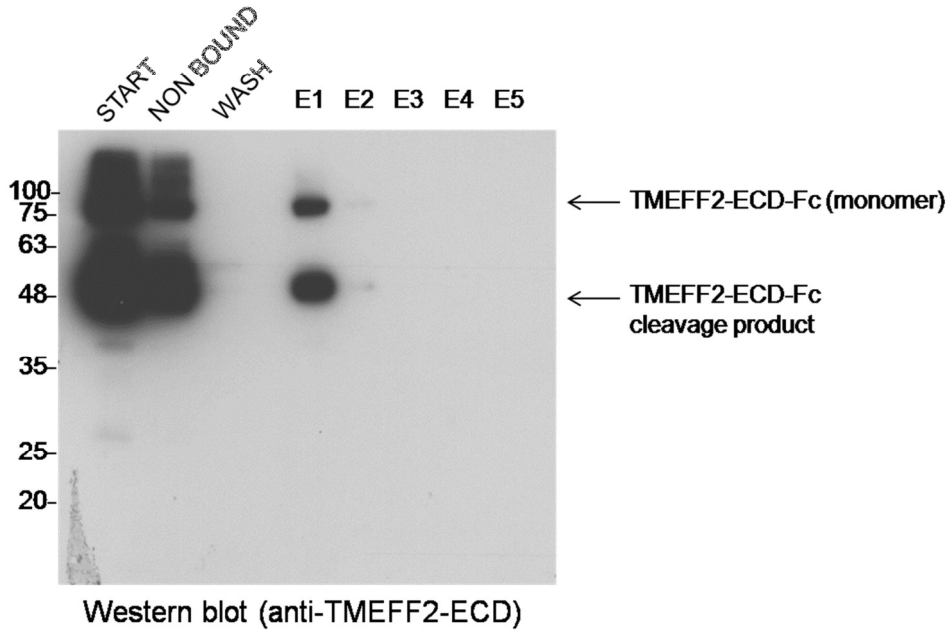

Figure 6.6 Analysis of TMEFF2-ECD-Fc purification on HIS-Select HF Nickel Affinity Gel by Western blotting.

10 µl of TMEFF2-ECD-Fc sample purified using protein G Sepharose (START), non-bound fraction and solution collected following washing of Nickel Affinity Gel as well as first five eluted fractions were analyzed by SDS-PAGE in reducing conditions. The ~75 kDa band corresponding to TMEFF-ECD-Fc monomer and the ~50 kDa band corresponding to cleaved TMEFF2-ECD-Fc were detected in the first eluted fraction (E1). These two bands were also seen in the non-bound fraction, indicating over-load of the HIS-Select Affinity Gel.

6.3.4 Analysis of TMEFF2-ECD-Fc purity using SDS-PAGE and silver staining.

To determine the purity of eluted TMEFF2-ECD-Fc as well as to investigate the origin of the ~50 kDa band recognized by anti-TMEFF2-ECD antibody the same samples were then analyzed by SDS-PAGE in reducing conditions followed by silver staining (Figure 6.7). In the starting sample, non-bound and wash fractions three major bands were detected: a ~27 kDa band corresponding to bovine IgG light chain (Figure 6.7 *), a ~55 kDa band corresponding to bovine IgG heavy chain (Figure 6.7 **) and a ~160 kDa protein corresponding to the whole IgG molecule (Figure 6.7 ***). None of these bands was found in eluted fractions E1-E5, indicating that the secondary purification removed the IgG contamination from the sample. In sample E1 four bands were detected by silver staining: a ~75 kDa TMEFF2-ECD-Fc monomer and a ~50 kDa protein recognized previously with the anti-TMEFF2-ECD antibody as well as two smaller proteins with apparent molecular sizes of ~38 kDa and ~33 kDa. In order to identify these two proteins all of the remaining E1 fraction was separated in 11% resolving gel in reducing conditions, stained with Coomassie Brilliant Blue and sent for mass spectroscopy analysis to Dr Ian A. Brewis, Central Biotechnology Services, Cardiff University School of Medicine. Due to the limited amount of protein available for this analysis only the ~38 kDa band was sequenced, revealing that it corresponded to human IgG with 96% confidence. As the only source of human IgG in the sample was the recombinant TMEFF2-ECD-Fc it was concluded that the ~38 kDa band and possibly also the ~33 kDa band were fragments of degraded TMEFF2-ECD-Fc. These fragments did not contain the TMEFF2-ECD sequence as they were not recognized by anti-TMEFF2-ECD antibody. Based on this information it was concluded that the ~50 kDa protein visualized with the anti-TMEFF2-ECD antibody was a TMEFF2-ECD-Fc cleavage product containing TMEFF2-ECD sequence.

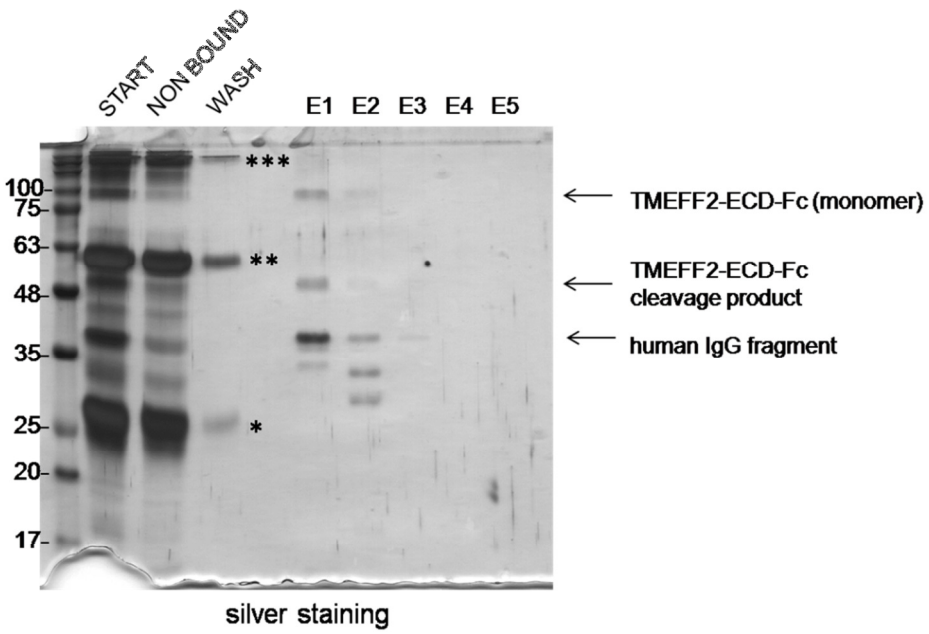

Figure 6.7 Analysis of TMEFF2-ECD-Fc purification on HIS-Select HF Nickel Affinity Gel by SDS-PAGE and silver staining.

10 µl of TMEFF2-ECD-Fc sample purified using protein G Sepharose (START), non-bound fraction and solution collected following washing of Nickel Affinity Gel as well as first five eluted fractions were analyzed by SDS-PAGE in reducing conditions using 11% resolving gel followed silver staining. This analysis indicated that second purification step removed bovine IgG from the sample (* IgG light chain, ** IgG heavy chain, *** whole IgG). ~75 kDa band corresponding to Fc-TMEFF-ECD was detected in the first eluted fraction (E1), together with ~50 kDa, ~38 kDa and ~33 kDa fragments, most probably generated by proteolytic processing of TMEFF2-ECD-Fc

As all of the purified TMEFF2-ECD-Fc (eluted fraction E1) was used for mass spectrometry analysis, a new batch of TMEFF2-ECD-Fc was purified using protein G Sepharose and HIS-Select HF Nickel Affinity Gel. The eluted fractions obtained during the second purification step (E1-E3) were then analyzed by SDS-PAGE using 10% resolving gel followed by staining with silver or Western blotting and labeling with anti-TMEFF2-ECD antibody. Samples were analyzed in the absence (Figure 6.8 A) or presence (Figure 6.8 B) of β-mercaptoethanol in order to establish whether the purified protein was purified as an intact, disulphide-linked TMEFF2-ECD-Fc dimer.

In the absence of β-mercaptoethanol a minor fraction of a >130 kDa full length TMEFF2-ECD-Fc dimer was detected in fractions E1-E3 by silver staining (Figure 6.8 A, left) and Western blotting (Figure 6.8 A, right). Additionally, two bands with apparent molecular masses of ~80 kDa and 90 kDa were detected on the gel and on the membrane. These bands are probably partially cleaved TMEFF2-ECD-Fc species, where the TMEFF2-ECD part was processed by proteases expressed by the host CHO cell line. A ~33 kDa band visualized by silver staining in fraction E1 was probably a degradation fragment of TMEFF2-ECD-Fc that did not contain the TMEFF2-ECD sequence as it was not recognized by anti-TMEFF2-ECD antibody. In the presence of β-mercaptoethanol in the sample loading buffer a faint ~80 kDa band corresponding to TMEFF2-ECD-Fc monomer was detected in sample E1 by Western blotting (Figure 6.8 B, right). The major component of fractions E1-E3 was the ~50 kDa TMEFF2 cleavage product. Staining with silver revealed the presence of the previously observed ~38 and ~33 kDa TMEFF2-ECD-Fc degradation fragments in samples E1-E3 (Figure 6.8 B, left).

The data obtained from this analysis indicated that the two-step purification of TMEFF2-ECD-Fc allowed removal of all impurities and obtain pure TMEFF2-ECD-Fc. However, the reduced amount of serum in conditioned medium of stably transfected CHO cells leads to increased protease activity and proteolytic processing of TMEFF2-ECD-Fc during purification. As a result, purified recombinant protein was a mixture of the full length TMEFF2-ECD-Fc dimer (>130 kDa) and at least two partially cleaved TMEFF2-ECD-Fc species (~80 kDa and ~90 kDa). Figure 6.9 shows a schematic picture of possible TMEFF2-ECD-Fc fragments generated by the cleavage of TMEFF2-ECD. In order to avoid TMEFF2-ECD-Fc processing during purification protease inhibitor cocktail should be added to the collected conditioned medium in future experiments.

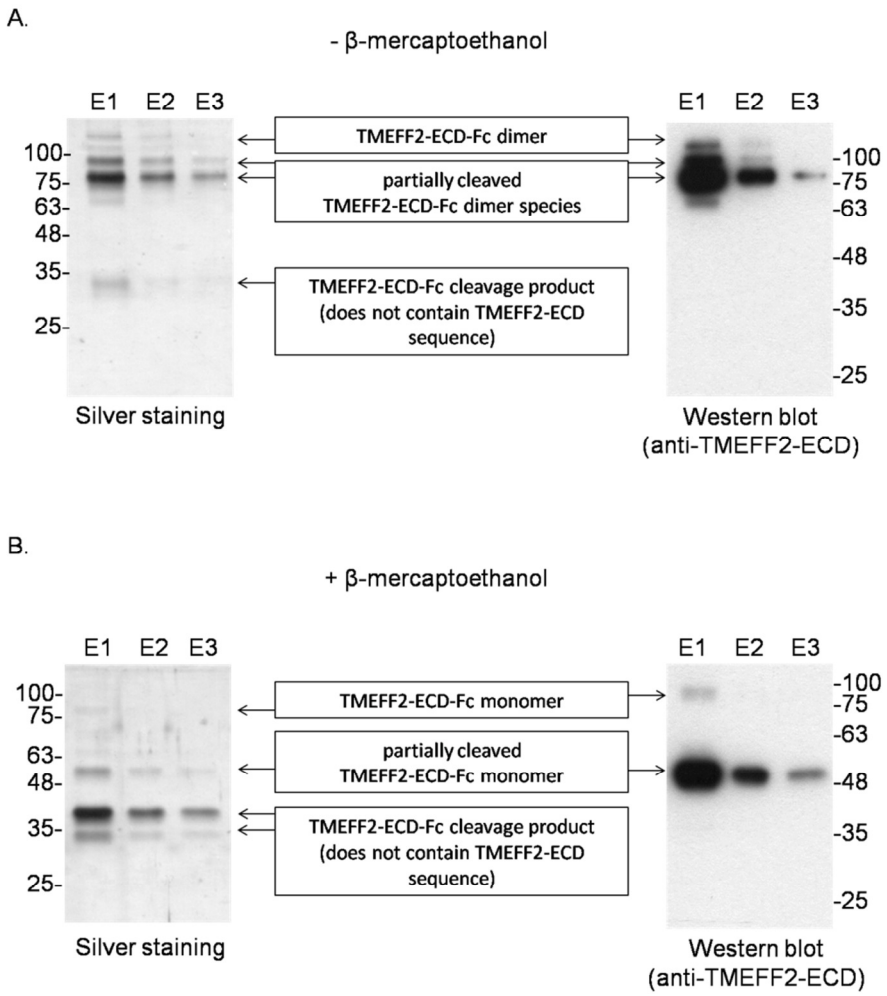

Figure 6.8 Analysis of the TMEFF2-ECD-Fc in fractions eluted from HIS-Select HF Nickel Affinity Gel.

10 µl of fractions E1, E2 and E3, eluted from HIS-Select HF-Nickel Affinity Gel were analyzed by SDS-PAGE in 10% resolving gel followed by silver staining or Western blotting and labeling with anti-TMEFF2-ECD antibody in the absence (A) or presence (B) of β-mercaptoethanol. In the absence of β-mercaptoethanol a >130 kDa band corresponding to TMEFF2-ECD-Fc dimer was detected in samples E1-E2 together with two partially cleaved dimers of TMEFF2-ECD-Fc (~80 kDa and ~90 kDa). When β-mercaptoethanol was present in the sample loading buffer, a minor fraction of ~80 kDa TMEFF2-ECD-Fc monomer was detected by Western blotting in sample E1. The major component of fractions E1-E2 was ~50 kDa TMEFF2-ECD-Fc cleavage product. Silver staining revealed that the samples contained also additional degradation fragments with apparent molecular masses of ~38 kDa and ~33 kDa.

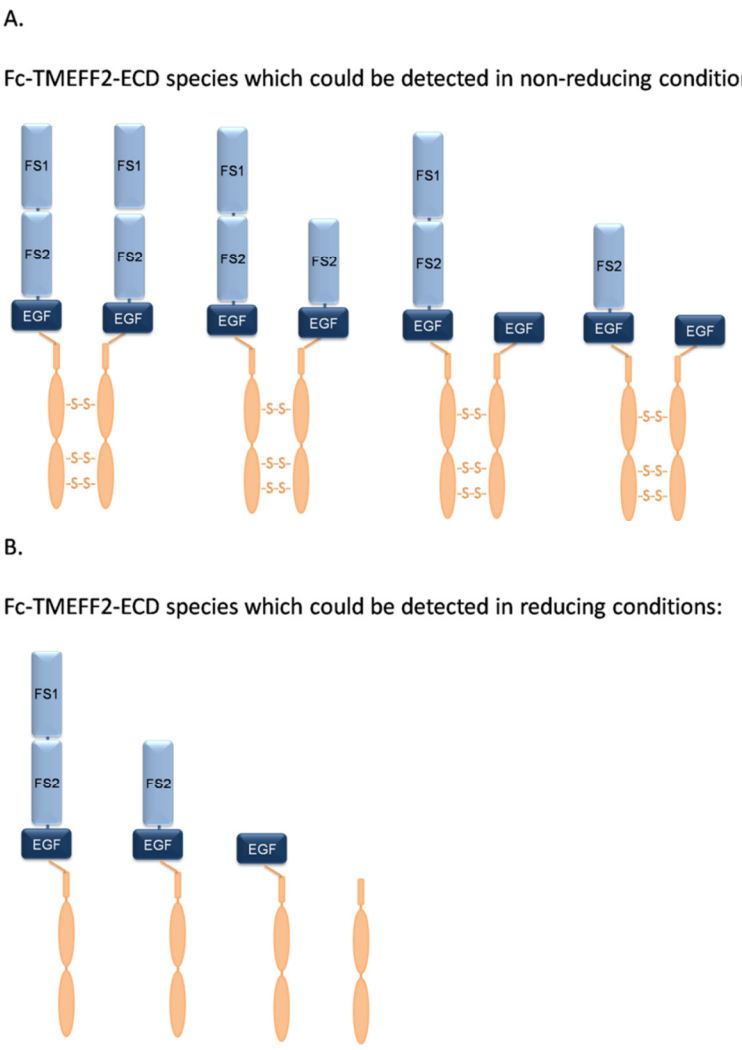

Figure 6.9 Potential TMEFF2-ECD-Fc fragments generated by proteolytic processing which could be detected in non-reducing (A) and reducing (B) conditions; FS – follistatin-like domain, EGF-EGF-like domain.

6.3.5 Analysis of ERK1/2 phosphorylation in PNT2-C2 and HEK293 cells in response to TMEFF2-ECD-Fc treatment.

The results presented in Chapter 5, where the ability of the MBP-tagged EGF-like domain from TMEFF2 to induce pERK1/2 phosphorylation was tested suggested that TMEFF2 is not a ligand for receptors from the ErbB family. However, expression of proteins in bacteria sometimes reduces their biological activity due to the lack of glycosylation and folding. As described by Glynne-Jones and co-workers, TMEFF2 is a glycoprotein and the glycosylation comprises approximately 21% of the TMEFF2 molecular weight as the removal of glycosylation by Peptide-N(4)-(N-acetyl-beta-D-glucosaminyl)asparagine amidase F (PNGaseF) reduced the molecular weight of TMEFF2 from 71 kDa to 56 kDa (Glynne-Jones et al. 2001). In order to examine if glycosylated fragments of the TMEFF2 ectodomain are able to activate ErbBs, purified TMEFF2-ECD-Fc, containing different TMEFF2-ECD-Fc species, were tested in ERK1/2 phosphorylation assays using the normal prostatic epithelial cell line PNT2-C2 (Figure 6.10) or human embryonic kidney cells HEK293 (Figure 6.11).

The experiment presented in Figure 6.10 was performed as previously described for PNT2-C2 treatment with MBP-tagged EGF-like domains. Briefly, PNT2-C2 cells were grown overnight in serum free medium with 25 µM GM6001 metalloprotease inhibitor in order to reduce ERK1/2 phosphorylation induced by endogenously shed ErbB ligands. After serum-starvation the cells were treated for 5 or 15 minutes with serum free medium containing different concentrations of TMEFF2-ECD-Fc (0 – 5.0 µg/ml) or medium supplemented with 10% FBS as a positive (+ve) control. The obtained result showed that TMEFF2-ECD-Fc did not activate ErbB receptors as no downstream phosphorylation of ERK1/2 was observed following 5 or 15 minutes treatment.

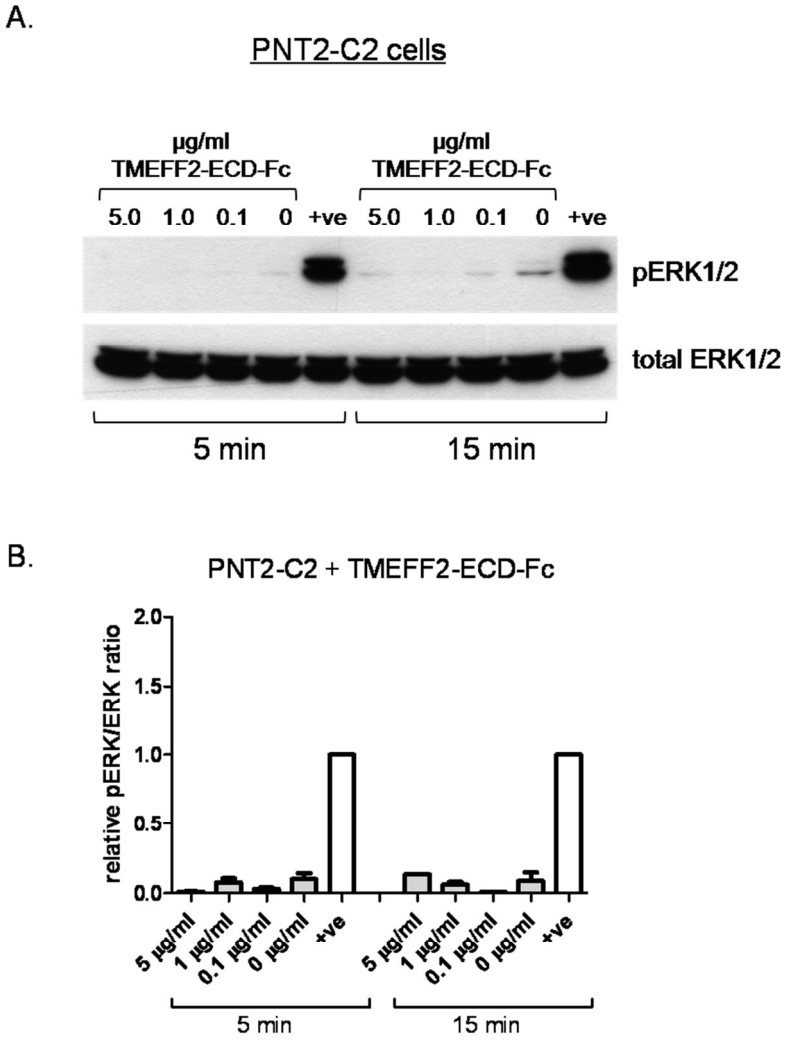

Figure 6.10 TMEFF2-ECD-Fc did not induce ERK1/2 phosphorylation in PNT2-C2 prostate epithelial cells.

PNT2-C2 cells were serum starved overnight in the presence of 25 µM GM6001 and treated for 5 or 15 minutes with different concentrations of TMEFF2-ECD-Fc. The medium containing 10% FBS was used as positive (+ve) control. Total cell lysates were analyzed by Western blotting for pERK1/2 and total ERK1/2 (A). The density of bands was analyzed using ImageJ software and presented as a relative pERK/ERK ratio (B). The Western blot is representative for three independent experiments and the histogram shows mean values from three experiments ±SEM.

Phosphorylation of ERK1/2 upon TMEFF2-ECD-Fc stimulation was also studied in HEK293 cells. HEK293 cells were chosen for this investigation because it was published previously that they responded to recombinant TMEFF2-ECD treatment by ERK1/2 phosphorylation (Ali & Knäuper 2007). This analysis was carried out similarly to PNT2-C2 stimulation; however experiments were performed in the absence of GM6001 as the level of constitutively activated ERK1/2 in HEK293 is very low. As presented in Figure 6.11, no ERK1/2 phosphorylation was induced following TMEFF2-ECD-Fc treatment of HEK293 cells. The discrepancy between the obtained result and previously published data, that TMEFF2-ECD induce ERK1/2 phosphorylation in HEK293 cells is probably caused by the different expression and purification methods used to obtain TMEFF2-ECD (Ali & Knäuper 2007). In the mentioned paper TMEFF2-ECD was expressed in mammalian cells as V5-tagged recombinant protein and purified in a single step process by affinity chromatography using anti-V5 agarose. Due to the shorter purification process it is possible that not all impurities were removed from the TMEFF2-ECD and the phosphorylation of ERK1/2 were induced by additional proteins present in the sample. The two-step purification method described in this study allowed to obtain pure, homogenous TMEFF2-ECD-Fc as no additional components were observed during SDS-PAGE and silver staining analysis (Figure 6.8 A). Another possibility, explaining ErbB activation by V5-tagged TMEFF2-ECD but not TMEFF2-ECD-Fc is that the large Fc-tag on the C-terminus hinders the interaction of TMEFF2-ECD-Fc with the receptor. In order to examine the influence of the tag location on TMEFF2-ECD biological activity, a recombinant TMEFF2-ECD tagged on the N-terminus was produced.

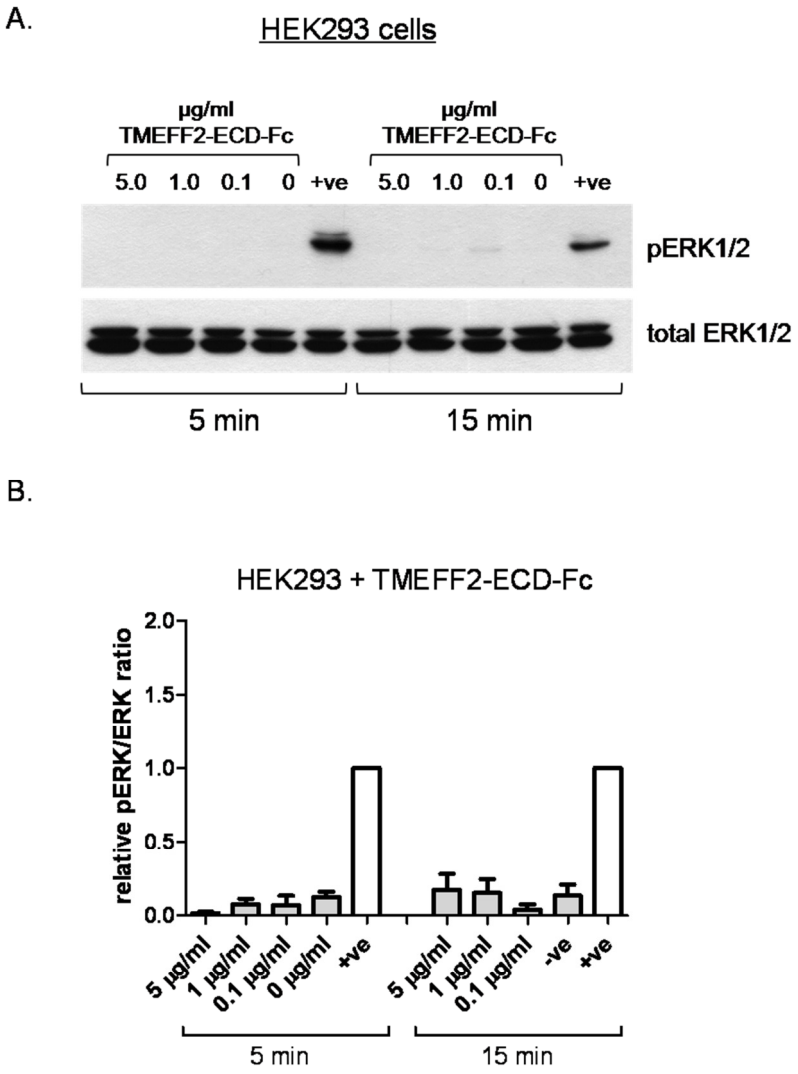

Figure 6.11 TMEFF2-ECD-Fc treatment of HEK293 cells did not induce ERK1/2 phosphorylation.

HEK293 cells were grown overnight in serum free medium followed by 5 or 15 minutes treatment with different concentrations of TMEFF2-ECD-Fc to induce ERK1/2 phosphorylation. The medium with 10% FBS was used as positive (+ve) control. Cell lysates were analyzed by Western blotting for pERK1/2 and total ERK1/2 (A). The density of bands was analyzed using ImageJ and presented as a relative pERK/ERK ratio (**B**). The Western blot is representative for three independent experiments and the histogram shows mean values from three experiments ±SEM.

6.3.6 Proliferation of PNT2-C2 cells in the presence of TMEFF2-ECD-Fc.

The biological activity of TMEFF2-ECD-Fc was also examined using a proliferation assay to investigate its influence on the growth of prostate epithelial cells. PNT2-C2 epithelial cells were grown in 96-wells plates in serum free RPMI containing 0.1-5.0 µg/ml of TMEFF2-ECD-Fc or 20 mM sodium phosphate pH 7.4 as a solvent control. On day 3 and day 4 the number of viable cells in each well was measured using Cell Proliferation Kit II (XTT) as described previously. Preliminary results from one experiment with eight repeats per condition are shown in Figure 6.12 and suggest that PNT2-C2 cells grew faster than control cells following stimulation with 0.1 and 1.0 µg/ml of TMEFF2-ECD-Fc in the medium. This result is in agreement with previously published data that described TMEFF2-ECD as a growth-promoting factor. Chen and co-workers showed that the conditioned medium from HEK293 cells expressing soluble TMEFF2-ECD had growth promoting activity on HEK293 as well as benign human prostatic RWPE1 cell line (Chen et al. 2011). The recombinant TMEFF2-ECD was also reported to increase proliferation of HEK293 cells (Ali & Knäuper 2007) and act as a survival factor for primary cultured neurons (Horie et al. 2000). It will be the matter of future investigation which receptors and signaling pathways are activated by TMEFF2-ECD and stimulate cell proliferation.

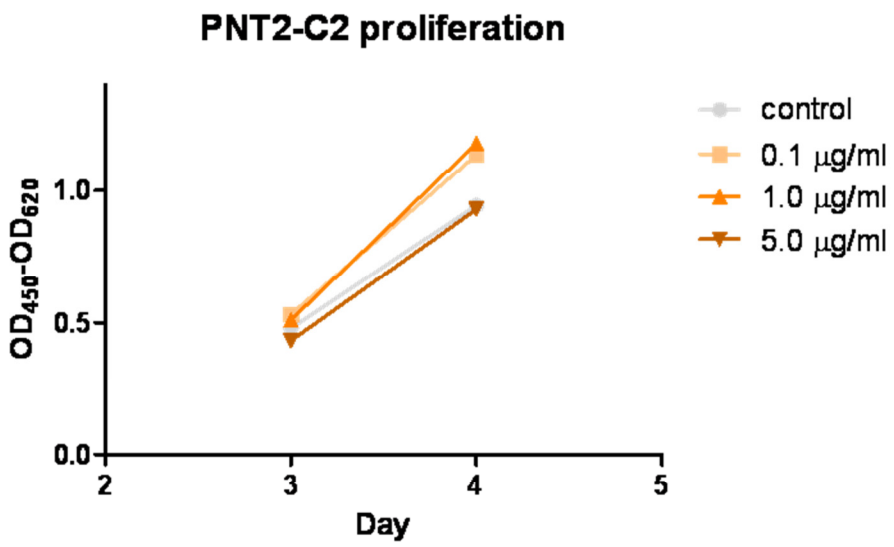

Figure 6.12 Proliferation of PNT2-C2 cells in the presence of TMEFF2-ECD-Fc.

PNT2-C2 cells were grown in 96-well plates in the presence of serum free medium containing different concentrations of TMEFF2-ECD-Fc or 20 mM sodium phosphate pH 7.4 as a control. The number of viable cells is each well was measured after 3 and 4 days of culture using Cell Proliferation Kit II (XTT) as described in Materials and methods. Graph shows mean values from one experiment with eight repeats per condition.

6.3.7 Expression of TMEFF2 fragments as N-terminal protein A fusion.

In addition to the TMEFF2-ECD-Fc, recombinant TMEFF2 fragments corresponding to predicted cleavage products generated by matriptase, hepsin and ADAMs were expressed in CHO cells as N-terminal protein A fusion proteins. Expression of TMEFF2-ECD with protein A on the N-terminus was performed in order to investigate the influence of the tag on TMEFF2-ECD biological activity as the function of N-protein A TMEFF2-ECD could be compared with TMEFF2-ECD tagged on the C-terminus with Fc.

To express proteins corresponding to TMEFF2 cleavage products fused with protein A, primers were designed to amplify sequences encoding TMEFF2-ECD, 2xFS, FS+EGF and EGF-like domain. Restriction sites were introduced in the primers and *BamHI* and *XhoI*-cleaved PCR products were then cloned into pcDNA5/FRT vector containing an IgG signal sequence followed by the protein A gene, as described in Materials and methods. The generated expression plasmids were sequenced and used to stably transfect CHO Flp-In cells according to Flp-In protocol (Appendix III). Following selection using cell culture medium containing 500 µg/ml of hygromycin B, stable cell lines were tested for the expression of recombinant proteins. Due to the presence of the signal sequence from human IgG upstream of the protein A gene, the protein A-tagged TMEFF2 fragments were secreted and were detected in the conditioned medium by Western blotting using anti-TMEFF2-ECD polyclonal antibody. The molecular sizes of the recombinant proteins were calculated from the amino acid sequence and are presented in Table 6.1 below:

Table 6.1 N-protein A TMEFF2 fusion proteins

Fusion protein	Calculated molecular mass
protein A – TMEFF2-ECD	52.9 kDa
protein A – 2xFS	46.0 kDa
protein A –FS+EGF	41.5 kDa
protein A – EGF	31.7 kDa

Figure 6.13 presents the analysis of 40 µl of conditioned medium from the parental CHO Flp-In cells or stably transfected CHO cell lines, supplemented with 10% FBS. Medium samples were analyzed by SDS-PAGE in non-reducing conditions, Western blotting and labeling with anti-TMEFF2-ECD polyclonal antibody. The apparent sizes of N-protein A-TMEFF2-ECD, 2xFS and FS+EGF fragments are much larger than calculated from the amino acid sequence, suggesting that these proteins form glycosylated dimers. The size of protein the A-EGF-like domain corresponded to the calculated molecular mass of the protein monomer. Conditioned medium from parental CHO cells was not stained for TMEFF2-ECD, indicating specific binding of the antibody.

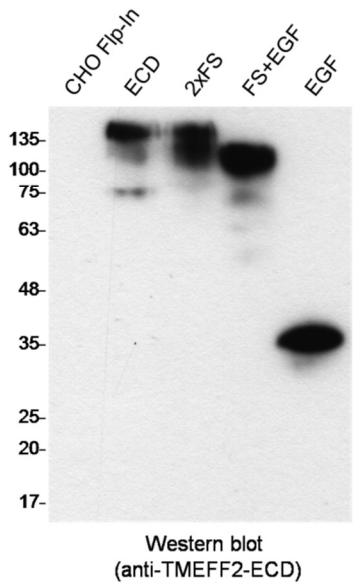

Figure 6.13 Analysis of N-protein A fusion TMEFF2 fragments in CHO conditioned medium under non-reducing conditions.

40 µl of conditioned medium from parental CHO Flp-In cells or stable cell lines expressing protein A-tagged ECD, 2xFS, FS+EGF and EGF-like TMEFF2 fragments were analyzed by separation in 11% resolving gel followed by Western blotting and labeling with anti-TMEFF2-ECD polyclonal antibody. The bands corresponding to protein A-tagged TMEFF2 fragments were detected in the samples from stable cell lines whereas no bands were seen in the medium from parental CHO Flp-In cells.

6.3.8 Purification of N-protein A TMEFF2 fragments from CHO conditioned medium.

The purification of N-protein A TMEFF2 fragments was established for TMEFF2-ECD. CHO cells stably expressing N-protein A TMEFF2-ECD were cultured in conditioned medium supplemented with 1% low IgG FBS. Following 3 days of culture, medium was collected as described in Materials and methods and filtered through 0.22 µm nitrocellulose membrane to remove cell debris. The medium was then applied onto previously equilibrated IgG Sepharose column at 4°C using the *ÄKTAprime* system with a flow rate of 1 ml/min. The IgG Sepharose was washed with TST buffer to remove non-bound proteins and 5 mM ammonium acetate pH 5.0 to wash away the IgG that may leak from the column material. Following washing, 0.1 M glycine-HCl pH 2.7 was applied to elute N-protein A TMEFF2-ECD which was monitored by measuring OD_{280} in eluted fractions. As shown in Figure 6.14, a broad, dispersed peak corresponding to eluted protein was observed upon applying the low pH elution buffer. To avoid the possibility that the eluted protein will be inactivated by the low pH, 0.5 ml of eluted fractions were collected into tubes containing 80 µl of 1M Tris-HCl pH 9.0.

10 µl of the 11 fractions with the highest OD_{280} were separated by SDS-PAGE in reducing conditions using 11% resolving gel, blotted and labeled with anti-TMEFF2-ECD antibody (Figure 6.15). This analysis showed a band corresponding to the glycosylated monomer of N-protein A TMEFF2-ECD in fractions 2-6. However, analysis of the same samples by SDS-PAGE and silver staining showed the presence of two other bands in addition to N-protein A TMEFF2-ECD (Figure 6.16). The apparent sizes of these proteins (50 kDa and 25 kDa) corresponded to heavy and light chain of IgG that likely leaked from the IgG Sepharose. Theoretically, N-protein A TMEFF2-ECD can be separated from IgG by ion-exchange chromatography using the differences of the isoelectric points between these two proteins. However, the quantity of the IgG impurities is much higher than the amount of target protein. For that reason the concentration of purified protein A TMEFF2-ECD will be too low to use this fusion protein in further experiments.

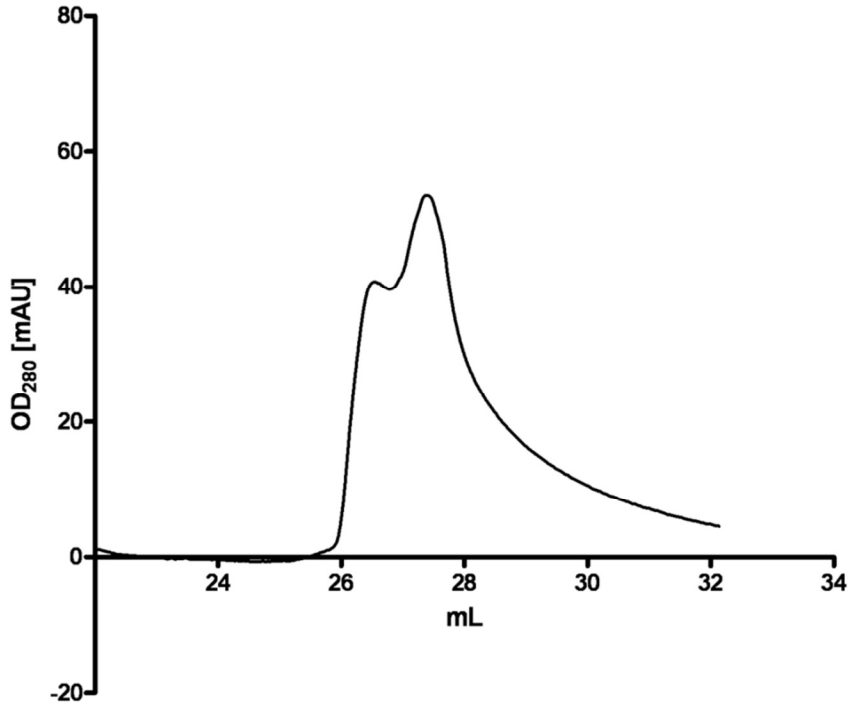

Figure 6.14 Elution of N-protein A TMEFF2-ECD from IgG Sepharose.

Conditioned medium from N-protein A TMEFF2-ECD expressing CHO cells was applied overnight into IgG Sepharose column and the fusion protein was eluted with 0.1 M glycine-HCl pH 2.7. Elution of the N-protein A TMEFF2-ECD was monitored by measuring the OD_{280} of the eluate.

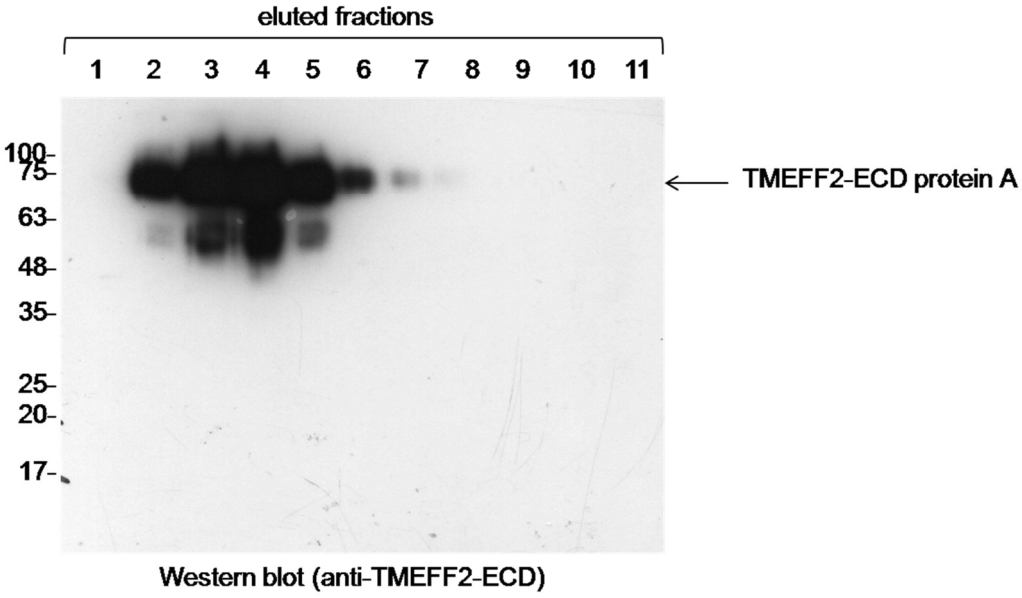

Figure 6.15 Analysis of N-protein A TMEFF2-ECD in eluted fractions by Western blotting.

The presence of N-protein A TMEFF2-ECD in 11 fractions eluted from IgG Sepharose was analyzed by Western blotting and labeling with anti-TMEFF2-ECD antibody. 10 µl of each fraction was loaded per lane. The monomer of N-protein A TMEFF2-ECD was detected in fractions 2-6.

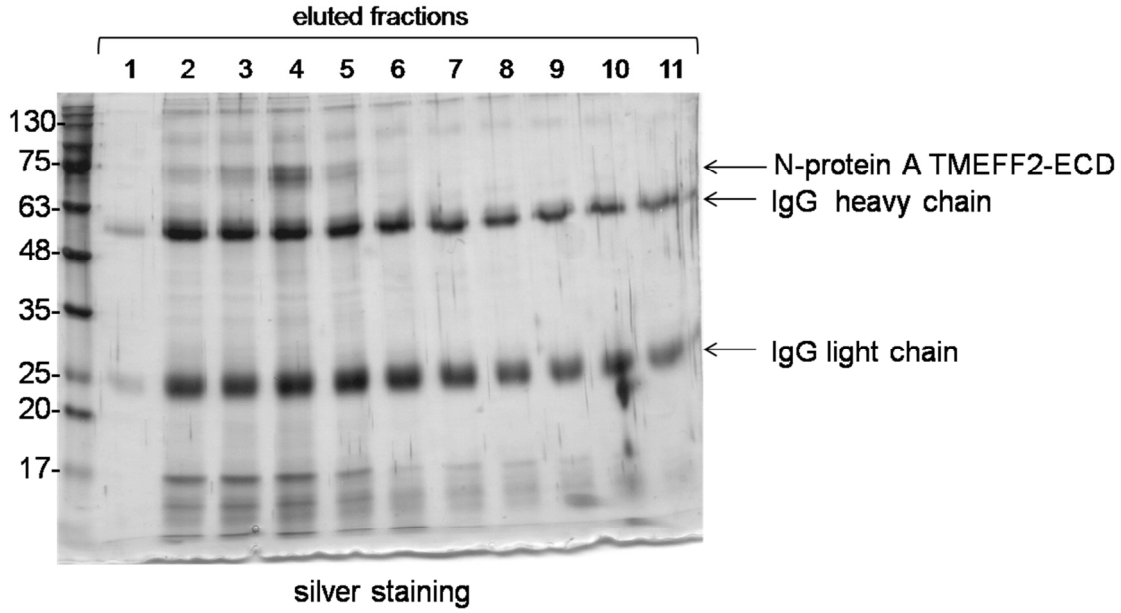

Figure 6.16 Analysis of N-protein A TMEFF2-ECD in eluted fractions by silver staining.

The purity of N-protein A TMEFF2-ECD was analyzed in11 fractions with the highest OD_{280} value that were eluted from IgG Sepharose. The samples were separated using 11% resolving gel and stained with silver. Except for N-protein A TMEFF2-ECD (fractions 2-5) two additional bands, corresponding to heavy and light chain of IgG were detected in all fractions.

6.3.9 Proliferation of CHO cells in the presence of N-protein A CHO fragments.

The data described in the previous section indicated that protein A-tagged TMEFF2 fragments were difficult to purify from the conditioned medium of stably transfected CHO cells due to the co-purification of IgG. Low expression level of protein A TMEFF2-ECD made the second purification step unrewarding as the ratio of the impurities exceeded the amount of the protein of interest by approximately 50 fold. For that reason the conditioned media from stable cell lines expressing N-protein A TMEFF2 fusion proteins were used to study the possible effect of TMEFF2 cleavage products on cell proliferation.

To obtain the conditioned medium $2x10^6$ of CHO Flp-In or stably transfected CHO cells expressing N-protein A TMEFF2-ECD, 2xFS, FS+EGF or EGF-like domain were seeded into 6-wells plates and grown in serum free medium for 48 hours. The collected medium was centrifuged to remove cell debris and added directly to CHO cells growing in 96-wells plates (Day 0). The number of viable cells in each well of the plate was assessed on Day 1, 2 and 3 using Cell Proliferation Kit II (XTT). The results from one experiment with eight repeats per condition are presented in Figure 6.17. The preliminary data indicate that the presence of TMEFF2-ECD and 2xFS fragments in conditioned medium decreased the proliferation rate of CHO cells, whereas the presence of EGF-like domain or FS+EGF TMEFF2 fragments did not influence cell proliferation. This result can be explained by the findings published by Lin and co-workers (Lin et al. 2011), showing that the presence of the first FS domain (or both FS domains) is required for interaction between TMEFF2 and PDGF-AA growth factor.

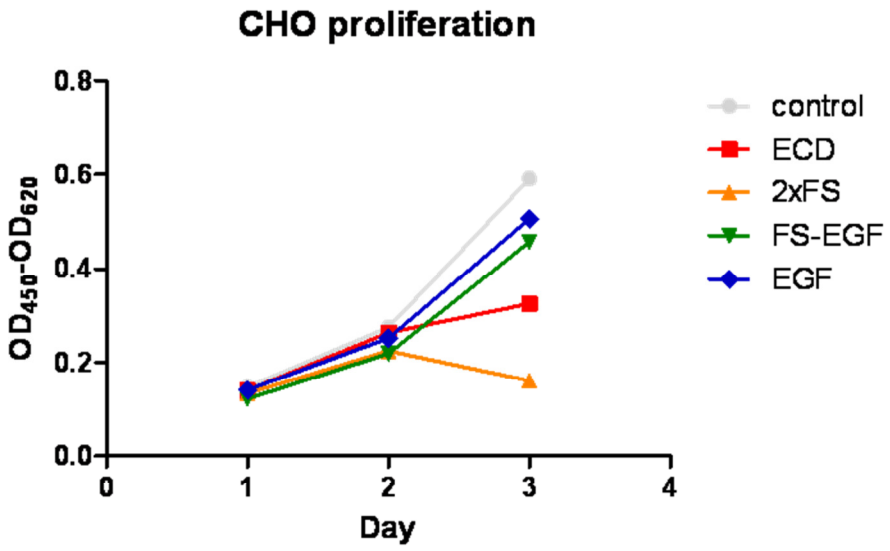

Figure 6.17 Proliferation of CHO cells in the presence of N-protein A TMEFF2 conditioned media.

CHO cells were grown in 96-well plates in the presence of serum free conditioned media from stable cell lines expressing N-protein A TMEFF2-ECD, 2xFS, FS+EGF and EGF-like domains or non transfected CHO cells as a control. Cell proliferation was monitored over 3 day period using Cell Proliferation Kit II (XTT) as described in Materials and methods. The presence of TMEFF2-ECD and 2xFS fragments decreased cell proliferation. Graph shows results from one preliminary experiment with eight repeats per condition.

6.4 Chapter summary.

The data presented in Chapter 5 described expression and purification protocol of MBP-tagged TMEFF2 EGF-like domain and ^{HR}EGF-like domain mutant in *E. coli*. However, due to the presence of several disulphide bonds within the FS domain, the TMEFF2-ECD, 2xFS and FS-EGF fragments were expressed but misfolded using a prokaryotic system. In this chapter mammalian expression was tested in order to obtain recombinant TMEFF2 fragments that can be used to investigate the influence of TMEFF2 cleavage products on prostate cancer cells *in vitro*.

The first method used to obtain recombinant TMEFF2 cleavage products was generation of stable CHO cell line releasing TMEFF2-ECD tagged at the C-terminus with the Fc fragment of human IgG_1. Purification of TMEFF2-ECD-Fc from the conditioned medium was performed using the affinity of the Fc-tag to protein G Sepharose. The Fc-tagged recombinant protein was eluted from the column material using low pH buffer and collected fractions were immediately mixed with 1 M Tris-HCl pH 9.0 to neutralize the pH and prevent destruction of protein's biological activity. The elution profile presented in Figure 6.4 indicated that the protein of interest was eluted from the column material as soon as the pH of the buffer inside the column decreased. Western blot analysis of collected fractions confirmed the presence of TMEFF2-ECD-Fc in eluted samples (Figure 6.5 B, fractions 2-8), however in addition to the ~75 kDa band corresponding to the TMEFF2-ECD-Fc monomer an additional ~50 kDa protein was detected. As this band was recognized by anti-TMEFF2-ECD antibody it was hypothesized that the ~50 kDa protein corresponded to partially cleaved TMEFF2-ECD-Fc. The cleavage of TMEFF2-ECD-Fc resulted from the culture conditions of CHO cells stably expressing TMEFF2-ECD-Fc. Prior to medium collection the cells were grown in conditioned medium containing 1% low IgG FBS instead of standard 10% FBS. In addition to grow factors serum contains also several protease inhibitors, such as alpha-1-antitrypsin (AAT), alpha-2-macroglobulin (α-2-M) and antithrombin (Gettins 2002; Armstrong & Quigley 1999). For that reason reduced amount of serum in the medium resulted in higher activity of proteases expressed by CHO cells and increased processing of TMEFF2-ECD-Fc that is known to be prone for proteolysis (Ali and Knäuper 2007, Chapter 4). In order to prevent TMEFF2-ECD-Fc during future purification, the conditioned medium should be supplemented with PMSF, EDTA and/or protease inhibitor cocktail immediately after collection from the cells.

The analysis of eluted fractions containing TMEFF2-ECD-Fc by SDS-PAGE and silver staining revealed that the purified protein was contaminated with bovine IgG (Figure 6.5 A), despite culturing the TMEFF2-ECD-Fc CHO cells in the presence of 1% low IgG FBS. To remove the IgG contamination from TMEFF2-ECD-Fc a second purification step was required.

The TMEFF2-ECD-Fc pcDNA5/FRT vector used to stably transfect CHO cells contained also a sequence encoding His tag, located downstream of the TMEFF2-ECD-Fc gene. The presence of the His tag allowed further purification of TMEFF2-ECD-Fc using HIS-Select HF Nickel Affinity Gel. Incubation of the sample containing TMEFF2-ECD-Fc and bovine IgG mixture resulted in binding of the TMEFF2-ECD-Fc to the HIS-Select affinity gel, whereas the bovine IgG remained in solution. To disrupt the interaction between TMEFF2-ECD-Fc and the affinity gel, the targeted protein was eluted using imidazole-containing buffer (Figure 6.6 and 6.7). The purity and folding of purified TMEFF2-ECD-Fc was then examined by SDS-PAGE and silver staining or Western blotting in the presence or absence of β-mercaptoethanol (Figure 6.8). In the absence of β-mercaptoethanol TMEFF2-ECD-Fc was present in the sample as a >130 kDa full length dimer as well as two partially cleaved dimers with apparent molecular masses of ~80 kDa and 90 kDa. Analysis of the same samples in the presence of β-mercaptoethanol in sample loading buffer revealed that the TMEFF2-ECD-Fc dimer species disintegrate into ~80 kDa full length TMEFF2-ECD-Fc monomer and cleaved ~50 kDa TMEFF2-ECD-Fc fragment. Silver staining revealed the presence of additional proteins in purified fractions which were not detected with anti-TMEFF2-ECD antibody. This proteins with apparent molecular masses of ~38 and ~33 kDa are more likely TMEFF2-ECD-Fc fragments which contain only the Fc-tag sequence, as confirmed for the ~38 kDa band by mass spec analysis. The schematic diagram of possible TMEFF2-ECD-Fc species which might be detected by Western blotting or silver staining in reducing and non-reducing conditions is presented in Figure 6.9.

Western blot and silver staining analysis showed that the IgG impurities were removed from the sample during the second purification procedure, however the recombinant TMEFF2-ECD-Fc was partially processed by proteases expressed by the CHO cells. Due to the time limitations the purification of TMEFF2-ECD-Fc in the presence of protease inhibitors in the collected medium could not be performed and the purified mixture of TMEFF2-ECD-Fc full length and cleaved dimers was used to investigate the biological activity of TMEFF2 cleavage products *in vitro*. In order to examine if the TMEFF2-ECD-Fc or its fragments are able to activate ErbB receptors, the ERK1/2 phosphorylation assays was performed using PNT2-C2 (Figure 6.10) and HEK293 cells (Figure 6.11). However, neither PNT2-C2 nor HEK293 cells responded to TMEFF2-ECD-Fc treatment in ERK1/2 phosphorylation. This result is in disagreement with the findings published previously by Ali and Knäuper, showing that HEK293 cells phosphorylate ERK1/2 following treatment with recombinant TMEFF2-ECD (Ali & Knäuper 2007). The reason behind this conflicting data is probably the use of different methods to express and purify TMEFF2-ECD. The mentioned study was performed using V5-tagged TMEFF2-ECD expressed in CHO cells and purified in a single step process using anti-V5 agarose. The lack of the second, “polishing” purification step might possibly leave some impurities

in the TMEFF2-ECD sample that induced ERK1/2 phosphorylation in HEK293 cells. The two step purification of TMEFF2-ECD-Fc described in this chapter allowed to obtain a sample containing pure, homogenous TMEFF2-ECD-Fc, as confirmed by the SDS-PAGE analysis and silver staining presented in Figure 6.8. The other explanation of the lack of ERK1/2 phosphorylation in response to TMEFF2-ECD-Fc treatment is the interference of the C-terminal Fc-tag with TMEFF2-ECD interaction with ErbB receptors. It is also possible that due to the proteolytic cleavage of TMEFF2-ECD-Fc the concentration of the ErbB-activating form of TMEFF2-ECD-Fc was too low to be able to detect receptor activation. For these reasons the *in vitro* experiments described in this chapter are considered as preliminary and should be repeated with TMEFF2-ECD-Fc that was purified in the presence of protease inhibitors.

The mixture of TMEFF2-ECD-Fc dimer species that was obtained was also used to investigate the proliferation of PNT2-C2 cells in the presence of soluble TMEFF2 fragments. Figure 6.12 shows the data obtained from one preliminary experiment where PNT2-C2 cells were grown in the presence of different concentrations of TMEFF2-ECD-Fc and the change in cell number was measured using Cell Proliferation Kit II (XTT). This result is in agreement with published data, showing that conditioned medium from TMEFF2-ECD expressing cells or recombinant TMEFF2-ECD has growth-promoting activity on HEK293 cells as well as benign human prostatic RWPE1 cell line (Ali & Knäuper 2007; Chen et al. 2011). However, the data from the ERK1/2 phosphorylation assays suggested that the proliferation-stimulating activity of TMEFF2-ECD is not mediated through ErbB receptors and activation of the MAPK/ERK signaling pathway. The receptor responding to TMEFF2 as well as the activated signaling pathway leading to increased proliferation need to be established in future studies.

An alternative system chosen to generate fragments corresponding to N-terminal TMEFF2 cleavage products was generation of stable CHO cell lines expressing TMEFF2-ECD, 2xFS, FS+EGF and EGF-like domain tagged on the N-terminus with a protein A tag. The presence of the protein A tag on the N-terminus of TMEFF2 fragments allowed comparison of the influence of the tag location on soluble TMEFF2 activity. Due to the presence of the signal sequence from the human IgG_1 TMEFF2 fragments were released and were purified from the conditioned medium using the affinity of protein A tag for IgG Sepharose. The purification protocol for protein A fusion proteins was established first for the N-protein A TMEFF2-ECD. The medium from stably transfected CHO cells was applied onto IgG Sepharose column and, following washing, the N-protein A TMEFF2-ECD was eluted using low pH buffer. The analysis of the elution profile shown in Figure 6.14 indicated that some protein was eluted from the column material as a broad, dispersed peak. The analysis of the eluted fractions by Western blotting and anti-TMEFF2-ECD labelling confirmed that the N-protein A TMEFF2-ECD was present in

fractions 2-6 (Figure 6.15). However, the analysis of the purity of obtained recombinant protein by SDS-PAGE and silver staining revealed the presence of two additional bands in all eluted fractions (Figure 6.16). The size of these proteins (~25 kDa and ~50 kDa) indicated that N-protein A TMEFF2-ECD was contaminated with IgG leaking from the column material or was co-purified from the conditioned medium due to the bovine IgG-protein A interactions. N-protein A TMEFF2-ECD could be further purified using ion exchange chromatography that protein separation based on the difference between their isoelectric points. In practice, however, the second purification step would dilute the targeted protein and the final concentration of N-protein A TMEFF2-ECD would be too low to perform next experiments. For that reason it was concluded that the expression of TMEFF2 as N-protein A fusion in CHO cells is not the optimal method to produce recombinant TMEFF2 fragments.

As the N-protein A TMEFF2 fragments were difficult to purify from the CHO medium, the complete conditioned media from stably transfected cells were used to investigate if the presence of TMEFF2-ECD, 2xFS, FS+EGF or EGF-like domain has any influence on cell proliferation. In these experiments the growth of cells was monitored using Cell Proliferation Kit II (XTT). Due to the time limitations only a pilot experiment was performed and Figure 6.15 presents the proliferation results with eight repeats per condition. This preliminary data showed decreased proliferation of CHO cells grown in the conditioned medium from TMEFF2-ECD and 2xFS expressing cells whereas the presence of FS-EGF and EGF-like domain in the medium did not influence CHO cell proliferation. This interesting observation could be explained based on the findings published by Lin and co-workers (Lin et al. 2011), showing that the first FS domain or both FS domains of TMEFF2 are able to bind and inactivate PDGF-AA. It could be then hypothesized that TMEFF2-ECD and 2xFS fragments bound and neutralized some growth factors required for the proliferation of CHO cells, most likely PDGF-AA. The other growth factors which could be potentially neutralized by soluble TMEFF2 are members of the transforming growth factor β (TGF-β) superfamily. The high sequence identity between FS domains of TMEFF2 and agrin suggest that TMEFF2 may interact with bone morphogenic factors (BMPs) and TGF-β1. Moreover, binding of the growth factors from the TGF-β family seems to be a common feature of many follistatin-like proteins. Fstl1 protein antagonize BMP-4 signaling during lung development (Geng et al. 2011) and recently discovered WFIKKN1 and WFIKKN2 proteins bind multiple TGF-β growth factors, including BMPs, TGF-β1 and growth differentiation factors (GDFs) (Kondás et al. 2008; Szláma et al. 2010).

The data described in Chapters 5 and 6 did not answer the question what is the biological role of TMEFF2 cleavage products but indicated some important activities of the soluble TMEFF2 fragments that should be investigated in the future. The tested soluble

TMEFF2 fragments did not induce ERK1/2 phosphorylation nor antagonize ErbB signaling pathway. It does however influence cell proliferation and the effect of TMEFF2-ECD seems to be cell type specific. CHO cells cultured in the presence of TMEFF2-ECD and 2xFS fragments grown slower than the control cells, possibly due to binding and neutralization of some growth factors by these fragments. Based on the literature data describing the role of other proteins containing FS domain it is hypothesized that the inhibitory effect of TMEFF2-ECD and 2xFS on CHO cells depends on their ability to bind members of the PDGF and/or TGF-β families. In contrast to the CHO cells, PNT2-C2 normal prostate epithelial cells grown faster in medium supplemented with 0.1-1.0 µg/ml of TMEFF2-ECD-Fc. As the TMEFF2-ECD-Fc does not activate ErbBs it will be interesting to investigate which receptors and signaling pathways are responsible for this growth-promoting effect of TMEFF2.

Chapter 7:

The fate of TMEFF2 cytoplasmic domain following ectodomain shedding

7.1 Introduction.

The data presented in Chapter 4 showed that TMEFF2 is processed by at least two groups of proteases that are expressed by prostate cancer cells – ADAMs and type II transmembrane serine proteases. TMEFF2 cleavage by these enzymes may play a critical role in the biological activity of TMEFF2 and deciphering the meaning of TMEFF2 processing may help to better understand the mechanism of prostate cancer progression. The experiments described in Chapters 5 and 6 were performed in order to investigate the biological function of extracellular products of TMEFF2 shedding. However, it should be emphasized that the proteolytic processing of TMEFF2 generates cytoplasmic fragment(s) that may have important biological functions inside prostate cancer cells.

7.1.1 The cytoplasmic domain of TMEFF2.

The evidence published by Ali and Knäuper indicated that the transmembrane fragment of TMEFF2 generated by ADAMs is further processed by the γ-secretase complex, resulting in the release of a small intracellular fragment (TMEFF2-ICD). Analysis of the TMEFF2-expressing cells treated with the γ-secretase inhibitor DAPT revealed the accumulation of TMEFF2 fragment corresponding to the membrane stump in the lysate (Ali & Knäuper 2007). Until very recently, there were no data regarding the fate of TMEFF2-ICD or interacting partners for the TMEFF2 cytoplasmic domain. However, in 2011 Chen and co-workers identified the first and currently the only known binding partner for the TMEFF2 cytoplasmic domain. MALDI-TOF/MS analysis of TMEFF2 complexes from stably transfected cells revealed that the cytoplasmic tail of TMEFF2 binds sarcosine dehydrogenase (SARDH) (Chen et al. 2011), an enzyme present mostly in the mitochondria but also in the cytoplasm that catalyses the conversion of sarcosine to glycine (Porter et al. 1985). TMEFF2-SARDH complexes were co-precipitated from LNCaP lysates and 22RV1 prostate cancer cells that express TMEFF2 endogenously. The biological significance of TMEFF2-SARDH interaction is not clear. However, decreased levels of sarcosine in the cytoplasm of TMEFF2 over-expressing cells suggested that interaction with TMEFF2 increased the catalytic activity of SARDH (Chen et al. 2011).

7.1.2 Atypical intracellular fate of pro-HB-EGF cytoplasmic domain.

Intracellular domains of several proteins that undergo ectodomain shedding are further processed by the γ-secretase complex. Liberated cytoplasmic domains of these proteins can translocate within the cell and might be involved in regulation of several processes, including activation of cytoplasmic kinases (Georgakopoulos et al. 2006), apoptosis (Vidal et al. 2005; Naresh et al. 2006) or gene transcription (Schroeter et al. 1998; Ni et al. 2001; Maetzel et al. 2009). However, not all proteins that undergo ectodomain shedding are further cleaved by γ-secretase but their intracellular domains

may still play an important role inside the cell. A very interesting example of this type of protein is the precursor of heparin-binding epidermal growth factor (pro-HB-EGF). Pro-HB-EGF is released from the cell surface by ectodomain shedding mediated by ADAM9, 10, 12 and 17 (Izumi et al. 1998; Asakura et al. 2002; Lemjabbar & Basbaum 2002; Sunnarborg et al. 2002; Yan et al. 2002). Immunolocalization experiments showed that following ADAM-mediated shedding the C-terminal part of pro-HB-EGF (HB-EGF-C) localized in the nucleus. However, the trafficking of the HB-EGF-C in cells expressing dominant-negative presenilin-1 mutant was not impaired, suggesting that the catalytic activity of the γ-secretase complex is not required for pro-HB-EGF translocation (Nanba et al. 2003). Further study showed that following ectodomain shedding HB-EGF-C is endocytosed and translocates to the nuclear envelope via retrograde transmembrane trafficking. Endocytic vesicles containing HB-EGF-C merge with the Golgi apparatus from which HB-EGF-C is targeted to the ER. From the ER HB-EGF-C diffuses or is actively transported to the inner nuclear membrane where it can interact with additional transcription factors (Hieda et al. 2008). A schematic diagram explaining HB-EGF-C trafficking inside the cell is presented in Figure 7.1. In the nucleus HB-EGF-C was shown to interact with two transcription repressors: B-cell lymphoma 6 protein (Bcl6) and promyelocytic leukemia zinc finger (PLZF) (Kinugasa et al. 2007; Nanba et al. 2003). Bcl6 is a mammalian transcriptional factor repressing the expression of cyclin D2 gene (Shaffer et al. 2000). Interaction of Bcl6 with HB-EGF-C reversed cyclin D2 repression by interfering with Bcl6 binding to the cyclin D2 gene promoter (Kinugasa et al. 2007).

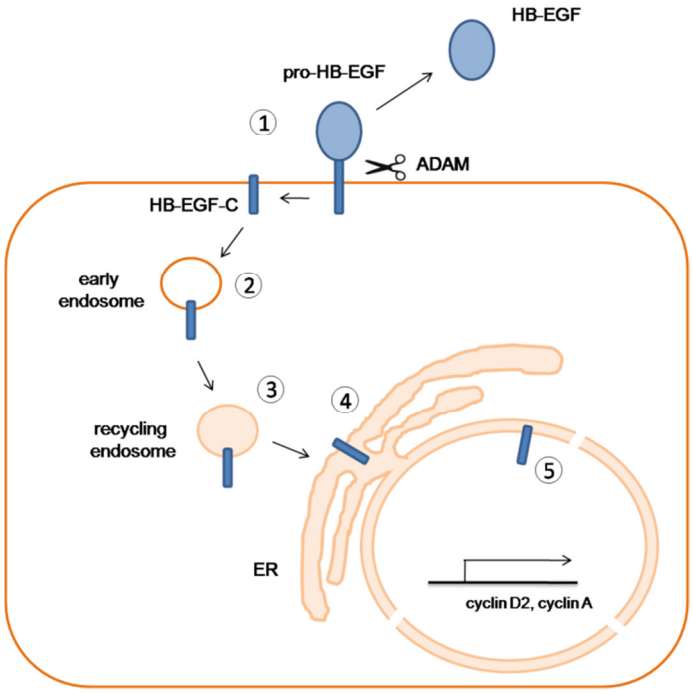

Figure 7.1 A model of HB-EGF-C trafficking to the inner nuclear membrane.

Pro-HB-EGF is expressed on the cell surface where it undergoes shedding mediated by ADAMs, releasing soluble HB-EGF (1). Membrane-anchored HB-EGF C-terminus (HB-EGF-C) is endocytosed (2) and possibly follows a retrograde transport pathway to the Golgi apparatus through recycling endosomes (3). From the Golgi apparatus HB-EGF-C is targeted to the ER (4) from where it diffuses or is actively transported to the inner nuclear membrane (5) and regulates transcription of cyclin genes (modified from M. Hieda et al. 2008).

PLZF, the other nuclear binding partner of HB-EGF-C, is a negative regulator of the cell cycle that repress the transcription of cyclin A and delays the entry or progression of cells into S-phase (Shaknovich et al. 1998; Yeyati et al. 1999). Binding of HB-EGF-C causes nuclear export of PLZF and reversal of cyclin A suppression (Nanba et al. 2003). Monitoring of the cell surface expression of pro-HB-EGF and nuclear accumulation of HB-EGF-C during cell cycle revealed that processing and translocation of HB-EGF correlates with cell cycle phases. Shedding of pro-HB-EGF occurs mostly during G_1-phase whereas HB-EGF-C accumulates in the nucleus in the beginning of S-phase causing nuclear export of PLZF in the late S-phase (Toki et al. 2005).

The role of HB-EGF-C in regulation of cyclin gene expression is even more interesting since the soluble HB-EGF is also involved in the modulation of the cell cycle. Binding of HB-EGF to ErbB receptors regulates the expression of cyclin D via the

Ras/MAPK signaling cascade and promotes progression into the G_1 phase of the cell cycle (Hackel et al. 1999). Therefore, pro-HB-EGF has two functional domains affecting mitogenic signaling, and the co-ordination of the dual mitogenic signals generated by the proteolytic processing may be important for cell cycle progression, as considered by Nanba and Higashiyama (Nanba & Higashiyama 2004).

7.2 Aims.

Chapter 7 describes preliminary data deciphering the role of TMEFF2 cytoplasmic fragments generated following ectodomain shedding. The experiments include:

- characterization of TMEFF2 cellular localization in HEK293 cells transfected with EGFP-TMEFF2 or TMEFF2-YFP and CHO cells expressing HA-TMEFF2-V5
- comparison of cellular localization of TMEFF2 and HB-EGF in stably transfected CHO cells
- analysis of TMEFF2 processing and cellular localization in the presence or absence of the γ-secretase inhibitor DAPT
- analysis of TMEFF2 C-terminal fragments in nuclear and cytoplasmic fractions from TMEFF2-expressing cells
- analysis of TMEFF2 C-terminal fragments generated by matriptase and hepsin-mediated cleavage in the presence or absence of γ-secretase and proteasome inhibitors.

7.3 Results

7.3.1 Localization of EGFP-TMEFF2 and TMEFF2-YFP in transfected HEK293 cells

One of the methods commonly used to examine intracellular localization of proteins is transfection of cells with expression construct encoding the protein of interest tagged with a fluorescent protein. This method allows trafficking of the studied protein in fixed, as well as live cells, to be monitored as it does not require additional labelling with antibodies. Cellular localization of TMEFF2 was examined in HEK293 cells transiently transfected with two constructs: TMEFF2 tagged on the N-terminus with enhanced green fluorescent protein (EGFP) and TMEFF2 tagged on the C-terminus with yellow fluorescent protein (YFP). 48 hours post-transfection the expression pattern of fluorescent TMEFF2 fusion proteins was analyzed and compared using the confocal microscope. As shown in Figure 7.2, EGFP-TMEFF2 expression was found mostly on the cell surface as well as membrane structures inside the cell, most likely corresponding to the ER. The green fluorescence signal detects only the full length EGFP-TMEFF2 or the EGFP-TMEFF2 cleavage products. Thus, cell surface fluorescence corresponds to the transmembrane EGFP-TMEFF2, whereas intracellular staining shows newly synthesized EGFP-TMEFF2. Additionally, at this stage of the investigation it is also possible that the full length EGFP-TMEFF2 or its N-terminal cleavage products are endocytosed and the green fluorescent staining in the cytoplasm corresponds to internalised protein. Figure 7.3 presents confocal microscope analysis of TMEFF2-YFP expression in HEK293 cells. Similarly to EGFP-TMEFF2, high TMEFF2-YFP fluorescent signal was detected on the cell surface. TMEFF2-YFP was also found in membrane structures within the cytoplasm as well as in the perinuclear area. HEK293 cells transiently transfected with TMEFF2-YFP were then used to monitor translocation of TMEFF2 cytoplasmic domain following PMA-mediated ectodomain shedding but due to the high amount of TMEFF2-YFP in the cytoplasm and the very bright fluorescent signal from YFP a change in TMEFF2 cytoplasmic domain localization could not be observed (data not shown). Therefore, further experiments were performed using CHO cells stably expressing TMEFF2 tagged on the C-terminus with V5 epitope which was visualized by labelling with mouse anti-V5 and anti-mouse AlexaFluor®594 antibodies. V5-tagged TMEFF2 was also preferred in this analysis as the literature data indicate that tagging short cytoplasmic domains with large fluorescent proteins may affect their trafficking and biological function (Nanba et al 2003).

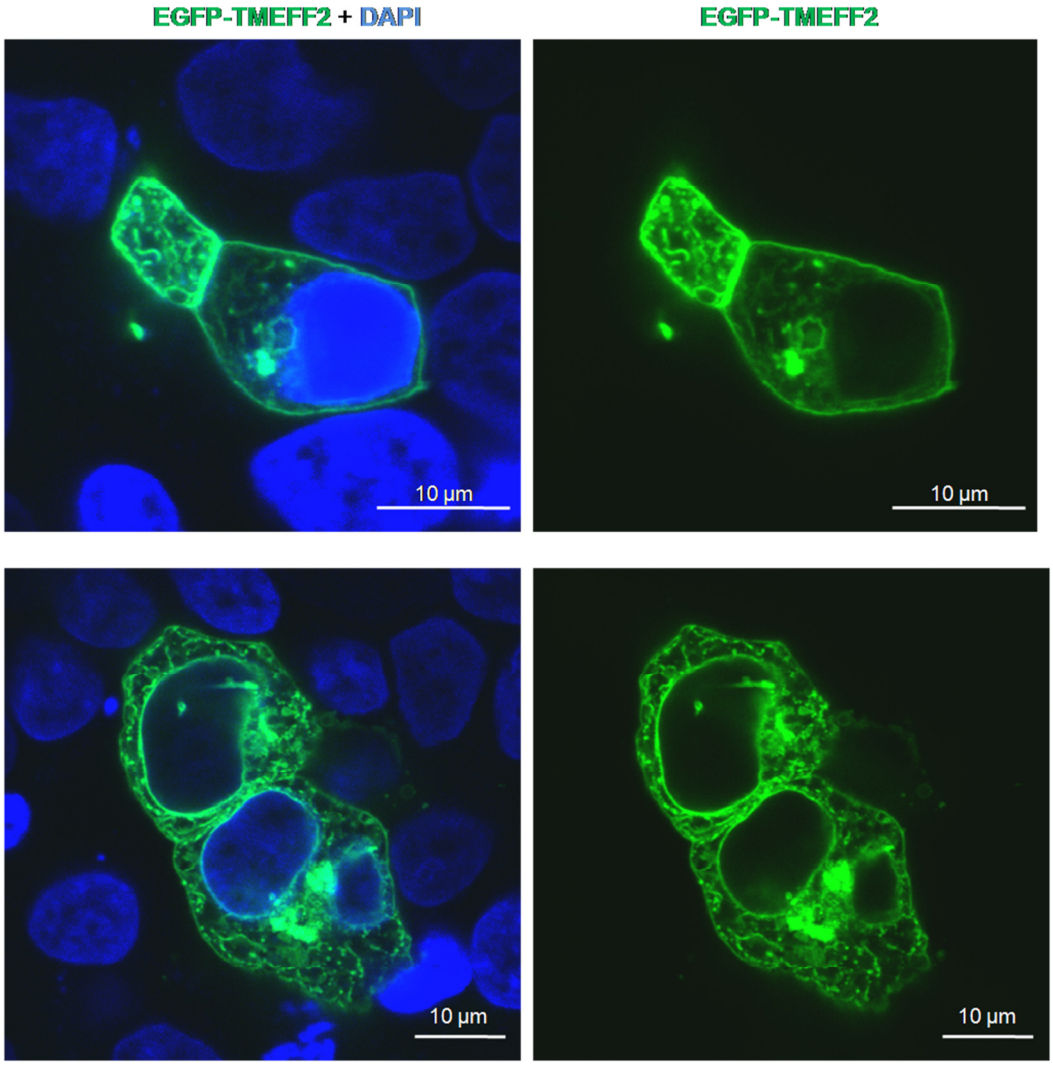

Figure 7.2 Localization of EGFP-TMEFF2 in transiently transfected HEK293 cells.

HEK293 cells were seeded on poly-L-lysine-coated cover slips in 6-well plates and transiently transfected with expression vector encoding TMEFF2 tagged on the extracellular domain (N-terminus) with enhanced green fluorescent protein (EGFP). 48 hours post-transfection HEK293 cells were fixed and cellular localization of EGFP-TMEFF2 was analyzed using confocal microscope. EGFP-TMEFF2 signal was detected mostly on the cell surface as well as in some membrane structures within the cytoplasm. Cell nuclei were visualised with DAPI (blue pseudocolor).

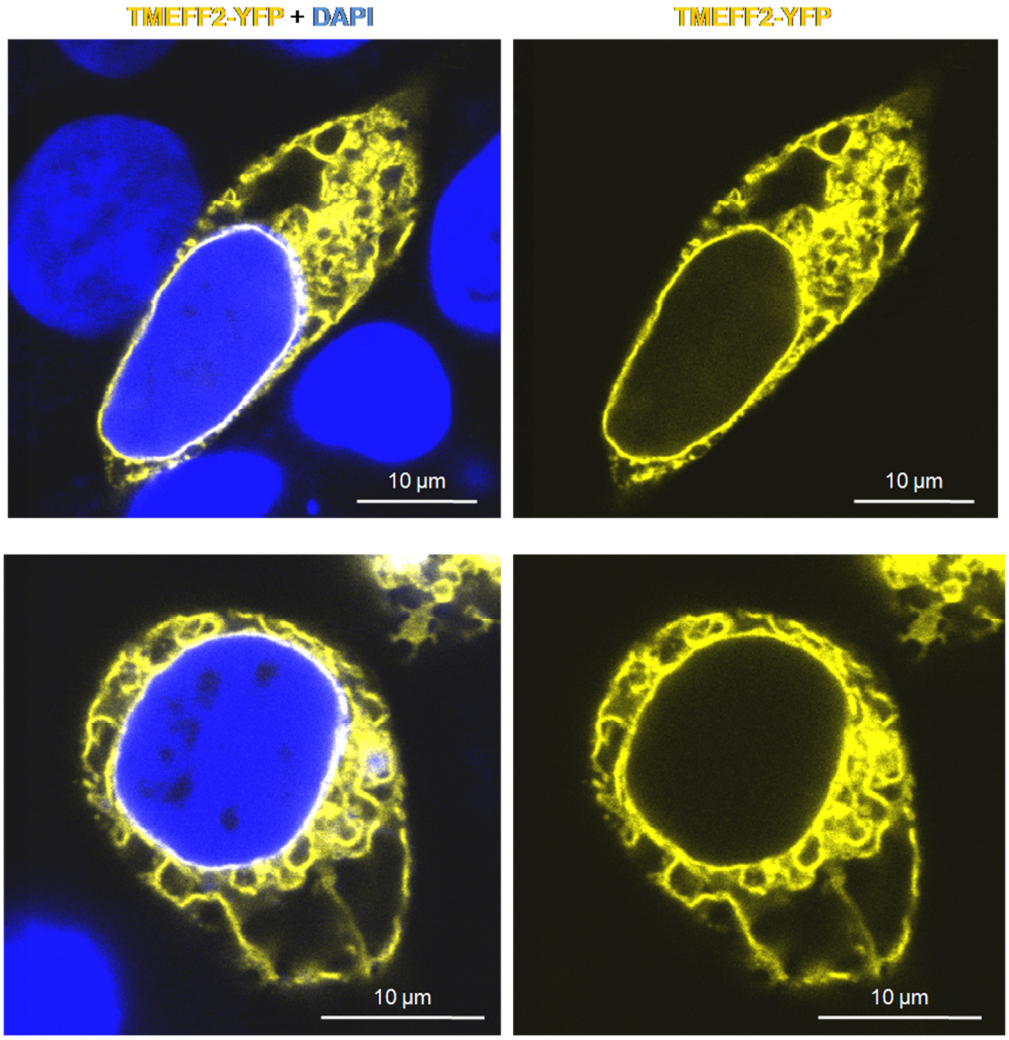

Figure 7.3 Localization of TMEFF2-YFP in transiently transfected HEK293 cells.

HEK293 cells were grown on poly-L-lysine-coated cover slips in 6-well plates and transiently transfected with expression construct encoding TMEFF2 tagged on the cytoplasmic domain (C-terminus) with yellow fluorescent protein (YFP). 48 hours post-transfection the cells were fixed and cellular localization of TMEFF2-YFP was monitored using the confocal microscope. TMEFF2-YFP was found on the cell surface as well as in some membrane structures within the cytoplasm and in the perinuclear region. Cell nuclei were visualised using DAPI (blue pseudocolor).

7.3.2 Comparison of HA/V5 TMEFF2 and AP/V5 HB-EGF expression pattern in stably transfected CHO cells.

The TMEFF2 expression pattern was characterized previously in HEK293 cells stably expressing HA/V5 TMEFF2 (Chapter 4, Figure 4.3). This analysis showed TMEFF2 localization on the cell surface, in the perinuclear region and within cytoplasmic structures, most likely corresponding to the ER. In this chapter TMEFF2 cellular localization was analyzed in stably transfected CHO cells, as it allowed comparison of TMEFF2 expression pattern with HB-EGF using a AP/V5 HB-EGF CHO cell line previously generated by Dr Vera Knäuper. The localization of TMEFF2 and HB-EGF cytoplasmic domains was analyzed in the presence or absence of PMA. HA/V5 TMEFF2 and AP/V5 HB-EGF CHO cells were grown in 6-well plates on poly-L-lysine-coated cover slips, serum starved for 1 hour and treated for 60 minutes with 100 ng/ml of PMA. Control cells were treated with DMSO solvent control. Cytoplasmic domains of HA/V5 TMEFF2 and AP/V5 HB-EGF were visualised using mouse monoclonal anti-V5 primary antibody and anti-mouse-AlexaFluor®594 secondary antibody. As shown in Figure 7.4 A, HA/V5 TMEFF2 in control cells was present on the cell surface as well as in the cytoplasm. Treatment with PMA increased cytoplasmic labelling of HA/V5 TMEFF2, suggesting translocation of V5-tagged TMEFF2 cytoplasmic fragment from the cell membrane into the cytoplasm. Anti-V5 labelling corresponding to HA/V5 TMEFF2 cytoplasmic domain did not localize in any vesicles or other structures, suggesting that intracellular part of TMEFF2 is rather not endocytosed following ectodomain shedding. However, this suggestion should be further verified by performing immunocolocalization of TMEFF2 and intracellular vesicles.

AP/V5 HB-EGF in control cells was found mostly in the cells membrane (Figure 7.4 B, left picture). PMA-induced ectodomain shedding significantly decreased cell surface labeling of AP/V5 HB-EGF and increased the cytoplasmic signal intensity (Figure 7.4 B, right picture). In the cytoplasm HB-EGF was detected within several vesicle structures that tended to gather close to the nucleus and are thought to be components of the endosome/Golgi/ER retrograde transport pathway that translocates HB-EGF-C to the inner nuclear membrane(Hieda et al. 2008).

Comparing the expression pattern of TMEFF2 and HB-EGF in stably transfected CHO cells it was concluded that both proteins were present on the cell surface and translocated to the cytoplasm upon PMA-mediated shedding. However, the pattern of TMEFF2 and HB-EGF labelling in the cytoplasm is different, indicating distinct intracellular trafficking of these proteins. PMA-treatment of AP/V5 HB-EGF CHO cells caused endocytosis of V5-tagged HB-EGF-C and accumulation of V5-positive endocytotic vesicles around the nucleus, which is in agreement with the literature data (Hieda et al. 2008). V5-tagged cytoplasmic domain of HA/V5 TMEFF2 was not detected in endocytotic structures.

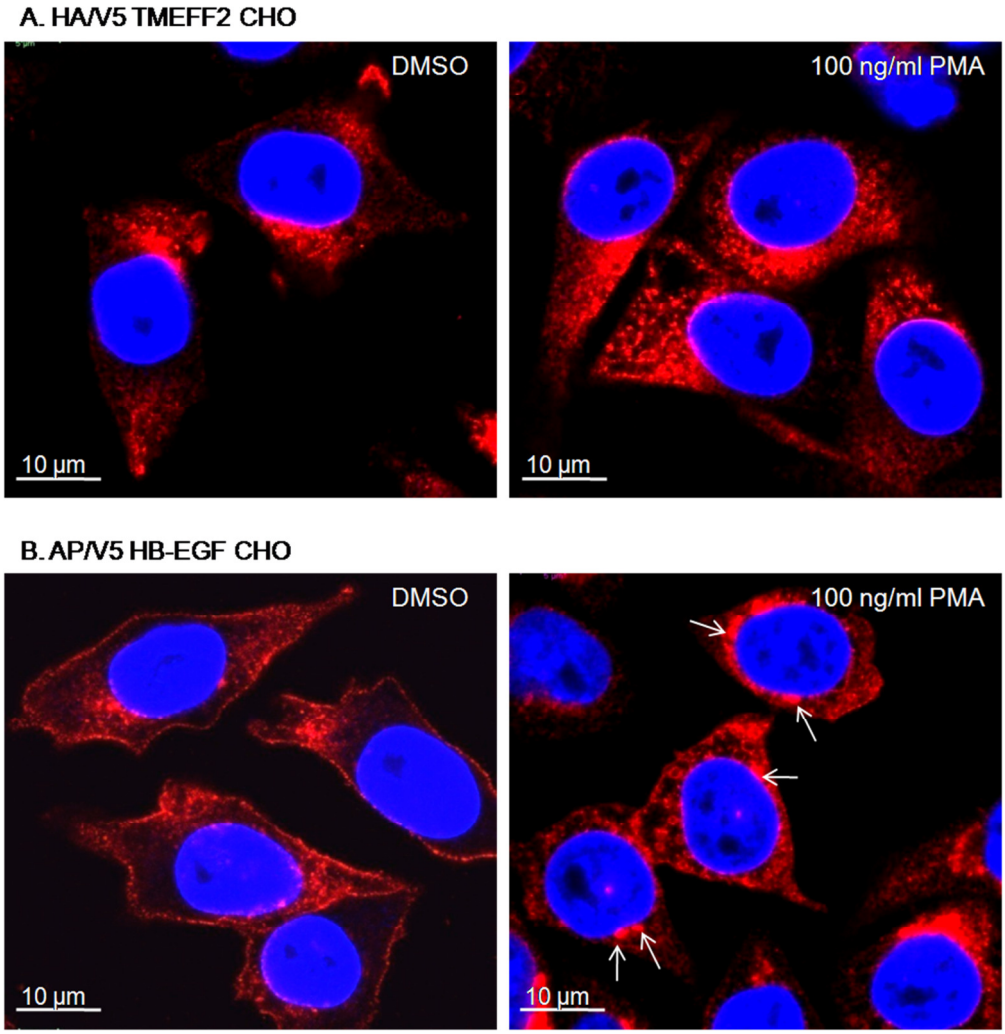

Figure 7.4. Localization of HA/V5 TMEFF2 or AP/V5 HB-EGF in CHO cells following PMA treatment.

CHO cells stably expressing HA/V5 TMEFF2 (A) or AP/V5 HB-EGF (B) were serum-starved for 1 hour and treated for 60 minutes with 100 ng/ml of PMA to induce ectodomain shedding. Control cells were treated with DMSO solvent control. Fixed and permeabilised cells were labelled with mouse anti-V5 primary and anti-mouse AlexaFluor®594 secondary antibody (red pseudocolour). Cell nuclei were visualised with DAPI (blue pseudocolour). In control cells HA/V5 TMEFF2 was present on the cell surface and in the cytoplasm. PMA treatment increased TMEFF2 staining in the cytoplasm, suggesting translocation of V5-tagged TMEFF2 cytoplasmic domain from cell membrane to the cytoplasm (A). AP/V5 HB-EGF in control cells was detected mostly on the cell surface. Treatment with PMA decreased membrane expression of AP/V5 HB-EGF and caused localization of V5-tagged cytoplasmic domain of HB-EGF in endosomes (B, white arrows).

7.3.3 Processing of TMEFF2 by the γ-secretase complex.

The data published by Ali and Knäuper showed that the shedding of AP/V5 TMEFF2 ectodomain leads to the generation of a ~17 kDa membrane-retained stub and a ~11 kDa free cytoplasmic fragment (TMEFF2-ICD) (Ali & Knäuper 2007). Analysis of AP/V5 TMEFF2 C-terminal cleavage products presented in Chapter 4 showed the presence of the ~17 kDa TMEFF2 fragment generated by metalloproteinases, whereas the ~ 10 kDa TMEFF2-ICD, produced by the γ-secretase, was detected only occasionally (Chapter 4, Figure 4.11). In order to confirm that the γ-secretase complex is involved in the processing of TMEFF2, HA/V5 TMEFF2 HEK293 cells were grown overnight in the presence of 5 µM γ-secretase inhibitor DAPT followed by 1 hour treatment with 100 ng/ml PMA to induce ectodomain shedding. Control cells were treated with DMSO solvent. Equal amounts of total cell lysates were analyzed by Western blotting using anti-V5 monoclonal antibody. As shown in Figure 7.5, the lysate from control cells lacked C-terminal AP/V5 TMEFF2 cleavage products (lane 1). PMA-treatment caused the accumulation of a ~17 kDa fragment corresponding to the transmembrane stub, generated by metalloproteinases (lane 2). Overnight treatment with DAPT also increased the amount of ~17 kDa TMEFF2 C-terminal fragment in the lysate (lane 3), whereas the greatest accumulation of a ~17 kDa TMEFF2 cleavage product was detected in the lysate from cells treated with DAPT and PMA (lane 4). Despite the fact that the ~11 kDa TMEFF2-ICD was not detected in this experiment it was concluded that the γ-secretase complex is involved in TMEFF2 processing as the presence of γ-secretase inhibitor DAPT led to the accumulation of ~17 kDa γ-secretase substrate. DAPT treatment prevented further processing of the TMEFF2 membrane stub generated by constitutively active metalloproteinases (lane 3) as well as PMA-activated enzymes (lane 4). The lack of ~11 kDa γ-secretase product in cell lysates was explained by rapid further processing or degradation of this C-terminal TMEFF2 fragment.

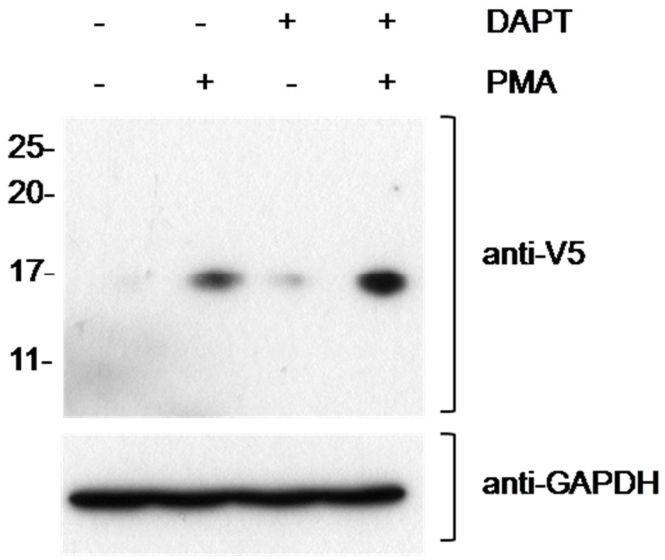

Figure 7.5 Analysis of HA/V5 TMEFF2 C-terminal processing in HEK293 cells following PMA treatment in the presence of γ-secretase inhibitor DAPT.

HA-V5 TMEFF2 HEK293 cells were grown overnight in the presence of 5 µM γ-secretase inhibitor DAPT followed by 1 hour treatment with 100 ng/ml PMA. 50 µg of total cell lysates were analyzed by Western blotting and labeling with anti-V5 antibody to detect C-terminal TMEFF2 cleavage products. Anti-GAPDH labeling served as a loading control. The amount of a ~17 kDa HA/V5 TMEFF2 fragment corresponding to the metalloproteinase product increased in the presence of DAPT, indicating that TMEFF2 is processed by the γ-secretase following ectodomain shedding.

Cellular trafficking of TMEFF2 C-terminal fragments was then monitored using HA/V5 TMEFF2 CHO cells grown overnight in the presence of metalloproteinase inhibitor GM6001, γ-secretase inhibitor DAPT or DMSO solvent control followed by 1 hour treatment with 100 ng/ml PMA (Figure 7.6). Localization of C-terminal HA/V5 TMEFF2 domain was visualized using mouse anti-V5 and anti-mouse AlexaFluor®594 antibodies and analyzed by confocal microscope. As observed previously, treatment with PMA increased the presence of C-terminal TMEFF2 fragment(s) in the cytoplasm (Figure 7.6, B). Pre-treatment with GM6001 inhibited HA/V5 TMEFF2 shedding by metalloproteinases and increased TMEFF2 labeling on the cell surface (Figure 7.6, C). A similar effect was observed when cells were grown overnight in the presence of DAPT (Figure 7.6, D). DAPT-treatment prevented γ-secretase processing of TMEFF2 membrane stub and translocation of TMEFF2-ICD from the cell membrane into the cytoplasm, retaining anti-V5 labeling on the cell surface.

Western blot analysis and immunolocalization experiments presented in Figures 7.5 and 7.6 gave indirect evidence that following ectodomain shedding TMEFF2 is processed γ-secretase, liberating free TMEFF2-ICD.

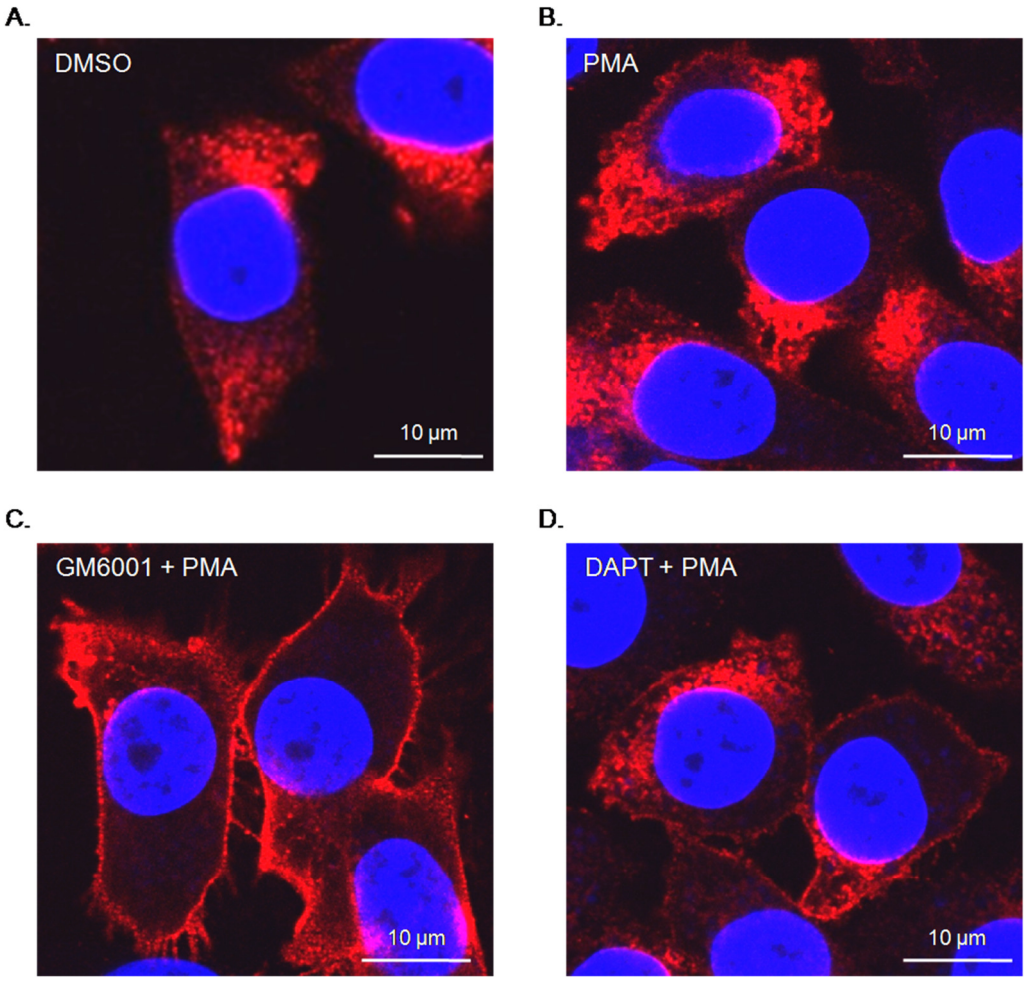

Figure 7.6 Cellular localization of HA/V5 TMEFF2 cytoplasmic domain in CHO cells in the presence of metalloproteinase or γ-secretase inhibitors.

HA/V5 TMEFF2 CHO cells were grown overnight in the presence of 25 µM GM6001 (metalloproteinase inhibitor), 5 µM DAPT (γ-secretase inhibitor) or DMSO (solvent control) followed by 1 hour treatment with 100 ng/ml PMA. The cells were fixed, permeabilised and labeled using mouse anti-V5 primary and anti-mouse AlexaFluor®594 secondary antibody (red pseudocolour). Cell nuclei were visualised with DAPI (blue pseudocolour). PMA treatment increased TMEFF2 labelling in the cytoplasm, whereas the presence of GM6001 or DAPT retained TMEFF2 signal on the cell surface.

7.3.4 Investigation of TMEFF2-ICD translocation to the nucleus.

Cytoplasmic domains of proteins undergoing RIPping follow several intracellular pathways, including translocation to the nucleus and regulation of gene expression. Analysis of TMEFF2 localization in CHO cells shown in previous figures did not indicate that TMEFF2-ICD translocates to the nucleus, even after TMEFF2 processing was induced with PMA. However, the immunolocalization experiment alone is not convincing enough to conclude that TMEFF2-ICD does not localize in the nucleus. For that reason translocation of TMEFF2-ICD to the nucleus was investigated further by separation of cytoplasmic and nuclear extracts from HA/V5 TMEFF2 HEK293 cells and analyzing them for the presence of V5-tagged TMEFF2-ICD.

7.3.4.1 Optimisation of the cytoplasmic and nuclear extraction protocol using HB-EGF-V5-expressing CHO cells.

The cytoplasmic and nuclear extraction method is based on two-step lysis protocol that allows separation of cytoplasmic and nuclear proteins. The cells are first mixed with a mild lysis buffer that disrupts plasma membranes but preserves nuclear envelopes. The cytoplasmic extract is then separated from the cell nuclei by centrifugation and gentle washing followed by disruption of cell nuclei with lysis buffer containing 10% glycerol. The cytoplasmic and nuclear extraction protocol used in this thesis was optimised first using HEK293 cells transfected with AP/V5 HB-EGF. It is known from the literature that the C-terminus of HB-EGF (HB-EGF-C) is endocytosed following ectodomain shedding and transported via endosome/ER/Golgi retrograde pathway to the inner nuclear membrane (Nanba et al. 2003; Hieda et al. 2008). Based on these data it was expected that HB-EGF-C will be found in nuclear extracts from transfected HEK293 cells. To induce HB-EGF shedding and generation of HB-EGF-C the cells were treated for 1 hour with 100 ng/ml PMA prior to preparing cytoplasmic and nuclear extracts. Equal amounts of cytoplasmic and nuclear proteins were then analyzed by Western blotting and labelling with anti-V5 antibody. To determine the efficiency of the extraction protocol, the Western blot membrane was stripped and re-probed with anti-β-tubulin antibody. The presence of β-tubulin in the nuclear fraction would indicate that the extraction protocol requires further optimisation in order to obtain pure nuclear extract, devoid of cytoplasmic proteins. As shown in Figure 7.7, a ~12 kDa protein corresponding in size to V5-tagged HB-EGF-C was detected in the cytoplasmic fraction of AP/V5 HB-EGF HEK293 cells, whereas HB-EGF fragments were not seen in the nuclear fraction. PMA treatment significantly increased the amount of V5-HB-EGF-C in the cytoplasmic extract and caused accumulation of the same protein in nuclear fraction. β-tubulin was found only in cytoplasmic fractions, indicating that the applied extraction protocol allows efficient separation of cytoplasmic and nuclear proteins.

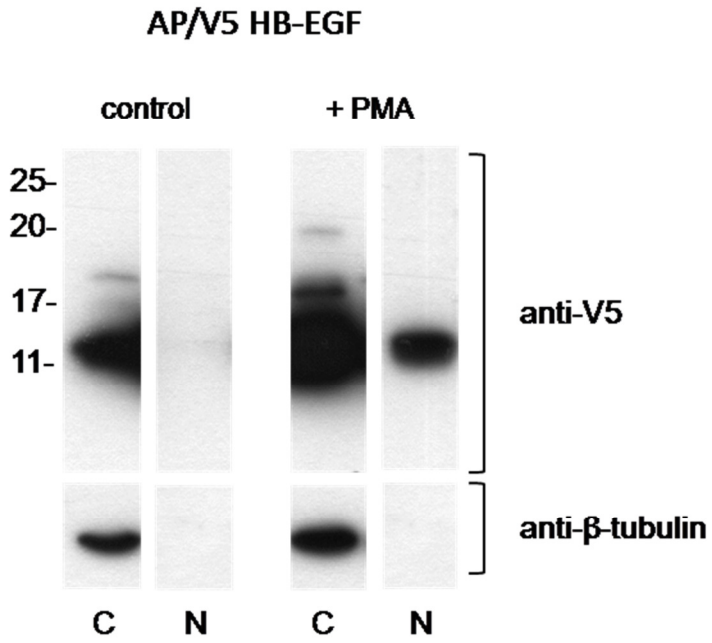

Figure 7.7 Analysis of the AP/V5 HB-EGF C-terminus in the cytoplasmic and nuclear extracts from transfected HEK293 cells.

HEK293 cells transiently transfected with AP/V5 HB-EGF were treated for 1 hour with 100 ng/ml PMA to induce ectodomain shedding. Control cells were grown in medium containing DMSO solvent. 30 µg of cytoplasmic (C) and nuclear (N) extracts from control and PMA-treated cells were analyzed by Western blotting and anti-V5 labelling. Stripped membrane was probed with anti- β-tubulin antibody to detect possible contamination of the nuclear fraction with cytoplasmic proteins. In control cells V5-tagged HB-EGF-C was detected cytoplasmic but not nuclear fraction. PMA treatment increased the amount of V5-HB-EGF-C in the cytoplasmic extract and caused accumulation of V5-tagged HB-EGF-C in the nuclear fraction.

7.3.4.2 Analysis of AP/V5 TMEFF2 cytoplasmic domain in nuclear and cytoplasmic extracts.

The optimised cytoplasmic and nuclear extraction protocol was used to analyze the presence of TMEFF2 C-terminal fragments in cytoplasmic and nuclear fractions. Similarly to AP/V5 HB-EGF-expressing cells, AP/V5 TMEFF2 HEK293 cells were treated for 1 hour with 100 ng/ml of PMA or DMSO as solvent control. Some of the cells were grown for 2 hours in the presence of10 ng/ml leptomycin B (LMB) prior to PMA treatment. LMB is a specific nuclear export inhibitor that covalently modifies exportin-1, an evolutionarily conserved receptor for the nuclear export signal of proteins (Kudo et al., 1999). As presented in Figure 7.8, treatment with PMA increased the amount of a ~ 17 kDaTMEFF2 fragment, corresponding to the metalloproteinase cleavage products in cytoplasmic extracts. C-terminal TMEFF2 fragments were not detected in nuclear extracts from control as well as PMA-treated cells. Pre-treatment with LMB did not cause accumulation of TMEFF2 fragments in the nuclear fraction and distribution of fragments was unaltered.

Based on the data obtained from immunolocalization experiments as well as analysis of TMEFF2 C-terminal fragments in cytoplasmic and nuclear extracts it was concluded that TMEFF2-ICD does not localize in the nucleus and thus is not directly involved in regulating gene expression. Moreover, the difficulty in TMEFF2-ICD detection suggest that this TMEFF2 fragment is very short lived and undergoes further cleavage or degradation immediately following γ-secretase processing.

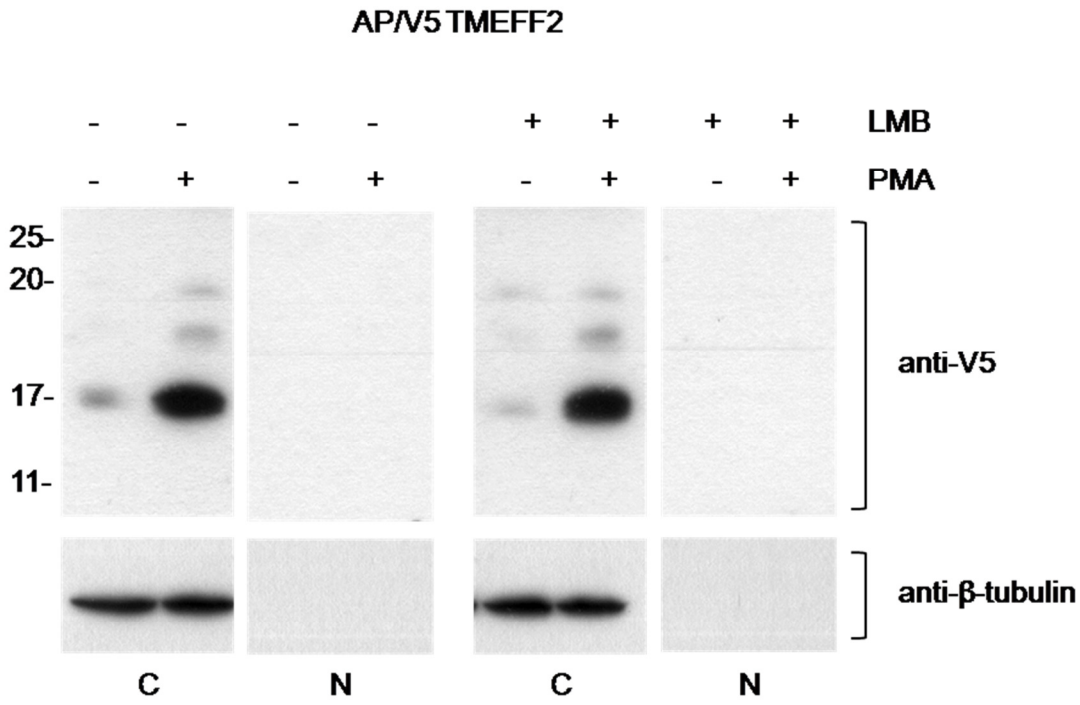

Figure 7.8 Analysis of the AP/V5 TMEFF2 C-terminal fragments in the cytoplasmic and nuclear fractions from transfectedHEK293 cells.

AP/V5 TMEFF2 HEK293 cells were grown for 2 hours in the presence of 10 ng/ml nuclear export inhibitor leptomycin B followed by 1 hour treatment with 100 ng/ml PMA. 50 µg of the cytoplasmic and nuclear extracts were analyzed by Western blotting and anti-V5 labelling. Stripped membranes were re-probed for β-tubulin in order to exclude possible contamination of the nuclear fraction with cytoplasmic proteins. PMA-treatment increased the amount of ~17 kDa TMEFF2 fragment generated by metalloproteinases in the cytoplasmic extracts. C-terminal TMEFF2 cleavage products were not detected in the nuclear extracts from control and PMA-treated cells, even following pre-incubation with LMB.

7.3.5 The fate of TMEFF2 C-terminal fragments generated by matriptase and hepsin.

The results presented in Chapter 4 indicated that TMEFF2 is processed not only by ADAMs and γ-secretase but also by type II transmembrane serine proteases – matriptase and hepsin. Moreover, the cleavage mediated by serine proteases occurs in different positions than ADAM-dependent processing, resulting in the generation of novel TMEFF2 fragments. The fate of the N-terminal TMEFF2 fragments released by matriptase and hepsin was analyzed in Chapters 5 and 6 whereas the fate of cytoplasmic fragments generated by serine proteases is investigated here.

In order to investigate if matriptase and hepsin-generated transmembrane TMEFF2 fragments are processed further by γ-secretase, HEK293 cells transiently transfected with AP/V5 TMEFF2 and matriptase, matriptase S-A, hepsin or hepsin S-A were treated overnight with 5 μM DAPT. Control cells were grown in the presence of DMSO solvent control. Equal amounts of total cell lysates were then analyzed by Western blotting and labelling with anti-V5 antibody. To compare differences in sample loading the Western blot membrane was stripped and re-probed for GAPDH. In all analyzed lysates a ~17 kDa protein corresponding to metalloproteinase-generated TMEFF2 fragment was detected (Figure 7.9). Cells transfected with inactive serine protease mutants treated with DAPT accumulated the ~17 kDa TMEFF2 cleavage product, confirming again that the γ-secretase complex is involved in processing of the ~17 kDa TMEFF2 transmembrane stub. As shown in Chapter 4, matriptase-mediated cleavage of TMEFF2 generates two fragments with apparent molecular masses of ~22 kDa and ~27 kDa whereas hepsin produce ~19 kDa C-terminal TMEFF2 stub (Chapter 4, Figure 4.11). DAPT treatment did not increase the amount of matriptase and hepsin-generated products (Figure 7.9), indicating that C-terminal fragments of TMEFF2 produced by matriptase and hepsin are not further cleaved by γ-secretase. In the lysate from hepsin-expressing cells a very faint ~11 kDa band corresponding in size to the γ-secretase product was visualised in the absence of DAPT. This band was undetectable in hepsin-transfected cells treated with DAPT, suggesting that the hepsin product is a novel substrate for the γ-secretase complex.

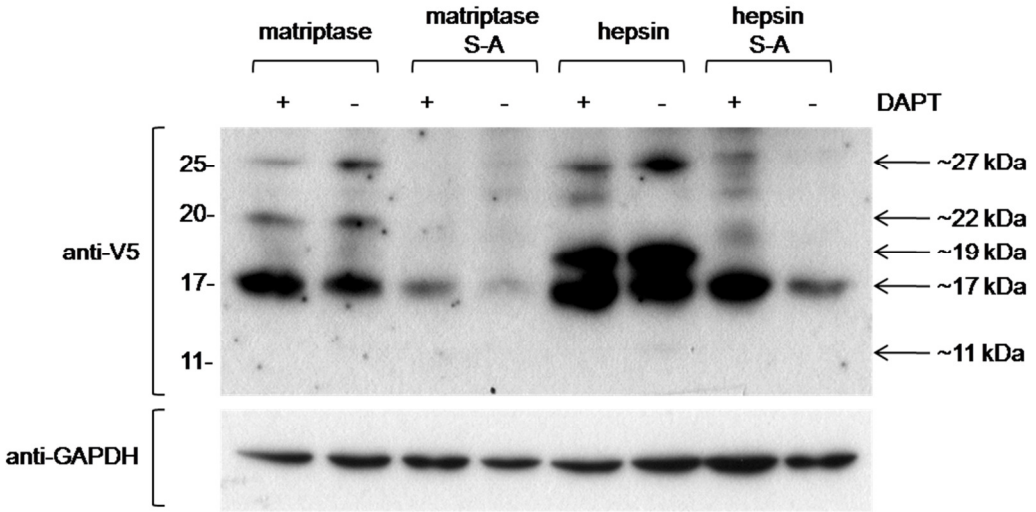

Figure 7.9 Analysis of TMEFF2 cytoplasmic fragments generated by serine proteases in the presence or absence of γ-secretase inhibitor DAPT.

AP/V5 TMEFF2 HEK293 cells transiently transfected with matriptase, hepsin or inactive S-A protease mutants were grown overnight in the presence of 5 µM DAPT or DMSO as a solvent control. 50 µg of cell lysates were then analyzed by Western blotting and anti-V5 labelling to detect C-terminal TMEFF2 cleavage products. Anti-GAPDH labelling served as a loading control. DAPT treatment caused accumulation of a ~17 kDa metalloproteinase product but did not increase the amount of matriptase (~22 kDa, ~27 kDa) and hepsin (~19 kDa)-generated fragments. In the lysate from hepsin-transfected cells a faint ~11 kDa band corresponding to the γ-secretase product was detected. This band was not found following treatment with DAPT.

To investigate the possibility that TMEFF2 C-terminal fragments generated by matriptase and hepsin as well as the TMEFF2-ICD released by the γ-secretase complex undergo proteasomal degradation, transfected cells were treated with the proteasome inhibitor epoxomicin. Epoxomicin, originally isolated from *Actinomycetes* strains, inactivates the proteasome by binding to its catalytic subunit but does not affect non-proteasomal proteases (Meng et al. 1999). AP/V5 TMEFF2 expressing cells, transfected with matriptase, hepsin or inactive S-A mutants were incubated for 4 hours with 5 μM epoxomicin. Prolonged exposure to higher doses of this inhibitor induces cell apoptosis and were therefore avoided (Meng et al. 1999). Analysis of the cell lysates by Western blotting and anti-V5 labeling is presented in Figure 7.10. Epoxomicin treatment caused accumulation of the ~17 kDa fragment generated by ADAMs as well as ~22 kDa matriptase product and ~19 kDa hepsin-generated fragment, suggesting that all these proteins are degraded in the proteasome. Interestingly, the ~11 kDa band corresponding to the γ-secretase product of TMEFF2 processing was also accumulated in response to epoxomicin treatment. This observation indicates that following RIPping TMEFF2-ICD undergoes proteasomal degradation and explains previous difficulties in the detection of TMEFF2-ICD by Western blotting.

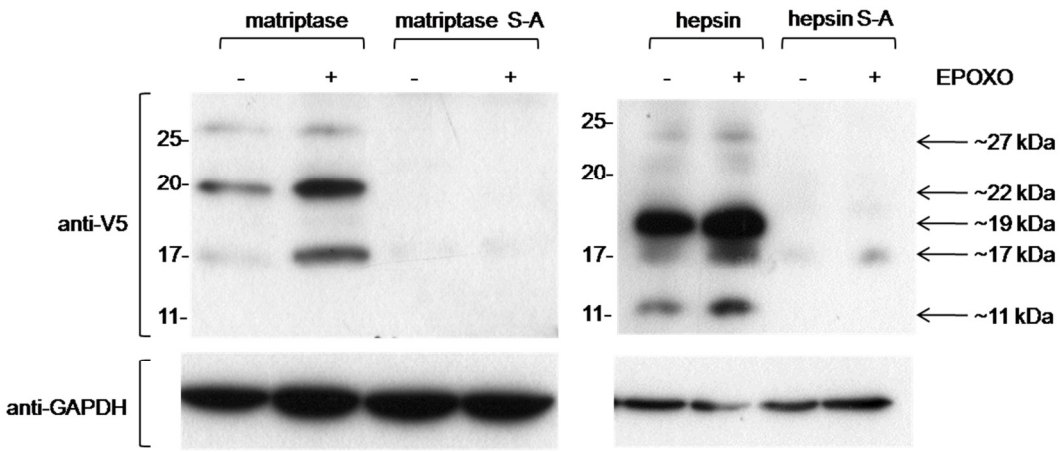

Figure 7.10 Analysis of TMEFF2 cytoplasmic fragments generated by serine proteases in the presence of proteasome inhibitor epoxomicin.

AP/V5 TMEFF2 HEK293 cells transiently transfected with matriptase, hepsin or inactive S-A protease mutants were treated for 4 hours with 5 μM proteasome inhibitor epoxomicin or DMSO as a solvent control. Cytoplasmic TMEFF2 fragments were then analyzed by Western blotting using anti-V5 antibody. 50 μg of total cell lysates were loaded per lane. Anti-GAPDH labelling served as a loading control. Epoxomicin treatment caused accumulation of a ~17 kDa metalloproteinase product, as well as hepsin-generated band and ~22 kDa matriptase products and ~11 kDa fragment generated by γ-secretase (grey arrow).

7.4 Chapter summary.

The experiments described in Chapter 7 focused on deciphering the cellular localization and fate of TMEFF2 C-terminal fragments following shedding of the ectodomain by ADAMs and serine proteases. Cytoplasmic domains of several proteins undergoing ectodomain shedding posses important biological functions, which are frequently independent and distinct from the biological activity of the ectodomain. Most of the transmembrane stumps generated during ectodomain shedding are further processed by the γ-secretase complex. Liberated cytoplasmic domains of these proteins translocate within the cell and are involved in activation of cytoplasmic kinases (Georgakopoulos et al. 2006), apoptosis (Vidal et al. 2005; Naresh et al. 2006) or gene transcription (Schroeter et al. 1998; Ni et al. 2001; Maetzel et al. 2009). To date, the knowledge about the fate of TMEFF2 cytoplasmic domain is very limited. Ali and Knäuper showed, that the membrane-retained stub of TMEFF2, generated by ADAMs, is a substrate for the γ-secretase (Ali & Knäuper 2007), however the cellular localization as well as the biological role of this fragment were not further investigated. In 2011 Chen and co-workers described that the cytoplasmic fragment of TMEFF2 interacts with sarcosine dehydrogenase (SARDH) and regulates cytoplasmic sarcosine levels by enhancing SARDH enzymatic activity (Chen et al. 2011). How γ-secretase processing of TMEFF2 influences TMEFF2-SARDH interactions and SARDH catalytic activity is not known. There are also no data about the fate of TMEFF2 C-terminal fragments generated by matriptase and hepsin, including their processing by the γ-secretase complex.

The cellular localization of TMEFF2 cytoplasmic domain was analyzed in two ways – by labeling of TMEFF2 C-terminus with fluorescently tagged antibody or using EGFP-TMEFF2 and TMEFF2-YFP protein expression constructs. HEK293 cells were transiently transfected with expression constructs encoding TMEFF2 tagged on the N-terminus with enhanced green fluorescent protein (EGFP-TMEFF2, Figure 7.2) and TMEFF2 tagged on the C-terminus with yellow fluorescent protein (TMEFF2-YFP, Figure 7.3). This analysis confirmed previous observations using antibody labelling. EGFP-TMEFF2 and TMEFF2-YFP localised mostly on the cell surface, membrane structures within the cytoplasm and in the perinuclear area. TMEFF2-YFP HEK293 cells were then used to monitor translocation of TMEFF2 C-terminus from the cell surface following PMA-mediated shedding. However, due to the high amount of TMEFF2-YFP in the cytoplasm and very bright fluorescent signal from YFP the change of TMEFF2 C-terminus localization could not be observed. For that reason further experiments were performed using CHO cells stably expressing HA/V5 TMEFF2. The advantage of this method is also the small size of the V5 tag that should not affect the trafficking and biological function of TMEFF2 C-terminus whereas the presence of large YFP tag could interfere with the cellular localization of TMEFF2 cytoplasmic domain.

The expression pattern of HA/V5 TMEFF2 in CHO cells was compared with the cellular localization of AP/V5 HB-EGF over-expressed in the same cell type, in the presence or absence of PMA. As shown in Figure 7.4, both proteins were present on the cell surface and translocated to the cytoplasm upon PMA-mediated shedding induction. However, the pattern of TMEFF2 and HB-EGF intracellular labelling is different, indicating distinct trafficking of these proteins. PMA-treatment of AP/V5 HB-EGF CHO cells caused endocytosis of V5-tagged HB-EGF-C and accumulation of V5-positive endocytotic vesicles around the nucleus, which is in agreement with the literature data (Hieda et al. 2008). V5-tagged cytoplasmic domain of HA/V5 TMEFF2 did not localize in endocytotic structures.

According to the literature data AP/V5 TMEFF2 ectodomain shedding generates a ~17 kDa membrane-retained stub that is further processed by the γ-secretase complex. This secondary cleavage releases a ~11 kDa AP/V5 TMEFF2 intracellular domain (TMEFF2-ICD) (Ali & Knäuper 2007). However, the ~11 kDa fragment was difficult to detect in previously described experiments (Chapter 4) and the involvement of the γ-secretase complex in TMEFF2 processing required further confirmation. Western blot analysis of AP/V5 TMEFF2 C-terminal cleavage products in the cells treated with γ-secretase inhibitor DAPT (Figure 7.5) confirmed further processing of TMEFF2 by the γ-secretase complex. A similar conclusion was made from the immunolabeling experiments, where the cellular localization of AP/V5 TMEFF2 cytoplasmic domain was compared between PMA, PMA+DAPT and PMA+GM6001-treated cells (Figure 7.6). The lack of TMEFF2 fragment corresponding to the γ-secretase product (TMEFF2-ICD) using Western blot analysis suggests that TMEFF2-ICD undergoes further processing or rapid degradation.

One of the possible intracellular functions of TMEFF2 cytoplasmic domain is translocation to the nucleus and regulation of targeted genes. Analysis of TMEFF2 cellular localization by immunolabeling and confocal microscopy shown in Figures 7.4 and 7.6, as well as in Chapter 4 Figure 4.3 did not indicate any nuclear signal, suggesting that TMEFF2 is not present in the nucleus. However, the confocal analysis alone is not convincing enough to conclude that the cytoplasmic domain of TMEFF2 does not localize in the nucleus. For that reason localization of TMEFF2 fragments in the nucleus was examined by cell fractionation. The protocol used in this investigation was first optimized using cells expressing HB-EGF as HB-EGF-C translocates to the nuclear envelope (Hieda et al. 2008) and could be detected by Western blotting in the nuclear extract from PMA-treated cells (Figure 7.7). Analysis of the cytoplasmic and nuclear fraction from AP/V5 TMEFF2 expressing cells revealed the presence of the ADAM-generated membrane stub in the cytoplasm but not in the nucleus (Figure 7.8). The TMEFF2-ICD was not detected either in the cytoplasm nor in the nuclear fraction, even when the cells were pre-treated

with a nuclear export inhibitor leptomycin B (LMB). Based on confocal analysis of TMEFF2-ICD localization as well as the cell fractionation data it could be concluded that TMEFF2-ICD does not translocate to the nucleus.

The fate of TMEFF2 C-terminal fragments generated by matriptase and hepsin was investigated. To analyze if these membrane-tethered proteins are recognized by the γ-secretase complex and further processed, AP/V5 TMEFF2 HEK293 cells expressing matriptase, hepsin or inactive S-A serine protease mutants were grown in the presence of DAPT inhibitor. As presented in Figure 7.9, DAPT treatment increased the amount of the ~17 kDa product of ADAM cleavage. However, the ~25 kDa and ~19 kDa matriptase, as well as the ~18 kDa hepsin cleavage products did not accumulate, indicating that they are not processed by γ-secretase. An analogous experiment was performed in the presence of the proteasome inhibitor epoxomicin in order to establish if TMEFF2 C-terminus is degraded following ADAM or serine protease shedding (Figure 7.10). Epoxomicin treatment resulted in the accumulation of ~17 kDa fragment generated by ADAMs, ~19 kDa matriptase product, ~18 kDa hepsin-generated fragment, suggesting that all these proteins undergo proteasomal degradation. The ~11 kDa TMEFF2 fragment cleaved by γ-secretase was also accumulated in epoxomicin-treated cells, suggesting that TMEFF2-ICD undergoes proteasomal degradation and explaining the inability to detect TMEFF2-ICD in previous Western blots.

The data described in this chapter indicate that the C-terminal products of TMEFF2 cleavage by ADAM, serine proteases and γ-secretase complex are most likely degraded by the proteasome. This findings should be further investigated in additional immunolocalization experiments or biochemical analysis using other inhibitors of protein degradation, for example lactacystin (Tomoda & Omura 2000). If these experiments would confirm that TMEFF2 C-terminal fragments undergo degradation it could be concluded that the main biological function of TMEFF2 involves its extracellular part and the C-terminal fragment does not play any additional role inside the cell. However, it could be also hypothesized that the degradation process itself has some biological meaning, for example by disrupting TMEFF2 interactions with its binding partners.

To date the only known binding partner of TMEFF2 C-terminus is SARDH (Chen et al. 2011), an enzyme catalyzing dehydrogenation of sarcosine to glycine (Porter et al. 1985). Interaction between TMEFF2 and SARDH was described in cells transfected with TMEFF2 as well as in prostate cancer cell lines that express TMEFF2 endogenously but the biological significance of TMEFF2-SARDH binding is not clear. Chen and co-workers reported that co-expression of TMEFF2 and SARDH significantly reduced the level of sarcosine in the cytoplasm (Chen et al. 2011) which would suggest that the interaction with TMEFF2 increased the activity of SARDH and enhanced the conversion of sarcosine into glycine. The involvement of TMEFF2 in the regulation of sarcosine levels in prostate

cancer cells is very interesting information as sarcosine is currently considered to be a novel, promising marker for the diagnosis of prostate cancer progression. In 2009 Sreekumar and co-workers published a large study in which they aimed to characterize the “metabolomic profile” of prostate cancer, identifying metabolites that can be detected in urine, blood or tissue biopsies from prostate cancer patients which would help to diagnose prostate cancer. They analyzed 1126 metabolites across 262 clinical samples related to prostate cancer using a combination of high throughput liquid and gas chromatography-based mass spectrometry and identified sarcosine as one of six differential metabolites. High levels of sarcosine were detected in 79% of metastatic samples, 42% samples from organ-localized prostate cancer and none of the samples from healthy individuals. Interestingly, the sarcosine levels can be assessed non-invasively in the urine. Their findings were also supported by *in vitro* studies, showing that sarcosine levels were higher in invasive prostate cancer cell lines comparing to benign prostate hyperplasia. Moreover, knockdown of the glycine-N-methyl transferase (GNMT), an enzyme that generates sarcosine from glycine, attenuated prostate cancer invasion (Sreekumar et al. 2009). The potential of sarcosine to be a novel marker for prostate cancer diagnosis was then disputed by Jentzmik and colleagues (Jentzmik et al. 2011) but other reports provide additional evidence that sarcosine is involved in the regulation of prostate cancer growth (Dahl et al. 2011). This could potentially help to diagnose prostate cancer patients with total serum PSA levels below 4 ng/ml (Lucarelli et al. 2012).

In the study by Chen et al. describing TMEFF2-SARDH interaction it was suggested that TMEFF2 binding to SARDH enhanced its enzymatic activity and decreased cytoplasmic sarcosine levels. Assuming that high levels of sarcosine are connected with more aggressive phenotype of prostate cancer it would suggest that TMEFF2 expression inhibits invasiveness of prostate cancer cells. Hypothetically, shedding of TMEFF2 by ADAMs or serine proteases followed by the degradation of TMEFF2 cytoplasmic domain would disrupt the interaction with SARDH, increase the accumulation of sarcosine in the cytoplasm, supporting the invasive phenotype of prostate cancer cell. However, the biological consequences of TMEFF2-SARDH binding as well as the role of ectodomain shedding and γ-secretase processing in regulating this interaction need to be considered in the future.

Chapter 8:

Final discussion and future experiments

8.1 TMEFF2 – potential target for novel prostate cancer therapies

Prostate cancer is the 2nd most common cancer worldwide for males, and the 5th most common cancer overall, with more than 670,000 new cases diagnosed every year. Thanks to the improved diagnostic procedures allowing to detect prostate cancer at early stages about 70% of patients diagnosed with prostate cancer survive more than 10 years. However, the lack of efficient treatment of hormone-insensitive, metastatic prostate cancer makes this disease the sixth most common cause of death from cancer in men worldwide (Cancer Research UK, May 2013). To design more effective anti-cancer therapies the mechanisms responsible for prostate cancer development, especially the transition from hormone-sensitive, organ-defined disease to hormone-refractory, metastatic prostate cancer need to be better understood. For that reason every newly identified protein expressed by prostate cancer cells is carefully investigated in order to better understand the mechanisms responsible for the development of an aggressive prostate cancer phenotype. One of these novel proteins potentially involved in the development and progression of prostate cancer and thus being a promising target for new anti-prostate cancer therapy is TMEFF2.

The role of TMEFF2 in the development and progression of prostate cancer is controversial. Several published data indicate that TMEFF2 has cancer-promoting activity (Glynne-Jones et al. 2001; Ali & Knäuper 2007), while others suggest that TMEFF2 inhibits progression of cancer (Liang et al. 2000; Gery et al. 2002; Gery & Koeffler 2003; Elahi et al. 2008). As a transmembrane protein TMEFF2 is exposed for proteolytic processing by membrane-anchored proteases, including members of a disintegrin and metalloprotease (ADAM) family (Ali & Knäuper 2007). Based on these reports, it was hypothesized that the opposing findings describing the role of TMEFF2 in prostate cancer biology result from proteolytic processing of TMEFF2 by different membrane-anchored proteases which are co-expressed with TMEFF2 in prostate cancer cells.

8.2 Expression of TMEFF2 and serine proteases in prostate cancer

In order to support the previously stated hypothesis the expression of TMEFF2 and several membrane serine proteases associated with prostate cancer was examined in prostate cancer cell lines and clinical samples. The results described in Chapter 3 showed that TMEFF2 is co-expressed with matriptase, hepsin and prostasin in prostate cancer-derived cell lines LNCaP and PC3 (Figures 3.2 and 3.4) as well as in lysates from cells isolated from prostate cancer patients (Figures 3.1 and 3.3). Co-expression of TMEFF2 and serine proteases in the same cells supported the hypothesis that the biological activity of TMEFF2 in prostate cancer could be differentially regulated by proteases. Prostate cancer cell lysates analyzed for TMEFF2 and serine protease expression corresponded to the $CD44^{+}/\alpha_2\beta_1^{hi}/CD133^{+}$ subpopulation of prostate cancer cells, described in the literature

as prostate cancer stem cells (Collins et al. 2001; Collins et al. 2005). Interestingly, TMEFF2 was detected in some but not all lysates from prostate cancer stem cells, raising a question about the functional difference between $CD44^+/\alpha_2\beta_1^{hi}/CD133^+/TMEFF2^+$ and $CD44^+/\alpha_2\beta_1^{hi}/CD133^+/TMEFF2^-$ cells that could be investigated in future experiments. The differences in motility, invasiveness and proliferation rates between TMEFF2-positive and TMEFF2-negative $CD44^+/\alpha_2\beta_1^{hi}/CD133^+$ prostate cancer cells could be analyzed *in vitro* using $CD44^+/\alpha_2\beta_1^{hi}/CD133^+/TMEFF2^+$ and $CD44^+/\alpha_2\beta_1^{hi}/CD133^+/TMEFF2^-$ subpopulation separated by immunolabeling and cell sorting. The behaviour of TMEFF2-negative and TMEFF2-positive prostate cancer cells could also be investigated *in vivo,* by implanting the cells into nude mice and monitoring the development of the tumour within the prostate.

8.3 Proteases involved in TMEFF2 processing

Proteolytic processing of TMEFF2 by enzymes expressed in normal prostate and prostate cancer cells, including membrane-anchored serine proteases (matriptase, matriptase-2, hepsin, prostasin) and ADAMs (ADAM 9, 12, 15A, 15B, 15C) was then analyzed *in vitro* using HEK293 cells over-expressing AP/V5 TMEFF2. In order to compare whether ADAMs and serine proteases cleave TMEFF2 within the same sequence analogous shedding experiments were performed using HEK293 cells expressing AP/V5 $\Delta_{303\text{-}320}$TMEFF2 mutant that is resistant to ADAM-mediated cleavage (Ali & Knäuper 2007). The results presented in Chapter 4 showed that co-expression of AP/V5 TMEFF2 with matriptase and hepsin significantly increased the release of AP-tagged TMEFF2 extracellular domain from the cell surface (Figure 4.10 A). This indicates that membrane-anchored serine proteases are involved in TMEFF2 processing. Interestingly, the release of AP/V5 $\Delta_{303\text{-}320}$TMEFF2 mutant was also elevated in matriptase and hepsin-expressing cells (Figure 4.10 B), suggesting that serine proteases and ADAMs cleave TMEFF2 in different positions. This finding was supported by the Western blot analysis of AP/V5 TMEFF2 C-terminal cleavage products. In the lysates from matriptase or hepsin-expressing cells novel TMEFF2 cytoplasmic fragments were detected in addition to the ~17 kDa ADAM-generated product (Figure 4.11). The molecular mass of C-terminal TMEFF2 fragments detected by Western blotting, as well as the fact that serine protease cleave their substrates after Arg or Lys allowed to propose several cleavage sites which could be accessible to matriptase and hepsin. Comparison of the suggested cleavage sites with TMEFF2 3D structural model (Figure 4.23) allowed the conclusion that the cleavage by matriptase occurs most probably within the sequence linking follistatin-like domains and additionally between the second follistatin module and the EGF-like domain. In contrast, hepsin likely cleaves TMEFF2 between the second follistatin module and the EGF-like domain but closer to the C-terminus of TMEFF2 than matriptase (Figure 4.24 and Figure 8.1 below).

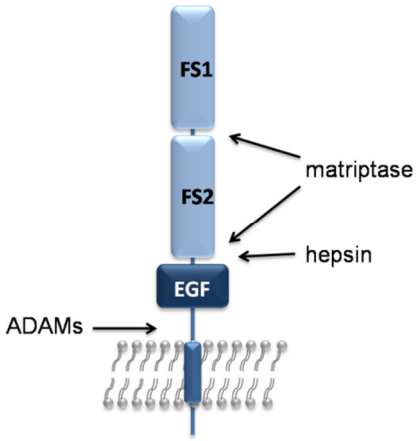

Figure 8.1 Schematic diagram of matriptase, hepsin and ADAM cleavage sites within TMEFF2 structure; FS1 - follistatin-like domain 1, FS2 – follistatin-like domain 2, EGF – EGF-like domain.

The precise determination of the matriptase and hepsin cleavage sites could be investigated by N-terminal sequencing of the 19 kDa, 22 kDa and 27 kDa TMEFF2 fragments detected by Western blotting. The Arg and Lys residues that are recognized by matriptase and hepsin could be identified by performing shedding assays using cells expressing AP/V5 TMEFF2 mutants containing R→A or K→A mutations within the proposed cleavage sites. However, the data presented in Chapter 4 are convincing enough to conclude that TMEFF2 is differentially processed by ADAMs and serine proteases. This processing results in the release of the full length TMEFF2-ECD, as well as fragments containing two follistatin-like modules or the second follistatin-like module and the EGF-like domain. All of these soluble TMEFF2 fragments have potentially different biological activities than the membrane-anchored TMEFF2 and may significantly influence the behaviour of prostate cancer cells. Generation of different soluble TMEFF2 fragments might be responsible for some biological changes described previously for prostate cancer cells over-expressing matriptase or hepsin, such as loss of viability and adhesion of hepsin-positive prostate cancer cells (Srikantan et al. 2002) or increased growth, proliferation and invasion of matriptase-positive prostate cancers cells (Saleem et al. 2006; Bergum & List 2010; Sanders et al. 2006).

AP/V5 TMEFF2 shedding by matriptase-2 and prostasin was also analyzed. Whereas the presence of prostasin did not influence AP/V5 TMEFF2 release, co-expression of matriptase-2 increased AP/V5 TMEFF2 shedding (Figure 4.10 A, Figure 4.16). However, further experiments showed that matriptase-2 increased TMEFF2 release indirectly, more likely through activation of ADAMs as the release of AP/V5 TMEFF2 from matriptase-2 expressing cells was impaired in the presence of metalloproteinase inhibitors (Figure 4.12) and the shedding of AP/V5 $\Delta_{303\text{-}320}$TMEFF2 mutant was not increased by

matriptase-2 (Figure 4.10 B). It was recently published that ADAM-mediated shedding can be regulated by activation of protease-activated receptors (PARs) and one of these receptors, PAR-2 was shown to be activated by matriptase (Abdallah et al. 2010; Takeuchi et al. 2000). The results presented in Chapter 4 suggest that AP/V5 TMEFF2 shedding from matriptase-2-expressing cells may be regulated by a similar mechanism. This hypothesis requires further verification, for example by performing shedding experiments in the presence of G protein-coupled receptor inhibitors, such as pertussis toxin. This exotoxin produced by *Bordetella pertussis* covalently modifies the α-subunit of G_i proteins and prevents the G-proteins from interacting with G protein-coupled receptors on the cell membrane (Burns 1988). The mechanism of TMEFF2 shedding in the presence of matriptase-2 could be also investigated using more specific, synthetic agonists and antagonists of PAR-2 (Lohman et al. 2012; Suen et al. 2012).

Shedding of TMEFF2 was also investigated by over-expression of ADAMs implicated in prostate cancer progression, including ADAM 9, ADAM 12 and three splice variants of ADAM 15: ADAM15A, ADAM15B and ADAM15C. Whereas expression of ADAM 9 and 12 in AP/V5 TMEFF2 HEK293 increased TMEFF2 shedding, none of the tested ADAM15 variants influenced AP/V5 TMEFF2 release (Figure 4.18). Interestingly, the level of AP/V5 TMEFF2 shedding was higher in cells expressing matriptase or hepsin when compared with ADAM-transfected cells, suggesting that serine proteases are more efficient TMEFF2 sheddases than ADAMs.

In addition to the proteases investigated in this thesis as potential TMEFF2 sheddases, there are other transmembrane enzymes expressed by prostate cancer cells which should be considered as TMEFF2 regulators. One of these proteases is TMPRSS2, a TTSP family member encoded by the *Tmprss2* gene (Lin, Ferguson, White, Wang, et al. 1999). It is believed, that *Tmprss2* gene contributes to prostate cancer progression in two distinct ways. First, it was shown by several groups that the 5' untranslated region of the *Tmprss2* gene, containing androgen-responsive elements, is frequently fused to coding sequences of transcription factors of the ETS family, making their expression androgen-inducible (Soller et al. 2006). Second, *Tmprss2* gene expression was found to be significantly upregulated in androgen-dependent prostate cancer compared to normal prostate epithelium or benign prostatic hyperplasia (Lin, Ferguson, White, Wang, et al. 1999; Vaarala et al. 2001). Another TTSP that might be involved in TMEFF2 processing is matriptase-3. This recently discovered member of the matriptase subfamily is characterized by high sequence homology with matriptase and significant expression in brain, skin, reproductive and oropharyngeal tissues (Szabo et al. 2005). Among proteases expressed by prostate cancer cells that should be investigated as potential TMEFF2 sheddases is also ADAM8, a catalytically active ADAM associated with unfavourable prognosis of prostate cancer (Fritzsche et al. 2006).

8.4 Investigating the biological activity of soluble TMEFF2 fragments

The next step was to investigate the physiological significance of TMEFF2 processing by serine proteases and ADAMs and to describe the biological role of soluble TMEFF2 fragments generated by these enzymes. For that reason recombinant TMEFF2 fragments corresponding to predicted cleavage products were expressed in *E. coli* (Chapter 5) and then in mammalian cells (Chapter 6). The *E. coli* expression system allowed to efficiently produce and purify recombinant EGF-like domain from TMEFF2, $^{H\text{-}R}$EGF-like domain TMEFF2 mutant and EGF-like domain from HB-EGF which served as a positive control in ERK1/2 phosphorylation experiments (Figure 5.10). Several proteins containing EGF-like domains display their biological activity through ErbB receptors. Activation of ErbBs can be measured by assessing the relative levels of the phosphorylated downstream kinases ERK1 and ERK2 (Ratan et al. 2003). To investigate whether the EGF-like domain from TMEFF2 acts as a ligand for ErbBs, purified recombinant EGF-like domains were tested *in vitro* in an ERK1/2 phosphorylation assay, using the normal prostate epithelial cell line PNT2-C2. Whereas PNT2-C2 cells responded to the EGF-like domain from HB-EGF treatment with ERK1/2 phosphorylation (Figure 5.12), none of the TMEFF2 EGF-like fragments (neither the EGF-like domain, nor the $^{H\text{-}R}$EGF-like domain mutant) induced phosphorylation of ERK1/2 (Figure 5.13, Figure 5.14). The lack of ERK1/2 phosphorylation in response to TMEFF2 EGF-like domain treatment suggested that TMEFF2 does not act through ErbB receptors. This finding is in agreement with some of the published data, indicating that TMEFF2 interacts with none of the ErbB receptors (Lin et al. 2011). However, there are some reports showing weak activation of ErbB-4 and EGFR by soluble TMEFF2-ECD (Uchida et al. 1999; Ali & Knäuper 2007). The lack of ErbBs activation by the TMEFF2 EGF-like domain reported in this thesis might be caused by the chosen expression system that impairs the function of TMEFF2 EGF-like domain. Expression of mammalian proteins in prokaryotic cells results in the lack of glycosylation that may significantly affect biological function of TMEFF2 EGF-like domain. As shown by Glynne-Jones et al. the glycosylation represents about 40% of the total TMEFF2 molecular mass (Glynne-Jones et al. 2001) so it was hypothesized that the glycosylation plays important role in determining TMEFF2 biological activity. Activation of ERK1/2 in cells treated with an EGF-like domain from HB-EGF, also produced in *E. coli* may depend only on the amino-acid sequence and do not require glycosylation.

Larger TMEFF2 fragments, including TMEFF2-ECD, 2xFS and ^{2nd}FS+EGF were also expressed in *E. coli* but did not fold properly, forming large, dysfunctional polymers (Figure 5.15). As mentioned in the Introduction, the structure of TMEFF2 is stabilized by several disulphide bonds, making the production of recombinant TMEFF2 fragments in prokaryotic cells very challenging, although *E. coli* strains enhancing disulphide bonds formation were used. In order to ensure proper folding and glycosylation of TMEFF2

fragments corresponding to matriptase, hepsin and ADAM-cleavage products, the proteins were expressed in mammalian cells.

Expression of recombinant TMEFF2 fragments in mammalian cells involved generation of a stable CHO cell line expressing TMEFF2-ECD tagged on the C-terminus with Fc fragment from human IgG_1 (Figure 6.1) and four CHO cell lines stably expressing TMEFF2-ECD, 2xFS, ^{2nd}FS+EGF and EGF-like domain tagged on the N-terminus with protein A (Figure 6.2). Production of two different TMEFF2-ECD variants, with tags located on the opposing ends of the proteins was performed in order to compare whether the tag location influences the protein activity.

TMEFF2-ECD-Fc was efficiently purified from the CHO conditioned medium using a two step purification process. However, due to proteolytic processing, the obtained protein was a mixture of at least three different TMEFF2-ECD-Fc species (Figure 6.8, Figure 6.9). In order to avoid TMEFF2-ECD-Fc proteolysis during future purifications, PMSF, EDTA and/or protease inhibitor cocktail should be present in the collected CHO conditioned medium. The purified TMEFF2-ECD-Fc species were then used to test its activity *in vitro*. First, the potential of the TMEFF2-ECD-Fc to induce ERK1/2 phosphorylation was examined using HEK293 and PNT2-C2 cell lines. HEK293 cells were chosen for this investigation because it was published previously that they phosphorylate ERK1/2 in response to recombinant TMEFF2-ECD treatment (Ali & Knäuper 2007). Activation of ErbB signaling by TMEFF2-ECD was also demonstrated using MKN28 gastric cells (Uchida et al. 1999). However, treatment of HEK293 and PNT2-C2 cell lines with 0.1 - 5.0 µg/ml of recombinant TMEFF2-ECD-Fc did not induce ERK1/2 phosphorylation (Figure 6.10, Figure 6.11). The disagreement between the obtained result and the published data might result from the different expression and purification methods used to obtain TMEFF2-ECD. In the published study HEK293 cells were treated with TMEFF2-ECD expressed in mammalian cells as V5-tagged recombinant protein and purified in a single step process by affinity chromatography using anti-V5 agarose (Ali & Knäuper 2007). Due to the shorter purification process it is possible that not all impurities were removed from the TMEFF2-ECD and the phosphorylation of ERK1/2 were induced by additional proteins present in the sample. The two-step purification method described in Chapter 6 obtained only TMEFF2-ECD-Fc species as no additional components were observed using silver stained SDS-PAGE gel (Figure 6.8). Another possibility, explaining ErbB activation by V5-tagged TMEFF2-ECD but not TMEFF2-ECD-Fc is that the large Fc-tag on the C-terminus hinders the interaction of TMEFF2-ECD-Fc with the receptor. However, in the study describing TMEFF2-ECD interaction with PDGF-AA the presence of the Fc-tag did not impair binding of TMEFF2-ECD to PDGF-AA (Lin et al. 2011). To summarize, the published data together with the results described in this thesis strongly suggest that TMEFF2 does not signal through ErbB receptors and ERK1/2 kinases,

despite the presence of the EGF-like domain within TMEFF2-ECD structure. The lack of ErbB activation by TMEFF2 EGF-like domain could explained by its atypical amino acid structure. In contrast to ErbB ligands, EGF-like domain from TMEFF2 contains His39 instead of Arg39 (Horie et al. 2000) and this amino acid substitution was shown to dramatically reduce the affinity of the EGF-like domains to ErbBs (D. A. Engler et al. 1990). The inability to activate ErbBs by the TMEFF2 EGF-like domain suggests that this part of TMEFF2 has some non-signaling functions in prostate cancer environment. One of the possible functions of the TMEFF2 EGF-like domain within the TMEFF2 structure is serving as a binding site for TMEFF2 interaction partners. This prediction is supported by the fact that the EGF-like domain from TMEFF1 is involved in TMEFF1 interaction with matriptase (Ge et al. 2006).

In addition to the ERK1/2 phosphorylation assay, the biological activity of purified TMEFF2-ECD-Fc was examined using proliferation assays and prostate epithelial cells. The preliminary results obtained from measuring the number of viable PNT2-C2 cells cultured in the presence of 0.1-5.0 µg/ml of TMEFF2-ECD-Fc indicated, that PNT2-C2 cells grew faster than control cells when 0.1 and 1.0 µg/ml of TMEFF2-ECD-Fc was added to the medium (Figure 6.12). This result is in agreement with previously published data describing TMEFF2-ECD as a growth-promoting factor. Chen and co-workers showed that the conditioned medium from HEK293 cells expressing soluble TMEFF2-ECD had growth promoting activity on HEK293 as well as benign human prostatic RWPE1 cell line (Chen et al. 2011). The recombinant TMEFF2-ECD was also reported to increase proliferation of HEK293 cells (Ali & Knäuper 2007) and act as a survival factor for primary cultured neurons (Horie et al. 2000).

In addition to the TMEFF2-ECD-Fc, the mammalian expression system was used to produce recombinant TMEFF2 fragments tagged on the N-terminus with protein A. Unfortunately, due to the low expression levels, co-purification of serum-derived IgG and limited time the N-protein A TMEFF2-ECD could not be purified to homogeneity. Additionally, the purification of Fc-TMFF2-ECD indicated that the expression of TMEFF2 fragments in CHO cells resulted in proteolytic cleavage of recombinant protein as evidenced by the presence of different molecular mass fragments in the conditioned medium. For that reason the conditioned media from stable cell lines expressing N-protein A fusion proteins were used in a preliminary experiment to investigate the possible influence of TMEFF2 cleavage products on cell proliferation. The results indicated that the presence of TMEFF2-ECD and 2xFS fragments in conditioned medium decreased the proliferation of CHO cells, whereas the addition of EGF-like domain or FS+EGF TMEFF2 fragments did not influence cell proliferation (Figure 6.17). Decreased proliferation rates of CHO cells grown in the presence of TMEFF2-ECD and 2xFS fragments could be explained based on the finding published by Lin and co-workers (Lin et al. 2011), showing

that the presence of the first FS domain (or both FS domains) is required for interaction between TMEFF2 and PDGF-AA growth factor. Thus, it is possible that the TMEFF2-ECD and 2xFS fragments present in the culture medium bind and neutralize some growth factors that are required for CHO proliferation. Binding of these growth factors is more likely mediated through the FS domains of TMEFF2.

8.5 Potential biological functions of soluble TMEFF2 fragments

The presence of the two FS domains within TMEFF2 structure allows the classification of TMEFF2 to the family of follistatin-related proteins. This family consists of follistatin, follistatin-like 1 (Fstl1) protein, TMEFF1, SPARC (secreted protein, acidic and rich in cysteine, also known as osteonectin or BM-40), agrin and large multidomain proteins WFIKKN1 and WFIKKN2 (Phillips & de Kretser 1998; Liepinsh et al. 2006; Kondás et al. 2008). Members of the follistatin-related protein family contain one up to nine FS modules. The FS domain has structural homology to EGF as the positioning of the backbone structure as well as the cysteine residues is partially maintained until the fourth cysteine unit. There are also important structural similarities between FS module and the Kazal family of enzyme inhibitors but none of the known follistatin-like proteins was found to possess an inhibitory activity (Phillips & de Kretser 1998). Comparison of the TMEFF2 FS domains sequences with the other follistatin-like proteins revealed significant structural similarities between TMEFF2 and agrin. The FS domains of TMEFF2 and agrin share 38.4% sequence identity and a region containing two putative glycosaminoglycan attachment sites is seen in both proteins (Horie et al. 2000). Agrin is a large proteoglycan expressed as two isoforms resulting from differential transcription. Both agrin isoforms are composed of the N-terminal part with nine FS and two laminin EGF-like domains, the middle region with a SEA (*sea* urchin sperm protein, enterokinase, and agrin) module and the C-terminal part containing four EGF and three laminin globular domains (Godfrey et al. 1984; Patthy & Nikolics 1993; Bork & Patthy 1995). The laminin globular domains are known to activate signaling pathways that regulate synaptic differentiation (Bezakova & Ruegg 2003). Until recently little was known about the function of the N-terminal part of agrin that contains the FS modules. In 2010 Bányai and co-workers used a surface plasmon resonance spectroscopy and a luciferase reporter assay to show that the N-terminal fragment of agrin binds to bone morphogenic factor-4 (BMP-4), BMP-6 and TGF-β1 with relatively high affinity, modulating their activity. Interaction with agrin inhibits the activity of BMP-4 and BMP-6 but enhances the activity of TGF-β1 (Bányai et al. 2010).

BMPs and TGF- β1 are classified to the TGF-β superfamily of growth factors. Members of this superfamily bind to type I and type II receptors that form heterotetrameric complexes and activate downstream signaling. In humans and other mammals five type I receptors and seven type II receptors for TGF-β proteins were described to date

(Moustakas & Heldin 2009). All these receptors contain a cytoplasmic serine/threonine kinase domain. Ligand binding links the constitutively active type II receptor to the dormant type I receptor, leading to the phosphorylation of the juxtamembrane part of the type I receptor by the type II receptor kinases. TGF-β1 interacts specifically with TβR-II type II receptor which associates with and activate TβR-I type I receptor. Type I receptor kinases transmit the signal by phosphorylating receptor-regulated Smad proteins (R-Smads) which in the "canonical" signaling pathway are Smad2 and Smad3. Phosphorylated R-Smads associate with common-mediator Smad (Co-Smad) – Smad4 and the R-Smad/Co-Smad complexes move into the nucleus where they regulate the expression of targeted genes, in the co-operation with other transcription factors, co-activators and co-repressors (Miyazono 2000; Miyazono et al. 2001; Miyazawa et al. 2002; Moustakas & Heldin 2009; Heldin & Moustakas 2012). BMPs bind type II (BMPRII, ActRIIA, ActRIIB) and type I (ALK3, ALK6) receptors and also signal through Smad proteins. However, in contrast with TGF-β1, BMPs activate the "noncanonical" signaling pathway, where the activation of the type I receptors by type II receptors leads to phosphorylation of Smad1, Smad5 and Smad8 (R-Smads) which then associate with Smad4 (Co-Smad). R-Smad/Co-Smad complexes translocate to the nucleus and regulate transcription of BMP-dependent genes. The BMP pathway can be antagonized by Smad6 and Smad7 (Moustakas & Heldin 2009). Schematic diagrams of "canonical" and "noncanonical" signaling pathways activated by TGF-β superfamily members are shown in Figure 8.2

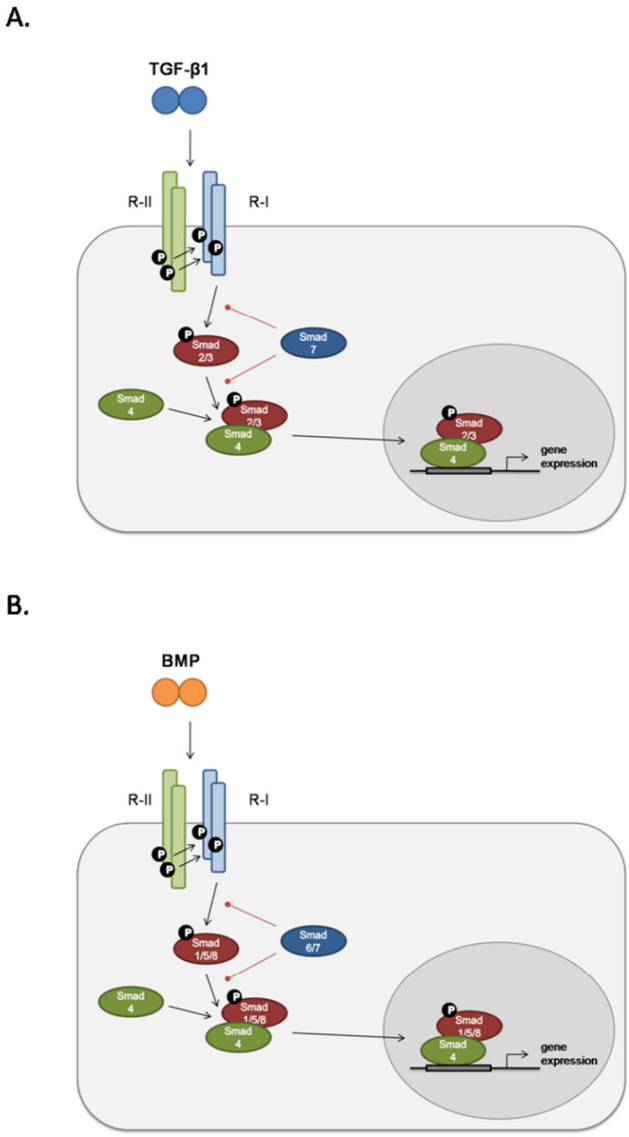

Figure 8.2. Schematic diagram of TGF-β1 (A) and BMPs (B) signaling.

Members of the TGF-β superfamily of growth factors transmits their biological signal into the cell through interaction with type II (R-II) and type I (R-I) serine/threonine kinase receptors. Upon ligand binding constitutively active type II receptors recruit and phosphorylate type I receptors. Type I receptors then activate receptor-regulated Smad proteins (R-Smads, indicated in red). In TGF-β1 signaling pathway ("canonical", A) type I receptors activate Smad 2/3, whereas in BMP pathway ("noncanonical", B) – Smad 1/5/7. R-Smads then associate with a common-mediator Smad (Co-Smad, indicated in green) – Smad4. The R-Smad/Co-Smad complexes move into the nucleus and regulate the expression of targeted genes. Smad signaling can be antagonized an inhibitory Smads (I-Smad, indicated in blue) – Smad7 and/or Smad7.

Due to the high structural homology of FS domains from TMEFF2 and agrin it could be hypothesized that the extracellular part of TMEFF2 interacts with growth factors from the TGF-β superfamily and modulates their function. Moreover, interaction with TGF-β1 or BMPs seems to be a common feature of proteins containing FS modules. Follistatin-like 1 (Fstl1) protein contains single FS module that interacts with BMP-4 as well as its type II receptor in the lung. The antagonistic effect of Fstl1 on BMP-4 signaling is important during lung development (Geng et al. 2011). WFIKKN1 and WFIKKN2 interact through their FS domains with BMP-2, BMP-4 and TGF-β1 as well as other members of the TGF-β superfamily – growth and differentiation factor 8 (GDF8) and GDF11. Interestingly, a luciferase reporter assay showed that the interaction with WFIKKN1 and WFIKKN2 inhibits biological activity of GDF8 and GDF11 but not BMP-2, BMP-4 and TGF-β1 (Kondás et al. 2008; Szláma et al. 2010). In order to investigate whether the extracellular part of full length, transmembrane TMEFF2 is able to bind and regulate the activity of TGF-β superfamily members, a future analysis should focus on phosphorylation of type I receptors and R-Smads upon stimulation with TGF-β1, BMPs or GDFs, in the cells with or without TMEFF2 expression. In addition, a luciferase reporter assay should be performed to investigate the expression of TGF-β1, BMPs or GDFs-dependent genes in the presence or absence of TMEFF2. The role of soluble TMEFF2 fragments generated by ADAMs or serine proteases could be analyzed in analogous phosphorylation assays, performed using cells co-expressing TMEFF2 and the sheddase.

The biological role of TMEFF2 might be similar to the function of its homologue, TMEFF1. These two proteins share 35.8% identity at the amino acid level, as well as some important structure similarities including the domain structure of the extracellular part, the presence of His39 within the EGF-like domain (Horie et al. 2000). TMEFF1 has been implicated in modulating another signaling cascade involving members of the TGF-β superfamily, the activin/Nodal pathway, regulating the left-right axis formation during early vertebrate development (Schier & Shen 2000). In this pathway binding of the ligand induces formation of a complex between the constitutively active type II receptor and the type I receptor ALK (activin receptor-like kinase) 4 and 7. As a result, the type I receptor is activated by phosphorylation. The activated ALK phosphorylates Smad2 and Smad3, which forms a heterotrimeric complex with Smad4, translocates to the nucleus to regulate gene expression, in conjunction with other transcription factors. Activin and Nodal use the same type II and type I receptors. However, Nodal also requires a membrane associated coreceptor Cripto (Massagué 1998). Although Cripto members are not required for activin signaling, overexpression of Cripto does influence activin activity by repressing the signal pathway (Gray et al. 2003). The schematic diagram of activin/Nodal signaling is presented in Figure 8.3.

As shown by Harms and Chang, TMEFF1 is an important regulator of Nodal signaling as it binds Cripto and prevents its interaction with Nodal. TMEFF1 does not interact with either Nodal or ALK4 (Harms & Chang 2003). It has not been investigated to date if TMEFF2 is also able to regulate Nodal/activin signalling through binding of Cripto. Thus, future investigations should focus on co-immunoprecipitation of TMEFF2 with Cripto, Nodal, ALK4 or ALK7 and analysis of downstream signaling molecules such as phosphorylated Smad2 and Smad3. The direct influence of TMEFF2 on Nodal-regulated gene expression could be analyzed using luciferase reporter assay.

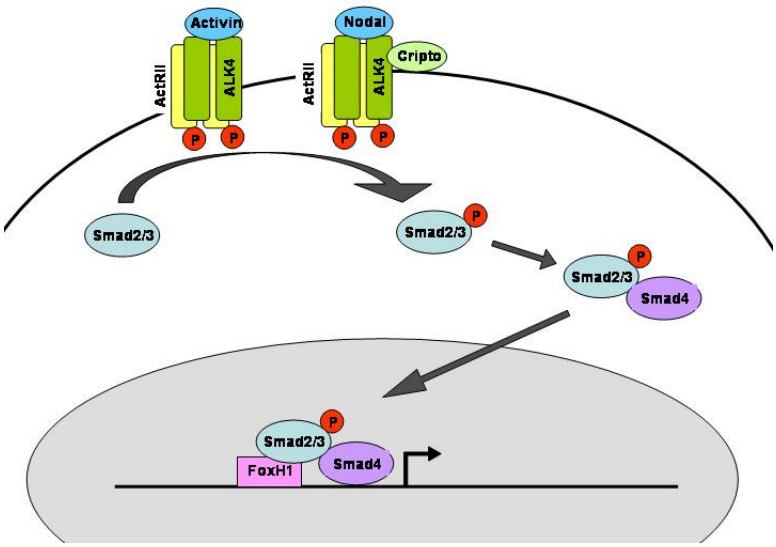

8.3 Schematic diagram of the activin/Nodal signaling (from http://www.cisreg.ca/tfe/)

Nodal interacts with activin receptors (ActRIIB,ALK4) and co-receptor protein Cripto. The activated receptor phosphorylates Smad2 or Smad3 and allows its association with Smad4. The Smad2/3/4 complex translocates to the nucleus where it binds to FoxH1transcription factor and regulates a spectrum of target gene expression. Activin triggers the same signaling without requirement of Cripto coreceptor.

Finally, TMEFF2 might be also involved in regulation of platelet-derived growth factors (PDGFs), similarly to other follistatin-related proteins. As shown by Raines and co-workers, SPARC is able to specifically interact with PDGF-B chain which prevents binding of PDGF-AB and BB to their cell surface receptors. This mechanism is thought to regulate the activity of specific PDGF isoforms in vascular injury, because the expression of both SPARC and PDGF-B chain is minimal in normal tissue and increases upon injury (Raines et al. 1992). The data published by Raines did not show if the FS domain is involved in the SPARC-PDGF-B chain binding. It could be hypothesized that the FS domains participates in SPARC-PDGF-B interaction as it was demonstrated recently that the FS domain of TMEFF2 binds PDGF-AA (Lin et al. 2011).

To summarize, analysis of the biological function of proteins structurally related to TMEFF2 allows the prediction that the extracellular part of TMEFF2 as well as soluble TMEFF2 fragments containing FS modules might be involved in the regulation of several signaling cascades, including TGF-β, PDGF and Nodal/activin signaling. It will be a matter of future investigation to determine which of these signaling pathways are regulated by TMEFF2 in prostate cancer cells and how this regulation influences the development and progression of prostate cancer.

8.6 Shedding of TMEFF2 in the presence of PDGF-AA

It was shown recently that the extracellular part of TMEFF2 interacts with a multifunctional cytokine PDGF-AA and prevents binding of PDGF-AA to its receptor, PDGFRα (Lin et al. 2011). In order to investigate if the interaction with PDGF-AA influences TMEFF2 shedding, the release of AP/V5 TMEFF2 in the presence of PGDF-AA was analyzed. Overnight treatment of AP/V5 TMEFF2 HEK293 cells with different concentrations of recombinant PDGF-AA did not influence AP/V5 TMEFF2 release, whether PDGFRα was expressed in the cells or not (Figure 4.21). Surprisingly, when AP/V5 TMEFF2 HEK293 cells were treated with PDGF-AA for 1 hour, the shedding was significantly reduced in a dose-dependent manner. This effect was however observed only in cells lacking PDGFRα expression (Figure 4.22), suggesting that the affinity of PDGF-AA is higher for the receptor than for TMEFF2. It could be speculated that decreased TMEFF2 release from PDGF-AA-treated cells results from the internalisation of the AP/V5 TMEFF2-PDGF-AA complex and down-regulation of cell surface AP/V5 TMEFF2 available for shedding. It is also possible that PDGF-AA binding to TMEFF2 masks the ADAM cleavage site and prevents TMEFF2 ectodomain shedding. The two possible scenarios could be investigated in the future, for example by immunolabeling of TMEFF2 and PDGF-AA followed by confocal microscopy analysis of their co-localization in the cell. This analysis should be complemented with PDGF-AA binding assays described by Lin

and co-workers (Lin et al. 2011) using immobilised $\Delta_{303-320}$TMEFF2 mutant and soluble PDGF-AA. The lack of PDGF-AA- $\Delta_{303-320}$TMEFF2 interaction would suggest that PDGF-AA binds to TMEFF2 within the sequence recognized by ADAMs, preventing TMEFF2 ectodomain shedding.

8.7 The fate of TMEFF2 cytoplasmic domain following ectodomain cleavage

The main part of this thesis describes the expression, purification and investigation of the biological function of extracellular TMEFF2 fragments that are released from the cell surface by ADAMs and serine proteases. However, the proteolytic processing of TMEFF2 generates also cytoplasmic fragment(s) that may play important biological functions inside cancer cells. To date, the knowledge about the fate of TMEFF2 cytoplasmic domain is very limited. It is known from the literature data that the membrane-retained stub of TMEFF2, generated by ADAMs is a substrate for the γ-secretase complex (Ali & Knäuper 2007). The cellular localization as well as the biological role of TMEFF2 cytoplasmic domain was not further investigated. The results presented in Chapter 7 focus on investigating the fate of TMEFF2 C-terminal fragments, generated by matriptase and hepsin. First, the intracellular expression pattern of TMEFF2 was compared with the expression of HB-EGF using immunolabeling and confocal microscopy. This analysis revealed that the trafficking of TMEFF2 and HB-EGF cytoplasmic domains differs significantly (Figure 7.4). In the absence of PMA both proteins were present on the cell surface and translocated to the cytoplasm upon PMA-mediated shedding induction. However, PMA-treatment of AP/V5 HB-EGF-expressing cells caused endocytosis of V5-tagged HB-EGF-C and accumulation of V5-positive endocytotic vesicles around the nucleus, which confirms previously published data (Hieda et al. 2008). V5-tagged cytoplasmic domain of HA/V5 TMEFF2 translocates from the cell membrane into the cytoplasm but did not localize in endocytotic structures. Comparison of HB-EGF and TMEFF2 trafficking indicated that the cytoplasmic domain of TMEFF2 does not translocate to the nuclear membrane via endocytotic vesicles pathway.

Trafficking of HB-EGF-ICD to the nuclear membrane is a very unique mechanism of protein translocation to the nucleus. More common trafficking pathway for cytoplasmic domains regulating gene expression is translocation from the cytoplasm into the nucleus through nuclear pores. Cytoplasmic domains of Notch receptor, EpCAM and ErbB-4, following γ-secretase processing, translocate to the nucleus through the pores (Artavanis-Tsakonas et al. 1995; Maetzel et al. 2009; Ni et al. 2001). To investigate the possibility, that the intracellular part of TMEFF2 is transported into the nucleus via nuclear pores, the localization of TMEFF2 fragments in the nucleus was examined by cell fractionation. Analysis of the cytoplasmic and nuclear fraction from AP/V5 TMEFF2 expressing cells

revealed the presence of the ADAM-generated membrane stub in the cytoplasmic but not in the nuclear fraction (Figure 7.8). The TMEFF2-ICD was detected neither in the cytoplasm nor in the nuclear fraction, even when the cells were pre-treated with a nuclear export inhibitor leptomycin B (LMB), suggesting the degradation of TMEFF2-ICD following γ-secretase processing. Based on confocal analysis of TMEFF2-ICD localization as well as the cell fractionation data it was concluded that TMEFF2-ICD does not translocate to the nucleus.

The fate of TMEFF2 cytoplasmic fragments generated by ADAMs, matriptase and hepsin was then analyzed in cells treated with the γ-secretase inhibitor DAPT. This analysis confirmed that the γ-secretase complex is involved in TMEFF2 processing following ADAM-mediated shedding (Figure 7.5) and showed that the C-terminal products of matriptase and hepsin cleavage are not further processed by the γ-secretase (Figure 7.9). Analysis of the cells treated with proteasome inhibitor epoxomicin showed that the C-terminal products of TMEFF2 cleavage by ADAM, serine proteases and γ-secretase complex are most likely degraded. Pre-treatment with epoxomicin significantly increased amounts of these fragments in cell lysates (Figure 7.10). Degradation of the cytoplasmic domain following γ-secretase processing is a mechanism of removing unnecessary fragments of transmembrane proteins where the biological function of transmembrane protein depends entirely on its ectodomain. An example of such protein is the IL-6 receptor (IL-6R). The membrane-attached as well as soluble ectodomain of IL-6R plays important roles in IL-6 signaling, whereas the cytoplasmic domain undergo lysosomal degradation following ectodomain release (Chalaris et al. 2010).

The data regarding the fate of TMEFF2 cytoplasmic fragments require further verification during biochemical analysis in the presence of other inhibitors of protein degradation, such as lactacystin (Tomoda & Omura 2000), or immunocolocalization of TMEFF2 C-terminus and proteasomal or lysosomal markers. Confirmation of the results described in this thesis would indicate that the biological function of TMEFF2 depends on its ectodomain. However, it might be speculated that the degradation of TMEFF2 C-terminal fragments has some biological meaning, for example by disrupting TMEFF2 interactions with its intracellular binding partners. To date the only known binding partner of TMEFF2 C-terminus is SARDH (Chen et al. 2011), an enzyme catalyzing dehydrogenation of sarcosine to glycine (Porter et al. 1985). The interaction of TMEFF2 with SARDH reduces cytoplasmic sarcosine levels, probably by enhancing the enzymatic activity of SARDH (Chen et al. 2011). Elevated sarcosine levels in the cytoplasm correlate with aggressive phenotype of prostate cancer, indicating that sarcosine might be a novel marker of prostate cancer progression (Sreekumar et al. 2009; Dahl et al. 2011). The correlation between TMEFF2 expression and decreased sarcosine levels in prostate cancer cells suggests that the full-length TMEFF2 inhibits invasiveness of prostate cancer

cells. Hypothetically, shedding of TMEFF2 by ADAMs or serine proteases followed by the degradation of TMEFF2 cytoplasmic domain would disrupt the TMEFF2-SARDH interaction, increase the accumulation of sarcosine in the cytoplasm, supporting the invasive phenotype of prostate cancer cell. For that reason the investigation of the biological consequences of TMEFF2-SARDH binding as well as the role of proteolysis in regulating this interaction will be an interesting part of the future investigation of TMEFF2 biological function in prostate cancer.

To summarize, the data presented in this thesis showed for the first time that TMEFF2, a transmembrane protein expressed in normal prostate and prostate cancer cells is proteolytically processed by at least two groups of cell surface enzymes: type II transmembrane serine proteases (matriptase and hepsin) and ADAMs (ADAM9, ADAM12). This processing results in the generation of several soluble TMEFF2 fragments that have potentially different function in prostate cancer environment. The biological role of these fragments is more likely dependent on the presence of the follistatin-like domain. Future experiments will focus on deciphering the signaling pathways regulated by soluble TMEFF2 cleavage products in prostate cancer cells as well as determination if the differential processing by ADAMs and TTSPs might be a general regulatory mechanism, involved in modulating the function of other transmembrane proteins.

Bibliography:

Abdallah, R.T. et al., 2010. Plasma kallikrein promotes epidermal growth factor receptor transactivation and signaling in vascular smooth muscle through direct activation of protease-activated receptors. *The Journal of biological chemistry*, 285(45), pp.35206–15.

Abram, C.L. et al., 2003. The adaptor protein fish associates with members of the ADAMs family and localizes to podosomes of Src-transformed cells. *The Journal of biological chemistry*, 278(19), pp.16844–51.

Adachi, M. et al., 2001. Activation of epithelial sodium channels by prostasin in Xenopus oocytes. *Journal of the American Society of Nephrology : JASN*, 12(6), pp.1114–21.

Afar, D.E. et al., 2001. Catalytic cleavage of the androgen-regulated TMPRSS2 protease results in its secretion by prostate and prostate cancer epithelia. *Cancer research*, 61(4), pp.1686–92.

Afar, D.E.H. et al., 2004. Preclinical validation of anti-TMEFF2-auristatin E-conjugated antibodies in the treatment of prostate cancer. *Molecular cancer therapeutics*, 3(8), pp.921–32.

Ahmed, S. et al., 2006. Identification of membrane-bound serine proteinase matriptase as processing enzyme of insulin-like growth factor binding protein-related protein-1 (IGFBP-rP1/angiomodulin/mac25). *The FEBS journal*, 273(3), pp.615–27.

Akerström, B., Nielsen, E. & Björck, L., 1987. Definition of IgG- and albumin-binding regions of streptococcal protein G. *The Journal of biological chemistry*, 262(28), pp.13388–91.

Al-Fakhri, N. et al., 2003. Increased expression of disintegrin-metalloproteinases ADAM-15 and ADAM-9 following upregulation of integrins alpha5beta1 and alphavbeta3 in atherosclerosis. *Journal of cellular biochemistry*, 89(4), pp.808–23.

Al-Hajj, M. et al., 2003. Prospective identification of tumorigenic breast cancer cells. *Proceedings of the National Academy of Sciences of the United States of America*, 100(7), pp.3983–8.

Ali, N. & Knäuper, V., 2007. Phorbol ester-induced shedding of the prostate cancer marker transmembrane protein with epidermal growth factor and two follistatin motifs 2 is mediated by the disintegrin and metalloproteinase-17. *The Journal of biological chemistry*, 282(52), pp.37378–88.

Amour, A. et al., 2002. The enzymatic activity of ADAM8 and ADAM9 is not regulated by TIMPs. *FEBS letters*, 524(1-3), pp.154–8.

Andriopoulos, B. et al., 2009. BMP6 is a key endogenous regulator of hepcidin expression and iron metabolism. *Nature genetics*, 41(4), pp.482–7.

Antalis, T.M. et al., 2010. The cutting edge: membrane-anchored serine protease activities in the pericellular microenvironment. *The Biochemical journal*, 428(3), pp.325–46.

Armstrong, P.B. & Quigley, J.P., 1999. Alpha2-macroglobulin: an evolutionarily conserved arm of the innate immune system. *Developmental and comparative immunology*, 23(4-5), pp.375–90.

Artavanis-Tsakonas, S., Matsuno, K. & Fortini, M.E., 1995. Notch signaling. *Science (New York, N.Y.)*, 268(5208), pp.225–32.

Asakura, M. et al., 2002. Cardiac hypertrophy is inhibited by antagonism of ADAM12 processing of HB-EGF: metalloproteinase inhibitors as a new therapy. *Nature medicine*, 8(1), pp.35–40.

Atfi, A. et al., 2007. The disintegrin and metalloproteinase ADAM12 contributes to TGF-beta signaling through interaction with the type II receptor. *The Journal of cell biology*, 178(2), pp.201–8.

Babitt, J.L. et al., 2006. Bone morphogenetic protein signaling by hemojuvelin regulates hepcidin expression. *Nature genetics*, 38(5), pp.531–9.

Baker, A.H., Edwards, D.R. & Murphy, G., 2002. Metalloproteinase inhibitors: biological actions and therapeutic opportunities. *Journal of cell science*, 115(Pt 19), pp.3719–27.

Baneyx, F. & Mujacic, M., 2004. Recombinant protein folding and misfolding in Escherichia coli. *Nature biotechnology*, 22(11), pp.1399–408.

Bányai, L., Sonderegger, P. & Patthy, L., 2010. Agrin binds BMP2, BMP4 and TGFbeta1. *PloS one*, 5(5), p.e10758.

Basel-Vanagaite, L. et al., 2007. Autosomal recessive ichthyosis with hypotrichosis caused by a mutation in ST14, encoding type II transmembrane serine protease matriptase. *American journal of human genetics*, 80(3), pp.467–77..

Bazil, V. & Strominger, J., 1994. Metalloprotease and serine protease are involved in cleavage of CD43, CD44, and CD16 from stimulated human granulocytes. Induction of cleavage of L-selectin via CD16. *Journal of immunology*, 152(3), pp.1314–22.

Beck, V. et al., 2005. ADAM15 decreases integrin alphavbeta3/vitronectin-mediated ovarian cancer cell adhesion and motility in an RGD-dependent fashion. *The international journal of biochemistry & cell biology*, 37(3), pp.590–603.

Becker, J.C. et al., 1991. Shedding of ICAM-1 from human melanoma cell lines induced by IFN-gamma and tumor necrosis factor-alpha. Functional consequences on cell-mediated cytotoxicity. *Journal of immunology (Baltimore, Md. : 1950)*, 147(12), pp.4398–401.

Béliveau, F. et al., 2011. Essential role of endocytosis of the type II transmembrane serine protease TMPRSS6 in regulating its functionality. *The Journal of biological chemistry*, 286(33), pp.29035–43.

Benaud, C. et al., 2002. Sphingosine 1-phosphate, present in serum-derived lipoproteins, activates matriptase. *The Journal of biological chemistry*, 277(12), pp.10539–46.

Benaud, C.M. et al., 2002. Deregulated activation of matriptase in breast cancer cells. *Clinical & experimental metastasis*, 19(7), pp.639–49.

Benson, M.C. et al., 1992. The use of prostate specific antigen density to enhance the predictive value of intermediate levels of serum prostate specific antigen. *The Journal of urology*, 147(3 Pt 2), pp.817–21.

Bergum, C. et al., 2012. Strong expression association between matriptase and its substrate prostasin in breast cancer. *Journal of cellular physiology*, 227(4), pp.1604–9.

Bergum, C. & List, K., 2010. Loss of the matriptase inhibitor HAI-2 during prostate cancer progression. *The Prostate*, 70(13), pp.1422–8.

Bertram, J. et al., 2006. Inhibition of the phosphatidylinositol 3'-kinase pathway promotes autocrine Fas-induced death of phosphatase and tensin homologue-deficient prostate cancer cells. *Cancer research*, 66(9), pp.4781–8.

Bertram, L., Lill, C.M. & Tanzi, R.E., 2010. The genetics of Alzheimer disease: back to the future. *Neuron*, 68(2), pp.270–81.

Bezakova, G. & Ruegg, M.A., 2003. New insights into the roles of agrin. *Nature reviews. Molecular cell biology*, 4(4), pp.295–308.

Bhatt, A.S. et al., 2005. Adhesion signaling by a novel mitotic substrate of src kinases. *Oncogene*, 24(34), pp.5333–43.

Bierhuizen, M.F. & Fukuda, M., 1992. Expression cloning of a cDNA encoding UDP-GlcNAc:Gal beta 1-3-GalNAc-R (GlcNAc to GalNAc) beta 1-6GlcNAc transferase by gene transfer into CHO cells expressing polyoma large tumor antigen. *Proceedings of the National Academy of Sciences of the United States of America*, 89(19), pp.9326–330.

Björck, L. & Kronvall, G., 1984. Purification and some properties of streptococcal protein G, a novel IgG-binding reagent. *Journal of immunology (Baltimore, Md.: 1950)*, 133(2), pp.969–74.

Black, R.A. et al., 1997. A metalloproteinase disintegrin that releases tumour-necrosis factor-alpha from cells. *Nature*, 385(6618), pp.729–33.

Blobel, C.P., 2005. ADAMs: key components in EGFR signalling and development. *Nature reviews. Molecular cell biology*, 6(1), pp.32–43.

Bonnet, D. & Dick, J.E., 1997. Human acute myeloid leukemia is organized as a hierarchy that originates from a primitive hematopoietic cell. *Nature medicine*, 3(7), pp.730–7.

Bork, P. & Patthy, L., 1995. The SEA module: a new extracellular domain associated with O-glycosylation. *Protein science : a publication of the Protein Society*, 4(7), pp.1421–5.

Borneman, A., Kuschel, R. & Fujisawa-Sehara, A., 2000. Analysis for transcript expression of meltrin alpha in normal, regenerating, and denervated rat muscle. *Journal of muscle research and cell motility*, 21(5), pp.475–80.

Bourd-Boittin, K. et al., 2008. RACK1, a new ADAM12 interacting protein. Contribution to liver fibrogenesis. *The Journal of biological chemistry*, 283(38), pp.26000–9.

Bowen, C. et al., 2000. Loss of NKX3.1 expression in human prostate cancers correlates with tumor progression. *Cancer research*, 60(21), pp.6111–5.

Boyd, A.W. & Lackmann, M., 2001. Signals from Eph and ephrin proteins: a developmental tool kit. *Science's STKE : signal transduction knowledge environment*, 2001(112), p.re20.

Brew, K. & Nagase, H., 2010. The tissue inhibitors of metalloproteinases (TIMPs): an ancient family with structural and functional diversity. *Biochimica et biophysica acta*, 1803(1), pp.55–71.

Brose, N. & Rosenmund, C., 2002. Move over protein kinase C, you've got company: alternative cellular effectors of diacylglycerol and phorbol esters. *Journal of cell science*, 115(Pt 23), pp.4399–411.

Brown, M.S. et al., 2000. Regulated intramembrane proteolysis: a control mechanism conserved from bacteria to humans. *Cell*, 100(4), pp.391–8.

Bugge, T.H., Antalis, T.M. & Wu, Q., 2009. Type II transmembrane serine proteases. *The Journal of biological chemistry*, 284(35), pp.23177–81.

Burns, D.L., 1988. Subunit structure and enzymic activity of pertussis toxin. *Microbiological sciences*, 5(9), pp.285–7.

Cairns, P. et al., 1997. Frequent inactivation of PTEN/MMAC1 in primary prostate cancer. *Cancer research*, 57(22), pp.4997–5000.

Cal, S. et al., 2005. Human polyserase-2, a novel enzyme with three tandem serine protease domains in a single polypeptide chain. *The Journal of biological chemistry*, 280(3), pp.1953–61.

Cal, S. et al., 2006. Identification and characterization of human polyserase-3, a novel protein with tandem serine-protease domains in the same polypeptide chain. *BMC biochemistry*, 7, p.9.

Campbell, I.D. & Bork, P., 1993. Epidermal growth factor-like modules. *Current Opinion in Structural Biology*, 3(3), pp.385–392.

Carey, L. et al., 2010. Triple-negative breast cancer: disease entity or title of convenience? *Nature reviews. Clinical oncology*, 7(12), pp.683–92.

Carl-McGrath, S. et al., 2005. The disintegrin-metalloproteinases ADAM9, ADAM12, and ADAM15 are upregulated in gastric cancer. *International journal of oncology*, 26(1), pp.17–24.

Carpenter, G. et al., 1975. Characterization of the Binding of 12 ” 1-Labeled Epidermal Growth Factor to Human Fibroblasts *. , 250(11), pp.4297–4304.

Carpenter, G. & Cohen, S., 1990. Epidermal growth factor. *The Journal of biological chemistry*, 265(14), pp.7709–12.

Carter, H.B. et al., 1992. Longitudinal evaluation of prostate-specific antigen levels in men with and without prostate disease. *JAMA*, 267(16), pp.2215–20.

Chalaris, A. et al., 2010. ADAM17-mediated shedding of the IL6R induces cleavage of the membrane stub by gamma-secretase. *Biochimica et biophysica acta*, 1803(2), pp.234–45.

Charrier, L. et al., 2005. ADAM-15 inhibits wound healing in human intestinal epithelial cell monolayers. *American journal of physiology. Gastrointestinal and liver physiology*, 288(2), pp.G346–53.

Charrier-Hisamuddin, L., Laboisse, C.L. & Merlin, D., 2008. ADAM-15: a metalloprotease that mediates inflammation. *FASEB journal : official publication of the Federation of American Societies for Experimental Biology*, 22(3), pp.641–53.

Chaves-Pérez, A. et al., 2012. EpCAM regulates cell cycle progression via control of cyclin D1 expression. *Oncogene*.

Chen, L.M., Hodge, G.B., et al., 2001. Down-regulation of prostasin serine protease: a potential invasion suppressor in prostate cancer. *The Prostate*, 48(2), pp.93–103.

Chen, L.M., Skinner, M.L., et al., 2001. Prostasin is a glycosylphosphatidylinositol-anchored active serine protease. *The Journal of biological chemistry*, 276(24), pp.21434–42.

Chen, L.-M. et al., 2006. Prostasin attenuates inducible nitric oxide synthase expression in lipopolysaccharide-induced urinary bladder inflammation. *American journal of physiology. Renal physiology*, 291(3), pp.F567–77.

Chen, L.-M. et al., 2009. Prostasin regulates iNOS and cyclin D1 expression by modulating protease-activated receptor-2 signaling in prostate epithelial cells. *The Prostate*, 69(16), pp.1790–801.

Chen, L.-M. & Chai, K.X., 2002. Prostasin serine protease inhibits breast cancer invasiveness and is transcriptionally regulated by promoter DNA methylation. *International journal of cancer. Journal international du cancer*, 97(3), pp.323–9.

Chen, L.-M., Zhang, X. & Chai, K.X., 2004. Regulation of prostasin expression and function in the prostate. *The Prostate*, 59(1), pp.1–12.

Chen, M. et al., 2010. Hepsin activates prostasin and cleaves the extracellular domain of the epidermal growth factor receptor. *Molecular and cellular biochemistry*, 337(1-2), pp.259–66.

Chen, M. et al., 2007. Prostasin induces protease-dependent and independent molecular changes in the human prostate carcinoma cell line PC-3. *Biochimica et biophysica acta*, 1773(7), pp.1133–40.

Chen, M. et al., 2008. The epidermal growth factor receptor (EGFR) is proteolytically modified by the Matriptase-Prostasin serine protease cascade in cultured epithelial cells. *Biochimica et biophysica acta*, 1783(5), pp.896–903.

Chen, T.R. et al., 2012. Generation and characterization of Tmeff2 mutant mice. *Biochemical and biophysical research communications*.

Chen, X. et al., 2011. The tumor suppressor activity of the transmembrane protein with epidermal growth factor and two follistatin motifs 2 (TMEFF2) correlates with its ability to modulate sarcosine levels. *The Journal of biological chemistry*, 286(18), pp.16091–100.

Chen, Y.-W. et al., 2010. Regulation of the matriptase-prostasin cell surface proteolytic cascade by hepatocyte growth factor activator inhibitor-1 during epidermal differentiation. *The Journal of biological chemistry*, 285(41), pp.31755–62.

Chen, Z. et al., 2003. Hepsin and maspin are inversely expressed in laser capture microdissectioned prostate cancer. *The Journal of urology*, 169(4), pp.1316–9.

Chesneau, V. et al., 2003. Catalytic properties of ADAM19. *The Journal of biological chemistry*, 278(25), pp.22331–40.

Cho, E.G. et al., 2001. N-terminal processing is essential for release of epithin, a mouse type II membrane serine protease. *The Journal of biological chemistry*, 276(48), pp.44581–9.

Cissé, M.A. et al., 2005. The disintegrin ADAM9 indirectly contributes to the physiological processing of cellular prion by modulating ADAM10 activity. *The Journal of biological chemistry*, 280(49), pp.40624–31.

Citri, A. & Yarden, Y., 2006. REVIEWS EGF – ERBB signalling : towards the systems level. , 7(July), pp.505–516.

Coates, D., 2003. The angiotensin converting enzyme (ACE). *The international journal of biochemistry & cell biology*, 35(6), pp.769–73.

Collins, A.T. et al., 2001. Identification and isolation of human prostate epithelial stem cells based on alpha(2)beta(1)-integrin expression. *Journal of cell science*, 114(Pt 21), pp.3865–72.

Collins, A.T. et al., 2005. Prospective identification of tumorigenic prostate cancer stem cells. *Cancer research*, 65(23), pp.10946–51.

Colombel, M. et al., 1992. Hormone-regulated apoptosis results from reentry of differentiated prostate cells onto a defective cell cycle. *Cancer research*, 52(16), pp.4313–9.

Cominetti, M.R. et al., 2009. Inhibition of platelets and tumor cell adhesion by the disintegrin domain of human ADAM9 to collagen I under dynamic flow conditions. *Biochimie*, 91(8), pp.1045–52.

Costa, V.L. et al., 2010. Three epigenetic biomarkers, GDF15, TMEFF2, and VIM, accurately predict bladder cancer from DNA-based analyses of urine samples. *Clinical cancer research : an official journal of the American Association for Cancer Research*, 16(23), pp.5842–51.

Croucher, P.I., Wang, F. & Hargreaves, P.G., 1999. Interleukin-6 receptor shedding: a possible role for members of the ADAM family. *Biochemical Society transactions*, 27(2), pp.224–228.

Crowe, P.D. et al., 1993. Specific induction of 80-kDa tumor necrosis factor receptor shedding in T lymphocytes involves the cytoplasmic domain and phosphorylation. *Journal of immunology (Baltimore, Md. : 1950)*, 151(12), pp.6882–90.

Crystal, A.S. et al., 2003. Membrane topology of gamma-secretase component PEN-2. *The Journal of biological chemistry*, 278(22), pp.20117–23.

Culig, Z. et al., 1994. Androgen receptor activation in prostatic tumor cell lines by insulin-like growth factor-I, keratinocyte growth factor, and epidermal growth factor. *Cancer research*, 54(20), pp.5474–8.

Dahl, M. et al., 2011. Sarcosine induces increase in HER2/neu expression in androgen-dependent prostate cancer cells. *Molecular biology reports*, 38(7), pp.4237–43.

Dale, B.A. et al., 1985. Expression of epidermal keratins and filaggrin during human fetal skin development. *The Journal of cell biology*, 101(4), pp.1257–69.

Dean, M., Fojo, T. & Bates, S., 2005. Tumour stem cells and drug resistance. *Nature reviews. Cancer*, 5(4), pp.275–84.

Deheuninck, J. & Luo, K., 2009. Ski and SnoN, potent negative regulators of TGF-beta signaling. *Cell research*, 19(1), pp.47–57.

DeMarzo, A.M. et al., 2003. Pathological and molecular aspects of prostate cancer. *Lancet*, 361(9361), pp.955–64.

Denda, K. et al., 2002. Functional characterization of Kunitz domains in hepatocyte growth factor activator inhibitor type 1. *The Journal of biological chemistry*, 277(16), pp.14053–9.

Denzel, S. et al., 2012. MMP7 is a target of the tumour-associated antigen EpCAM. *International journal of experimental pathology*, 93(5), pp.341–53.

Dhanasekaran, S.M. et al., 2001. Delineation of prognostic biomarkers in prostate cancer. *Nature*, 412(6849), pp.822–6.

Doedens, J.R. & Black, R.A., 2000. Stimulation-induced down-regulation of tumor necrosis factor-alpha converting enzyme. *The Journal of biological chemistry*, 275(19), pp.14598–607.

Du, X. et al., 2008. The serine protease TMPRSS6 is required to sense iron deficiency. *Science (New York, N.Y.)*, 320(5879), pp.1088–92.

Dyczynska, E. et al., 2008. Breast cancer-associated mutations in metalloprotease disintegrin ADAM12 interfere with the intracellular trafficking and processing of the protein. *International journal of cancer. Journal international du cancer*, 122(11), pp.2634–40.

Dyczynska, E. et al., 2007. Proteolytic processing of delta-like 1 by ADAM proteases. *The Journal of biological chemistry*, 282(1), pp.436–44.

Edwards, D., Handsley, M.M. & Pennington, C.J., 2008. The ADAM metalloproteinases. *Molecular aspects of medicine*, 29(5), pp.258–89.

Edwards, J. & Bartlett, J.M.S., 2005. The androgen receptor and signal-transduction pathways in hormone-refractory prostate cancer. Part 1: Modifications to the androgen receptor. *BJU international*, 95(9), pp.1320–6.

Ehrmann, M. & Clausen, T., 2004. Proteolysis as a regulatory mechanism. *Annual review of genetics*, 38, pp.709–24.

Elahi, A. et al., 2008. HPP1-mediated tumor suppression requires activation of STAT1 pathways. *International journal of cancer. Journal international du cancer*, 122(7), pp.1567–72..

Ellwood-Yen, K. et al., 2003. Myc-driven murine prostate cancer shares molecular features with human prostate tumors. *Cancer cell*, 4(3), pp.223–38.

Emery, A.E.H., 2002. The muscular dystrophies. *Lancet*, 359(9307), pp.687–95.

Engler, D. a, Montelione, G.T. & Niyogi, S.K., 1990. Human epidermal growth factor. Distinct roles of tyrosine 37 and arginine 41 in receptor binding as determined by site-directed mutagenesis and nuclear magnetic resonance spectroscopy. *FEBS letters*, 271(1-2), pp.47–50.

Engler, D.A., Montelione, G.T. & Niyogi, S.K., 1990. Human epidermal growth factor. Distinct roles of tyrosine 37 and arginine 41 in receptor binding as determined by site-directed mutagenesis and nuclear magnetic resonance spectroscopy. *FEBS letters*, 271(1-2), pp.47–50.

English, W.R., Corvol, P. & Murphy, G., 2012. LPS activates ADAM9 dependent shedding of ACE from endothelial cells. *Biochemical and biophysical research communications*, 421(1), pp.70–5.

Epstein, 2010. An update of the Gleason grading system. *The Journal of urology*, 183(2), pp.433–40.

Eto, K. et al., 2000. RGD-independent binding of integrin alpha9beta1 to the ADAM-12 and -15 disintegrin domains mediates cell-cell interaction. *The Journal of biological chemistry*, 275(45), pp.34922–30.

Evans, R.M., 1988. The steroid and thyroid hormone receptor superfamily. *Science (New York, N.Y.)*, 240(4854), pp.889–95.

Fan, B. et al., 2007. Hepatocyte growth factor activator inhibitor-1 (HAI-1) is essential for the integrity of basement membranes in the developing placental labyrinth. *Developmental biology*, 303(1), pp.222–30.

Fan, B. et al., 2005. Identification of hepatocyte growth factor activator inhibitor-1B as a potential physiological inhibitor of prostasin. *The Journal of biological chemistry*, 280(41), pp.34513–20.

Fang, D. et al., 2005. A tumorigenic subpopulation with stem cell properties in melanomas. *Cancer research*, 65(20), pp.9328–37.

Fang, J.-D. et al., 2011. Endogenous expression of matriptase in neural progenitor cells promotes cell migration and neuron differentiation. *The Journal of biological chemistry*, 286(7), pp.5667–79.

Favre, A., 1989. Identification of filaggrin in Hassall's corpuscle by histochemical and immunohistochemical methods. *Acta anatomica*, 135(1), pp.71–6.

Fenton, M.A. et al., 1997. Functional characterization of mutant androgen receptors from androgen-independent prostate cancer. *Clinical cancer research : an official journal of the American Association for Cancer Research*, 3(8), pp.1383–8.

Finberg, K.E. et al., 2008. Mutations in TMPRSS6 cause iron-refractory iron deficiency anemia (IRIDA). *Nature genetics*, 40(5), pp.569–71.

Folgueras, A.R. et al., 2008. Membrane-bound serine protease matriptase-2 (Tmprss6) is an essential regulator of iron homeostasis. *Blood*, 112(6), pp.2539–45.

Fonseca, P. & Light, A., 1983. The purification and characterization of bovine enterokinase from membrane fragments in the duodenal mucosal fluid. *The Journal of biological chemistry*, 258(23), pp.14516–20.

Fortini, M.E., 2002. Gamma-secretase-mediated proteolysis in cell-surface-receptor signalling. *Nature reviews. Molecular cell biology*, 3(9), pp.673–84.

Fortini, M.E. & Bilder, D., 2009. Endocytic regulation of Notch signaling. *Current opinion in genetics & development*, 19(4), pp.323–8.

Fortna, R.R. et al., 2004. Membrane topology and nicastrin-enhanced endoproteolysis of APH-1, a component of the gamma-secretase complex. *The Journal of biological chemistry*, 279(5), pp.3685–93.

Fourie, A.M. et al., 2003. Catalytic activity of ADAM8, ADAM15, and MDC-L (ADAM28) on synthetic peptide substrates and in ectodomain cleavage of CD23. *The Journal of biological chemistry*, 278(33), pp.30469–77.

Franzke, C.-W. et al., 2004. Shedding of collagen XVII/BP180: structural motifs influence cleavage from cell surface. *The Journal of biological chemistry*, 279(23), pp.24521–9.

Frateschi, S. et al., 2011. PAR2 absence completely rescues inflammation and ichthyosis caused by altered CAP1/Prss8 expression in mouse skin. *Nature communications*, 2, p.161.

Friis, S. et al., 2011. Transport via the transcytotic pathway makes prostasin available as a substrate for matriptase. *The Journal of biological chemistry*, 286(7), pp.5793–802.

Fritzsche, F.R. et al., 2006. ADAM8 expression in prostate cancer is associated with parameters of unfavorable prognosis. *Virchows Archiv : an international journal of pathology*, 449(6), pp.628–36.

Fritzsche, F.R., Jung, M., et al., 2008. ADAM9 expression is a significant and independent prognostic marker of PSA relapse in prostate cancer. *European urology*, 54(5), pp.1097–106.

Fritzsche, F.R., Wassermann, K., et al., 2008. ADAM9 is highly expressed in renal cell cancer and is associated with tumour progression. *BMC cancer*, 8, p.179.

Fröhlich, C. et al., 2011. ADAM12 produced by tumor cells rather than stromal cells accelerates breast tumor progression. *Molecular cancer research : MCR*, 9(11), pp.1449–61.

Fröhlich, C. et al., 2006. Molecular profiling of ADAM12 in human bladder cancer. *Clinical cancer research : an official journal of the American Association for Cancer Research*, 12(24), pp.7359–68.

Fry, J.L. & Toker, A., 2010. Secreted and membrane-bound isoforms of protease ADAM9 have opposing effects on breast cancer cell migration. *Cancer research*, 70(20), pp.8187–98.

Galliano, M.F. et al., 2000. Binding of ADAM12, a marker of skeletal muscle regeneration, to the muscle-specific actin-binding protein, alpha -actinin-2, is required for myoblast fusion. *The Journal of biological chemistry*, 275(18), pp.13933–9.

Ganesan, R. et al., 2012. An allosteric anti-hepsin antibody derived from a constrained phage display library. *Protein engineering, design & selection : PEDS*, 25(3), pp.127–33.

Ganesan, R. et al., 2011. Proteolytic activation of pro-macrophage-stimulating protein by hepsin. *Molecular cancer research : MCR*, 9(9), pp.1175–86.

Gao, A.C. et al., 1997. CD44 is a metastasis suppressor gene for prostatic cancer located on human chromosome 11p13. *Cancer research*, 57(5), pp.846–9.

Ge, W. et al., 2006. Protein interaction analysis of ST14 domains and their point and deletion mutants. *The Journal of biological chemistry*, 281(11), pp.7406–12.

Geng, Y. et al., 2011. Follistatin-like 1 (Fstl1) is a bone morphogenetic protein (BMP) 4 signaling antagonist in controlling mouse lung development. *Proceedings of the National Academy of Sciences of the United States of America*, 108(17), pp.7058–63.

Georgakopoulos, A. et al., 2006. Metalloproteinase/Presenilin1 processing of ephrinB regulates EphB-induced Src phosphorylation and signaling. *The EMBO journal*, 25(6), pp.1242–52.

Gery, S. et al., 2002. TMEFF2 is an androgen-regulated gene exhibiting antiproliferative effects in prostate cancer cells. *Oncogene*, 21(31), pp.4739–46.

Gery, S. & Koeffler, H.P., 2003. Repression of the TMEFF2 promoter by c-Myc. *Journal of molecular biology*, 328(5), pp.977–83.

Gettins, P.G.W., 2002. Serpin structure, mechanism, and function. *Chemical reviews*, 102(12), pp.4751–804.

Gilpin, B.J. et al., 1998. A novel, secreted form of human ADAM 12 (meltrin alpha) provokes myogenesis in vivo. *The Journal of biological chemistry*, 273(1), pp.157–66.

Gleason, D., 1966. Classification of prostate carcinomas. *Cancer Chemother Rep*, (50), pp.125–128.

Glenner, G.G. & Wong, C.W., 1984. Alzheimer's disease: initial report of the purification and characterization of a novel cerebrovascular amyloid protein. *Biochemical and biophysical research communications*, 120(3), pp.885–90.

Glynne-Jones, E. et al., 2001. TENB2, a proteoglycan identified in prostate cancer that is associated with disease progression and androgen independence. *International journal of cancer. Journal international du cancer*, 94(2), pp.178–84.

Godfrey, E.W. et al., 1984. Components of Torpedo electric organ and muscle that cause aggregation of acetylcholine receptors on cultured muscle cells. *The Journal of cell biology*, 99(2), pp.615–27.

Goel, M.M. et al., 2011. Hepsin immunohistochemical expression in prostate cancer in relation to Gleason's grade and serum prostate specific antigen. *Indian journal of pathology & microbiology*, 54(3), pp.476–81.

Gonzales, P.E. et al., 2004. Inhibition of the tumor necrosis factor-alpha-converting enzyme by its pro domain. *The Journal of biological chemistry*, 279(30), pp.31638–45.

Graille, M. et al., 2000. Crystal structure of a Staphylococcus aureus protein A domain complexed with the Fab fragment of a human IgM antibody: structural basis for recognition of B-cell receptors and superantigen activity. *Proceedings of the National Academy of Sciences of the United States of America*, 97(10), pp.5399–404.

Gray, P.C., Harrison, C.A. & Vale, W., 2003. Cripto forms a complex with activin and type II activin receptors and can block activin signaling. *Proceedings of the National Academy of Sciences of the United States of America*, 100(9), pp.5193–8.

Gregory, C.W. et al., 2001. Androgen receptor stabilization in recurrent prostate cancer is associated with hypersensitivity to low androgen. *Cancer research*, 61(7), pp.2892–8.

Gregory, C.W. et al., 2004. Epidermal growth factor increases coactivation of the androgen receptor in recurrent prostate cancer. *The Journal of biological chemistry*, 279(8), pp.7119–30.

Groot, A.J. & Vooijs, M.A., 2012. The role of Adams in Notch signaling. *Advances in experimental medicine and biology*, 727, pp.15–36.

Grützmann, R. et al., 2004. ADAM9 expression in pancreatic cancer is associated with tumour type and is a prognostic factor in ductal adenocarcinoma. *British journal of cancer*, 90(5), pp.1053–8.

Guillem, F. et al., 2008. Two nonsense mutations in the TMPRSS6 gene in a patient with microcytic anemia and iron deficiency. *Blood*, 112(5), pp.2089–91.

Guipponi, M. et al., 2007. Mice deficient for the type II transmembrane serine protease, TMPRSS1/hepsin, exhibit profound hearing loss. *The American journal of pathology*, 171(2), pp.608–16.

Guipponi, M. et al., 2002. The transmembrane serine protease (TMPRSS3) mutated in deafness DFNB8/10 activates the epithelial sodium channel (ENaC) in vitro. *Human molecular genetics*, 11(23), pp.2829–36.

Guo, Z. et al., 2009. A novel androgen receptor splice variant is up-regulated during prostate cancer progression and promotes androgen depletion-resistant growth. *Cancer research*, 69(6), pp.2305–13.

Hackel, P.O. et al., 1999. Epidermal growth factor receptors: critical mediators of multiple receptor pathways. *Current opinion in cell biology*, 11(2), pp.184–9.

Ham, C. et al., 2002. ADAM15 is an adherens junction molecule whose surface expression can be driven by VE-cadherin. *Experimental cell research*, 279(2), pp.239–47.

Hamburger, A.W. & Salmon, S.E., 1977. Primary bioassay of human tumor stem cells. *Science (New York, N.Y.)*, 197(4302), pp.461–3.

Harms, P.W. & Chang, C., 2003. Tomoregulin-1 (TMEFF1) inhibits nodal signaling through direct binding to the nodal coreceptor Cripto. *Genes & development*, 17(21), pp.2624–9.

Hart, S. et al., 2005. GPCR-induced migration of breast carcinoma cells depends on both EGFR signal transactivation and EGFR-independent pathways. *Biological chemistry*, 386(9), pp.845–55.

Hayashida, K. et al., 2010. Molecular and cellular mechanisms of ectodomain shedding. *Anatomical record (Hoboken, N.J. : 2007)*, 293(6), pp.925–37.

Heldin, C.-H. & Moustakas, A., 2012. Role of Smads in TGFβ signaling. *Cell and tissue research*, 347(1), pp.21–36.

Heppner, G.H., 1984. Tumor heterogeneity. *Cancer research*, 44(6), pp.2259–65.

Herreman, A. et al., 2003. gamma-Secretase activity requires the presenilin-dependent trafficking of nicastrin through the Golgi apparatus but not its complex glycosylation. *Journal of cell science*, 116(Pt 6), pp.1127–36.

Herren, B. et al., 2001. ADAM15 overexpression in NIH3T3 cells enhances cell-cell interactions. *Experimental cell research*, 271(1), pp.152–60.

Herren, B., Raines, E.W. & Ross, R., 1997. Expression of a disintegrin-like protein in cultured human vascular cells and in vivo. *FASEB journal : official publication of the Federation of American Societies for Experimental Biology*, 11(2), pp.173–80.

Herter, S. et al., 2005. Hepatocyte growth factor is a preferred in vitro substrate for human hepsin, a membrane-anchored serine protease implicated in prostate and ovarian cancers. *The Biochemical journal*, 390(Pt 1), pp.125–36.

Hieda, M. et al., 2008. Membrane-anchored growth factor, HB-EGF, on the cell surface targeted to the inner nuclear membrane. *The Journal of cell biology*, 180(4), pp.763–9.

Hooper, J.D. et al., 2003. Mouse matriptase-2: identification, characterization and comparative mRNA expression analysis with mouse hepsin in adult and embryonic tissues. *The Biochemical journal*, 373(Pt 3), pp.689–702.

Hooper, J.D. et al., 2001. Type II transmembrane serine proteases. Insights into an emerging class of cell surface proteolytic enzymes. *The Journal of biological chemistry*, 276(2), pp.857–60.

Horie, M. et al., 2000. Identification and characterization of TMEFF2, a novel survival factor for hippocampal and mesencephalic neurons. *Genomics*, 67(2), pp.146–52.

Horiuchi, K. et al., 2003. Potential role for ADAM15 in pathological neovascularization in mice. *Molecular and cellular biology*, 23(16), pp.5614–24.

Horiuchi, K. et al., 2007. Substrate selectivity of epidermal growth factor-receptor ligand sheddases and their regulation by phorbol esters and calcium influx. *Molecular biology of the cell*, 18(1), pp.176–88.

Hotoda, N. et al., 2002. A secreted form of human ADAM9 has an alpha-secretase activity for APP. *Biochemical and biophysical research communications*, 293(2), pp.800–5.

Hougaard, S. et al., 2000. Trafficking of human ADAM 12-L: retention in the trans-Golgi network. *Biochemical and biophysical research communications*, 275(2), pp.261–7.

Howard, L. et al., 1999. Interaction of the metalloprotease disintegrins MDC9 and MDC15 with two SH3 domain-containing proteins, endophilin I and SH3PX1. *The Journal of biological chemistry*, 274(44), pp.31693–9.

Howard, L., Maciewicz, R.A. & Blobel, C.P., 2000. Cloning and characterization of ADAM28: evidence for autocatalytic pro-domain removal and for cell surface localization of mature ADAM28. *The Biochemical journal*, 348 Pt 1, pp.21–7.

Hsieh, T.Y. et al., 1996. Regulation of growth, PSA/PAP and androgen receptor expression by 1 alpha,25-dihydroxyvitamin D3 in the androgen-dependent LNCaP cells. *Biochemical and biophysical research communications*, 223(1), pp.141–6.

Huang, J., Bridges, L.C. & White, J.M., 2005. Selective modulation of integrin-mediated cell migration by distinct ADAM family members. *Molecular biology of the cell*, 16(10), pp.4982–91.

Huang, S. et al., 2002. Stat1 negatively regulates angiogenesis, tumorigenicity and metastasis of tumor cells. *Oncogene*, 21(16), pp.2504–12.

Huusko, P. et al., 2004. Nonsense-mediated decay microarray analysis identifies mutations of EPHB2 in human prostate cancer. *Nature genetics*, 36(9), pp.979–83.

Iba, K. et al., 2000. The cysteine-rich domain of human ADAM 12 supports cell adhesion through syndecans and triggers signaling events that lead to beta1 integrin-dependent cell spreading. *The Journal of cell biology*, 149(5), pp.1143–56.

Ieguchi, K. et al., 2010. Direct binding of the EGF-like domain of neuregulin-1 to integrins ({alpha}v{beta}3 and {alpha}6{beta}4) is involved in neuregulin-1/ErbB signaling. *The Journal of biological chemistry*, 285(41), pp.31388–98.

Ihara, S. et al., 2002. Prometastatic effect of N-acetylglucosaminyltransferase V is due to modification and stabilization of active matriptase by adding beta 1-6 GlcNAc branching. *The Journal of biological chemistry*, 277(19), pp.16960–7.

Inouye, K. et al., 2010. Identification of the matriptase second CUB domain as the secondary site for interaction with hepatocyte growth factor activator inhibitor type-1. *The Journal of biological chemistry*, 285(43), pp.33394–403.

Ito, N. et al., 2004. ADAMs, a disintegrin and metalloproteinases, mediate shedding of oxytocinase. *Biochemical and biophysical research communications*, 314(4), pp.1008–13.

Ivetic, A. et al., 2004. Mutagenesis of the ezrin-radixin-moesin binding domain of L-selectin tail affects shedding, microvillar positioning, and leukocyte tethering. *Journal of Biological Chemistry*.

Izumi, Y. et al., 1998. A metalloprotease-disintegrin, MDC9/meltrin-gamma/ADAM9 and PKCdelta are involved in TPA-induced ectodomain shedding of membrane-anchored heparin-binding EGF-like growth factor. *The EMBO journal*, 17(24), pp.7260–72.

Jacobsen, J. et al., 2008. Catalytic properties of ADAM12 and its domain deletion mutants. *Biochemistry*, 47(2), pp.537–47.

Janes, P.W. et al., 2005. Adam meets Eph: an ADAM substrate recognition module acts as a molecular switch for ephrin cleavage in trans. *Cell*, 123(2), pp.291–304.

Jenkins, R.B. et al., 1997. Detection of c-myc oncogene amplification and chromosomal anomalies in metastatic prostatic carcinoma by fluorescence in situ hybridization. *Cancer research*, 57(3), pp.524–31.

Jentzmik, F. et al., 2011. Sarcosine in prostate cancer tissue is not a differential metabolite for prostate cancer aggressiveness and biochemical progression. *The Journal of urology*, 185(2), pp.706–11.

Jin, C. et al., 2003. Cooperation between ectopic FGFR1 and depression of FGFR2 in induction of prostatic intraepithelial neoplasia in the mouse prostate. *Cancer research*, 63(24), pp.8784–90..

Jørgensen, L.H. et al., 2007. Transgenic overexpression of ADAM12 suppresses muscle regeneration and aggravates dystrophy in aged mdx mice. *The American journal of pathology*, 171(5), pp.1599–607.

Josson, S. et al., 2011. Inhibition of ADAM9 expression induces epithelial phenotypic alterations and sensitizes human prostate cancer cells to radiation and chemotherapy. *The Prostate*, 71(3), pp.232–40.

Jost, L.M., Kirkwood, J.M. & Whiteside, T.L., 1992. Improved short- and long-term XTT-based colorimetric cellular cytotoxicity assay for melanoma and other tumor cells. *Journal of immunological methods*, 147(2), pp.153–65.

Kahn, J. et al., 1998. Calmodulin Regulates L-Selectin Adhesion Molecule Expression and Function through a Protease-Dependent Mechanism. *Cell*, 92(6), pp.809–818.

Kang, Q., Cao, Y. & Zolkiewska, A., 2000. Metalloprotease-disintegrin ADAM 12 binds to the SH3 domain of Src and activates Src tyrosine kinase in C2C12 cells. *The Biochemical journal*, 352 Pt 3, pp.883–92.

Kansas, G.S. et al., 1994. A role for the epidermal growth factor-like domain of P-selectin in ligand recognition and cell adhesion. *The Journal of cell biology*, 124(4), pp.609–18.

Kapust, R.B. & Waugh, D.S., 1999. Escherichia coli maltose-binding protein is uncommonly effective at promoting the solubility of polypeptides to which it is fused. *Protein science : a publication of the Protein Society*, 8(8), pp.1668–74.

Karadag, A., Zhou, M. & Croucher, P.I., 2006. ADAM-9 (MDC-9/meltrin-gamma), a member of the a disintegrin and metalloproteinase family, regulates myeloma-cell-induced interleukin-6 production in osteoblasts by direct interaction with the alpha(v)beta5 integrin. *Blood*, 107(8), pp.3271–8.

Kataoka, H. et al., 2003. Roles of hepatocyte growth factor (HGF) activator and HGF activator inhibitor in the pericellular activation of HGF/scatter factor. *Cancer metastasis reviews*, 22(2-3), pp.223–36.

Kazama, Y. et al., 1995. Hepsin, a putative membrane-associated serine protease, activates human factor VII and initiates a pathway of blood coagulation on the cell surface leading to thrombin formation. *The Journal of biological chemistry*, 270(1), pp.66–72.

Kelly, K.A. et al., 2008. Detection of early prostate cancer using a hepsin-targeted imaging agent. *Cancer research*, 68(7), pp.2286–91.

Kilpatrick, L.M. et al., 2006. Initiation of plasminogen activation on the surface of monocytes expressing the type II transmembrane serine protease matriptase. *Blood*, 108(8), pp.2616–23.

Kim, C. et al., 2005. Filamin is essential for shedding of the transmembrane serine protease, epithin. *EMBO reports*, 6(11), pp.1045–51.

Kim, C.F.B. et al., 2005. Identification of bronchioalveolar stem cells in normal lung and lung cancer. *Cell*, 121(6), pp.823–35.

Kinugasa, Y. et al., 2007. The carboxyl-terminal fragment of pro-HB-EGF reverses Bcl6-mediated gene repression. *The Journal of biological chemistry*, 282(20), pp.14797–806.

Kirchhofer, D. et al., 2005. Hepsin activates pro-hepatocyte growth factor and is inhibited by hepatocyte growth factor activator inhibitor-1B (HAI-1B) and HAI-2. *FEBS letters*, 579(9), pp.1945–50.

Kiyomiya, K. et al., 2006. Matriptase activation and shedding with HAI-1 is induced by steroid sex hormones in human prostate cancer cells, but not in breast cancer cells. *American journal of physiology. Cell physiology*, 291(1), pp.C40–9.

Kleino, I. et al., 2009. Alternative splicing of ADAM15 regulates its interactions with cellular SH3 proteins. *Journal of cellular biochemistry*, 108(4), pp.877–85.

Kleino, I., Ortiz, R.M. & Huovila, A.-P.J., 2007. ADAM15 gene structure and differential alternative exon use in human tissues. *BMC molecular biology*, 8, p.90.

Klezovitch, O. et al., 2004. Hepsin promotes prostate cancer progression and metastasis. *Cancer cell*, 6(2), pp.185–95.

Kodama, T. et al., 2004. ADAM12 is selectively overexpressed in human glioblastomas and is associated with glioblastoma cell proliferation and shedding of heparin-binding epidermal growth factor. *The American journal of pathology*, 165(5), pp.1743–53.

Kojima, K. & Inouye, K., 2011. Activation of matriptase zymogen. *Journal of biochemistry*, 150(2), pp.123–5.

Komuro, A. et al., 2003. WW domain-containing protein YAP associates with ErbB-4 and acts as a co-transcriptional activator for the carboxyl-terminal fragment of ErbB-4 that translocates to the nucleus. *The Journal of biological chemistry*, 278(35), pp.33334–41.

Kondás, K. et al., 2008. Both WFIKKN1 and WFIKKN2 have high affinity for growth and differentiation factors 8 and 11. *The Journal of biological chemistry*, 283(35), pp.23677–84.

Kopan, R. & Ilagan, M.X.G., 2009. The canonical Notch signaling pathway: unfolding the activation mechanism. *Cell*, 137(2), pp.216–33.

Koschubs, T. et al., 2012. Allosteric antibody inhibition of human hepsin protease. *The Biochemical journal*, 442(3), pp.483–94.

Krätzschmar, J., Lum, L. & Blobel, C.P., 1996. Metargidin, a membrane-anchored metalloprotease-disintegrin protein with an RGD integrin binding sequence. *The Journal of biological chemistry*, 271(9), pp.4593–6.

Kronqvist, P. et al., 2002. ADAM12 alleviates the skeletal muscle pathology in mdx dystrophic mice. *The American journal of pathology*, 161(5), pp.1535–40.

Kuefer, R. et al., 2006. ADAM15 disintegrin is associated with aggressive prostate and breast cancer disease. *Neoplasia (New York, N.Y.)*, 8(4), pp.319–29.

Kumar, V.L. & Majumder, P.K., 1995. Prostate gland: structure, functions and regulation. *International urology and nephrology*, 27(3), pp.231–43.

Kurisaki, T. et al., 2003. Phenotypic analysis of Meltrin alpha (ADAM12)-deficient mice: involvement of Meltrin alpha in adipogenesis and myogenesis. *Molecular and cellular biology*, 23(1), pp.55–61.

Kveiborg, M. et al., 2005. A role for ADAM12 in breast tumor progression and stromal cell apoptosis. *Cancer research*, 65(11), pp.4754–61.

Kveiborg, M. et al., 2008. Cellular roles of ADAM12 in health and disease. *The international journal of biochemistry & cell biology*, 40(9), pp.1685–702.

Lakhal, S. et al., 2011. Regulation of type II transmembrane serine proteinase TMPRSS6 by hypoxia-inducible factors: new link between hypoxia signaling and iron homeostasis. *The Journal of biological chemistry*, 286(6), pp.4090–7.

Lander, E.S. et al., 2001. Initial sequencing and analysis of the human genome. *Nature*, 409(6822), pp.860–921.

Landers, K.A. et al., 2005. Use of multiple biomarkers for a molecular diagnosis of prostate cancer. *International journal of cancer. Journal international du cancer*, 114(6), pp.950–6.

Lang, J.C. & Schuller, D.E., 2001. Differential expression of a novel serine protease homologue in squamous cell carcinoma of the head and neck. *British journal of cancer*, 84(2), pp.237–43.

Lee, H.-J. et al., 2002. Presenilin-dependent gamma-secretase-like intramembrane cleavage of ErbB4. *The Journal of biological chemistry*, 277(8), pp.6318–23.

Lee, M., Fridman, R. & Mobashery, S., 2004. Extracellular proteases as targets for treatment of cancer metastases. *Chemical Society reviews*, 33(7), pp.401–9.

Lee, S.L., Dickson, R.B. & Lin, C.Y., 2000. Activation of hepatocyte growth factor and urokinase/plasminogen activator by matriptase, an epithelial membrane serine protease. *The Journal of biological chemistry*, 275(47), pp.36720–5.

Lee, W.H. et al., 1994. Cytidine methylation of regulatory sequences near the pi-class glutathione S-transferase gene accompanies human prostatic carcinogenesis. *Proceedings of the National Academy of Sciences of the United States of America*, 91(24), pp.11733–7.

Lemjabbar, H. & Basbaum, C., 2002. Platelet-activating factor receptor and ADAM10 mediate responses to Staphylococcus aureus in epithelial cells. *Nature medicine*, 8(1), pp.41–6..

Lendeckel, U. et al., 2005. Increased expression of ADAM family members in human breast cancer and breast cancer cell lines. *Journal of cancer research and clinical oncology*, 131(1), pp.41–8.

Letellier, M. et al., 1990. Mechanism of formation of human IgE-binding factors (soluble CD23): III. Evidence for a receptor (Fc epsilon RII)-associated proteolytic activity. *Journal of Experimental Medicine*, 172(3), pp.693–700.

Leytus, S.P. et al., 1988. A novel trypsin-like serine protease (hepsin) with a putative transmembrane domain expressed by human liver and hepatoma cells. *Biochemistry*, 27(3), pp.1067–74.

Leyvraz, C. et al., 2005. The epidermal barrier function is dependent on the serine protease CAP1/Prss8. *The Journal of cell biology*, 170(3), pp.487–96.

Li, C. et al., 2007. Identification of pancreatic cancer stem cells. *Cancer research*, 67(3), pp.1030–7.

Li, H. et al., 2012. An essential role of metalloprotease-disintegrin ADAM12 in triple-negative breast cancer. *Breast cancer research and treatment*, 135(3), pp.759–69.

Li, H., Wolfe, M.S. & Selkoe, D.J., 2009. Toward structural elucidation of the gamma-secretase complex. *Structure (London, England : 1993)*, 17(3), pp.326–34.

Liang, G. et al., 2000. The gene for a novel transmembrane protein containing epidermal growth factor and follistatin domains is frequently hypermethylated in human tumor cells. *Cancer research*, 60(17), pp.4907–12.

Lichtenthaler, S.F., 2006. Ectodomain shedding of the amyloid precursor protein: cellular control mechanisms and novel modifiers. *Neuro-degenerative diseases*, 3(4-5), pp.262–9.

Liepinsh, E. et al., 2006. Second Kunitz-type protease inhibitor domain of the human WFIKKN1 protein. *Journal of biomolecular NMR*, 35(1), pp.73–8.

Lilja, H., 1985. A kallikrein-like serine protease in prostatic fluid cleaves the predominant seminal vesicle protein. *The Journal of clinical investigation*, 76(5), pp.1899–903.

Lilja, H., Ulmert, D. & Vickers, A.J., 2008. Prostate-specific antigen and prostate cancer: prediction, detection and monitoring. *Nature reviews. Cancer*, 8(4), pp.268–78.

Lin, B., Ferguson, C., White, J.T., Wang, S., et al., 1999. Prostate-localized and androgen-regulated expression of the membrane-bound serine protease TMPRSS2. *Cancer research*, 59(17), pp.4180–4.

Lin, C.Y., Anders, J., Johnson, M., Sang, Q.A., et al., 1999. Molecular cloning of cDNA for matriptase, a matrix-degrading serine protease with trypsin-like activity. *The Journal of biological chemistry*, 274(26), pp.18231–6.

Lin, C.Y., Anders, J., Johnson, M. & Dickson, R.B., 1999. Purification and characterization of a complex containing matriptase and a Kunitz-type serine protease inhibitor from human milk. *The Journal of biological chemistry*, 274(26), pp.18237–42.

Lin, H. et al., 2003. Tomoregulin ectodomain shedding by proinflammatory cytokines. *Life sciences*, 73(13), pp.1617–27.

Lin, K. et al., 2011. TMEFF2 is a PDGF-AA binding protein with methylation-associated gene silencing in multiple cancer types including glioma. *PloS one*, 6(4), p.e18608.

Lin, Y. & Clinton, G., 1991. A soluble protein related to the HER-2 proto-oncogene product is released from human breast carcinoma cells. *Oncogene*, 6(4), pp.639–43.

Linggi, B. & Carpenter, G., 2006. ErbB-4 s80 intracellular domain abrogates ETO2-dependent transcriptional repression. *The Journal of biological chemistry*, 281(35), pp.25373–80..

List, K., Szabo, R., et al., 2006. Delineation of matriptase protein expression by enzymatic gene trapping suggests diverging roles in barrier function, hair formation, and squamous cell carcinogenesis. *The American journal of pathology*, 168(5), pp.1513–25.

List, K. et al., 2005. Deregulated matriptase causes ras-independent multistage carcinogenesis and promotes ras-mediated malignant transformation. *Genes & development*, 19(16), pp.1934–50.

List, K. et al., 2003. Loss of proteolytically processed filaggrin caused by epidermal deletion of Matriptase/MT-SP1. *The Journal of cell biology*, 163(4), pp.901–10.

List, K. et al., 2002. Matriptase / MT-SP1 is required for postnatal survival , epidermal barrier function , hair follicle development , and thymic homeostasis. *Oncogene*, 21(February), pp.3765–79.

List, K., Bugge, T.H. & Szabo, R., 2006. Matriptase: potent proteolysis on the cell surface. *Molecular medicine (Cambridge, Mass.)*, 12(1-3), pp.1–7.

Lobstein, J. et al., 2012. SHuffle, a novel Escherichia coli protein expression strain capable of correctly folding disulfide bonded proteins in its cytoplasm. *Microbial cell factories*, 11(1), p.56.

Loechel, F. et al., 2000. ADAM 12-S cleaves IGFBP-3 and IGFBP-5 and is inhibited by TIMP-3. *Biochemical and biophysical research communications*, 278(3), pp.511–5.

Loechel, F. et al., 1998. Human ADAM 12 (meltrin alpha) is an active metalloprotease. *The Journal of biological chemistry*, 273(27), pp.16993–7.

Loechel, F. et al., 1999. Regulation of human ADAM 12 protease by the prodomain. Evidence for a functional cysteine switch. *The Journal of biological chemistry*, 274(19), pp.13427–33.

Lohman, R.-J. et al., 2012. An antagonist of human protease activated receptor-2 attenuates PAR2 signaling, macrophage activation, mast cell degranulation, and collagen-induced arthritis in rats. *FASEB journal : official publication of the Federation of American Societies for Experimental Biology*, 26(7), pp.2877–87.

Lorenzen, I. et al., 2012. The membrane-proximal domain of A Disintegrin and Metalloprotease 17 (ADAM17) is responsible for recognition of the interleukin-6 receptor and interleukin-1 receptor II. *FEBS letters*, 586(8), pp.1093–100.

Lorenzen, I., Trad, A. & Grötzinger, J., 2011. Multimerisation of A disintegrin and metalloprotease protein-17 (ADAM17) is mediated by its EGF-like domain. *Biochemical and biophysical research communications*, 415(2), pp.330–6.

Lu, D. et al., 1997. Bovine proenteropeptidase is activated by trypsin, and the specificity of enteropeptidase depends on the heavy chain. *The Journal of biological chemistry*, 272(50), pp.31293–300.

Lu, T.-Y. et al., 2010. Epithelial cell adhesion molecule regulation is associated with the maintenance of the undifferentiated phenotype of human embryonic stem cells. *The Journal of biological chemistry*, 285(12), pp.8719–32.

Lucarelli, G. et al., 2012. Serum sarcosine increases the accuracy of prostate cancer detection in patients with total serum PSA less than 4.0 ng/ml. *The Prostate*, 72(15), pp.1611–21.

Lucas, N. & Day, M.L., 2009. The role of the disintegrin metalloproteinase ADAM15 in prostate cancer progression. *Journal of cellular biochemistry*, 106(6), pp.967–74.

Lum, L., Reid, M.S. & Blobel, C.P., 1998. Intracellular maturation of the mouse metalloprotease disintegrin MDC15. *The Journal of biological chemistry*, 273(40), pp.26236–47.

Luo, Jun et al., 2001. Human Prostate Cancer and Benign Prostatic Hyperplasia : Molecular Dissection by Gene Expression Profiling Advances in Brief Human Prostate Cancer and Benign Prostatic Hyperplasia : Molecular Dissection by. *Cancer Res.*, pp.4683–4688.

Luo, J et al., 2001. Human prostate cancer and benign prostatic hyperplasia: molecular dissection by gene expression profiling. *Cancer research*, 61(12), pp.4683–8

Maaser, K. & Borlak, J., 2008. A genome-wide expression analysis identifies a network of EpCAM-induced cell cycle regulators. *British journal of cancer*, 99(10), pp.1635–43.

Macfarlane, S.R. et al., 2001. Proteinase-activated receptors. *Pharmacological reviews*, 53(2), pp.245–82.

Madu, C.O. & Lu, Y., 2010. Novel diagnostic biomarkers for prostate cancer. *Journal of Cancer*, 1, pp.150–77.

Maeda, Y. et al., 1996. Expression of a bifunctional chimeric protein A-Vargula hilgendorfii luciferase in mammalian cells. *BioTechniques*, 20(1), pp.116–21.

Maetzel, D. et al., 2009. Nuclear signalling by tumour-associated antigen EpCAM. *Nature cell biology*, 11(2), pp.162–71.

Magee, J.A. et al., 2001. Expression profiling reveals hepsin overexpression in prostate cancer. *Cancer research*, 61(15), pp.5692–6.

Mahimkar, R.M. et al., 2005. The disintegrin domain of ADAM9: a ligand for multiple beta1 renal integrins. *The Biochemical journal*, 385(Pt 2), pp.461–8.

Maitland, N.J. & Collins, A., 2005. A tumour stem cell hypothesis for the origins of prostate cancer. *BJU international*, 96(9), pp.1219–23.

Maretzky, T., Yang, G., et al., 2009. Characterization of the catalytic activity of the membrane-anchored metalloproteinase ADAM15 in cell-based assays. *The Biochemical journal*, 420(1), pp.105–13.

Maretzky, T., Le Gall, S.M., et al., 2009. Src stimulates fibroblast growth factor receptor-2 shedding by an ADAM15 splice variant linked to breast cancer. *Cancer research*, 69(11), pp.4573–6.

Markholt, S. et al., 2012. Global gene analysis of oocytes from early stages in human folliculogenesis shows high expression of novel genes in reproduction. *Molecular human reproduction*, 18(2), pp.96–110.

Martin, J. et al., 2002. The role of ADAM 15 in glomerular mesangial cell migration. *The Journal of biological chemistry*, 277(37), pp.33683–9.

De Marzo, A.M. et al., 2004. Pathological and molecular mechanisms of prostate carcinogenesis: implications for diagnosis, detection, prevention, and treatment. *Journal of cellular biochemistry*, 91(3), pp.459–77.

Massagué, J., 2008. TGFbeta in Cancer. *Cell*, 134(2), pp.215–30.

Massagué, J., 1998. TGF-beta signal transduction. *Annual review of biochemistry*, 67, pp.753–91.

Matsuo, T. et al., 2008. Expression of the serine protease hepsin and clinical outcome of human endometrial cancer. *Anticancer research*, 28(1A), pp.159–64.

Matthews, V. et al., 2003. Cellular cholesterol depletion triggers shedding of the human interleukin-6 receptor by ADAM10 and ADAM17 (TACE). *The Journal of biological chemistry*, 278(40), pp.38829–39.

Maurer, E., Gütschow, M. & Stirnberg, M., 2012. Matriptase-2 (TMPRSS6) is directly up-regulated by hypoxia inducible factor-1: identification of a hypoxia-responsive element in the TMPRSS6 promoter region. *Biological chemistry*, 393(6), pp.535–40.

Mazzocca, A. et al., 2005. A secreted form of ADAM9 promotes carcinoma invasion through tumor-stromal interactions. *Cancer research*, 65(11), pp.4728–38.

Meng, L. et al., 1999. Epoxomicin, a potent and selective proteasome inhibitor, exhibits in vivo antiinflammatory activity. *Proceedings of the National Academy of Sciences of the United States of America*, 96(18), pp.10403–8.

Migaki, G.I., 1995. Mutational analysis of the membrane-proximal cleavage site of L- selectin: relaxed sequence specificity surrounding the cleavage site. *Journal of Experimental Medicine*, 182(2), pp.549–557.

De Miguel, P. et al., 1999. Immunohistochemical comparative analysis of transforming growth factor alpha, epidermal growth factor, and epidermal growth factor receptor in normal, hyperplastic and neoplastic human prostates. *Cytokine*, 11(9), pp.722–7.

Miyazawa, K. et al., 2002. Two major Smad pathways in TGF-beta superfamily signalling. *Genes to cells : devoted to molecular & cellular mechanisms*, 7(12), pp.1191–204.

Miyazono, K., 2000. Positive and negative regulation of TGF-beta signaling. *Journal of cell science*, 113 (Pt 7, pp.1101–9.

Miyazono, K., Kusanagi, K. & Inoue, H., 2001. Divergence and convergence of TGF-beta/BMP signaling. *Journal of cellular physiology*, 187(3), pp.265–76.

Mochizuki, S. & Okada, Y., 2007. ADAMs in cancer cell proliferation and progression. *Cancer science*, 98(5), pp.621–8.

Moghadaszadeh, B. et al., 2003. Compensation for dystrophin-deficiency: ADAM12 overexpression in skeletal muscle results in increased alpha 7 integrin, utrophin and associated glycoproteins. *Human molecular genetics*, 12(19), pp.2467–79.

Mohan, S. et al., 2002. ADAM-9 is an insulin-like growth factor binding protein-5 protease produced and secreted by human osteoblasts. *Biochemistry*, 41(51), pp.15394–403.

Mok, S.C. et al., 2001. Prostasin, a potential serum marker for ovarian cancer: identification through microarray technology. *Journal of the National Cancer Institute*, 93(19), pp.1458–64.

Montero, J.C. et al., 2002. Mitogen-activated protein kinase-dependent and -independent routes control shedding of transmembrane growth factors through multiple secretases. *The Biochemical journal*, 363(Pt 2), pp.211–21.

Moran, P. et al., 2006. Pro-urokinase-type plasminogen activator is a substrate for hepsin. *The Journal of biological chemistry*, 281(41), pp.30439–46.

Mori, S. et al., 2003. PACSIN3 binds ADAM12/meltrin alpha and up-regulates ectodomain shedding of heparin-binding epidermal growth factor-like growth factor. *The Journal of biological chemistry*, 278(46), pp.46029–34.

Moss, M.L. et al., 2011. ADAM9 inhibition increases membrane activity of ADAM10 and controls α-secretase processing of amyloid precursor protein. *The Journal of biological chemistry*, 286(47), pp.40443–51.

Moss, M.L. et al., 2007. The ADAM10 prodomain is a specific inhibitor of ADAM10 proteolytic activity and inhibits cellular shedding events. *The Journal of biological chemistry*, 282(49), pp.35712–21.

Moustakas, A. & Heldin, C.-H., 2009. The regulation of TGFbeta signal transduction. *Development (Cambridge, England)*, 136(22), pp.3699–714.

Müllberg, J. et al., 1994. The soluble human IL-6 receptor. Mutational characterization of the proteolytic cleavage site. *Journal of immunology (Baltimore, Md.: 1950)*, 152(10), pp.4958–68.

Münz, M. et al., 2004. The carcinoma-associated antigen EpCAM upregulates c-myc and induces cell proliferation. *Oncogene*, 23(34), pp.5748–58.

Murphy, G., 2011. Tissue inhibitors of metalloproteinases. *Genome biology*, 12(11), p.233.

Nagata, S. et al., 2012. Aberrant DNA methylation of tumor-related genes in oral rinse: A noninvasive method for detection of oral squamous cell carcinoma. *Cancer*.

Nagle, R.B. et al., 1995. Expression of hemidesmosomal and extracellular matrix proteins by normal and malignant human prostate tissue. *The American journal of pathology*, 146(6), pp.1498–507.

Najy, A.J., Day, K.C. & Day, M.L., 2008a. ADAM15 supports prostate cancer metastasis by modulating tumor cell-endothelial cell interaction. *Cancer research*, 68(4), pp.1092–9.

Najy, A.J., Day, K.C. & Day, M.L., 2008b. The ectodomain shedding of E-cadherin by ADAM15 supports ErbB receptor activation. *The Journal of biological chemistry*, 283(26), pp.18393–401.

Nakamura, K. et al., 2008. Hepsin inhibits the cell growth of endometrial cancer. *International journal of molecular medicine*, 22(3), pp.389–97.

Nakamura, K. et al., 2006. Hepsin shows inhibitory effects through apoptotic pathway on ovarian cancer cell lines. *International journal of oncology*, 28(2), pp.393–8.

Nanba, D. et al., 2003. Proteolytic release of the carboxy-terminal fragment of proHB-EGF causes nuclear export of PLZF. *The Journal of cell biology*, 163(3), pp.489–502.

Nanba, D. & Higashiyama, S., 2004. Dual intracellular signaling by proteolytic cleavage of membrane-anchored heparin-binding EGF-like growth factor. *Cytokine & Growth Factor Reviews*, 15(1), pp.13–19.

Nandana, S. et al., 2010. Hepsin cooperates with MYC in the progression of adenocarcinoma in a prostate cancer mouse model. *The Prostate*, 70(6), pp.591–600.

Naresh, A. et al., 2006. The ERBB4/HER4 intracellular domain 4ICD is a BH3-only protein promoting apoptosis of breast cancer cells. *Cancer research*, 66(12), pp.6412–20.

Narla, G. et al., 2001. KLF6, a candidate tumor suppressor gene mutated in prostate cancer. *Science (New York, N.Y.)*, 294(5551), pp.2563–6.

Nath, D. et al., 1999. Interaction of metargidin (ADAM-15) with alphavbeta3 and alpha5beta1 integrins on different haemopoietic cells. *Journal of cell science*, 112 (Pt 4, pp.579–87.

Netzel-Arnett, S. et al., 2006. Evidence for a matriptase-prostasin proteolytic cascade regulating terminal epidermal differentiation. *The Journal of biological chemistry*, 281(44), pp.32941–5.

Netzel-Arnett, S. et al., 2003. Membrane anchored serine proteases: a rapidly expanding group of cell surface proteolytic enzymes with potential roles in cancer. *Cancer metastasis reviews*, 22(2-3), pp.237–58.

Ni, C.Y. et al., 2001. gamma -Secretase cleavage and nuclear localization of ErbB-4 receptor tyrosine kinase. *Science (New York, N.Y.)*, 294(5549), pp.2179–81.

Nicolas, G. et al., 2002. The gene encoding the iron regulatory peptide hepcidin is regulated by anemia, hypoxia, and inflammation. *The Journal of clinical investigation*, 110(7), pp.1037–44.

Nilsson, J. et al., 1997. Affinity fusion strategies for detection, purification, and immobilization of recombinant proteins. *Protein expression and purification*, 11(1), pp.1–16.

O'Brien, C.A. et al., 2007. A human colon cancer cell capable of initiating tumour growth in immunodeficient mice. *Nature*, 445(7123), pp.106–10.

O'Shea, C. et al., 2003. Expression of ADAM-9 mRNA and protein in human breast cancer. *International journal of cancer. Journal international du cancer*, 105(6), pp.754–61.

Oberst, M. et al., 2001. Matriptase and HAI-1 are expressed by normal and malignant epithelial cells in vitro and in vivo. *The American journal of pathology*, 158(4), pp.1301–11.

Oberst, M.D., Singh, B., et al., 2003. Characterization of matriptase expression in normal human tissues. *The journal of histochemistry and cytochemistry : official journal of the Histochemistry Society*, 51(8), pp.1017–25.

Oberst, M.D. et al., 2002. Expression of the serine protease matriptase and its inhibitor HAI-1 in epithelial ovarian cancer: correlation with clinical outcome and tumor clinicopathological parameters. *Clinical cancer research : an official journal of the American Association for Cancer Research*, 8(4), pp.1101–7.

Oberst, M.D. et al., 2005. HAI-1 regulates activation and expression of matriptase, a membrane-bound serine protease. *American journal of physiology. Cell physiology*, 289(2), pp.C462–70.

Oberst, M.D., Williams, C.A., et al., 2003. The activation of matriptase requires its noncatalytic domains, serine protease domain, and its cognate inhibitor. *The Journal of biological chemistry*, 278(29), pp.26773–9.

Odet, F., Verot, A. & Le Magueresse-Battistoni, B., 2006. The mouse testis is the source of various serine proteases and serine proteinase inhibitors (SERPINs): Serine proteases and SERPINs identified in Leydig cells are under gonadotropin regulation. *Endocrinology*, 147(9), pp.4374–83.

Le Pabic, H. et al., 2003. ADAM12 in human liver cancers: TGF-beta-regulated expression in stellate cells is associated with matrix remodeling. *Hepatology (Baltimore, Md.)*, 37(5), pp.1056–66.

Pace, G., Pomante, R. & Vicentini, C., 2012. Hepsin in the diagnosis of prostate cancer. *Minerva urologica e nefrologica = The Italian journal of urology and nephrology*, 64(2), pp.143–8.

Parekh, N. et al., 2008. Associations of lifestyle and physiologic factors with prostate-specific antigen concentrations: evidence from the National Health and Nutrition Examination Survey (2001-2004). *Cancer epidemiology, biomarkers & prevention*, 17(9), pp.2467–72.

Park, S.Y. et al., 2011. Promoter CpG island hypermethylation during breast cancer progression. *Virchows Archiv : an international journal of pathology*, 458(1), pp.73–84.

Parr, C. et al., 2007. Matriptase-2 inhibits breast tumor growth and invasion and correlates with favorable prognosis for breast cancer patients. *Clinical cancer research : an official journal of the American Association for Cancer Research*, 13(12), pp.3568–76.

Parry, D.A. et al., 2009. Loss of the metalloprotease ADAM9 leads to cone-rod dystrophy in humans and retinal degeneration in mice. *American journal of human genetics*, 84(5), pp.683–91.

Patthy, L. & Nikolics, K., 1993. Functions of agrin and agrin-related proteins. *Trends in neurosciences*, 16(2), pp.76–81.

Pearson, H.A. & Peers, C., 2006. Physiological roles for amyloid beta peptides. *The Journal of physiology*, 575(Pt 1), pp.5–10.

Peduto, L. et al., 2006. ADAM12 is highly expressed in carcinoma-associated stroma and is required for mouse prostate tumor progression. *Oncogene*, 25(39), pp.5462–6.

Peduto, L. et al., 2005. Critical function for ADAM9 in mouse prostate cancer. *Cancer research*, 65(20), pp.9312–9.

Phillips, D.J. & de Kretser, D.M., 1998. Follistatin: a multifunctional regulatory protein. *Frontiers in neuroendocrinology*, 19(4), pp.287–322.

Phong, M.-C. et al., 2003. Molecular mechanisms of L-selectin-induced co-localization in rafts and shedding [corrected]. *Biochemical and biophysical research communications*, 300(2), pp.563–9.

Pienta, K.J., 2009. Critical appraisal of prostate-specific antigen in prostate cancer screening: 20 years later. *Urology*, 73(5 Suppl), pp.S11–20..

Poghosyan, Z. et al., 2002. Phosphorylation-dependent interactions between ADAM15 cytoplasmic domain and Src family protein-tyrosine kinases. *The Journal of biological chemistry*, 277(7), pp.4999–5007.

Porter, D.H., Cook, R.J. & Wagner, C., 1985. Enzymatic properties of dimethylglycine dehydrogenase and sarcosine dehydrogenase from rat liver. *Archives of biochemistry and biophysics*, 243(2), pp.396–407.

Porteu, F. & Nathan, C., 1990. Shedding of tumor necrosis factor receptors by activated human neutrophils. *Journal of Experimental Medicine*, 172(2), pp.599–607.

Pound, C.R. et al., 1999. Natural history of progression after PSA elevation following radical prostatectomy. *JAMA : the journal of the American Medical Association*, 281(17), pp.1591–7.

Prenzel, N. et al., 1999. EGF receptor transactivation by G-protein-coupled receptors requires metalloproteinase cleavage of proHB-EGF. *Nature*, 402(6764), pp.884–8.

Qiu, D. et al., 2007. Roles and regulation of membrane-associated serine proteases. *Biochemical Society transactions*, 35(Pt 3), pp.583–7.

Quayle, S.N. & Sadar, M.D., 2006. A truncated isoform of TMEFF2 encodes a secreted protein in prostate cancer cells. *Genomics*, 87(5), pp.633–7.

Raines, E.W. et al., 1992. The extracellular glycoprotein SPARC interacts with platelet-derived growth factor (PDGF)-AB and -BB and inhibits the binding of PDGF to its receptors. *Proceedings of the National Academy of Sciences of the United States of America*, 89(4), pp.1281–5.

Ralhan, R. et al., 2010. EpCAM nuclear localization identifies aggressive thyroid cancer and is a marker for poor prognosis. *BMC cancer*, 10, p.331.

Ramsay, A.J., Hooper, J.D., et al., 2009. Matriptase-2 (TMPRSS6): a proteolytic regulator of iron homeostasis. *Haematologica*, 94(6), pp.840–9.

Ramsay, A.J., Quesada, V., et al., 2009. Matriptase-2 mutations in iron-refractory iron deficiency anemia patients provide new insights into protease activation mechanisms. *Human molecular genetics*, 18(19), pp.3673–83.

Ratan, H.L. et al., 2003. ErbB receptors : possible therapeutic targets in prostate cancer ?

Ray, A., Dhar, S. & Ray, B.K., 2010. Transforming growth factor-beta1-mediated activation of NF-kappaB contributes to enhanced ADAM-12 expression in mammary carcinoma cells. *Molecular cancer research : MCR*, 8(9), pp.1261–70.

Reddy, P. et al., 2000. Functional analysis of the domain structure of tumor necrosis factor-alpha converting enzyme. *The Journal of biological chemistry*, 275(19), pp.14608–14.

Ricci-Vitiani, L. et al., 2007. Identification and expansion of human colon-cancer-initiating cells. *Nature*, 445(7123), pp.111–5.

Riddick, A.C.P. et al., 2005. Identification of degradome components associated with prostate cancer progression by expression analysis of human prostatic tissues. *British journal of cancer*, 92(12), pp.2171–80.

Riggs, P., 2000. Expression and purification of recombinant proteins by fusion to maltose-binding protein. *Molecular biotechnology*, 15(1), pp.51–63.

Rio, C. et al., 2000. Tumor necrosis factor-alpha-converting enzyme is required for cleavage of erbB4/HER4. *The Journal of biological chemistry*, 275(14), pp.10379–87.

Rose-John, S. et al., 2006. Interleukin-6 biology is coordinated by membrane-bound and soluble receptors: role in inflammation and cancer. *Journal of leukocyte biology*, 80(2), pp.227–36.

Rose-John, S. & Heinrich, P.C., 1994. Soluble receptors for cytokines and growth factors: generation and biological function. *The Biochemical journal*, 300 (Pt 2, pp.281–90.

Roy, R. et al., 2004. ADAM 12 cleaves extracellular matrix proteins and correlates with cancer status and stage. *The Journal of biological chemistry*, 279(49), pp.51323–30.

Roy, R. et al., 2011. ADAM12 transmembrane and secreted isoforms promote breast tumor growth: a distinct role for ADAM12-S protein in tumor metastasis. *The Journal of biological chemistry*, 286(23), pp.20758–68.

Sahin, U. et al., 2004. Distinct roles for ADAM10 and ADAM17 in ectodomain shedding of six EGFR ligands. *The Journal of cell biology*, 164(5), pp.769–79.

Saleem, M. et al., 2006. A novel biomarker for staging human prostate adenocarcinoma: overexpression of matriptase with concomitant loss of its inhibitor, hepatocyte growth factor activator inhibitor-1. *Cancer epidemiology, biomarkers & prevention : a publication of the American Association for Cancer Research, cosponsored by the American Society of Preventive Oncology*, 15(2), pp.217–27.

Sanders, A.J. et al., 2006. Genetic reduction of matriptase-1 expression is associated with a reduction in the aggressive phenotype of prostate cancer cells in vitro and in vivo. *Journal of experimental therapeutics & oncology*, 6(1), pp.39–48.

Sanders, A.J. et al., 2008. Genetic upregulation of matriptase-2 reduces the aggressiveness of prostate cancer cells in vitro and in vivo and affects FAK and paxillin localisation. *Journal of cellular physiology*, 216(3), pp.780–9.

Sanders, A.J. et al., 2007. Suppression of hepatocyte growth factor activator inhibitor-1 leads to a more aggressive phenotype of prostate cancer cells in vitro. *International journal of molecular medicine*, 20(4), pp.613–9.

Sato, F. et al., 2002. Aberrant methylation of the HPP1 gene in ulcerative colitis-associated colorectal carcinoma. *Cancer research*, 62(23), pp.6820–2.

Satomi, S. et al., 2001. A role for membrane-type serine protease (MT-SP1) in intestinal epithelial turnover. *Biochemical and biophysical research communications*, 287(4), pp.995–1002.

Schäfer, B., Gschwind, A. & Ullrich, A., 2004. Multiple G-protein-coupled receptor signals converge on the epidermal growth factor receptor to promote migration and invasion. *Oncogene*, 23(4), pp.991–9.

Schier, A.F. & Shen, M.M., 2000. Nodal signalling in vertebrate development. *Nature*, 403(6768), pp.385–9.

Schild, L. & Kellenberger, S., 2001. Structure function relationships of ENaC and its role in sodium handling. *Advances in experimental medicine and biology*, 502, pp.305–14.

Schlomann, U. et al., 2002. The metalloprotease disintegrin ADAM8. Processing by autocatalysis is required for proteolytic activity and cell adhesion. *The Journal of biological chemistry*, 277(50), pp.48210–9.

Schroeter, E.H., Kisslinger, J.A. & Kopan, R., 1998. Notch-1 signalling requires ligand-induced proteolytic release of intracellular domain. *Nature*, 393(6683), pp.382–6.

Schulze, W.X., Deng, L. & Mann, M., 2005. Phosphotyrosine interactome of the ErbB-receptor kinase family. *Molecular systems biology*, 1, p.2005.0008.

Schuurmans, A.L., Bolt, J. & Mulder, E., 1988. Androgens and transforming growth factor beta modulate the growth response to epidermal growth factor in human prostatic tumor cells (LNCaP). *Molecular and cellular endocrinology*, 60(1), pp.101–4.

Scudiero, D.A. et al., 1988. Evaluation of a soluble tetrazolium/formazan assay for cell growth and drug sensitivity in culture using human and other tumor cell lines. *Cancer research*, 48(17), pp.4827–33.

Seals, D.F. et al., 2005. The adaptor protein Tks5/Fish is required for podosome formation and function, and for the protease-driven invasion of cancer cells. *Cancer cell*, 7(2), pp.155–65.

Seals, D.F. & Courtneidge, S.A., 2003. The ADAMs family of metalloproteases: multidomain proteins with multiple functions. *Genes & development*, 17(1), pp.7–30.

Seiki, M., 1999. Membrane-type matrix metalloproteinases. *APMIS : acta pathologica, microbiologica, et immunologica Scandinavica*, 107(1), pp.137–43.

Selzer-Plon, J. et al., 2009. Expression of prostasin and its inhibitors during colorectal cancer carcinogenesis. *BMC cancer*, 9, p.201.

Semenov, A. V. et al., 1999. Production of soluble P-selectin by platelets and endothelial cells. *Biochemistry*, 64(11), pp.1326–1335.

Shaffer, A.L. et al., 2000. BCL-6 represses genes that function in lymphocyte differentiation, inflammation, and cell cycle control. *Immunity*, 13(2), pp.199–212.

Shaffer, D. et al., 2005. Evidence for a p27 tumor suppressive function independent of its role regulating cell proliferation in the prostate. *Proceedings of the National Academy of Sciences of the United States of America*, 102(1), pp.210–5.

Shah, S. et al., 2005. Nicastrin functions as a gamma-secretase-substrate receptor. *Cell*, 122(3), pp.435–47.

Shaknovich, R. et al., 1998. The promyelocytic leukemia zinc finger protein affects myeloid cell growth, differentiation, and apoptosis. *Molecular and cellular biology*, 18(9), pp.5533–45.

Sheeley, D.M., Merrill, B.M. & Taylor, L.C., 1997. Characterization of monoclonal antibody glycosylation: comparison of expression systems and identification of terminal alpha-linked galactose. *Analytical biochemistry*, 247(1), pp.102–10.

Shi, Y.E. et al., 1993. Identification and Characterization of a Novel Matrix-degrading Protease from Hormone-dependent Human Breast Cancer Cells. *Cancer Res.*, 53(6), pp.1409–15.

Shibata, D.M. et al., 2002. Hypermethylation of HPP1 is associated with hMLH1 hypermethylation in gastric adenocarcinomas. *Cancer research*, 62(20), pp.5637–40.

Shintani, Y. et al., 2004. Overexpression of ADAM9 in non-small cell lung cancer correlates with brain metastasis. *Cancer research*, 64(12), pp.4190–6.

Shipway, A. et al., 2004. Biochemical characterization of prostasin, a channel activating protease. *Biochemical and biophysical research communications*, 324(2), pp.953–63.

Siegel, D.A. et al., 2006. Tomoregulin-2 is found extensively in plaques in Alzheimer's disease brain. *Journal of neurochemistry*, 98(1), pp.34–44.

Silvestri, L. et al., 2008. The serine protease matriptase-2 (TMPRSS6) inhibits hepcidin activation by cleaving membrane hemojuvelin. *Cell metabolism*, 8(6), pp.502–11.

Simons, K. & Ikonen, E., 1997. Functional rafts in cell membranes. *Nature*, 387(6633), pp.569–72.

Singh, D. et al., 2002. Gene expression correlates of clinical prostate cancer behavior. *Cancer cell*, 1(2), pp.203–9.

Singh, R.J.R. et al., 2005. Cytokine stimulated vascular cell adhesion molecule-1 (VCAM-1) ectodomain release is regulated by TIMP-3. *Cardiovascular research*, 67(1), pp.39–49.

Singh, S.K. et al., 2003. Identification of a cancer stem cell in human brain tumors. *Cancer research*, 63(18), pp.5821–8.

Sjöblom, T. et al., 2006. The consensus coding sequences of human breast and colorectal cancers. *Science (New York, N.Y.)*, 314(5797), pp.268–74.

Soller, M.J. et al., 2006. Confirmation of the high frequency of the TMPRSS2/ERG fusion gene in prostate cancer. *Genes, chromosomes & cancer*, 45(7), pp.717–9.

Solomon, E. et al., 2010. The role of SnoN in transforming growth factor beta1-induced expression of metalloprotease-disintegrin ADAM12. *The Journal of biological chemistry*, 285(29), pp.21969–77.

Sørensen, H.P. et al., 2008. Heparan sulfate regulates ADAM12 through a molecular switch mechanism. *The Journal of biological chemistry*, 283(46), pp.31920–32.

Sreekumar, A. et al., 2009. Metabolomic profiles delineate potential role for sarcosine in prostate cancer progression. *Nature*, 457(7231), pp.910–4.

Srikantan, V., Valladares, M. & Rhim, J.S., 2002. HEPSIN Inhibits Cell Growth / Invasion in Prostate Cancer Cells HEPSIN Inhibits Cell Growth / Invasion in Prostate Cancer Cells 1. *Cancer research*, pp.6812–6816.

Stautz, D. et al., 2010. ADAM12 localizes with c-Src to actin-rich structures at the cell periphery and regulates Src kinase activity. *Experimental cell research*, 316(1), pp.55–67.

Stautz, D., Wewer, U.M. & Kveiborg, M., 2012. Functional analysis of a breast cancer-associated mutation in the intracellular domain of the metalloprotease ADAM12. *PloS one*, 7(5), p.e37628.

Stenflo, J., 1991. Structure-function relationships of epidermal growth factor modules in vitamin K-dependent clotting factors. *Blood*, 78(7), pp.1637–51.

Stephan, C. et al., 2004. Hepsin is highly over expressed in and a new candidate for a prognostic indicator in prostate cancer. *The Journal of urology*, 171(1), pp.187–91.

Stirnberg, M. et al., 2010. Proteolytic processing of the serine protease matriptase-2: identification of the cleavage sites required for its autocatalytic release from the cell surface. *The Biochemical journal*, 430(1), pp.87–95.

Subramanian, S. V, Fitzgerald, M.L. & Bernfield, M., 1997. Regulated shedding of syndecan-1 and -4 ectodomains by thrombin and growth factor receptor activation. *The Journal of biological chemistry*, 272(23), pp.14713–20.

Suen, J.Y. et al., 2012. Modulating human proteinase activated receptor 2 with a novel antagonist (GB88) and agonist (GB110). *British journal of pharmacology*, 165(5), pp.1413–23.

Sun, P., Tropea, J.E. & Waugh, D.S., 2011. Enhancing the solubility of recombinant proteins in Escherichia coli by using hexahistidine-tagged maltose-binding protein as a fusion partner. *Methods in molecular biology (Clifton, N.J.)*, 705, pp.259–74.

Sundberg, C. et al., 2004. Regulation of ADAM12 cell-surface expression by protein kinase C epsilon. *The Journal of biological chemistry*, 279(49), pp.51601–11.

Sung, S.-Y. et al., 2006. Oxidative stress induces ADAM9 protein expression in human prostate cancer cells. *Cancer research*, 66(19), pp.9519–26.

Sunnarborg, S.W. et al., 2002. Tumor necrosis factor-alpha converting enzyme (TACE) regulates epidermal growth factor receptor ligand availability. *The Journal of biological chemistry*, 277(15), pp.12838–45.

Suzuki, M., 1997. Matrix Metalloproteinase-3 Releases Active Heparin-binding EGF-like Growth Factor by Cleavage at a Specific Juxtamembrane Site. *Journal of Biological Chemistry*, 272(50), pp.31730–31737.

Szabo, R. et al., 2007. Matriptase inhibition by hepatocyte growth factor activator inhibitor-1 is essential for placental development. *Oncogene*, 26(11), pp.1546–56.

Szabo, R. et al., 2005. Matriptase-3 is a novel phylogenetically preserved membrane-anchored serine protease with broad serpin reactivity. *The Biochemical journal*, 390(Pt 1), pp.231–42.

Szabo, R. et al., 2003. Type II transmembrane serine proteases. *Thrombosis and haemostasis*, 90(2), pp.185–93.

Szabo, R. & Bugge, T.H., 2008. Type II transmembrane serine proteases in development and disease. *The international journal of biochemistry & cell biology*, 40(6-7), pp.1297–316.

Szláma, G. et al., 2010. WFIKKN1 and WFIKKN2 bind growth factors TGFβ1, BMP2 and BMP4 but do not inhibit their signalling activity. *The FEBS journal*, 277(24), pp.5040–50.

Takahashi, S. et al., 2003. Down-regulated expression of prostasin in high-grade or hormone-refractory human prostate cancers. *The Prostate*, 54(3), pp.187–93.

Takeda, S. et al., 2006. Crystal structures of VAP1 reveal ADAMs' MDC domain architecture and its unique C-shaped scaffold. *The EMBO journal*, 25(11), pp.2388–96.

Takenobu, H. et al., 2003. The stress- and inflammatory cytokine-induced ectodomain shedding of heparin-binding epidermal growth factor-like growth factor is mediated by p38 MAPK, distinct from the 12-O-tetradecanoylphorbol-13-acetate- and lysophosphatidic acid-induced signaling ca. *The Journal of biological chemistry*, 278(19), pp.17255–62.

Takeuchi, T. et al., 2000. Cellular localization of membrane-type serine protease 1 and identification of protease-activated receptor-2 and single-chain urokinase-type plasminogen activator as substrates. *The Journal of biological chemistry*, 275(34), pp.26333–42.

Tanaka, M. et al., 2004. ADAM binding protein Eve-1 is required for ectodomain shedding of epidermal growth factor receptor ligands. *The Journal of biological chemistry*, 279(40), pp.41950–9.

Tanaka, Y. et al., 2003. Protein kinase C promotes apoptosis in LNCaP prostate cancer cells through activation of p38 MAPK and inhibition of the Akt survival pathway. *The Journal of biological chemistry*, 278(36), pp.33753–62.

Tanida, S. et al., 2004. The mechanism of cleavage of EGFR ligands induced by inflammatory cytokines in gastric cancer cells. *Gastroenterology*, 127(2), pp.559–69..

Tanimoto, H. et al., 1997. Hepsin, a cell surface serine protease identified in hepatoma cells, is overexpressed in ovarian cancer. *Cancer research*, 57(14), pp.2884–7.

Thabard, W. et al., 2001. Protein kinase C delta and eta isoenzymes control the shedding of the interleukin 6 receptor alpha in myeloma cells. *The Biochemical journal*, 358(Pt 1), pp.193–200.

Thodeti, C.K. et al., 2003. ADAM12/syndecan-4 signaling promotes beta 1 integrin-dependent cell spreading through protein kinase Calpha and RhoA. *The Journal of biological chemistry*, 278(11), pp.9576–84.

Tilley, W.D. et al., 1996. Mutations in the androgen receptor gene are associated with progression of human prostate cancer to androgen independence. *Clinical cancer research : an official journal of the American Association for Cancer Research*, 2(2), pp.277–85.

Toki, F. et al., 2005. Ectodomain shedding of membrane-anchored heparin-binding EGF like growth factor and subcellular localization of the C-terminal fragment in the cell cycle. *Journal of cellular physiology*, 202(3), pp.839–48.

Tomoda, H. & Omura, S., 2000. Lactacystin, a proteasome inhibitor: discovery and its application in cell biology. *Yakugaku zasshi : Journal of the Pharmaceutical Society of Japan*, 120(10), pp.935–49.

Tong, Z. et al., 2004. Prostasin, a membrane-anchored serine peptidase, regulates sodium currents in JME/CF15 cells, a cystic fibrosis airway epithelial cell line. *American journal of physiology. Lung cellular and molecular physiology*, 287(5), pp.L928–35.

Tripathi, M. et al., 2011. Laminin-332 cleavage by matriptase alters motility parameters of prostate cancer cells. *The Prostate*, 71(2), pp.184–96.

Tripathi, M. et al., 2008. Laminin-332 is a substrate for hepsin, a protease associated with prostate cancer progression. *The Journal of biological chemistry*, 283(45), pp.30576–84.

Trochon-Joseph, V. et al., 2004. Evidence of antiangiogenic and antimetastatic activities of the recombinant disintegrin domain of metargidin. *Cancer research*, 64(6), pp.2062–9.

Truksa, J. et al., 2006. Bone morphogenetic proteins 2, 4, and 9 stimulate murine hepcidin 1 expression independently of Hfe, transferrin receptor 2 (Tfr2), and IL-6. *Proceedings of the National Academy of Sciences of the United States of America*, 103(27), pp.10289–93.

Tseng, I.-C. et al., 2010. Matriptase activation, an early cellular response to acidosis. *The Journal of biological chemistry*, 285(5), pp.3261–70.

Tsuji, A. et al., 1991. Hepsin, a cell membrane-associated protease. Characterization, tissue distribution, and gene localization. *The Journal of biological chemistry*, 266(25), pp.16948–53.

Tsuzuki, S. et al., 2005. Evidence for the occurrence of membrane-type serine protease 1/matriptase on the basolateral sides of enterocytes. *The Biochemical journal*, 388(Pt 2), pp.679–87.

Tuzi, N.L. & Gullick, W.J., 1994. eph, the largest known family of putative growth factor receptors. *British journal of cancer*, 69(3), pp.417–21.

Uchida, T. et al., 1999. A novel epidermal growth factor-like molecule containing two follistatin modules stimulates tyrosine phosphorylation of erbB-4 in MKN28 gastric cancer cells. *Biochemical and biophysical research communications*, 266(2), pp.593–602.

Uhland, K., 2006. Matriptase and its putative role in cancer. *Cellular and molecular life sciences : CMLS*, 63(24), pp.2968–78.

Umbas, R. et al., 1994. Decreased E-cadherin expression is associated with poor prognosis in patients with prostate cancer. *Cancer research*, 54(14), pp.3929–33.

Urban, S. & Freeman, M., 2002. Intramembrane proteolysis controls diverse signalling pathways throughout evolution. *Current opinion in genetics & development*, 12(5), pp.512–8.

Vaarala, M.H. et al., 2001. The TMPRSS2 gene encoding transmembrane serine protease is overexpressed in a majority of prostate cancer patients: detection of mutated TMPRSS2 form in a case of aggressive disease. *International journal of cancer. Journal international du cancer*, 94(5), pp.705–10.

Vasioukhin, V., 2004. Hepsin paradox reveals unexpected complexity of metastatic process. *Cell cycle (Georgetown, Tex.)*, 3(11), pp.1394–7.

Velasco, G. et al., 2002. Matriptase-2, a membrane-bound mosaic serine proteinase predominantly expressed in human liver and showing degrading activity against extracellular matrix proteins. *The Journal of biological chemistry*, 277(40), pp.37637–46.

Veldscholte, J. et al., 1990. Unusual specificity of the androgen receptor in the human prostate tumor cell line LNCaP: high affinity for progestagenic and estrogenic steroids. *Biochimica et biophysica acta*, 1052(1), pp.187–94.

Verghese, G.M., Gutknecht, M.F. & Caughey, G.H., 2006. Prostasin regulates epithelial monolayer function: cell-specific Gpld1-mediated secretion and functional role for GPI anchor. *American journal of physiology. Cell physiology*, 291(6), pp.C1258–70.

Vidal, G.A. et al., 2005. Presenilin-dependent gamma-secretase processing regulates multiple ERBB4/HER4 activities. *The Journal of biological chemistry*, 280(20), pp.19777–83.

Vis, A.N. & Schröder, F.H., 2009. Key targets of hormonal treatment of prostate cancer. Part 1: the androgen receptor and steroidogenic pathways. *BJU international*, 104(4), pp.438–48.

Visakorpi, T. et al., 1995. In vivo amplification of the androgen receptor gene and progression of human prostate cancer. *Nature genetics*, 9(4), pp.401–6.

Vogel, L.K. et al., 2006. The ratio of Matriptase/HAI-1 mRNA is higher in colorectal cancer adenomas and carcinomas than corresponding tissue from control individuals. *BMC cancer*, 6, p.176.

Wadhawan, V. et al., 2012. From prediction to experimental validation: desmoglein 2 is a functionally relevant substrate of matriptase in epithelial cells and their reciprocal relationship is important for cell adhesion. *The Biochemical journal*, 447(1), pp.61–70.

Wallrapp, C. et al., 2000. A novel transmembrane serine protease (TMPRSS3) overexpressed in pancreatic cancer. *Cancer research*, 60(10), pp.2602–6.

Wang, J.-K. et al., 2009. Polarized epithelial cells secrete matriptase as a consequence of zymogen activation and HAI-1-mediated inhibition. *American journal of physiology. Cell physiology*, 297(2), pp.C459–70.

Wang, M.M., 2011. Notch signaling and Notch signaling modifiers. *The international journal of biochemistry & cell biology*, 43(11), pp.1550–62.

Wang, S.I., Parsons, R. & Ittmann, M., 1998. Homozygous deletion of the PTEN tumor suppressor gene in a subset of prostate adenocarcinomas. *Clinical cancer research : an official journal of the American Association for Cancer Research*, 4(3), pp.811–5..

Wang, X. et al., 2006. Cytoplasmic domain phosphorylation of heparin-binding EGF-like growth factor. *Cell structure and function*, 31(1), pp.15–27.

Weber, S. & Saftig, P., 2012. Ectodomain shedding and ADAMs in development. *Development (Cambridge, England)*, 139(20), pp.3693–709.

Went, P. et al., 2006. Frequent high-level expression of the immunotherapeutic target Ep-CAM in colon, stomach, prostate and lung cancers. *British journal of cancer*, 94(1), pp.128–35.

Werner, R.G., 1998. Innovative and economic potential of mammalian cell culture. *Arzneimittel-Forschung*, 48(4), pp.423–6.

Weskamp, G. et al., 1996. MDC9, a widely expressed cellular disintegrin containing cytoplasmic SH3 ligand domains. *The Journal of cell biology*, 132(4), pp.717–26..

Weskamp, G. et al., 2002. Mice lacking the metalloprotease-disintegrin MDC9 (ADAM9) have no evident major abnormalities during development or adult life. *Molecular and cellular biology*, 22(5), pp.1537–44.

Wewer, U.M. et al., 2006. ADAM12 is a four-leafed clover: the excised prodomain remains bound to the mature enzyme. *The Journal of biological chemistry*, 281(14), pp.9418–22.

Wheeler, D.L. et al., 2003. Protein kinase Cepsilon is linked to 12-O-tetradecanoylphorbol-13-acetate-induced tumor necrosis factor-alpha ectodomain shedding and the development of metastatic squamous cell carcinoma in protein kinase Cepsilon transgenic mice. *Cancer research*, 63(19), pp.6547–55.

Williams, C.C. et al., 2004. The ERBB4/HER4 receptor tyrosine kinase regulates gene expression by functioning as a STAT5A nuclear chaperone. *The Journal of cell biology*, 167(3), pp.469–78.

Wilson, K.J. et al., 2009. Functional selectivity of EGF family peptide growth factors: implications for cancer. *Pharmacology & therapeutics*, 122(1), pp.1–8.

Wittig-Blaich, S.M. et al., 2011. Matrix-dependent regulation of AKT in Hepsin-overexpressing PC3 prostate cancer cells. *Neoplasia (New York, N.Y.)*, 13(7), pp.579–89.

Wolfe, M.S. et al., 1999. Two transmembrane aspartates in presenilin-1 required for presenilin endoproteolysis and gamma-secretase activity. *Nature*, 398(6727), pp.513–7.

Wolfsberg, T.G. et al., 1995. ADAM, a novel family of membrane proteins containing A Disintegrin And Metalloprotease domain: multipotential functions in cell-cell and cell-matrix interactions. *The Journal of cell biology*, 131(2), pp.275–8.

Wolfsberg, T.G. et al., 1993. The precursor region of a protein active in sperm-egg fusion contains a metalloprotease and a disintegrin domain: structural, functional, and evolutionary implications. *Proceedings of the National Academy of Sciences of the United States of America*, 90(22), pp.10783–7.

Wouters, M.A. et al., 2005. Evolution of distinct EGF domains with specific functions. *Protein science : a publication of the Protein Society*, 14(4), pp.1091–103.

Wu, Q. et al., 1998. Generation and characterization of mice deficient in hepsin, a hepatic transmembrane serine protease. *The Journal of clinical investigation*, 101(2), pp.321–6.

Wu, S.-R. et al., 2010. Matriptase is involved in ErbB-2-induced prostate cancer cell invasion. *The American journal of pathology*, 177(6), pp.3145–58.

Wyble, C. et al., 1997. TNF-α and IL-1 Upregulate Membrane-Bound and Soluble E-Selectin through a Common Pathway. *Journal of Surgical Research*, 73(2), pp.107–112.

Xing, P. et al., 2011. Clinical and biological significance of hepsin overexpression in breast cancer. *Journal of investigative medicine : the official publication of the American Federation for Clinical Research*, 59(5), pp.803–10.

Yamada, D. et al., 2007. Increased expression of ADAM 9 and ADAM 15 mRNA in pancreatic cancer. *Anticancer research*, 27(2), pp.793–9.

Yamaoka, K. et al., 1998. Cloning and characterization of the cDNA for human airway trypsin-like protease. *The Journal of biological chemistry*, 273(19), pp.11895–901.

Yan, W. et al., 1999. Corin, a mosaic transmembrane serine protease encoded by a novel cDNA from human heart. *The Journal of biological chemistry*, 274(21), pp.14926–35.

Yan, Y., Shirakabe, K. & Werb, Z., 2002. The metalloprotease Kuzbanian (ADAM10) mediates the transactivation of EGF receptor by G protein-coupled receptors. *The Journal of cell biology*, 158(2), pp.221–6.

Yasuoka, S. et al., 1997. Purification, characterization, and localization of a novel trypsin-like protease found in the human airway. *American journal of respiratory cell and molecular biology*, 16(3), pp.300–8.

Yeyati, P.L. et al., 1999. Leukemia translocation protein PLZF inhibits cell growth and expression of cyclin A. *Oncogene*, 18(4), pp.925–34.

Young, J. et al., 2001. HPP1: a transmembrane protein-encoding gene commonly methylated in colorectal polyps and cancers. *Proceedings of the National Academy of Sciences of the United States of America*, 98(1), pp.265–70.

Yu, J.X., Chao, L. & Chao, J., 1995. Molecular cloning, tissue-specific expression, and cellular localization of human prostasin mRNA. *The Journal of biological chemistry*, 270(22), pp.13483–9.

Yu, J.X., Chao, L. & Chao, J., 1994. Prostasin is a novel human serine proteinase from seminal fluid. Purification, tissue distribution, and localization in prostate gland. *The Journal of biological chemistry*, 269(29), pp.18843–8.

Yuan, X. et al., 1998. Structure of murine enterokinase (enteropeptidase) and expression in small intestine during development. *The American journal of physiology*, 274(2 Pt 1), pp.G342–9.

Zacharski, L.R. et al., 1998. Expression of the factor VII activating protease, hepsin, in situ in renal cell carcinoma. *Thrombosis and haemostasis*, 79(4), pp.876–7.

Zhang, L. & Esko, J.D., 1994. Amino acid determinants that drive heparan sulfate assembly in a proteoglycan. *The Journal of biological chemistry*, 269(30), pp.19295–9.

Zhang, X.P. et al., 1998. Specific interaction of the recombinant disintegrin-like domain of MDC-15 (metargidin, ADAM-15) with integrin alphavbeta3. *The Journal of biological chemistry*, 273(13), pp.7345–50.

Zhao, X.-Y. et al., 2005. Targeting tomoregulin for radioimmunotherapy of prostate cancer. *Cancer research*, 65(7), pp.2846–53.

Zhao, Z. et al., 2004. Interaction of the disintegrin and cysteine-rich domains of ADAM12 with integrin alpha7beta1. *Experimental cell research*, 298(1), pp.28–37.

Zhong, J.L. et al., 2008. Distinct functions of natural ADAM-15 cytoplasmic domain variants in human mammary carcinoma. *Molecular cancer research : MCR*, 6(3), pp.383–94.

Zigrino, P. et al., 2007. Role of ADAM-9 disintegrin-cysteine-rich domains in human keratinocyte migration. *The Journal of biological chemistry*, 282(42), pp.30785–93.

Appendix I: Buffers and solutions

AP buffer

100 mM Tris-HCl pH 9.5

100 mM NaCl

20 mM $MgCl_2$

Buffer C

10 mM HEPES pH 7.9

10 mM KCl

0.1 mM EDTA

Add freshly: 1 mM DTT (Sigma-Aldrich), 8 mM β-glycerophosphate (Sigma-Aldrich), 300 µM sodium ortovanadate (Sigma-Aldrich), protease inhibitor cocktail (Sigma-Aldrich, 10 µl per 1 ml of buffer)

Buffer N

20 mM HEPES pH 7.9

10% glycerol (v/v)

0.4 M NaCl

1 mM EDTA

1 mM EGTA

Add freshly: 1 mM DTT (Sigma-Aldrich), 8 mM β-glycerophosphate (Sigma-Aldrich), 300 µM sodium ortovanadate (Sigma-Aldrich), protease inhibitor cocktail (Sigma-Aldrich, 10 µl per 1 ml of buffer)

Column buffer

20 mM Tris-HCl pH 7.4

200 mM NaCl

1 mM EDTA (Melford)

Coomassie Brilliant Blue R-250 staining solution

3 % Coomassie Brilliant Blue R-250

10 % acetic acid

45% methanol

Coomassie distain solution

10% acetic acid

50% methanol

His-select elution buffer

50 mM Tris-HCl pH 8.0

300 mM NaCl

250 mM imidazole (Sigma-Aldrich)

His-Select equilibration and wash buffer

50 mM Tris-HCl pH 8.0

300 mM NaCl

10 mM imidazole (Sigma-Aldrich)

Luria-Bertani broth (LB broth, 1 liter)

10g trypton

5g yeast extract

10g NaCl

Phosphate buffered saline (PBS)

10 PBS tablets (OXOID)/1L H_2O

Reducing sample buffer (2x)

3.5 ml dH_2O

1.25 ml 0.5M Tris-HCl pH 6.8

2.5 ml glycerol

2 ml 10% SDS

0.2 ml 0.5% bromophenol blue

0.5 ml 2-mercaptoethanol (Sigma-Aldrich)

Rich broth (1liter)

10g tryptone

5g yeast extract

5g NaCl

2g glucose (Acros Organics)

RIPA lysis buffer

20 mM sodium phosphate pH 7.4

150 mM NaCl

1% v/v Triton-X-100

SDS-PAGE Running buffer

25 mM Tris

190 mM glycine

0.1% SDS

TEA buffer

40 mM Tris acetate

1 mM EDTA

Tris buffered saline (TBS)

50 mM Tris pH 8.0

150 mM NaCl

TBS/Tween 20 (TBST)

TBS + 0.01% Tween-20 (v/v, Sigma)

TST

50 mM Tris-HCl pH 7.6

150 mM NaCl

0.05% Tween 20

Western blot stripping buffer:

62.5 mM Tris-HCl pH 6.8

2% SDS

100 mM β-mercaptoethanol

Western blot transfer buffer

25 mM Tris

190 mM glycine

20% methanol

1% agarose gel

1g agarose

99 ml TEA buffer

10 µl ethidium bromide (Sigma-Aldrich)

1.5% agar plates

7.5 g agar

500 ml LB broth

4% stacking gel

3.2 ml ddH_20

0.5 ml 40% acrylamide/bis-acrylamide solution, 19:1 (Geneflow)

1.25 ml 1 M Tris-HCl pH 6.8

100 µl 10% ammonium persulfate (Sigma-Aldrich)

10 µl TEMED (Sigma-Aldrich)

10% resolving gel

4.9 ml dH_2O

2.5 ml 40% acrylamide/bis-acrylamide solution, 19:1 (Geneflow)

2.5 ml 1.5 M Tris-HCl pH 8.8

100 µl 10% ammonium persulfate (Sigma-Aldrich)

10 µl TEMED

11% resolving gel

4.5 ml dH_2O

3.0 ml 40% acrylamide/bis-acrylamide solution, 19:1 (Geneflow)

2.5 ml 1.5 M Tris-HCl pH 8.8

100 µl 10% ammonium persulfate (Sigma-Aldrich)

10 µl TEMED

12.5% resolving gel

4.2 ml dH_2O

3.2 ml 40% acrylamide/bis-acrylamide solution, 19:1 (Geneflow)

2.5 ml 1.5 M Tris-HCl pH 6.8

100 µl 10% ammonium persulfate (Sigma-Aldrich)

10 µl TEMED

Appendix II : Sequence of MBP-tagged fusion proteins

- MBP TMEFF2-ECD, Mw=76,4 kDa

MKIKTGARILALSALTTMMFSASALAKIEEGKLVIWINGDKGYNGLAEVGKKFEKDTGI
KVTVEHPDKLEEKFPQVAATGDGPDIIFWAHDRFGGYAQSGLLAEITPDKAFQDKLY
PFTWDAVRYNGKLIAYPIAVEALSLIYNKDLLPNPPKTWEEIPALDKELKAKGKSALMF
NLQEPYFTWPLIAADGGYAFKYENGKYDIKDVGVDNAGAKAGLTFLVDLIKNKHMNA
DTDYSIAEAAFNKGETAMTINGPWAWSNIDTSKVNYGVTVLPTFKGQPSKPFVGVLS
AGINAASPNKELAKEFLENYLLTDEGLEAVNKDKPLGAVALKSYEEELAKDPRIAATM
ENAQKGEIMPNIPQMSAFWYAVRTAVINAASGRQTVDEALKDAQTNSSSNNNNNNN
NNNLGIEGRISEFAAFPTSLSDQTPTGWNCSGYDDRENDLFLCDTNTCKFDGECLRI
GDTVTCVCQFKCNNDYVPVCGSNGESYQNECYLRQAACKQQSEILVVSEGSCATD
AGSGSGDGVHEGSGETSQKETSTCDICQFGAECDEDAEDVWCVCNIDCSQTNFNP
LCASDGKSYDNACQIKEASCQKQEKIEVMSLGRCQDNTTTTTKSEDGHYARTDYAE
NANKLEESAREHHIPCPEHYNGFCMHGKCEHSINMQEPSCRCDAGYTGQHCEKKD
YSVLYVVPGPVRFQYV

- MBP 2xFS TMEFF2 V5-6xHis, Mw= 71.7 kDa

MKIKTGARILALSALTTMMFSASALAKIEEGKLVIWINGDKGYNGLAEVGKKFEKDTGI
KVTVEHPDKLEEKFPQVAATGDGPDIIFWAHDRFGGYAQSGLLAEITPDKAFQDKLY
PFTWDAVRYNGKLIAYPIAVEALSLIYNKDLLPNPPKTWEEIPALDKELKAKGKSALMF
NLQEPYFTWPLIAADGGYAFKYENGKYDIKDVGVDNAGAKAGLTFLVDLIKNKHMNA
DTDYSIAEAAFNKGETAMTINGPWAWSNIDTSKVNYGVTVLPTFKGQPSKPFVGVLS
AGINAASPNKELAKEFLENYLLTDEGLEAVNKDKPLGAVALKSYEEELAKDPRIAATM
ENAQKGEIMPNIPQMSAFWYAVRTAVINAASGRQTVDEALKDAQTNSSSNNNNNNN
NNNLGIEGRISEFAAFPTSLSDQTPTGWNCSGYDDRENDLFLCDTNTCKFDGECLRI
GDTVTCVCQFKCNNDYVPVCGSNGESYQNECYLRQAACKQQSEILVVSEGSCATD
AGSGSGDGVHEGSGETSQKETSTCDICQFGAECDEDAEDVWCVCNIDCSQTNFNP
LCASDGKSYDNACQIKEASCQKQEKIEVMSLGRCQDNTTTTTKSEDGHYARTDYAE
LESRGPFEGKPIPNPLLGLDSTRTGHHHHHH

- MBP 2nd FS+EGF TMEFF2, Mw=65 kDa

MKIKTGARILALSALTTMMFSASALAKIEEGKLVIWINGDKGYNGLAEVGKKFEKDTGI
KVTVEHPDKLEEKFPQVAATGDGPDIIFWAHDRFGGYAQSGLLAEITPDKAFQDKLY
PFTWDAVRYNGKLIAYPIAVEALSLIYNKDLLPNPPKTWEEIPALDKELKAKGKSALMF
NLQEPYFTWPLIAADGGYAFKYENGKYDIKDVGVDNAGAKAGLTFLVDLIKNKHMNA
DTDYSIAEAAFNKGETAMTINGPWAWSNIDTSKVNYGVTVLPTFKGQPSKPFVGVLS
AGINAASPNKELAKEFLENYLLTDEGLEAVNKDKPLGAVALKSYEEELAKDPRIAATM
ENAQKGEIMPNIPQMSAFWYAVRTAVINAASGRQTVDEALKDAQTNSSSNNNNNNN
NNNLGIEGRISEFGVHEGSGETSQKETSTCDICQFGAECDEDAEDVWCVCNIDCSQT
NFNPLCASDGKSYDNACQIKEASCQKQEKIEVMSLGRCQDNTTTTTKSEDGHYART
DYAENANKLEESAREHHIPCPEHYNGFCMHGKCEHSINMQEPSCRCDAGYTGQHC
EKKDYSVLYVVPGPVRFQYV

- MBP EGF TMEFF2 V5-His, Mw=57.23 kDa

MKIKTGARILALSALTTMMFSASALAKIEEGKLVIWINGDKGYNGLAEVGKKFEKDTGI
KVTVEHPDKLEEKFPQVAATGDGPDIIFWAHDRFGGYAQSGLLAEITPDKAFQDKLY
PFTWDAVRYNGKLIAYPIAVEALSLIYNKDLLPNPPKTWEEIPALDKELKAKGKSALMF
NLQEPYFTWPLIAADGGYAFKYENGKYDIKDVGVDNAGAKAGLTFLVDLIKNKHMNA
DTDYSIAEAAFNKGETAMTINGPWAWSNIDTSKVNYGVTVLPTFKGQPSKPFVGVLS
AGINAASPNKELAKEFLENYLLTDEGLEAVNKDKPLGAVALKSYEEELAKDPRIAATM
ENAQKGEIMPNIPQMSAFWYAVRTAVINAASGRQTVDEALKDAQTNSSSNNNNNNN
NNNLGIEGRISEFGSGHYARTDYAENANKLEESAREHHIPCPEHYNGFCMHGKCEH
SINMQEPSCRCDAGYTGQHCEKKDYSVLYVLESRGPFEGKPIPNPLLGLDSTRTGH
HHHHH

- MBP $^{H\text{-}R}$EGF TMEFF2, Mw=54.8 kDa

MKIKTGARILALSALTTMMFSASALAKIEEGKLVIWINGDKGYNGLAEVGKKFEKDTGI
KVTVEHPDKLEEKFPQVAATGDGPDIIFWAHDRFGGYAQSGLLAEITPDKAFQDKLY
PFTWDAVRYNGKLIAYPIAVEALSLIYNKDLLPNPPKTWEEIPALDKELKAKGKSALMF
NLQEPYFTWPLIAADGGYAFKYENGKYDIKDVGVDNAGAKAGLTFLVDLIKNKHMNA
DTDYSIAEAAFNKGETAMTINGPWAWSNIDTSKVNYGVTVLPTFKGQPSKPFVGVLS
AGINAASPNKELAKEFLENYLLTDEGLEAVNKDKPLGAVALKSYEEELAKDPRIAATM
ENAQKGEIMPNIPQMSAFWYAVRTAVINAASGRQTVDEALKDAQTNSSSNNNNNNN
NNNLGIEGRISEFGHYARTDYAENANKLEESAREHHIPCPEHYNGFCMHGKCEHSIN
MQEPSCRCDAGYTGQRCEKKDYSVLYVVPGPVRFQYV

- MBP EGF HB-EGF V5-His, Mw=56.7 kDa

MKIKTGARILALSALTTMMFSASALAKIEEGKLVIWINGDKGYNGLAEVGKKFEKDTGI
KVTVEHPDKLEEKFPQVAATGDGPDIIFWAHDRFGGYAQSGLLAEITPDKAFQDKLY
PFTWDAVRYNGKLIAYPIAVEALSLIYNKDLLPNPPKTWEEIPALDKELKAKGKSALMF
NLQEPYFTWPLIAADGGYAFKYENGKYDIKDVGVDNAGAKAGLTFLVDLIKNKHMNA
DTDYSIAEAAFNKGETAMTINGPWAWSNIDTSKVNYGVTVLPTFKGQPSKPFVGVLS
AGINAASPNKELAKEFLENYLLTDEGLEAVNKDKPLGAVALKSYEEELAKDPRIAATM
ENAQKGEIMPNIPQMSAFWYAVRTAVINAASGRQTVDEALKDAQTNSSSNNNNNNN
NNNLGIEGRISEFGSKGLGKKRDPCLRKYKDFCIHGECKYVKELRAPSCICHPGYHG
ERCHGLSLPVENRLYTYDHTTILALESRGPFEGKPIPNPLLGLDSTRTGHHHHHH

Appendix III: Flp-In System (Invitrogen)

The Flp-In System allows stable expression of the gene of interest in mammalian cells by taking advantage of a *Saccharomyces cerevisiae*-derived DNA recombination system. It involves introduction of a Flp Recombination Target (FRT) site into the genome of the mammalian cell line of choice followed by the incorporation of an expression vector into the genome via Flp recombinase-mediated DNA recombination at the FRT site.

Generation of a mammalian cell line stably expressing gene of interest requires transfection with three different vectors in two steps. In the first step pFRT/*lac*Zeo target site vector is used to generate a Flp-In host cell line. The vector contains a *lacZ-Zeocin* fusion gene whose expression is controlled by the SV40 early promoter and a FRT site just downstream of the ATG initiation codon of the *lacZ-Zeocin* fusion gene. Cells transfected with the pFRT/l*ac*Zeo plasmid are selected for Zeocin resistance and the resulting Flp-In host cell line contains an integrated FRT site and expresses the *lacZ-Zeocin* fusion gene. Second step requires co-transfection of the Flp-In host cell line with pOG44 plasmid which constitutively expresses the Flp recombinase under the control of the human CMV promoter and pcDNA5/FRT vector containing cloned gene of interest. The pcDNA5/FRT vector contains also the hygromycin resistance gene that lacks a promoter and the ATG initiation codon with a FRT site embedded in the 5' coding region. Upon co-transfection the Flp recombinase expressed from the pOG44 mediates a homologous recombination between the FRT sites in the genome on Flp-In host cell line and the pcDNA5/FRT plasmid. It results in the integration of the pcDNA5/FRT construct into the genome. Insertion of pcDNA5/FRT at the FRT site brings the SV40 promoter and the ATG initiation codon from pFRT/*lac*Zeo into proximity and frame with the hygromycin resistance gene, and inactivates the *lacZ-Zeocin* fusion gene. Thus, stable Flp-In expression cell lines can be selected for hygromycin resistance, Zeocin sensitivity, lack of β-galactosidase activity, and expression of the recombinant protein of interest (see diagram below).

Flp-In System (Invitrogen)

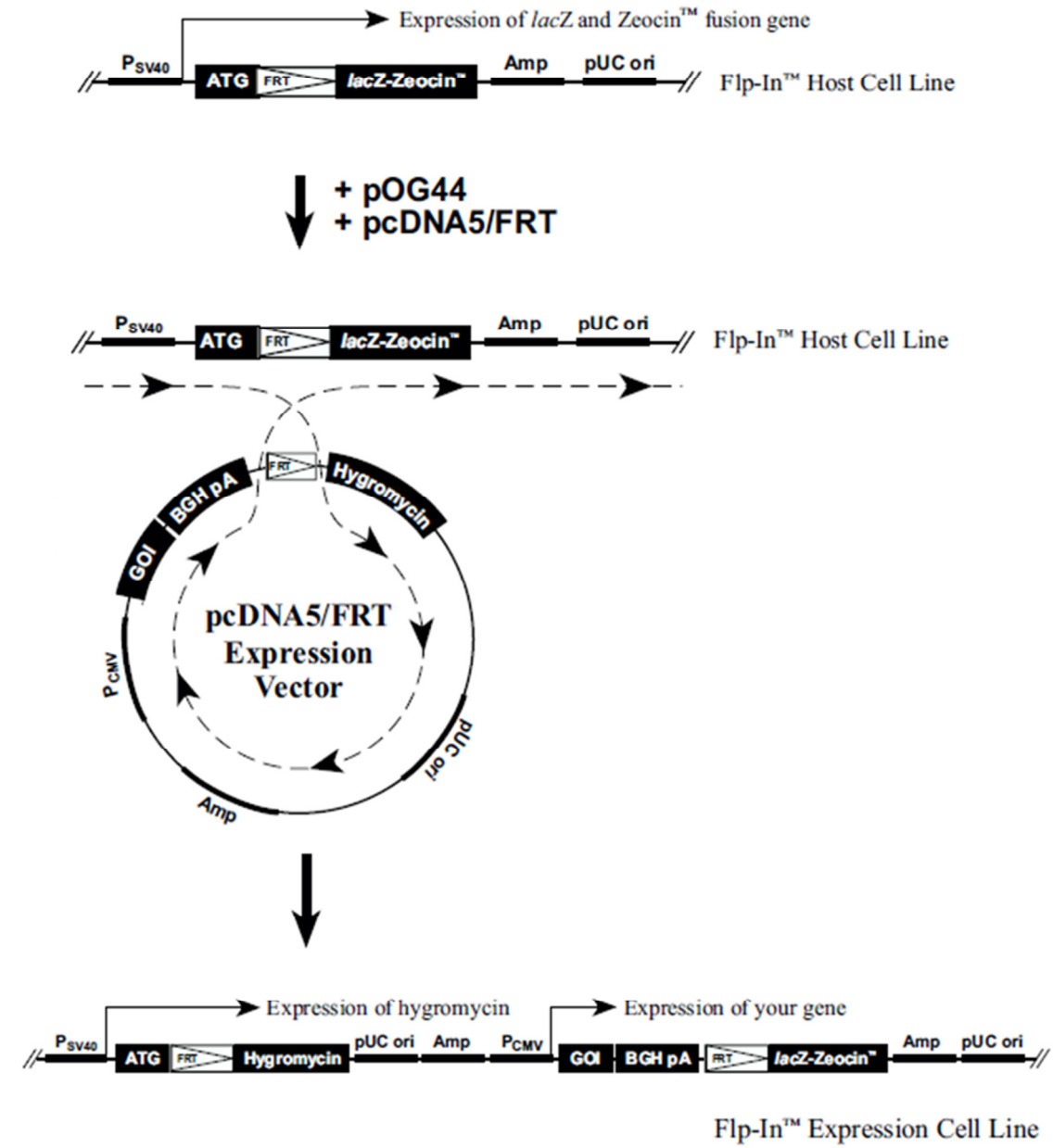

(from www.invitrogen.com)

Appendix IV: N-protein A TMEFF2 fragments protein sequence

- **IgG-protein A-ECD**, Mw= 52.9 kDa

PPWLPSTAASVLEFGLGISTMETDTLLLWVLLLWVPGSTGDYPYDVPDYAGAQPALPVEL
KTAALAQHDEAVDNKFNKEQQNAFYEILHLPNLNEEQRNAFIQSLKDDPSQSANLLAEAK
KLNDAQAPKVDNKFNKEQQNAFYEILHLPNLNEEQRNAFIQLSKDDPSQSANLLAEAKKL
NGAQAPKVDANSAGKSTTGSAFPTSLSDCQTPTGWNCSGYDDRENDLFLCDTNTCKFD
GECLRIGDTVTCVCQFKCNNDYVPVCGSNGESYQNECYLRQAACKQQSEILVVSEGSC
ATDAGSGSGDGVHEGSGETSQKETSTCDICQFGAECDEDAEDVWCVCNIDCSQTNFNP
LCASDGKSYDNACQIKEASCQKQEKIEVMSLGRCQDNTTTTTKSEDGHYARTDYAENAN
KLEESAREHHIPCPEHYNGFCMHGKCEHSINMQEPSCRCDAGYTGQHCEKKDYSVLYV
VPGPVRFQYV

- **IgG-protein A-2xFS**, Mw = 46.0 kDa

PPWLPSTAASVLEFGLGISTMETDTLLLWVLLLWVPGSTGDYPYDVPDYAGAQPALPVEL
KTAALAQHDEAVDNKFNKEQQNAFYEILHLPNLNEEQRNAFIQSLKDDPSQSANLLAEAK
KLNDAQAPKVDNKFNKEQQNAFYEILHLPNLNEEQRNAFIQLSKDDPSQSANLLAEAKKL
NGAQAPKVDANSAGKSTTGSAFPTSLSDCQTPTGWNCSGYDDRENDLFLCDTNTCKFD
GECLRIGDTVTCVCQFKCNNDYVPVCGSNGESYQNECYLRQAACKQQSEILVVSEGSC
ATDAGSGSGDGVHEGSGETSQKETSTCDICQFGAECDEDAEDVWCVCNIDCSQTNFNP
LCASDGKSYDNACQIKEASCQKQEKIEVMSLGRCQDNTTTTTKSEDGHYARTDYAENAN
KLEESARE

- **IgG-protein A-FS-EGF**, Mw = 41.5 kDa

PPWLPSTAASVLEFGLGISTMETDTLLLWVLLLWVPGSTGDYPYDVPDYAGAQPALPVEL
KTAALAQHDEAVDNKFNKEQQNAFYEILHLPNLNEEQRNAFIQSLKDDPSQSANLLAEAK
KLNDAQAPKVDNKFNKEQQNAFYEILHLPNLNEEQRNAFIQLSKDDPSQSANLLAEAKKL
NGAQAPKVDANSAGKSTTGSGVHEGSGETSQKETSTCDICQFGAECDEDAEDVWCVC
NIDCSQTNFNPLCASDGKSYDNACQIKEASCQKQEKIEVMSLGRCQDNTTTTTKSEDGH
YARTDYAENANKLEESAREHHIPCPEHYNGFCMHGKCEHSINMQEPSCRCDAGYTGQH
CEKKDYSVLYVVPGPVRFQYV

- **IgG-protein A-EGF**, Mw = 31.7 kDa

PPWLPSTAASVLEFGLGISTMETDTLLLWVLLLWVPGSTGDYPYDVPDYAGAQPALPVEL
KTAALAQHDEAVDNKFNKEQQNAFYEILHLPNLNEEQRNAFIQSLKDDPSQSANLLAEAK
KLNDAQAPKVDNKFNKEQQNAFYEILHLPNLNEEQRNAFIQLSKDDPSQSANLLAEAKKL
NGAQAPKVDANSAGKSTTGSKSEDGHYARTDYAENANKLEESAREHHIPCPEHYNGFC
MHGKCEHSINMQEPSCRCDAGYTGQHCEKKDYSVLYVVPGPVRFQYV

Appendix V: TMEFF2-ECD-Fc protein sequence

MVLWESPRQCSSWTLCEGFCWLLLLPVMLLIVARPVKLAAFPTSLSDCQTPTGWNCSG
YDDRENDLFLCDTNTCKFDGECLRIGDTVTCVCQFKCNNDYVPVCGSNGESYQNECYL
RQAACKQQSEILVVSEGSCATDAGSGSGDGVHEGSGETSQKETSTCDICQFGAECDED
AEDVWCVCNIDCSQTNFNPLCASDGKSYDNACQIKEASCQKQEKIEVMSLGRCQDNTTT
TTKSEDGHYARTDYAENANKLEESAREHHIPCPEHYNGFCMHGKCEHSINMQEPSCRC
DAGYTGQHCEDYKDDDDKGIDEPKSCDKTHTCPPCPAPELLGGPSVFLFPPKPKDTLMI
SRTPEVTCVVVDVSHEDPEVKFNWYVDGVEVHNAKTKPREEQYNSTYRVVSVLTVLHQ
DWLNGKEYKCKVSNKALPAPIEKTISKAKGQPREPQVYTLPPSREEMTKNQVSLTCLVK
GFYPSDIAVEWESNGQPENNYKTTPPVLDSDGSFFLYSKLTVDKSRWQQGNVFSCSVM
HEALHNHYTQKSLFLSPGKTGVHHHHHH